

Proanthocyanidins and Glucose Homeostasis:  
An Analysis of Bioavailability and Mechanisms in Rats

by

Kaiyuan Yang

A thesis submitted in partial fulfillment of the requirements for the degree of

Doctor of Philosophy

in

Nutrition and Metabolism

Department of Agricultural, Food and Nutritional Science  
University of Alberta

© Kaiyuan Yang, 2015

## Abstract

Proanthocyanidins (PAC) belong to a highly consumed class of flavonoids and their consumption has been linked to beneficial effects on glycemic control in type 2 diabetes. However, limited gastrointestinal absorption occurs due to the structure complexity of polymeric PAC and the mechanisms by which PAC exerts such benefits are largely unknown. We hypothesized that hydrolysis of the PAC polymer would increase bioavailability, thus leading to enhanced beneficial effects on glucose homeostasis. We further hypothesized that PAC effects *in vivo* would be associated with improved pancreatic  $\beta$ -cell function and hepatic insulin sensitivity by acting on specific signalling pathways that could be detected using *in vitro* techniques. PAC-rich pea seed coats (PSC) were supplemented in a high fat diet (HFD) either in native (PAC) or hydrolyzed (HPAC) form and fed to HFD-induced glucose intolerant rats for 4 weeks. HFD or low fat diet (LFD) groups were controls. PAC-derived compounds were characterized in both PSC and serum. The results showed that hydrolysis significantly decreased the degree of polymerization (DP). Meanwhile increased PAC-derived metabolites were detected in the serum of HPAC-fed rats compared to PAC-fed rats, suggesting hydrolysis of PSC enhanced PAC bioavailability. This was associated with ~18% less ( $P < 0.05$ ) weight gain compared to HFD without affecting food intake, as well as improvement in glucose tolerance *in vivo*. There was a 50% decrease of the  $\alpha/\beta$ -cell area ratio and a 2.5-fold increase ( $P < 0.05$ ) in glucose-stimulated insulin secretion (GSIS) from isolated islets of HPAC-fed rats. These results demonstrate that hydrolysis of PSC-derived PAC increased the bioavailability of PAC-derived products, which is critical for enhancing beneficial effects on glucose homeostasis and pancreatic  $\beta$ -cell function. The results from the *in vitro* study of a PAC metabolite on INS-1 cell line showed that a low but physiologically

relevant concentration of epicatechin (EC, 0.3  $\mu$ M) rectified stearic acid (SFA)-impaired insulin secretion via activation of CaMKII pathway, although it failed to attenuate elevated reactive oxygen species (ROS) production induced by high glucose and H<sub>2</sub>O<sub>2</sub>; whereas 30  $\mu$ M EC effectively suppressed ROS production but showed no effects on insulin secretion. These results indicate that EC effects are concentration-dependent, and that EC can act as a molecule in regulating cell signaling pathways at physiological concentrations. Hepatic insulin sensitivity was assessed using the insulin tolerance test (ITT). PAC and HPAC had decreased glucose recovery rates during ITT ( $P < 0.05$  for both), indicating suppressed hepatic glucose production compared with HFD. Correspondingly, we detected reduced phosphoenolpyruvate carboxykinase (PEPCK) content in the livers of PAC ( $P < 0.05$ ) and HPAC ( $P = 0.1$ ). Furthermore, hepatic glycogen content and total glutathione were increased in PAC but not in HPAC compared with HFD, suggesting PAC alleviated hepatocyte insulin resistance via relief of oxidative stress, whereas HPAC was not as effective. In summary, reducing the structural complexity of PAC can improve bioavailability, leading to enhanced glycemic control in the condition of glucose intolerance. This is related to improvements in pancreatic islet function, especially insulin secretion from pancreatic  $\beta$ -cells as well as better-controlled hepatic glucose production. The present study also supports the theory that bioavailable PAC-derived compounds can exert effects via modulating cellular signaling pathways.

## Preface

All of the work presented in this dissertation was conducted in University of Alberta. The research project, of which this thesis is a part, received research ethics approval from the University of Alberta Research Ethics Board, Project Name “fat metabolism and signalling in uncoupling protein-2 knockout mice”, No. 523, Feb 1, 2009, renewed Feb 1, 2010, renewed Feb 1, 2011, renewed Feb 1, 2012, ended Jan 31, 2013. The guidelines of the Canadian Council on Animal Care and the International Guide and Care of Laboratory Animals were followed in all animal experiments. Protocols were approved by the Animal Care and Use Committee of the University of Alberta.

A version of Chapter 3 was accepted by *The Journal of Nutritional Biochemistry*, manuscript (DOI: 10.1016/j.jnutbio.2015.03.002) entitled “Hydrolysis enhances bioavailability of proanthocyanidin-derived metabolites and improves  $\beta$ -cell function in glucose intolerant rats” by Kaiyuan Yang, Zohre Hashemi, Wei Han, Alena Jin, Han Yang, Jocelyn Ozga, Liang Li and Catherine B. Chan. I led the study, prepared animal diets, conducted *in vivo* studies, tissue collection, serum analyses, immunohistochemistry and morphometry as well as islet studies, statistical analyses and drafted the manuscript. Zohre Hashemi also prepared diets and assisted with *in vivo* studies and tissue collection. Han Yang, Alena Jin and Jocelyn Ozga were responsible for preparing the pea seed coats and their quantitative analysis; Jocelyn Ozga also edited the manuscript. Wei Han and Liang Li conducted the studies of proanthocyanidin metabolites by mass spectroscopy. Catherine B. Chan oversaw the entire study, acquired the research grants and edited the manuscript. It also contributed to a Report of Invention as a prelude to a full patent application: ‘Pea (*Pisum Sativum* L.) Seed Coats



and Seed Coat Fractions', by OZGA, Jocelyn; CHAN, Catherine; JIN, Alena; HAN, Yang; HASHEMI, Seyede; YANG, Kaiyuan. United States Provisional Patent Application Serial No. 62/041,277 (Appendix 1).

Chapter 4 is being prepared in manuscript format and will be submitted to a relevant journal. I led the study, conducted all the experiments and data collection and analyses, and drafted the manuscript. Catherine B. Chan oversaw the entire study and edited the manuscript.

In the study presented in Chapter 5, Han Yang, Alena Jin and Jocelyn Ozga were responsible for preparing the pea seed coats. I led the study, prepared animal diets, conducted *in vivo* studies, serum analyses and tissue collection and analyses. Zohre Hashemi also prepared diets and assisted with *in vivo* studies and tissue collection. Catherine B. Chan oversaw the entire study.

In Chapter 6, the data in Table 6-1 was provided by Tao Huan and Liang Li, and I analyzed these data. I conducted *in vivo* studies, serum analyses and collected and analyzed the data in Figure 6-1 and 6-2. Zohre Hashemi assisted with *in vivo* studies and serum collection. Part of the data in Figure 6-1 was used with permission from Hashemi et al. (2015) of which I am a co-author.

## Dedication

To my family

*If you can dream—and not make dreams your master*

*If you can think—and not make thoughts your aim*

*If you can meet with Triumph and Disaster*

*And treat those two impostors just the same*

*-- Rudyard Kipling*

## Acknowledgments

First and foremost, I would like to thank my supervisor Dr. Catherine (Cathy) Chan. It has been a great honour to be one of her students. I am grateful for all her patience, time, advice, encouragement, and guidance throughout this research project, making my PhD experience exciting and productive. She had faith in me even during tough times. I am indebted to her more than she knows. I am also thankful for the excellent example she has provided as a successful woman professor. The joy and enthusiasm she has for her research is motivational and inspiring for me in the pursuit of PhD and future career. I also thank my committee members Dr. Yves Sauvé and Dr. Catherine Field for being extremely supportive and encouraging, and proving their insightful thoughts and constructive comments to my project. I am grateful for their crucial contribution and guidance during my study.

The members of the Chan group have contributed immensely to my personal and professional time at University of Alberta. They have been a valuable source of friendships as well as good advice. I thank Dr. Zohre Hashemi who has been helping me out during my entire study. We worked together on all the animal feeding trials, and I appreciated her enthusiasm and collaboration. Feiyue Deng has always been a wonderful friend to me ever since the day we both were in Canada. She helped me get through all the darkest times, and has been nothing but supportive and thoughtful, which I would never forget. I would like to thank Dr. Xiaofeng Wang who joined the Chan group only recently, but has given me invaluable advice in my later work of cell culture experiments. I also appreciated the assistance from Nicole Coursen in animal care and handling. She was the first one who showed me around in the animal facility and taught me all the animal handling technique (“tricks”). I also appreciated the friendships from Ghada Assad, Hebah Salawi and Hui Huang. I am grateful for the help, laughs and joys shared with them. Collective and individual acknowledgments also go to all who have worked with me in the Chan lab: the former members Dr. Zahra Fatehi-Hassanabad, Anne Harasym, Diana Cristina Soria Contreras and Aramsri Meeprom; and student volunteers Joel Gupta, Grace Xu, Rebecca Fuller, Karissa Frederick, Lisa Kocizky, Homun Yee, Kevin Whitlock.

In regard to collaborations, I would like to acknowledge Dr. Jocelyn Ozga, Dr. Alena Jin and Han Yang for preparing the pea seed coats and analysis of their components. Many

thanks also go to Dr. Liang Li, Wei Han and Tao Huan in the Department of Chemistry for their valuable work on the metabolomic analysis of proanthocyanidins.

I am deeply grateful for technical support from Kunimasa Suzuki and Gregory Plummer. I would also like to acknowledge Anne-Francoise Close from Dr. Jean Buteau's lab for teaching me all the techniques in cell culture experiments.

I very much appreciated the funding sources that made my PhD work possible. I was funded by the China Scholarship Council and University of Alberta from Sept., 2010 to Aug., 2014. From Sept. to Dec., 2014, my work was supported by a stipend from the Canadian Institutes of Health Research (CIHR) to Dr. Yves Sauvé. Then I was funded by scholarships from the Department of Agricultural, Food and Nutritional Science (AFNS) and my supervisor Dr. Catherine Chan. I also thank all the travel awards from the Faculty of Graduate Studies and Research, the Department of AFNS, Alberta Diabetes Institute and CIHR.

My time at University of Alberta was made enjoyable in large part due to the many friends that became a part of my life. I am grateful for time spent with roommates and friends, and our memorable trips into the mountains, and for many other people and memories.

Lastly, I would like to thank my family for all their love and encouragement. For my parents who raised me with a love of science and supported me in all my pursuits. Thank you.

## Table of Contents

Abstract.....	ii
Preface.....	iv
Dedication.....	vi
Acknowledgments.....	vii
Table of Contents .....	ix
List of Tables.....	xv
List of Figures .....	xvi
List of Abbreviations.....	xviii
Chapter 1 Introduction .....	1
1.1 Proanthocyanidins .....	1
1.1.1 Flavonoids.....	1
1.1.2 Flavan-3-ols and proanthocyanidins.....	3
1.1.3 Occurrence in food and dietary intake of catechins and proanthocyanidins.....	4
1.1.4 Absorption, bioavailability and metabolism of proanthocyanidins.....	4
1.1.5 Health related properties of proanthocyanidins .....	9
1.2 Glucose homeostasis.....	13
1.2.1 Glucose uptake .....	13
1.2.2 Glucose output .....	21
1.3 Definition and pathology of prediabetes .....	22

1.3.1 Prediabetes .....	22
1.3.2 Pathology of prediabetes.....	22
1.4 The effects and proposed mechanisms of proanthocyanidins on glucose homeostasis.....	24
1.4.1 Proanthocyanidins' effects on glucose homeostasis .....	24
1.4.2 Proposed mechanisms .....	29
Chapter 2 Study Rationale, Hypotheses and Objectives .....	38
2.1 Rationale.....	38
2.2 Overall hypothesis.....	39
2.3 Specific hypothesis and objectives .....	39
2.3.1 Bioavailability of PAC and HPAC and effects on pancreatic islet function (Chapter 3).....	39
2.3.2 Effects of PAC-derived compounds, epicatechin (EC) on insulin secreting INS- 1 cell lines (Chapter 4) .....	40
2.3.3 Effects of PAC and HPAC on hepatic glucose metabolism (Chapter 5) .....	40
Chapter 3 Hydrolysis enhances bioavailability of proanthocyanidin-derived metabolites and improves $\beta$ -cell function in glucose intolerant rats .....	42
3.1 Introduction.....	42
3.2 Methods.....	45
3.2.1 Chemicals and reagents .....	45
3.2.2 Preparation of pea seed coat diets.....	45
3.2.3 Animal feeding trial .....	47

3.2.4	Glucose and insulin tolerance tests .....	47
3.2.5	Tissue collection .....	48
3.2.6	Soluble PAC and anthocyanin quantitation .....	48
3.2.7	Analysis of PAC-derived compounds in PSC and serum samples.....	49
3.2.8	Analysis of plasma insulin and glucagon .....	50
3.2.9	Immunohistochemistry .....	50
3.2.10	Glucose stimulated insulin secretion from isolated islets .....	50
3.2.11	Statistical analyses.....	51
3.3	Results.....	52
3.3.1	Hydrolysis depolymerized PAC and increased metabolites in serum .....	52
3.3.2	HPAC improved body composition without affecting food intake.....	56
3.3.3	HPAC diet improved insulin resistance induced by HFD .....	58
3.3.4	HPAC preserved pancreatic islet morphology and function .....	61
3.4	Discussion .....	64
Chapter 4 Epicatechin potentiates glucose-stimulated insulin secretion in INS-1 cells		
	through CaMKII activation.....	68
4.1	Introduction.....	68
4.2	Materials and methods.....	71
4.2.1	Cell culture .....	71
4.2.2	Measurement of EC modulation of glucose-induced ROS production .....	71
4.2.3	Measurement of EC modulation of H <sub>2</sub> O <sub>2</sub> -induced ROS production.....	72
4.2.4	Evaluation of cell viability .....	72

4.2.5 Glucose stimulated insulin secretion.....	73
4.2.6 Western blot analysis .....	73
4.2.7 Statistical analysis.....	74
4.3 Results.....	75
4.3.1 EC (30 $\mu$ M) protects against high glucose-induced ROS in INS-1 cells .....	75
4.3.2 EC at 30 $\mu$ M protects against H <sub>2</sub> O <sub>2</sub> -induced ROS in INS-1 cells .....	76
4.3.3 EC at 0.3 $\mu$ M is not effective in improving cell viability of INS-1 cells treated with SFA .....	77
4.3.4 EC at 0.3 $\mu$ M enhances insulin secretion from INS-1 cells treated with SFA ..	78
4.3.5 CaMKII inhibitor KN-93 reverses EC-enhanced GSIS from INS-1 cells treated with SFA .....	81
4.3.6 CaMKII phosphorylation is normalized by EC in INS-1 cells treated with SFA .....	82
4.4 Discussion .....	85
Chapter 5 Flavan-3-ols improvement of insulin sensitivity and modulation of hepatic glucose production is associated with suppression of PEPCK expression in glucose intolerant rats .....	92
5.1 Introduction.....	92
5.2 Methods.....	95
5.2.1 Preparation of pea seed coat diets .....	95
5.2.2 Animal feeding trial .....	96
5.2.3 Glucose and insulin tolerance tests .....	96



5.2.4 Tissue collection .....	96
5.2.5 Analysis of plasma insulin and glucagon.....	96
5.2.6 Antioxidant assay .....	97
5.2.7 Total glutathione (tGSH) assay.....	97
5.2.8 Measurement of hepatic glycogen concentrations.....	98
5.2.9 Western blot analysis.....	98
5.2.10 Statistical analysis.....	99
5.3 Results .....	100
5.3.1 PAC- and HPAC-feeding decrease body weight gain induced by HFD .....	100
5.3.2 HPAC has marginally decreased fasting plasma insulin and glucagon.....	100
5.3.3 PAC increases hepatic glutathione and glycogen content .....	101
5.3.4 HPAC reverses glucose intolerance induced by HFD.....	103
5.3.5 HPAC affects hepatic glucose output during insulin challenge.....	103
5.3.6 Effects of PAC and HPAC on the expression of hepatic enzymes .....	105
5.4 Discussion .....	107
Chapter 6 General Discussion .....	111
6.1 Summary of hypotheses and results.....	111
6.2 Impact of DP on the bioavailability of PAC.....	114
6.3 PAC's effects on glucose handling.....	117
6.4 PAC/HPAC effects on pancreatic islets and insulin secreting $\beta$ -cells.....	121
6.4.1 PAC/HPACs effects on the morphology of pancreatic islets .....	121

6.4.2 PAC/HPAC effects on insulin secretion from pancreatic islets and $\beta$ -cell lines	122
6.4.3 The mechanism of EC effects on insulin secretion.....	124
6.5 PAC/HPAC effects on liver function and glucose production .....	125
6.6 Contributions and implications of present thesis research .....	129
6.7 Conclusions .....	131
Bibliography.....	132
Appendix A.....	157

## **List of Tables**

Table 1-1. Classification, structure and food sources of dietary flavonoids.....	2
Table 1-2. Summary of studies on PAC effects in humans. ....	27
Table 1-3. Summary of studies on PAC effects in vivo and in vitro. ....	32
Table 3-1. Experimental diet formulas. ....	46
Table 3-2. PAC-derived compounds in pea seed coats and rat serum. ....	52
Table 3-3. Food intake and body composition .....	56
Table 5-1. Experimental diet formulas. ....	95
Table 5-2. Energy Intake, body weight and tissue weights.....	100
Table 5-3. Antioxidant, glucose, insulin, glucagon in blood and HOMA-IR.....	101
Table 6-1. PAC-derived metabolites from microbial metabolism in serum and urine....	116

## List of Figures

Figure 1-1. Structure of 2-phenylbenzopyran (C6-C3-C6) skeleton .....	1
Figure 1-2. Proposed schema of PAC absorption and metabolism in the body .....	7
Figure 1-3. Glucose stimulated insulin secretion from pancreatic $\beta$ -cells .....	15
Figure 1-4. The regulation of glucose metabolism by insulin in the liver. ....	17
Figure 1-5. AMPK signaling pathway in the liver. ....	20
Figure 3-1. ESI-MS spectrum of the HPAC serum extract showing the epicatechin-3'-O-glucuronide (A, B) and 4'-O-methyl-epigallocatechin (C, D).....	54
Figure 3-2. Structures of PAC-derived compounds.....	55
Figure 3-3. Effects of diet on body weight change during the feeding trial. ....	57
Figure 3-4. Blood glucose concentrations and insulin release after glucose challenge. ..	59
Figure 3-5. Blood glucose responses after insulin challenge.....	60
Figure 3-6. Effects of different diets on pancreatic morphology, fasted insulin and glucagon.....	63
Figure 3-7. Effects of different diets on glucose-stimulated insulin secretion from isolated islets. ....	63
Figure 4-1. EC at 30 $\mu$ M protects against high glucose-induced ROS in INS-1 cells.....	76
Figure 4-2. EC at 30 $\mu$ M protects against H <sub>2</sub> O <sub>2</sub> -induced ROS in INS-1 cells. ....	77
Figure 4-3. EC (A) and NAC (B) at 0.3 $\mu$ M is not effective in improving cell viability of INS-1 cells treated with SFA. ....	78
Figure 4-4. EC at 0.3 $\mu$ M enhances insulin secretion from INS-1 cells treated with SFA.	79
Figure 4-5. EC and SFA's effects on total insulin synthesized in GSIS from INS-1 cells.	80
Figure 4-6 CaMKII inhibitor KN-93 reverses EC-enhanced GSIS from INS-1 cells treated with SFA.....	81

Figure 4-7 Expression of proteins involved in EC-enhanced GSIS from INS-1 cells treated with SFA.....	84
Figure 4-8. Structure of epicatechin (EC, A) and catechin (B).....	87
Figure 4-9 Schematic diagram of the possible pathways of CaMKII and PKA in insulin secretion in pancreatic $\beta$ -cells. ....	89
Figure 5-1. Effects of PAC and HPAC on total glutathione concentrations in the liver.	102
Figure 5-2 Effects of PAC and HPAC on hepatic glycogen content.....	102
Figure 5-3 Glucose and insulin responses after oral glucose challenge. ....	104
Figure 5-4. Effects of PAC and HPAC on the expression of hepatic enzymes.....	106
Figure 6-1 Schematic diagram of the effects and possible mechanisms of PAC and HPAC on improving disrupted glucose homeostasis under glucose intolerant condition.....	113
Figure 6-2 Comparison of PAC and nonPAC during intraperitoneal glucose tolerance test (IPGTT).....	118
Figure 6-3 Comparison of PAC and HS during intraperitoneal glucose tolerance test (IPGTT).....	119

## List of Abbreviations

ABTS	2,2'-azino-bis(3-ethylbenzthiazoline-6-sulfonic acid)
ACC	acetyl-coenzyme A carboxylase
ADA	American Diabetes Association
ADP	adenosine diphosphate
Akt/PKB	protein kinase B, PKB, as known as Akt
AMP	adenosine 5'-monophosphate
AMPK	AMP-activated protein kinase
ANOVA	analysis of variation
ATP	adenosine triphosphate
AUC	area under the curve
BMI	body mass index
BSA	bovine serum albumin
CaMKII	Ca <sup>2+</sup> /calmodulin-dependent protein kinase II
CaMKK $\beta$	Ca <sup>2+</sup> /calmodulin-dependent protein kinase kinase $\beta$
cAMP	cyclic adenosine monophosphate
CNS	central nervous system
CREB	cAMP response element binding protein
CRP	c-reactive protein
DCF	2', 7' -dichlorofluorescein
DCFDA	2',7' -dichlorofluorescein diacetate
DNA	deoxyribonucleic acid
DP	degree of polymerization
DPPH	1,1-diphenyl-2-picrylhydrazyl

DTNB	5,5'-dithiobis(2-nitrobenzoic acid)
dUTP	2'-deoxyuridine 5'-triphosphate
EC	epicatechin
EGCG	epigallocatechin gallate
EGP	endogenous glucose production
ELISA	enzyme linked immunosorbent assay
eNOS	endothelial nitric oxide synthase
ER	endoplasmic reticulum
ERK	extracellular-regulated kinase
ESI	electrospray ionization
FAS	fatty-acid synthase
FBS	fetal bovine serum
FFA	free fatty acid
FPG	fasting plasma glucose
FPI	fasting plasma insulin
G-6-P	glucose-6-phosphate
G6Pase	glucose 6-phosphatase
G-6-PDH	glucose-6- phosphate dehydrogenase
GAPDH	glyceraldehyde-3-phosphate dehydrogenase
GI	gastrointestinal
GIP	gastric inhibitory polypeptide
GK	glucokinase
GLP-1	glucagon-like peptide 1
GLUT	glucose transporter
GSH	glutathione
GSIS	glucose stimulated insulin secretion

GSK-3	glycogen synthase kinase-3
GSP	grape seed proanthocyanidins
GSSG	glutathione disulfide
GTE	green tea extract
GTT	glucose tolerance test
HbA <sub>1c</sub>	glycated hemoglobin A <sub>1c</sub>
HBSS	Hanks' Balanced salt solution
HEPES	4-(2-hydroxyethyl)-1-piperazineethanesulfonic acid
HFD	high fat diet
HGP	hepatic glucose production
HILIC	hydrophilic interaction chromatography
HK	hexokinase
HMG-CoA	3-hydroxy-3-methylglutaryl-coenzyme A
HOMA-IR	homeostasis model assessment-estimated insulin resistance index
HOMA- $\beta$	homeostasis model assessment-estimated $\beta$ -cell function index
HPAC	hydrolyzed proanthocyanidin-containing pea seed coats
HPLC	high-performance liquid chromatography
IAUC	incremental area under the curve
IC <sub>50</sub>	half maximal inhibitory concentration
IFG	impaired fasting glucose
IFN	Interferon
IGT	impaired glucose tolerance
IHC	immunohistochemistry
IL	Interleukin
IPGTT	intraperitoneal glucose tolerance test



IR	insulin resistance
IRS	insulin receptor substrate
ISI	insulin sensitivity index
ITT	insulin tolerance test
KRB	Krebs–Ringer bicarbonate buffer
LFD	low fat diet
LKB1	liver kinase B1
LTP	long-term potentiation
MAP-2	microtubule-associated protein 2
MAPK	mitogen-activated protein kinase
MCP	monocyte chemoattractant protein
MDA	malondialdehyde
MPA	metaphosphoric acid
MS	mass spectrometer
MTT	3-(4,5-dimethylthiazol-2-yl)-2,5-diphenyltetrazolium bromide
NAC	N-acetyl cysteine
NADP	nicotinamide adenine dinucleotide phosphate
NF-E	nuclear factor-erythroid
NF- $\kappa$ B	nuclear factor kappa-light-chain-enhancer of activated B cells
Nrf2	nuclear factor-erythroid (NF-E) 2-related factor 2
OGTT	oral glucose tolerance test
PAC	proanthocyanidin-containing pea seed coat
pAMPK $\alpha$	phosphorylated 5'-adenosine monophosphate (AMP) -activated protein kinase $\alpha$
pCaMKII	phosphorylated Ca <sup>2+</sup> /calmodulin-dependent protein kinase II
PDK1	phosphoinositide-dependent kinase 1

PDX-1	pancreatic and duodenal homeobox 1
PEPCK	phosphoenolpyruvate carboxykinase
pERK	phosphorylated extracellular-regulated kinase
PGC-1 $\alpha$	peroxisome proliferator-activated receptor gamma coactivator-1 $\alpha$
PI3K	phosphatidylinositol 3-kinase
p-JNK	phosphorylated c-Jun N-terminal protein kinase
PKA	protein kinase A
PKB	protein kinase B
PP1	protein phosphatase-1
p-PKA	phosphorylated protein kinase A
PSC	pea seed coat
PUFA	polyunsaturated fatty acid
QUICKI	quantitative insulin sensitivity check index
RIPA	radioimmunoprecipitation assay
ROS	reactive oxygen species
RPMI	Roswell Park Memorial Institute
SAA	serum amyloid A
SD	Sprague-Dawley
SDS	sodium dodecyl sulfate
SEM	standard error of the mean
SFA	saturated fatty acid-stearic acid
SOD	superoxide dismutase
STZ	streptozotocin
sVCAM	soluble vascular cell adhesion molecule
T2D	type 2 diabetes
t-BOOH	tert-butylhydroperoxide

TAC	total antioxidant capacity
tGSH	total glutathione
TNF	tumor necrosis factor
TUNEL	terminal deoxynucleotidyl transferase 2'-deoxyuridine 5'-triphosphate (dUTP) nick end labeling
UCP-1	uncoupling protein-1
USDA	United States Department of Agriculture
UV	ultraviolet
WAG	Wistar Albino Glaxo
WHO	World Health Organization

# Chapter 1

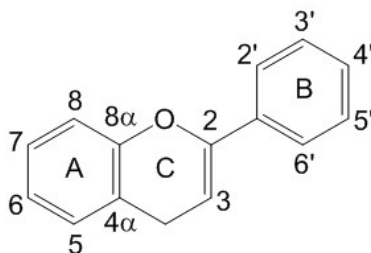
## Introduction

### 1.1 Proanthocyanidins

#### 1.1.1 Flavonoids

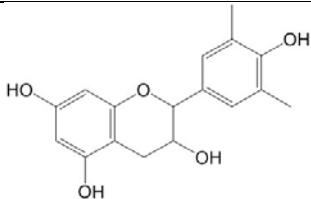
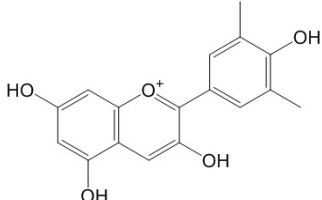
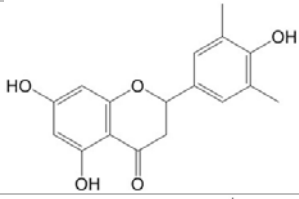
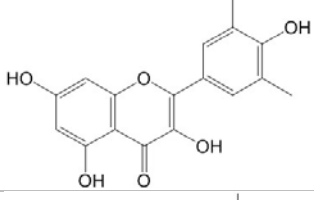
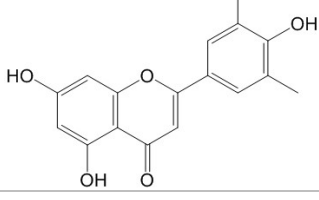
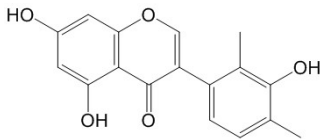
Flavonoids are a group of plant phenolic secondary metabolites. They exist ubiquitously and contribute to the flavor and color of many vegetables and fruits, and therefore are an important part of human diets. In plants, they are important for plant physiology by being involved in plant growth and reproduction, as well as protecting plants against bioaggressors [1]. Due to the antioxidant and free-radical scavenging properties of flavonoids, interest has been drawn on the biological effects of flavonoids in chronic diseases, such as cardiovascular diseases and cancers [2].

Flavonoids have a common 2-phenylbenzopyran (C<sub>6</sub>-C<sub>3</sub>-C<sub>6</sub>) skeleton (Figure 1-1). The A ring has a characteristic hydroxylation pattern at the 5 and 7 position, whereas the B ring is usually 4', 3'4', or 3'4'5'-hydroxylated [3]. Based on variations in the heterocyclic C-ring, flavonoids can be divided into six subgroups: flavones, flavonols, flavanones, flavan-3-ols (catechins and proanthocyanidins), anthocyanidins, and isoflavones (Table 1-1) [4].



**Figure 1-1. Structure of 2-phenylbenzopyran (C<sub>6</sub>-C<sub>3</sub>-C<sub>6</sub>) skeleton**

**Table 1-1. Classification, structure and food sources of dietary flavonoids**

Class	General Structure	Flavonoid	Substitution Pattern	Dietary Sources
Flavan-3-ols (catechins)		(+)-catechin	3,5,7,3',4'-OH	Tea, cocoa, grape seeds
		(-)-epicatechin	3,5,7,3',4'-OH	
Anthocyanidins		cyanidin	3,5,7,4'-OH,3,5-OMe	Cherry, raspberry, strawberry
Flavanones		naringenin	5,7,4'-OH	Citrus fruits
Flavonols		kaempferol	3,5,7,4'-OH	Leek, broccoli, grapefruit
		quercetin	3,5,7,3',4'-OH	Onion, broccoli, red wine, berries
Flavones		apigenin	5,7,4'-OH	Parsley, celery
		luteolin	5,7,3',4'-OH	Red pepper
Isoflavones		genistein	5,7,4'-OH	Soybean
		daidzein	7,4'-OH	

### **1.1.2 Flavan-3-ols and proanthocyanidins**

Flavan-3-ols are a major group of flavonoids. As shown in Table 1-1 the heterocyclic C ring of flavan-3-ols has a saturated C<sub>3</sub> element [4]. The monomeric flavan-3-ols are commonly named catechins, while the oligomers and polymers are known as proanthocyanidins (PAC, or condensed tannins). They are a unique class of flavonoids that possess properties characterized by the presence of hydroxyl groups and interflavan bonds with different numbers and positions in a wide range of molecular sizes varying from 300 to 55000 Da [5].

PAC are made mainly of (+)-catechin and (-)-epicatechin, with degree of polymerization (DP), which reflects the number of flavanol units, up to 20 or even higher [5]. The carbon-carbon linkage of the interflavan bond is not easy to break, usually requiring strong hot acidic environment [6]. PAC oligomers and polymers can form complexes with proteins, which confers some of their sensory and digestive properties. For example, astringency of most PAC-rich foods results from the interaction of PAC with proline-rich salivary proteins in the mouth, whereas bitterness is due to an interaction between polar molecules and the lipid portion of the taste papillae membrane [7,8]. PAC can also react with food-derived proteins, digestive enzymes and cell membrane proteins in the gastrointestinal (GI) tract, exerting influence on the functions of the GI tract [9].

The chemical structure of PAC also features extensive hydroxyl groups, which makes PAC not only water soluble even with a relatively large DP [5], but also capable of readily donating hydrogen (electron) to stabilize radical species, especially with the B-ring catechol groups (dihydroxylated B-rings) [10–12]. In addition, PAC-derived radicals are more stable and less harmful than the initial radical species [13]. Therefore they are well known as potent antioxidants.

### **1.1.3 Occurrence in food and dietary intake of catechins and proanthocyanidins**

PAC and their derivatives are widely present in the bark, leaves, fruits and seeds of many plants, where they provide protection against microbial pathogens, insect pests and herbivores [14]. PAC contribute mainly to the flavor of bitterness and astringency, and colors of yellow, orange, red, purple and blue [15]. They are among the main phenolic compounds found in seeds and nuts, spices, fruits, wine, and tea (Table 1-1), and contribute a major fraction of total flavonoid intake in western diet [16–20]. The content of PAC in food depends on the species, origins, degree of ripeness, food processing, and food storage conditions. For example, 100g of apple (Red Delicious) adds ~144mg of PAC to the diet, and ~200ml of brewed tea adds 20-70mg [5]. Total PAC concentrations in different berries are 23-664 mg/100g of fresh weight [21]. Dehulling, peeling, grinding and juice filtration can decrease total PAC content. Higher PAC levels are found in fresh fruits than in dried fruits [15]. Flavonoid content in milk is dependent on the animal feed [22]. The estimated average dietary intake of PAC varies from 95-227mg/d in different populations [18–20,23,24]. However, the intake of PAC may be underestimated because the available United States Department of Agriculture (USDA) database does not report PAC, especially compounds with DP>3 content for all foods, due to the insolubility of the compounds and limitations of the analytical technology [25,26].

### **1.1.4 Absorption, bioavailability and metabolism of proanthocyanidins**

A number of research studies have attempted to address the metabolism of PAC in the body because both human and animal studies indicate that PAC can be absorbed and metabolized [27–30]. Nonetheless, there are still questions regarding the absorption and metabolic transformations of PAC that remain unsolved.

#### **1.1.4.1 Effects of structure**

After ingestion of foods containing PAC, it is reported that PAC remain intact in the stomach, as the breakdown of interflavan bonds requires a strong, hot, acidic environment [31]. After entering the small intestine, hydrophilic PAC (due to the presence of abundant hydroxyl groups) are solubilized and accessible to enterocytes [32]. PAC with low molecular weight, i.e. monomers, dimers and trimers are reported to be rapidly absorbed directly by enterocytes, whereas PAC polymers remain in the lumen of GI tract [33]. However, very little is known of the mechanisms of direct absorption of PAC in the small intestine. So far no transporters have been found for PAC transport through cell membranes. Deprez et al. suggest that PAC with low molecular weight may be absorbed by paracellular transport [34].

Phase II metabolism is the biochemical modification of xenobiotics by phase II enzymes, leading to glucuronidation, acetylation and sulfation reactions [32,33]. The absorbed PAC monomers are firstly subjected to phase II metabolism in enterocytes, and then in hepatocytes after they reach the liver from the portal blood stream, forming methylated, glucuronidated or sulfated conjugates [35]. These monomers and metabolites are detected in plasma and various organs; notably some of these compounds are able to pass the brain-blood barrier and accumulate in the brain [36–38]. In contrast, oligomers detected in plasma are unconjugated. Several studies have detected procyanidin dimers and trimers without conjugation or methylation in rat plasma after ingestion of PAC-rich extracts [38–40]. Unchanged dimeric procyanidins were also found in human plasma [41]. Nonetheless, Shoji et al. reported very low levels of methylated PAC dimers and trimers in rats fed apple procyanidins [40]. A few studies also demonstrate that a portion of PAC oligomers ( $DP \leq 3$ ) can be degraded into catechins internally [42,43]. Those results suggest that phase II metabolism of PAC is dependent on their structures, and the extent of metabolism needs



further characterization.

PAC monomers and oligomers that are absorbed in the small intestine account for about 30% of the ingested PAC [27,30]. The remaining PAC in the lumen (mostly polymers) will eventually move to the colon. In addition, some metabolites may be recycled back to the small intestine in the bile by hepatic elimination [44]. In the GI tract, PAC may interact with digestive enzymes, and associate with cell membrane proteins and polysaccharides, thus exerting local biological activities in the GI tract [45,46]. Upon reaching the colon, PAC become fermentable substrates for colonic microflora, and are degraded into small phenolic acids and valerolactones, which are absorbed into the circulation, subjected to hepatic phase II metabolism, and eventually excreted out of the body [47,48]. The major microbial catabolites detected in blood and urine include phenylvalerolactones, and phenylvaleric, phenylpropionic, phenylacetic, and benzoic acid derivatives [32].

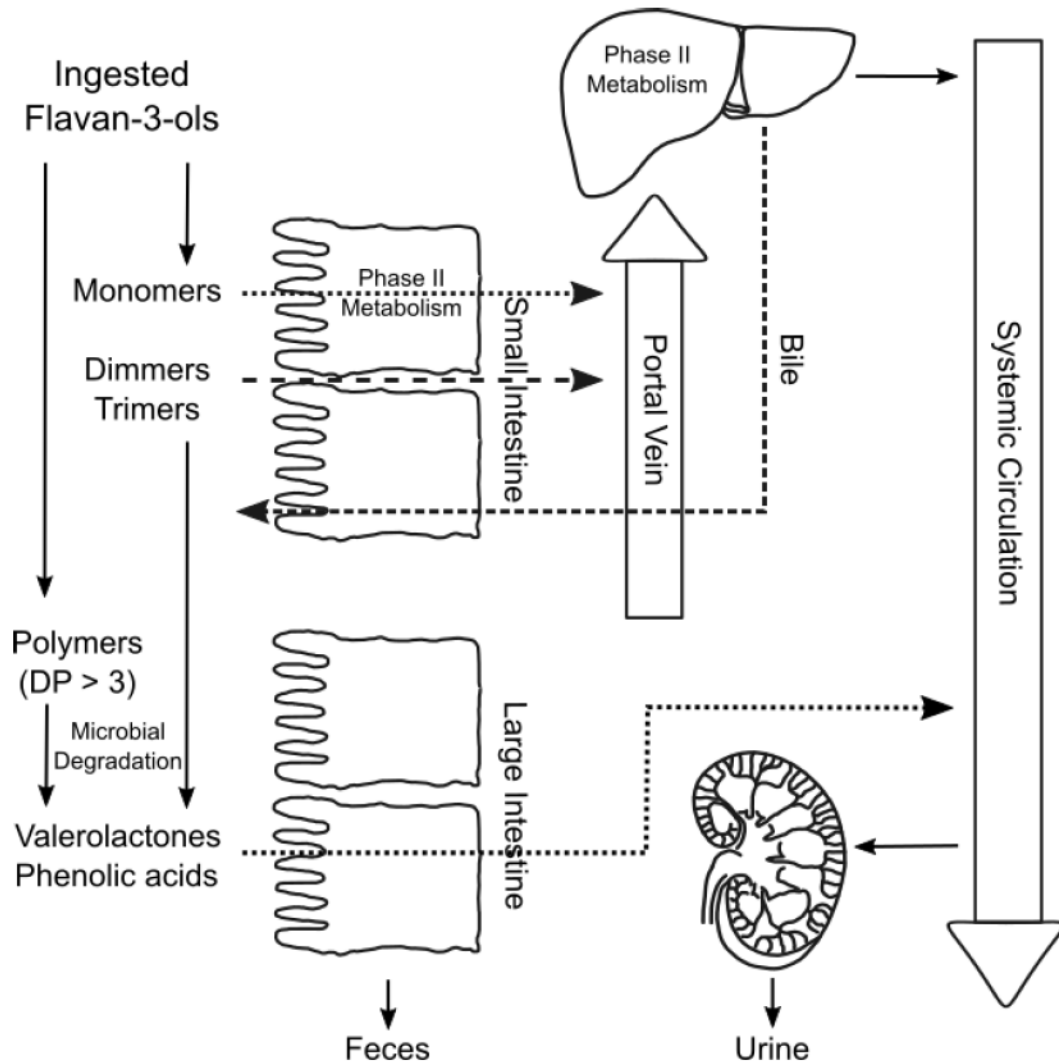


**Figure 1-2. Proposed schema of PAC absorption and metabolism in the body**

Having been ingested, flavan-3-ols with  $DP \leq 3$  can be absorbed directly and metabolized by enterocytes in the small intestine. These compounds and metabolites enter the liver through portal vein, go through phase II metabolism there, and finally enter systemic circulation, transporting to various organs. Some of the compounds in the liver may be recycled back to the small intestine in the bile. They reach the colon together with flavan-3-ols with  $DP \geq 3$ , and are degraded into valerolactones and phenolic acids by colonic microbiota. Some of those compounds can be absorbed in the colon and enter systemic circulation. In the end, all the compounds and metabolites are eliminated from the body in feces and urine. [32,33]

#### 1.1.4.2 Effects of food matrix

Food matrix is an important factor that can affect PAC bioavailability. For instance, different formulations of tea have been suggested to alter tea flavan-3-ol bioavailability. An *in vitro* study by Green et al. reports that milk (bovine, soy, rice) enhances catechin recovery when formulated with green tea [49]. However, van der Burg-Koorevaar et al. find no effect of milk on absorption of black tea catechin *in vitro* [50]. Tea flavan-3-ol bioavailability isn't affected by consuming with milk in two human studies [51,52]. These results suggest that adding milk to tea has limited impact on tea flavan-3-ol bioavailability. When green tea is formulated with ascorbic acid and citrus juice (orange, grapefruit, lemon, and lime), digestive recovery of catechins is significantly improved [49]. A study also finds that green tea extract supplementation is better absorbed compared with tea infusion [53]. In addition, food matrix composition (with bread, glucose or cheese) shows no influence on the absorption, metabolism, and excretion of flavan-3-ols [54].

Cocoa and chocolate are another important source of dietary PAC. Their food matrix composition is very likely to modulate the absorption and pharmacokinetics of flavan-3-ols. Sucrose is able to increase peak serum concentrations of catechins, whereas lipid and milk protein decrease or have minimal effect on flavanol absorption [55–61]. The physical form of cocoa and chocolate products is also considered to play a role in flavanol absorption. Ingestion of milk-containing cocoa beverages results in higher peak serum concentrations of epicatechin (EC) than chocolate confections formulated with or without milk, which may be the result of rapid emptying of beverages from the stomach [59].

Other food components could also affect the bioavailability of PAC. For example, A starch-rich meal decreases the absorption of PAC *in vitro* and *in vivo* [28]. When comparing between PAC-rich wine and juices, alcohol content has no effect on the bioavailability of

PAC in humans [62]. Nonetheless, non-extractable PAC that mainly associates with dietary fiber is fermentable by colonic microbiota, and their metabolites are bioavailable for 24 hours after ingestion [63]. What's more, it's suggested that dietary fiber may even increase the yield of PAC metabolites [64].

### **1.1.5 Health related properties of proanthocyanidins**

#### **1.1.5.1 Proanthocyanidins as antioxidants**

As mentioned above, the hydroxyl group-rich structure makes PAC a potent antioxidant. When compared to  $\alpha$ -tocopherol, PAC show similar or stronger effects on scavenging 1,1-diphenyl-2-picrylhydrazyl (DPPH) radicals and inhibition of autoxidation of linoleic acid *in vitro* [65]. They also suppress NADPH-dependent lipid peroxidation in rat liver microsomes similar to  $\alpha$ -tocopherol [65]. PAC can also protect polyunsaturated fatty acids (PUFA) in micellar systems against ultraviolet (UV) light-induced oxidation [66,67]. In these micellar systems, PAC are as effective as  $\alpha$ -tocopherol and have a role in  $\alpha$ -tocopherol recycling [67]. When supplemented with 75mg PAC for 9 weeks, an increase in superoxide dismutase (SOD) activity is found in the rat brain, together with decreases in lipid peroxidation and protein oxidation [68].

#### **1.1.5.2 Proanthocyanidins modulate bacteria in the gastrointestinal tract**

The anti-bacterial effects of PAC start in the mouth, where PAC extracts act against a Gram-negative anaerobic bacterium *Porphyromonas gingivalis*, which contributes to the progression of periodontitis [69]. PAC-rich grape seed extract is found positively responsive toward 10 different Gram-positive and Gram-negative bacteria strains [70]. Whereas in the large intestine, 3 weeks of condensed tannin (PAC) diets results in a shift in the predominant bacteria towards tannin-resistant gram-negative *Enterobacteriaceae* and *Bacteroides* species in the rat [71]. However, the extent and mechanisms of

antibacterial activity of PAC are poorly understood. It is suggested that PAC might be able to deplete iron and affect activities of key enzymes in the bacteria [72].

#### **1.1.5.3 Proanthocyanidins as anti-cancer agents**

Consideration of PAC as anti-cancer agents is based on their chemopreventive, anti-proliferative and pro-apoptotic activities [73]. PAC can neutralize carcinogenic agents in the gut to prevent cancer formation. The viability of esophageal adenocarcinoma cells is significantly reduced by procyanidins from apples, and the action is positively related with DP [74]. Pro-apoptotic activation of the androgen receptor by grape seed PAC is demonstrated in human colorectal cancer cell line and colon adenocarcinoma cells [75,76].

On the other hand, it's known that high levels of antioxidants, e.g.  $\beta$ -carotene,  $\alpha$ -tocopherol, N-acetylcysteine and flavonoids, can become prooxidants when redox-active metals (copper, iron) are available at the same time, causing deoxyribonucleic acid (DNA) damage and cell apoptosis [77,78]. Sakano et al. have demonstrated that 20  $\mu$ M of procyanidin B2 is effective in preventing DNA damage, whereas 200  $\mu$ M of procyanidin B2 together with Cu(II) induced DNA damage [79]. Similar results are reported when catechin is used to generate cellular ROS causing cell damage [80]. In addition, the level of copper in cancer cells is reported to be elevated already [81]. Therefore, in cancer cells, PAC can also act as prooxidants, mobilizing endogenous copper ions, producing reactive oxygen species to increase oxidative stress, and catalyzing DNA degradation in cancer cells, therefore exert their anticancer properties.

#### **1.1.5.4 Proanthocyanidins' anti-inflammatory effects**

Epidemiological studies show that higher intake of flavonoids is associated with lower plasma concentrations of inflammatory markers, e.g. C-reactive protein (CRP), interleukin (IL)-8 and soluble vascular cell adhesion molecule (sVCAM)-1 [82,83].

Postprandial hyperlipidaemia and hyperglycaemia following meals rich in lipids and carbohydrate induces a relative oxidative stress, which is typically accompanied by postprandial inflammation [84]. Several studies demonstrate that the phenolic compounds in fruit are bioavailable and can increase the antioxidant capacity of the plasma acutely and after long-term consumption [85–89]. Supplementation with PAC/PAC-rich extracts is demonstrated to up-regulate reduced glutathione concentration [90] and reduce plasma inflammatory markers, including CRP, monocyte chemoattractant protein (MCP)-1, IL-8, serum amyloid A (SAA), interferon (IFN)- $\alpha$  [91–93]. When PAC/PAC-rich extracts are administered to different animal models, higher antioxidant capacity in plasma, increased activity and levels of antioxidant enzymes, and decreased production of NO, malondialdehyde (MDA) and pro-inflammatory cytokines (e.g. tumor necrosis factor (TNF)- $\alpha$ , IL-6 and CRP) in plasma, pancreas, liver or adipose tissue are observed [94–101]. Mechanism studies suggest that PAC ameliorates inflammation by reducing nuclear factor kappa-light-chain-enhancer of activated B cells (NF- $\kappa$ B)-regulated transcriptional activity, and down-regulating phosphorylation of extracellular-regulated kinase 1/2 (ERK1/2) [95,102].

#### **1.1.5.5 Proanthocyanidins' preventative effects on neuro-degeneration**

There is an increasing prevalence of both Alzheimer's disease and Parkinson's disease in our aging societies. Dietary intake of flavonoid-rich foods has been associated with preservation of cognition with ageing [103], reduction of the risk for Parkinson's disease [104] and delay in the onset of Alzheimer's disease [105]. PAC may protect neurons against oxidative stress [106,107], reduce neurodegeneration during aging [108,109], and protect against A $\beta$ -induced neuronal injury [110]. By interactions with the ERK and phosphatidylinositol-3-OH kinase (PI3K)/Akt/PKB (protein kinase B, PKB, as known as Akt) signaling pathways, PAC increase the expression of neuroprotective and

neuromodulatory proteins and increase the number and strength of connections between neurons [111,112]. Moreover, several PAC metabolites have also been identified in the brain of mouse and rat following feeding with PAC-supplemented diets [110,113,114], suggesting that PAC are likely to be candidates for direct neuroprotective and neuromodulatory actions.

## **1.2 Glucose homeostasis**

### **1.2.1 Glucose uptake**

#### **1.2.1.1 The fate of glucose**

After a meal and until the storage of glycogen is depleted, glucose is the major source of fuel for the whole body except heart muscle. Under normoglycemia, plasma glucose is maintained tightly between 4 and 7 mM. This is controlled by the balance of glucose absorption from intestine, uptake and metabolism in the liver and peripheral tissues [115].

After a meal, of 100g glucose ingested, 30 g (30%) is taken up by the liver and 70 g (70%) is released into the systemic circulation. Of this 70 g, the brain uses 15 g (~20%) for energy, skeletal muscles uptake 27 g (~40%) for both energy and storage, the liver extracts another 15 g (~20%) from the circulation, kidneys uptake 8 g (~10%), 5 g (~7%) is taken up by adipose tissue, and the remainder is taken up by skin and blood cells. Glucose uptake in the liver, skeletal muscles and adipose tissue is controlled by insulin [116–118].

#### **1.2.1.2 Glucose stimulated insulin secretion from pancreatic islets**

The endocrine tissues of the pancreas are called the islets of Langerhans [119]. These micro-organs are distributed throughout the pancreas, accounting for 1-2% of the total mass of the organ. There are five main cell types in the islets, including insulin-secreting  $\beta$ -cells, glucagon-secreting  $\alpha$ -cells, somatostatin-secreting  $\delta$ -cells, pancreatic polypeptide-producing PP-cells and ghrelin-secreting  $\epsilon$ -cells. The  $\beta$ -cells are the most abundant followed by  $\alpha$ -cells, and the hormones they secrete are critical for the regulation of blood glucose homeostasis [120,121].

Insulin secretion from the  $\beta$ -cells is tightly controlled by nutrients (glucose, fatty acids, amino acids, etc.), hormones, and neurotransmitters. Under physiological conditions, the



increase in extracellular glucose concentration ( $> 4$  mM) is sensed by the low affinity, high capacity glucose transporters (GLUT1 in humans and GLUT2 in rodents) [122]. Upon entry into the pancreatic  $\beta$ -cells, glucose is phosphorylated by glucokinase and metabolized through glycolysis and the tricarboxylic acid cycle. Enhanced glucose metabolism increases the cellular adenosine triphosphate (ATP)/adenosine diphosphate (ADP) ratio, which leads to the closure of ATP-sensitive  $K^+$  channels ( $K_{ATP}$  channels) in the plasma membrane [123,124]. This depolarizes the cell membrane thus opening voltage-dependent  $Ca^{2+}$  channels. Influx of  $Ca^{2+}$  increases the intracellular  $Ca^{2+}$  concentrations, which serves as the triggering signal in glucose-induced insulin secretion [125]. The  $Ca^{2+}$  entry activates various kinases in  $\beta$ -cells, such as protein kinase A (PKA) [126],  $Ca^{2+}$ /calmodulin-dependent protein kinase II (CaMKII) [122,125] and extracellular signal-regulated kinase (ERK) 1/2 [126]. It's suggested that the activation of CaMKII plays an important role in the process of insulin secretion. CaMKII activation coincides with insulin secretion [127,128], while disruption of this kinase activation impairs  $Ca^{2+}$  entry and insulin secretion during glucose stimulation [129,130]. There also exist glucose-dependent metabolic amplifying pathways that contribute to about 50% of insulin secretion [131]. However, their molecular and cellular mechanisms have not yet been understood completely.

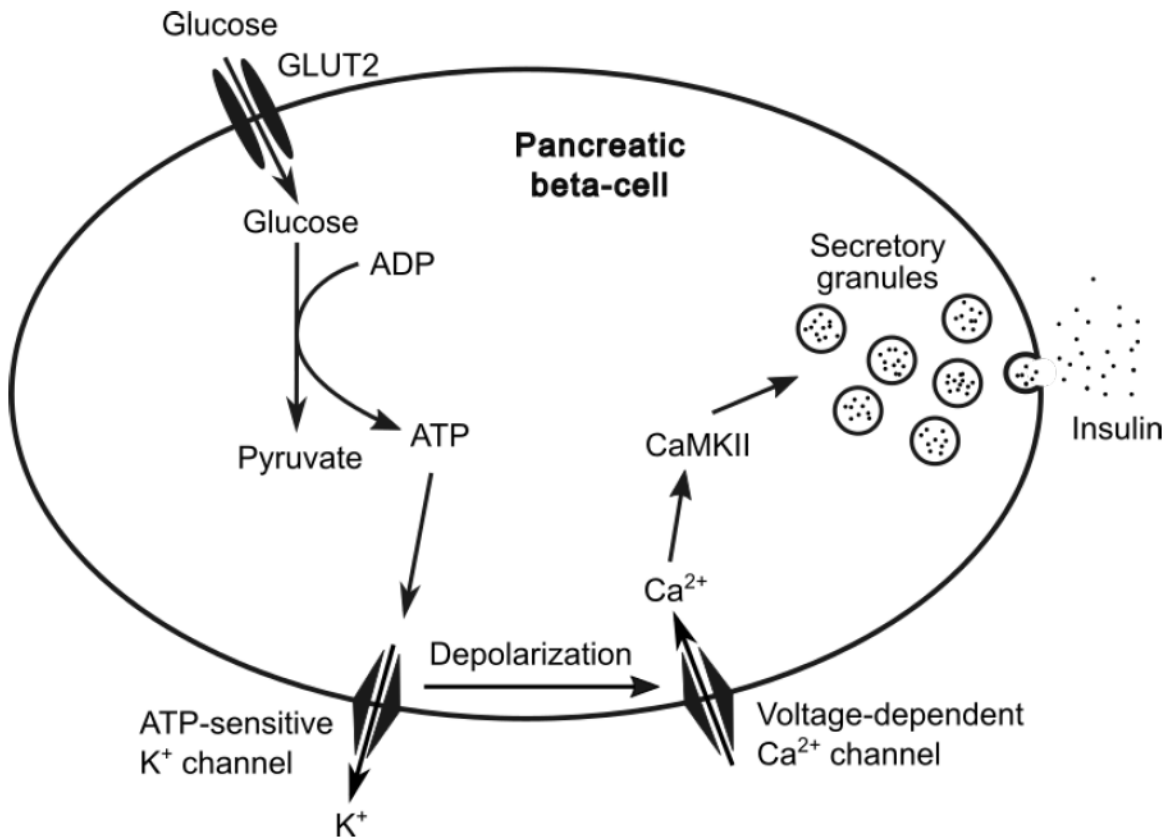


**Figure 1-3. Glucose stimulated insulin secretion from pancreatic  $\beta$ -cells**

Increase in cellular adenosine triphosphate (ATP)/adenosine diphosphate (ADP) ratio by glycolysis closes ATP-sensitive K<sup>+</sup> channels. This depolarizes the cell membrane thus opens voltage-dependent Ca<sup>2+</sup> channels. Influx of Ca<sup>2+</sup> increases the intracellular Ca<sup>2+</sup> concentrations, which activates Ca<sup>2+</sup>/calmodulin-dependent protein kinase II (CaMKII) and serves as the triggering signal in glucose-induced insulin secretion.

### 1.2.1.3 Insulin action in glucose metabolism in the liver

The liver is the central organ in the maintenance of glucose homeostasis. It can both consume and produce substantial amounts of glucose. As mentioned above, it is responsible for the disposal of about 1/3 of ingested glucose [116]. Glucose is taken up into the hepatocytes by GLUT2, which is a membrane bound transporter with a high K<sub>m</sub> for glucose [132]. Therefore hepatic glucose uptake and release is closely related with glucose

concentrations rather than insulin, however, the liver's response to hyperglycemia will be impaired when insulin is deficient [132].

As shown in Figure 1-4, in the hepatocyte, insulin binds to the extracellular  $\alpha$ -subunit of the insulin receptor and increases tyrosine kinase activity of the intracellular  $\beta$ -subunit [133]. Then insulin receptor substrate 1/2 (IRS 1/2) will be phosphorylated, which activates the PI3K catalytic subunit. Activated PI3K leads to activation of phosphoinositide-dependent kinase 1 (PDK1), one of the serine kinases that phosphorylates and activates the serine/threonine kinase Akt/PKB [115]. Akt inhibits the activity of glycogen synthase kinase-3 (GSK-3) [134]. This leads to activation of glycogen synthesis. Akt also inhibits expression of phosphoenolpyruvate carboxykinase (PEPCK) and glucose-6-phosphatase (G6Pase) thus repressing glucose production by gluconeogenesis [135]. Insulin also promotes glucose utilization and storage by stimulating the expression of enzymes for glycolysis (glucokinase), glycogenesis (glycogen synthase) and fatty acid synthesis (acetyl-coenzyme A carboxylase, ACC; fatty-acid synthase, FAS) [136].

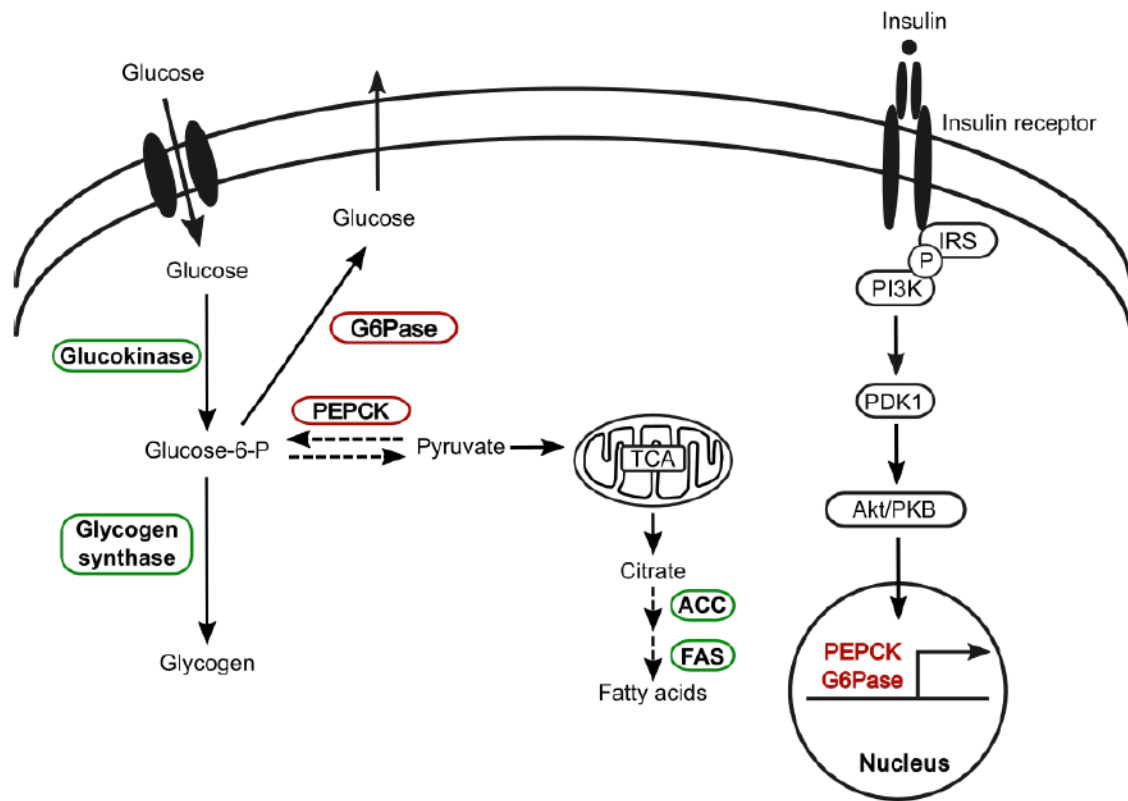


**Figure 1-4. The regulation of glucose metabolism by insulin in the liver.**

Insulin binds to insulin receptors on the membrane of hepatocytes and activates cellular signaling cascades. It stimulates the utilization and storage of glucose as lipid and glycogen, while repressing glucose synthesis and release through regulation of enzyme synthesis and activity. Insulin increases the activity of glycogen synthase, stimulates the expression of genes for glycolytic and fatty-acid synthetic enzymes (in green), while inhibiting the expression of those encoding gluconeogenic enzymes (in red). Glucose-6-P, glucose-6-phosphate; G6Pase, glucose-6-phosphatase; PEPCK, phosphoenolpyruvate carboxykinase; ACC, acetyl-coenzyme A carboxylase; FAS, fatty-acid synthase.

In the post-absorptive state, the liver contributes about 90% of endogenous glucose production, about 45% from glycogenolysis and 47-56% from gluconeogenesis [137]. During the postprandial period, the liver starts to suppress glucose production in response to increased insulin, while taking up and storing glucose as glycogen [135]. In type 2 diabetes (T2D), there is slightly elevated (~10-25%) or unchanged glucose release from the liver when blood glucose and insulin concentrations are elevated [137]. The abnormal glucose production is almost completely due to the failure of suppression of gluconeogenesis [137].

#### **1.2.1.4 Insulin action in glucose uptake and metabolism in skeletal muscle and adipose tissue**

Skeletal muscle and adipose tissue are responsible for another 1/3 of the postprandial glucose disposal, therefore are also important in reducing the glycaemic response to a meal. Insulin can upregulate glucose uptake in skeletal muscles and adipose tissue. This action begins with insulin binding to the insulin receptor on the cell membrane, which activates and autophosphorylates the tyrosine kinase domain [133]. Then the insulin receptor phosphorylates insulin receptor substrate 1 (IRS-1). IRS-1 is able to activate PI3K, which activates the serine/threonine kinase Akt/PKB. This leads to the translocation of the glucose transporter GLUT4 from intracellular sites to the cell surface, therefore increases glucose uptake [138]. On the other hand, insulin stimulates glycolysis, lipogenesis, glycogen and protein synthesis, and inhibits lipolysis, glycogenolysis and protein breakdown in muscles and fat [115].

#### **1.2.1.5 AMPK signaling pathway in glucose metabolism**

In addition to insulin signaling pathways, 5'-adenosine monophosphate (AMP) -activated protein kinase (AMPK) pathway (Figure 1-5) also plays an important role in regulating

glucose homeostasis. AMPK is a serine/threonine protein kinase that acts as a sensor of cellular energy status in all eukaryotic cells. Under metabolic stress that either reduce adenosine triphosphate (ATP) production (e.g., deprivation of glucose or oxygen) or increase ATP consumption (e.g., muscle contraction), increased cellular AMP:ATP can activate AMPK via phosphorylation at a specific threonine residue on the  $\alpha$  subunit (Thr172) by liver kinase B1 (LKB1) [139]. AMPK can also be activated by  $\text{Ca}^{2+}$ /calmodulin-dependent protein kinase kinase  $\beta$  (CaMKK  $\beta$ ) in response to elevated intracellular  $\text{Ca}^{2+}$  [140]. Activation of AMPK in general stimulates catabolic pathways that generate ATP (e.g. glucose uptake, glycolysis), while inhibiting anabolic pathways that consume ATP (e.g. synthesis of glycogen, fatty acids, cholesterol and protein) [141]. In the liver, activated AMPK suppresses glucose production from gluconeogenesis by decreasing gene transcription of PEPCK and G6Pase, meanwhile, it also inhibits the synthesis of fatty acids and cholesterol via reducing the activity of ACC and 3-hydroxy-3-methylglutaryl-coenzyme A (HMG-CoA) reductase [142,143]. AMPK also promotes fatty acid  $\beta$ -oxidation. This is a result of decreased activity of ACC, which causes a subsequent decrease in malonyl-CoA concentrations. The decreased malonyl-CoA in turn prevents inhibition of carnitine palmitoyltransferase 1 (CPT1), an enzyme responsible for importing long-chain fatty acids into mitochondria for  $\beta$ -oxidation, leading to an increase in fatty acid oxidation [140]. (Figure 1-5). In addition, AMPK activation promotes glucose uptake in muscles and adipose tissue by translocation of GLUT4 to cell membrane, as well as upregulation of GLUT4 expression [144].

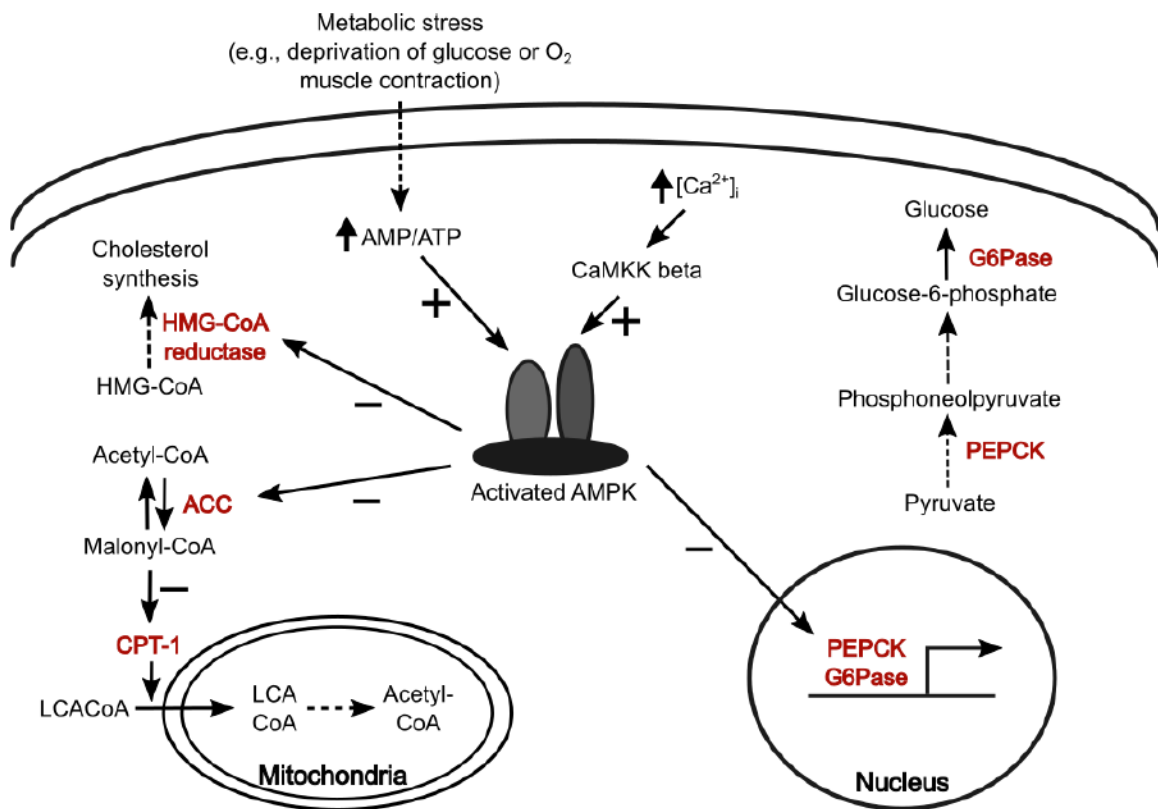


**Figure 1-5. AMPK signaling pathway in the liver.**

Increase in cellular 5'-adenosine monophosphate (AMP): adenosine triphosphate (ATP) induced by metabolic stress (e.g., deprivation of glucose or oxygen, muscle contraction) can activate AMP-activated protein kinase (AMPK) pathway. AMPK can also be activated by Ca<sup>2+</sup>/calmodulin-dependent protein kinase kinase  $\beta$  (CaMKK  $\beta$ ) in response to elevated intracellular Ca<sup>2+</sup>. Activated AMPK suppresses glucose production from gluconeogenesis by decreasing gene transcription of PEPCK and G6Pase, meanwhile, it inhibits the synthesis of fatty acids and cholesterol via reducing the activity of acetyl-coenzyme A carboxylase (ACC) and 3-hydroxy-3-methylglutaryl-coenzyme A (HMG-CoA) reductase. AMPK also promotes fatty acid  $\beta$ -oxidation. This is a result of decreased activity of ACC, which causes a subsequent decrease in malonyl-CoA concentrations. The decreased malonyl-CoA levels in turn prevent inhibition of carnitine palmitoyltransferase 1 (CPT1), leading to an increase in fatty acid oxidation. LCACoA, long-chain acyl-CoA.

### **1.2.2 Glucose output**

Sustaining blood glucose during fasting is mainly regulated by glucagon through stimulating hepatic glucose production. Glucagon is a 29-amino acid peptide hormone secreted by pancreatic  $\alpha$ -cells. Its secretion increases when circulating glucose falls below the normal range [145]. Glucagon exerts effects by binding to the glucagon receptor, which is a transmembrane G protein-coupled receptor [146]. The binding leads to the activation of the coupled G proteins,  $G_{\alpha}$  and  $G_q$ . Activated  $G_{\alpha}$  is able to increase intracellular cyclic adenosine monophosphate (cAMP) levels by activating adenylate cyclase, resulting in the activation of protein kinase A (PKA). PKA acts via the activation of glycogen phosphorylase to increase glycogenolysis, the inactivation of glycogen synthase to inhibit glycogenesis, and the upregulation the expression of phosphoenolpyruvate carboxykinase (PEPCK) to enhance gluconeogenesis. Whereas the activation of  $G_q$  leads to the activation of phospholipase C, production of inositol 1,4,5-triphosphate, and subsequent release of intracellular  $Ca^{2+}$ . All of those responses increase the release of glucose from hepatic pool into blood. [145,147]



### **1.3 Definition and pathology of prediabetes**

#### **1.3.1 Prediabetes**

Prediabetes is used to describe the state in which glucose concentrations are higher than normal, but not meeting the diagnostic criteria for diabetes. It is characterized by the World Health Organization (WHO)/International Diabetes Foundation as impaired fasting glucose (IFG), defined as a fasting plasma glucose (FPG) concentration between 6.1 and 7.0 mmol/L; with or without impaired glucose tolerance (IGT), defined as a 2-hour postload plasma glucose concentration between 7.8 and 11.1 mmol/L during a 75 g oral glucose tolerance test (OGTT) [148]. Although using the same criteria for IGT, the American Diabetes Association (ADA) applies a lower IFG (FPG 5.6–6.9 mmol/L), and recommends a glycated hemoglobin A1c (HbA1c) of 5.7-6.4% for diagnosing prediabetes [149]. People with prediabetes are at high risk of developing T2D. About 6.9% of adults worldwide are estimated to have prediabetes [150]. Among them, 5-10% become diabetic every year, with the same proportion converting back to normoglycemia, and 70% eventually develop T2D [151].

#### **1.3.2 Pathology of prediabetes**

##### **1.3.2.1 Impaired glucose metabolism**

After a meal, elevated blood insulin suppresses endogenous glucose production (EGP) and stimulates whole body glucose uptake in a healthy subject. However due to manifestation of insulin resistance (IR) in different organs, those responses are less pronounced in prediabetes and diabetes.

In T2D, IR in the liver leads to a slightly elevated (10-25%) or unchanged EGP from liver when blood glucose and insulin concentrations are elevated [137]. The abnormal glucose production is almost completely due to the failure of suppression of gluconeogenesis [137].

Meanwhile, about 85–90% of dysregulation of glucose disposal in T2D is related to skeletal muscle IR [152]. Glycogen synthesis in skeletal muscle is decreased in T2D [153]. Impaired muscle glucose transportation and phosphorylation are also present in people with IR or T2D [154,155]. Defects in IRS-1 tyrosine phosphorylation and PI3K and Akt activation are known as the underlying causes of glucose dysregulation in the liver and skeletal muscle [156,157]. As for prediabetes, subjects with IFG have hepatic IR with normal/near normal insulin sensitivity in skeletal muscle. In contrast, individuals with IGT have IR in skeletal muscle with only a modest increase in hepatic IR [158,159].

### **1.3.2.2 Impaired $\beta$ -cell function**

The dysfunction of pancreatic  $\beta$ -cells is responsible for the progression from prediabetes to T2D. With T2D onset, there is already a ~50% decrease in  $\beta$ -cell mass [160] and apparent  $\beta$ -cell dysfunction in humans [161]. Under the prediabetic state,  $\beta$ -cell function decreases corresponding to the increase in FPG, which is similar to the changes in peripheral and hepatic insulin sensitivity [162]. Subjects with IFG and/or IGT have a decrease in  $\beta$ -cell glucose sensitivity [163]. First-phase insulin secretion is deficient in both IFG and IGT, whereas second-phase insulin secretion is impaired in IGT only [158,163–166].

## **1.4 The effects and proposed mechanisms of proanthocyanidins on glucose homeostasis**

### **1.4.1 Proanthocyanidins' effects on glucose homeostasis**

Foods rich in PAC or their derivatives are reported to be beneficial for T2D. Results from cohort studies in the US suggest that higher intake of anthocyanins and anthocyanin-rich fruit is significantly associated with a lower risk of T2D [24]. Tea (rich in catechins) consumption is inversely associated with the incidence of T2D in a European population [167]. Findings from a meta-analysis confirm an inverse association between consumption of coffee, decaffeinated coffee and tea and subsequent risk of T2D [168]. Although those epidemiological studies cannot provide causative evidence, they are useful in generating hypotheses about PAC's effects on glucose homeostasis, which would encourage human and in vivo/vitro studies to elucidate the relationship between PAC and glucose homeostasis. However, caution is warranted in interpreting findings from different epidemiological studies. Firstly, they are based on dietary intake assessment using self-report and although validated nutrient databases are used, many food items with PAC may not be included or clearly distinguished in the databases, e.g. herb teas versus tea leaves, red versus white wines, different berries. This may also explain the variations in PAC intake found in various studies. A comprehensive database is needed to estimate the content of PAC in foods, especially those with different cultivars, growing conditions and post-harvest processing. The frequently used USDA database for the PAC content of selected foods is the most up-to-date database, yet continuous efforts are needed to refine quantitation of the PAC content of foods.

A number of PAC-rich foods were tested in clinical trials for their effects on glucose regulation. Consumption of berries rich in polyphenols can improve postprandial glycemic control after sucrose ingestion, and moderately increase plasma glucagon-like

peptide (GLP)-1 in healthy subjects [169,170]. Improvement in insulin sensitivity and lowered fasting blood glucose are observed in randomized controlled clinical trials that evaluated the therapeutic potential of cinnamon amongst healthy and T2D subjects [171–173]. Black tea is effective in reducing late phase of postprandial glycemia when consumed at a dose of 1 cup/day (1g of dry tea) [174]. Grape seed procyanidins (GSP; 100, 300 mg) supplementation is able to reduce postprandial glucose at 15 and 30 min compare to a high-carbohydrate diet alone in healthy subjects [175]. In hypertensive patients with impaired glucose tolerance, adding a 100g dark chocolate bar to the diet leads to improved insulin sensitivity and  $\beta$ -cell function [176]. T2D patients treated with Pycnogenol® (PAC-rich pine bark extract) together with their medications have significantly reduced fasting glucose and HbA<sub>1c</sub> [177,178].

The clinical trials mentioned above (summarized in Table 2) reflect the potential action of PAC and PAC-rich foods on glucose homeostasis. For example, postprandial glycemia, fasting glucose and insulin sensitivity can be affected in response to PAC intake.

Furthermore, they provide valuable information on the doses of PAC that can be tolerated by people, which is also useful as a reference in mechanistic studies *in vivo* and *in vitro*. Nonetheless, it should also be noticed that none of the cited studies measure PAC-derived biomarkers in plasma or urine, therefore the exposure of subjects to PAC is unknown. There is limited information on the bioavailability and metabolism of PAC, even though several metabolites have been suggested as biomarkers of PAC intake recently [32,33]. Further validation of PAC biomarkers and pharmacokinetics is needed to illustrate the PAC exposure of subjects, as the amount and rate of absorption of PAC from different food matrices may be as or more important than the quantity consumed. In addition, knowing inter-individual differences in PAC bioavailability and biotransformation is important in interpreting results from human studies, especially

those with limited subject number. Besides, differences in sources and doses of PAC can also contribute to the variance in the results seen among those studies. Therefore, to improve our understanding of PAC influence on glucose homeostasis it will be necessary to standardize PAC intake in different studies using validated PAC biomarkers or other indicators.

**Table 1-2. Summary of studies on PAC effects on glucose homeostasis in humans.**

Source	Daily dose	Duration	Characteristics of participants	N	Beneficial effects	Reference
Black tea (39.0 mg/g flavan-3-ols)	1g in 250mL water	OGTT after single dose on 4 separate days	Healthy (12 female, 4 male) Age: 35.5 ± 1.5 yr BMI: 23.8 ± 0.7 kg/m <sup>2</sup>	16	↓ plasma glucose at 120min ↑ plasma insulin at 90 and 150min	[174]
Berries	150g mixed berry purée	OGTT after single dose	Healthy (11 female, 1 male) Age: 54.2 yr BMI: 25.4 kg/m <sup>2</sup>	12	↓ plasma glucose at 15 and 30min	[170]
Berries	150g mixed berry purée	OGTT after single dose	Healthy (10 female, 2 male) Age: 58 yr BMI: 24.3 kg/m <sup>2</sup>	12	Plasma glucose ↓ at 15min and ↑ at 90min Plasma insulin ↓ at 15min and ↑ at 90 and 120min ↑ GLP-1 AUC	[169]
Berries	150g mixed berry purée	OGTT after single dose	Healthy females Age: 52.3 yr BMI: 24.2 kg/m <sup>2</sup>	48	Plasma insulin ↓ at 15, 30min and ↑ at 120min, ↓ insulin AUC modest reduction of 0-30min glucose	[179]
GSP	100, 300mg	OGTT after single dose	Healthy (5 female, 4 male) Age: 21.25 ± 3.69 yr BMI: 20.28 ± 1.40 kg/m <sup>2</sup>	9	↓ plasma glucose at 15, 30min ↑ glucose AUC	[175]
Cinnamon	6g in a 330kcal meal	OGTT after single dose	Healthy (6 female, 8 male) Age: 25.6 ± 4.8 yr BMI: 22.6 ± 2.2 kg/m <sup>2</sup>	14	↓ plasma glucose at 15, 30 and 45min	[171]
Cinnamon	1, 3g in a 330kcal meal	OGTT after single dose	Healthy (6 female, 9 male) Age: 24.6 ± 1.9 yr BMI: 22.5 ± 2.7 kg/m <sup>2</sup>	15	No effects on glucose, GIP and ghrelin 3g cinnamon: ↓ plasma insulin at 60min and AUC (0-120min) ↑ GLP-1	[172]
Cinnamon	1, 3, 6g	40 days intervention 20 days washout	T2D (30 female, 30 male) Age: 52.0 ± 6.32 yr	60	↓ FPG 1g cinnamon: ↓ FPG after 20-day washout	[173]
Pycnogenol® (pine bark extract)	100mg	12 weeks	T2D (33 female, 44 male) Age: 56 yr	77	↓ FPG ↓ HbA <sub>1c</sub>	[178]

Pycnogenol® (pine bark extract)	50, 100, 200, 300mg	12 weeks (each dose for 3 weeks)	T2D (12 female, 18 male) Age: 28–64 yr BMI: 22–34 kg/m <sup>2</sup>	30	↓ FPG dose dependently (300mg has no stronger effect) ↓ HbA <sub>1c</sub> at 9 and 12 weeks	[177]
Dark chocolate bar	100g	15 days	Hypertensive patient with IGT (8 female, 11 male) Age: 44.8 ± 8.0 yr BMI: 26.5 ± 1.9 kg/m <sup>2</sup>	19	↓ insulin resistance (HOMA-IR) ↑ insulin sensitivity (QUICKI, ISI and ISI <sub>0</sub> ) ↑ β-cell function (CIR <sub>120</sub> )	[176]

## **1.4.2 Proposed mechanisms**

### **1.4.2.1 Modulation of hepatic glucose output**

The liver is one of two major sites (the other is enterocytes) for PAC metabolism in the body. Most of PAC absorbed will first be processed in the liver, and then enter the systemic circulation [33]. Therefore, it's likely that hepatocytes can be affected by PAC.

Administration of 80 mg/kg GSP in high fat diet (HFD)-fed mice for 6 weeks raises hepatic glucokinase activity when compared with control mice fed HFD [180]. Insulin resistant HepG2 cell glucose uptake is increased compared with control when treated with 6.25 µg/mL GSP [180]. Of great interest, hepatic AMPK is activated by several natural compounds, including PAC [181] and epigallocatechin gallate (EGCG) [182]. Activation of AMPK and suppression of gluconeogenesis are found in diabetic mice fed a 22.0 g/kg black soybean seed coat extract (rich in anthocyanins and procyanidins) [181] or a 27 g/kg anthocyanin-rich bilberry extract [183]. An *in vitro* study using HepG2 cells found that EGCG at 1 µM is effective in suppressing hepatic gluconeogenesis, by activating AMPK through Ca<sup>2+</sup>/calmodulin-dependent protein kinase kinase (CaMKK), without affecting insulin signaling pathway [184]. In contrast, when treating HepG2 cells with cocoa extract (10 µg/mL), or (-)-epicatechin (EC, 5 or 10 µM), insulin signaling via PI3K/AKT pathway is activated, in addition to AMPK pathway [185] consistent with an *in vivo* study, in which GSP (100 mg/kg) activates PI3K/AKT pathway in high fat-fructose diet-fed Wistar rats [186].

### **1.4.2.2 Effects on pancreatic β-cell functions**

#### **1.4.2.2.1 Alleviation of oxidative stress**



Due to its well-known antioxidant properties, PAC's protective effects against oxidative insults in pancreatic  $\beta$ -cells are extensively studied. GSP is effective in ameliorating the damage to pancreatic islets induced by low-dose streptozotocin (STZ) and high-carbohydrate/high-fat diet [187], STZ alone [187] and alloxan [101]. Some endoplasmic reticulum (ER) stress markers are downregulated by GSP [187]. GSP treatment increases pancreatic glutathione levels [101], inhibits lipid peroxidation [101,188], and decreases nitrite content in  $\beta$ -cells [101,188]. EC is also able to promote pancreatic  $\beta$ -cell regeneration in response to STZ or alloxan insults [100,189]. There is a dose-response of EC in decreasing nitrite content in STZ-treated islets [100]. Pretreatment of cells with EC prevents oxidative stress induced by tert-butylhydroperoxide (t-BOOH) in INS-1E  $\beta$ -cells [190].

#### **1.4.2.2.2 Regulation of insulin secretion**

PAC and EC can preserve insulin secretion by protecting pancreatic  $\beta$ -cells from oxidative stress as mentioned above. In addition, PAC and EC are considered to be insulin secretagogues in  $\beta$ -cell lines [191,192]. When fed to healthy rats or applied to normal isolated islets, EC enhances glucose stimulated insulin secretion (GSIS) [193]. PAC's ability to stimulate insulin secretion appears to depend on the number of hydroxyl groups in B ring of the compounds [194]. A PAC-rich cranberry supplement reverses the aging-induced reduction in plasma insulin concentrations in rats [195]. In addition, cranberry increases insulin release from INS-1 cells [195]. Another study testing various doses and durations of EC treatment finds that, in healthy rats, low-dose treatment with GSP (5 mg/kg for 21 days; 15 mg/kg for 36 days) increases plasma insulin, whereas a high dose (25 mg/kg for 36 days) decreases it [196]. In addition, after 45-day treatment with 25 mg/kg GSP, isolated rat islets show limited insulin secretion [196]. There is downregulation of insulin gene expression, insulin synthesis and expression of genes

related to insulin secretion [196]. A proteomic profile study using Zucker fatty rats treated 2 months with 35 mg/kg GSP identifies downregulation of protein and gene expression involved in insulin synthesis and secretion [197].

#### **1.4.2.2.3 Effects on $\beta$ -cell survival and proliferation**

When  $\beta$ -cells are under stress induced by oxidative reagents or aging, PAC and EC are able to reduce reactive oxygen/nitrogen species and promote  $\beta$ -cell proliferation and regeneration. GSP increases cell viability in the presence of STZ [198]. As an indicator of apoptosis, terminal deoxynucleotidyl transferase 2'-deoxyuridine 5'-triphosphate (dUTP) nick end labeling (TUNEL) staining within pancreatic islets is reduced by PAC administration in diabetic animals [187,198]. STZ-induced pancreatic  $\beta$ -cell loss recovers to 60% of control with EC treatment [100]. A study by Fernández-Millán et al. [199] shows that catechin-rich cocoa feeding is effective in protecting  $\beta$ -cell mass and function in obese Zucker diabetic rats. In addition, EC increases total DNA synthesis in healthy islets[193]. On the contrary, another group reports a decrease in antiproliferation gene expression in INS-1E cells treated with GSP (25 mg/L for 24 hours) [200].

**Table 1-3. Summary of studies on PAC effects *in vivo* and *in vitro*.**

Extract	Dose	Duration	Model	Oxidative stress	Glucose	Insulin	$\beta$ -cell	Reference
Urticaceae extract	10, 50, 100, 250 $\mu$ g/mL	1 hour	STZ-treated	RINm5F cells		$\uparrow$ GSIS		[198]
				Islets from healthy BALB/c mice	$\downarrow$ ROS $\downarrow$ peroxynitrite and NO $\downarrow$ lipid peroxidation		$\uparrow$ GSIS	
Cranberry powder	100, 250, 500 mg/kg	28 days	BALB/c mice		$\downarrow$ FPG	$\uparrow$ FPI	$\uparrow$ islet integrity $\downarrow$ apoptotic cells in islets	[195]
				Male Fisher rats	No changes in glucose	$\uparrow$ FPI $\uparrow$ OGTT insulin peak	$\uparrow$ $\beta$ -cell mass and PDX-1	
GSP	2% (w/w) of food	6-22 months	Healthy			$\uparrow$ GSIS		[187]
				INS-1 cells				
GSP	125, 250, 500 mg/kg	16 weeks	Low-dose STZ; High-CHO /high-fat diet		$\downarrow$ FPG $\downarrow$ OGTT glucose at 30min (dose 250 and 500)	$\uparrow$ insulin content in islets	$\uparrow$ HOMA- $\beta$ $\downarrow$ apoptotic cells within islets	[101]
				Male Sprague-Dawley rats	$\downarrow$ ER stress markers			
GSP	50, 100 mg/kg	24, 48, 72 hours	Alloxan-treated		$\downarrow$ FPG (dose 100 after 48h and both dose after 72h)	$\uparrow$ FPI (dose 100 after 72h)		[196]
				Male Wistar rats	$\uparrow$ glutathione (GSH) $\downarrow$ lipid peroxidation $\downarrow$ nitrate/nitrite			
GSP	25 mg/L	24 hours	Healthy			$\downarrow$ GSIS; $\uparrow$ insulin content		[196]
				INS-1 cells				
				Female Wistar rats		$\downarrow$ FPI		
						$\uparrow$ FPI		

GSP	25 mg/L	24 hours	Healthy	INS-1 cells						↑ proapoptotic and antiproliferation effects ↓ expression of proteins for insulin synthesis and secretion ↓ expression of antiapoptotic proteins	[200]
GSP	35 mg/kg	2 months	Diabetic	Female Zucker fatty rats	↓ expression of ER chaperones	No changes	No changes				[197]
Epicatechin	30 mg/kg	5 days, twice daily	Alloxan-treated	Albino rats		↓ FPG		↑ FPI		regeneration of β-cell	[189]
Epicatechin	30 mg/kg	6 days	STZ-treated	Male Sprague-Dawley (SD) rats		↓ OGTT glucose		↑ FPI to 50% of normal		↑ β-cell mass to 60% of normal	[100]
	0.8 mM	1 hour		Islets from healthy SD rats	↓ nitrite content			↑ GSIS to normal			
Cocoa epicatechin	5, 10, 20 μM	20 hours	t-BOOH treated	INS-1E cells	↑ GSH ↓ ROS			↑ GSIS to normal		↑ cell viability ↓ p-JNK	[190]
Epicatechin	200, 400, 600, 800, 1000 μM	incubation for 1 hour; perfusion for 30 min	Healthy	Islets from male WAG rats				↑ GSIS dose dependently (significant difference at 1000)		No structural change in islets after exposed to EC for 5 days; ↑ total DNA synthesis after 4 days in dose 500	[193]
	30 mg/kg	4 days, twice daily		Male WAG rats				↑ GSIS and insulin content by 30%			

Synthesized epicatechin	20, 40, 100, 200 $\mu$ M	1 hour	Healthy	MIN6 cells			$\uparrow$ GSIS	[192]
-------------------------	--------------------------	--------	---------	------------	--	--	-----------------	-------

### **1.4.2.3 An analysis of mechanistic studies in $\beta$ -cells: doses, models, and compound sources**

As discussed in above, human dietary intake of total PAC is estimated to be around 100-200 mg/d. The average body weight of an adult is about 62 kg [201]. Therefore, the estimated intake of PAC in humans is about 1.6 – 3.2 mg/kg/d. In human clinical trials, 300 mg of GSP (95% PAC w/w) has been used to study the acute effect on postprandial glucose [175]. Whereas 150 g berry purée equals approximately 200 – 996 mg of PAC [25]. Taking into account the average adult body weight, the intake is 3.4 – 16 mg/kg. As summarized in Table 3, most doses adopted in animal feeding trials are exceeding a reasonable human intake. Only Castell-Auví et al. tested the effects of 5 and 15 mg/kg of GSP in healthy Wistar rats. Even with lower doses compared to other studies, increases in fasting plasma insulin are found in both dose groups [196].

Supplementation of rat chow with 2% (w/w) cranberry powder, which equals ~26mg/kg intake [25], leads to improved fasting plasma insulin and  $\beta$ -cell mass in aged rats [195]. However, 25 or 50 mg/kg dose of GSP fails to enhance fasting insulin in healthy rats while lower doses (5 and 15 mg/kg) are effective [196]. In addition, after treating Zucker fatty rats with 35 mg/kg GSP for 2 months, no improvements are detected in glycemic control, whereas proteins for antiapoptosis and insulin synthesis and secretion are downregulated [197]. These findings suggest that a moderate dose of PAC may be beneficial when there is modest glucose dysregulation present. In contrast, 30 mg/kg EC can enhance insulin secretion in both healthy and STZ/alloxan treated rats [100,189,193]. Higher concentrations (50 – 500 mg/kg) of PAC seem to be effective in improving glucose and insulin profiles in rats with more severe STZ/alloxan induced diabetes [101,187,198].

In pancreatic islets and  $\beta$ -cell lines, a wide range of concentrations of PAC and EC are used: PAC, 10 – 500  $\mu$ g/mL; EC, 5 – 1000  $\mu$ M. Despite the differences in the experimental settings,

all EC concentrations tested enhance GSIS from islets and  $\beta$ -cell lines to some extent, whereas PAC effects are inconsistent. Urticaceae extract (10, 50, 100, 250  $\mu\text{g}/\text{mL}$  for 1 hour) increases insulin secretion from STZ-treated RINm5F cells and mouse islets at high glucose [198], and cranberry powder (250, 500  $\mu\text{g}/\text{mL}$  for 72 hours) enhances insulin secretion from healthy INS-1 cells [195]. However 25  $\mu\text{g}/\text{mL}$  GSP application doesn't improve GSIS from healthy INS-1 cells after 24 hours treatment [196], and increases in proapoptotic and antiproliferation effects of PAC are reported by Cedó et al. [200]. One of the reasons for the variance in PAC effects may be that the sources and purity of PAC-rich extracts are different among those studies. The GSP used by Cedó et al. is a highly pure mixture of PAC (monomeric (21.3%), dimeric (17.4%), trimeric (16.3%), tetrameric (13.3%), and oligomeric (5–13 U; 31.7%) procyanidins). However the exact compositions of Urticaceae extract and cranberry powder are not reported by the authors. It's possible that those two extracts are not as pure as GSP, so the actual amount of PAC applied to cells are even lower. What's more, the beneficial effects of other existing compounds in Urticaceae extract and cranberry powder cannot be ruled out either.

Recently, a few *in vitro* studies suggest a role of bacterially-derived phenolic metabolites of PAC in protecting pancreatic  $\beta$ -cells. One of them, caffeic acid (1  $\mu\text{M}$ ) is reported to enhance GSIS in INS-1E cells after a 1-hour treatment [202], whereas a 72-hour treatment affect the expression of genes that involved in  $\beta$ -cell stress, survival and function, e.g. *Ins1*, *Pdx1*, *Casp3*, *Bcl2* [202]. 3,4-dihydroxyphenylacetic acid (DHPAA, 5  $\mu\text{M}$ ) and 3-hydroxyphenylpropionic acid (HPPA, 1  $\mu\text{M}$ ) are also effective in potentiation glucose-stimulated insulin secretion (GSIS) in INS-1E cells and isolated rat pancreatic islets after 20 hours' treatment [203]. Besides, pretreatment with DHPAA and HPPA is able to protect INS-1E cells from oxidative damages [203].

In summary, PAC may be able to improve a disrupted glucose homeostatic state, whereas monomeric EC's beneficial effects are more pronounced in both normal and dysregulated glycemia. It's important to clarify the amount of components of PAC-rich extracts to

understand the exact effects of PAC itself. The state of glucose homeostasis disturbance to be used in investigating PAC's effects is another question worth consideration. Besides, challenges remain in understanding the metabolism of PAC and differentiation of the effects of different compounds.



## Chapter 2

### Study Rationale, Hypotheses and Objectives

#### 2.1 Rationale

As reviewed in section 1.4 in Chapter 1, proanthocyanidins (PAC) have been shown to exert compelling effects in maintaining glucose homeostasis. Epidemiological studies have suggested a positive correlation between PAC-rich food consumption and reduced risk of type 2 diabetes (section 1.4.1). Existing clinical trials also support the favorable role of PAC intake with glycemic control (section 1.4.1), despite the limitations in sample size and treatment duration. The mechanistic studies using animal models and cell lines suggest several possible mechanisms of PAC's effects on glucose modulation, however, these studies fail to consider PAC's bioavailability. For bioactive compounds to exert a biological effect *in vivo*, an appropriate amount at target tissues is crucial. Although PAC exists ubiquitously in the food items, the bioavailability of PAC is limited. It's estimated that about 70% of PAC consumed has a degree of polymerization (DP) > 3 [16], which makes direct absorption in the small intestine not possible due to the polymeric structure [33]. Although the polymeric PAC will become bioavailable after microbial degradation in the colon in forms of phenolic acids [32], the effects of these compounds might be quite different from their parent compounds. Besides, regarding the dosages adopted in these mechanistic studies, although a high dose may lead to better effects, PAC's limited bioavailability may impose an upper limit on efficacy. Thus, to better understand the effects of PAC related with their DP, we compare between PAC with reduced DP by acid hydrolysis (HPAC) and native PAC. In this way, we are able to differentiate the effects of PAC regarding the bioavailability. In addition, we use a PAC-rich pea seed coat (PSC) as the source of PAC in current study. This pea cultivar 'Solido' is an Alberta-grown crop that used mainly for producing pea butter. The seed coats are by-products containing high concentrations of PAC

( $264.1 \pm 14.6$  mg/100 g dry weight of PSC [204]). In comparison with the existing PAC products available in the market, the 'Solido' PSC could provide a low cost source of PAC. The PAC-rich PSCs are prepared and supplemented to a high fat diet in a way to ensure tolerable fiber content, therefore the amount of PAC in the diets are nutritionally and physiologically relevant.

## **2.2 Overall hypothesis**

The overall hypothesis of this project is that hydrolysis of PAC leads to improved bioavailability thus enhancing benefits on glucose homeostasis.

## **2.3 Specific hypothesis and objectives**

### **2.3.1 Bioavailability of PAC and HPAC and effects on pancreatic islet function (Chapter 3)**

The hypotheses are:

- 1) Hydrolysis will depolymerize PAC and increase its bioavailability;
- 2) Hydrolyzed PAC (HPAC) will be more effective in improving insulin sensitivity in glucose-intolerant rats compared with PAC;
- 3) HPAC will be more effective in reversing HFD-induced impairments in pancreatic islets compared with PAC.

To address these hypotheses, the objectives are:

- 1) To measure and compare the bioavailability of PAC and HPAC;
- 2) To assess and compare the effects of PAC and HPAC on glucose tolerance and insulin sensitivity;
- 3) To evaluate and compare the morphology and function of pancreatic islets from PAC and HPAC.

### **2.3.2 Effects of PAC-derived compounds, epicatechin (EC) on insulin secreting INS-1 cell lines (Chapter 4)**

The hypotheses are:

- 1) EC at a physiological relevant concentration (0.3  $\mu\text{M}$ ) will enhance insulin secretion from INS-1 cells via modulating CaMKII as a cellular signaling molecule;
- 2) EC at a high concentration (30  $\mu\text{M}$ ) will protect against oxidative stress in INS-1 cells as an antioxidant and improve cell viability.

To address these hypotheses, the objectives are:

- 1) To evaluate cell viability in INS-1 cells treated with 0.3  $\mu\text{M}$  and 30  $\mu\text{M}$  EC;
- 2) To assess GSIS and CaMKII pathway activation in INS-1 cells treated with EC;
- 3) To determine the effects of EC at 0.3  $\mu\text{M}$  and 30  $\mu\text{M}$  on elevated reactive oxygen species (ROS) induced by high glucose and  $\text{H}_2\text{O}_2$ .

### **2.3.3 Effects of PAC and HPAC on hepatic glucose metabolism (Chapter 5)**

The hypotheses are:

- 1) HPAC will be more effective in suppressing hepatic glucose production (HGP) compared with PAC;
- 2) HPAC suppresses HGP by activation of AMPK or Akt signaling pathways to reduce PEPCK content, a key rate-limiting enzyme in gluconeogenesis;
- 3) HPAC will have improved hepatic function compared with PAC.

To address these hypotheses, the objectives are:

- 1) To measure and compare the effects of PAC and HPAC on HGP;
- 2) To determine and compare the content of key enzymes involved in modulation of HGP in livers from PAC and HPAC;

3) To assess and compare markers for liver function related to HGP in PAC and HPAC livers.

## Chapter 3

### Hydrolysis enhances bioavailability of proanthocyanidin-derived metabolites and improves $\beta$ -cell function in glucose intolerant rats

#### 3.1 Introduction

Plant-based foods provide a significant amount of phytochemicals in our diet. Phytochemicals are non-nutrient compounds that have biological activity in the body [205]. Among them, flavonoids have been extensively studied because they exhibit a variety of physiological effects [1]. A subgroup of flavonoids, proanthocyanidins (PAC, or condensed tannins) are the oligomers and polymers of flavan-3-ols [26]. They exist in a variety of foods such as peas, beans, nuts, spices, fruits, wine and tea, and contribute the most to total flavonoid intake in the diet [206]. The estimated average dietary intake of PAC varies from 95 – 227 mg/d in different populations [18–20,23,24].

The availability of the phenolic hydrogens as hydrogen-donating radical scavengers and singlet oxygen quenchers predicts PAC antioxidant activity [207,208]. PAC as well as their monomeric flavan-3-ol subunits and hydrolysis-derived anthocyanin products can scavenge free radicals and reactive oxygen species (ROS) such as hydroxyl and peroxy radicals [207,208], which play a significant role in inducing oxidative stress [209]; hence, research has been focused on their effects on alleviating oxidative stress.

Evidence is emerging to support that consumption of PAC-rich foods improves glycemic control. Black tea [174] and berries [169] reduced postprandial glycemia and moderately increased plasma glucagon-like peptide-1 in healthy subjects. Improvement in insulin sensitivity and lowered fasting blood glucose were observed in randomized clinical trials that evaluated the therapeutic potential of cinnamon amongst diabetic and insulin-resistant patients [210].

Animal studies suggest that PAC may exert effects on the endocrine pancreas. Grape seed PAC extracts alleviated oxidative stress in alloxan-induced diabetic rats by increasing pancreatic glutathione concentrations and reducing lipid peroxidation [101]. Green tea epicatechin preserved pancreatic islet morphology and function against streptozotocin (STZ) toxicity both *in vivo* and *in vitro* [100]. Grape seed PAC extracts favorably modulated proteins involved in insulin synthesis and secretion [197]. PAC also prevented  $\beta$ -cell loss caused by aging and apoptosis [187,195,197].

Thus, findings from studies both *in vivo* and *in vitro* indicate PAC's physiological role in modulating glucose homeostasis in the body, potentially by acting on cell signalling pathways to improve pancreatic  $\beta$ -cell function. However, plant-derived PAC are polymeric structures with a wide degree of polymerization (DP) range; therefore, the absorption and bioavailability of native PAC is limited [5]. Many *in vitro* mechanistic studies tested PAC concentrations not relevant to dietary intake and absorption, whereas the amount of PAC absorbed into the body was not quantified in most *in vivo* studies. Other obstacles included lack of knowledge of the metabolism of PAC in humans, lack of biomarkers specific for PAC intake and insufficiently sensitive analytical methods for PAC and metabolites. The existing bioavailability studies only detect trace amounts of PAC with  $DP \leq 3$ , usually pmol/L or nmol/L, in the urine and plasma [27,29,211,212]. This concentration range of PAC is not likely to have antioxidant actions in the body [213]. To confirm the physiological roles of PAC, it is important to consider the bioavailability of those compounds when evaluating their effects.

PAC-rich PSC were tested in our previous studies [214]. Compared to PSC with minimal to not detectable PAC content, additional benefits of PAC on glucose homeostasis were marginal, which may have been due to the limited absorption and bioavailability of PAC polymers. Since the interflavan linkages of PACs can be cleaved upon acid hydrolysis producing flavan-3-ol (from PAC terminal units) and anthocyanin monomers (from the PAC extension units) [215], we

prepared an acid-hydrolyzed PAC seed coat fraction to reduce the polymeric nature of PAC. In the present study, we used the seed coats of the pea (*Pisum sativum*) cultivar 'Solido', a marrowfat-type field pea with brown seed coats containing primarily prodelphinidin-type PAC with B-type PAC linkages and a mean DP of 5 [204]. Our aim was to compare the bioavailability and effects of both PAC and hydrolyzed PAC (HPAC) PSC fractions on glucose homeostasis in rats. We hypothesized that the hydrolyzed PAC (HPAC) fraction would have enhanced bioavailability and therefore better effects on glycemic control.

## **3.2 Methods**

### **3.2.1 Chemicals and reagents**

(-)-Epicatechin (purity  $\geq$  98%) and (-)-gallocatechin (purity  $\geq$  98%) were purchased from Sigma-Aldrich Co. LLC. (Oakville, ON, Canada). Delphinidin chloride (purity  $\geq$  97%) was purchased from Extrasynthese (Genay Cedex, France). All other HPLC solvents and reagents were purchased from Sigma-Aldrich Co. LLC. (Markham, ON, Canada) and were of high performance liquid chromatography (HPLC) grade.

### **3.2.2 Preparation of pea seed coat diets**

Seed coats of pea (*Pisum sativum* L.) cultivar 'Solido' were obtained from Mountain Meadows Food Processing Ltd. (Legal, Alberta). The smaller seed fragments were removed from the bulk PSC sample using a 1.0 mm screen (Canadian Standard sieve series #18, W.S. Tyler Co. of Canada, St. Catherines, ON). The cleaned PSC were then ground into a powder using a standard electric coffee grinder for rat feeding studies. A portion of the ground samples were used unprocessed (PAC fraction) and a portion was subjected to acid hydrolysis (HPAC fraction). For acid hydrolysis, a 2N HCl solution (1L total volume consisting of 170 mL food grade HCl, 330 mL deionized water and 500 mL ethanol) was added to ~200 g of ground 'Solido' PSC, making a slurry. Acid hydrolysis was performed by placing the PSC slurry into a 100°C water bath for 1 h (from the time the slurry came to a boil). After 1 h of slurry boiling, the mixture was cooled down to approximately room temperature using an ice bath. Saturated NaOH solution (approximately 78 g NaOH) was slowly added into the slurry to neutralize the excess HCl. After neutralization, the PSC slurry was lyophilized using a freeze dryer. PAC and HPAC fractions were added to a high fat diet (Table 3-1) such that the final concentration of both was 0.8% (w/w). A preliminary trial indicated that 1.6% (w/w) of PAC or HPAC did not have superior effects to 0.8% (w/w). Since the fractions also contained fibre and protein (Table 3-1), the diets were adjusted to ensure that they were isonitrogenous and equal in fibre content.



**Table 3-1. Experimental diet formulas.**

Ingredient (g)	HFD	PAC	HPAC	LFD
Canola stearine *	99.5	99.5	99.5	29.85
Flaxseed oil †	6	6	6	1.8
Sunflower oil ‡	94.5	94.5	94.5	28.35
Casein §	270	254	254	270
L-Methionine ¶	2.5	2.5	2.5	2.5
Dextrose §	189	189	189	255
Corn Starch ‡	169	169	169	245
Cellulose §	100	0	0	100
'Solido' seed coat (raw or hydrolyzed)	0	193	193	0
Mineral mix Bernhart & Tomarelli §	51	51	51	51
Vitamin mix AIN-93-VX §	10	10	10	7.6
Inositol ¶	6.3	6.3	6.3	6.3
Choline Chloride ¶	2.8	2.8	2.8	2.8

Note: To avoid other dietary factors' effects on the outcomes, the nutrient contents of both raw and hydrolyzed pea seed coats (PSC) were analyzed (data not shown). The amount of added PSC was calculated to ensure diets were equal in total fat (20.0% w/w), protein (27.9% w/w), carbohydrate (35.8% w/w) and fibre (10.0% w/w) and thus were equal in caloric density, except for LFD (total fat 6.0% w/w, protein 27.9% w/w, carbohydrate 49.9% w/w, and fibre 10.0% w/w). PAC content was  $264.1 \pm 14.6$  mg/100 g dry weight of PSC.

\* Richardson Oilseed, † Shoppers Drug Mart, ‡ Canada Safeway, § Harlan, ¶ MP Biomedicals.

### **3.2.3 Animal feeding trial**

The guidelines of the Canadian Council on Animal Care and the International Guide and Care of Laboratory Animals were followed in all animal experiments. Protocols were approved by the Animal Care and Use Committee of the University of Alberta. Male Sprague-Dawley (SD) rats (n=84) were obtained from Charles River Canada (St. Constant, QC) at 8 weeks of age and housed 2 per cage. All the animals had 1 week of acclimatization with access to standard chow and water ad libitum. Then they were randomized into 4 groups, i.e. high fat diet (HFD), low fat diet (LFD), PAC-supplemented HFD (PAC), and HPAC-supplemented HFD (HPAC). LFD group remained on standard chow. All the others were introduced to a 6-week HFD regimen to induce glucose intolerance, which was confirmed using an oral glucose tolerance test (GTT as described below; data not shown). The 4 groups of rats were switched to the experimental diets (Table 3-1) for 4 weeks. The rationale for the treatment period is that for rats at ages from 8 weeks to 7 months, 1 rat day equals to 34.8 human days [216]. Thus, treating rats for 4 weeks equals a ~2.5 years' treatment in humans. A more prolonged treatment period may lead to secondary adaption, which would mask the outcomes directly from primary adaptation to the treatments. The rat age and treatment time frame is similar to that used in our published study [214] and therefore allows us to make inter-study comparisons.

Body weights were measured weekly and food intake was recorded daily. At the end of the feeding trial, rats' lean and fat mass was determined by an EchoMRI Whole Body Composition Analyzer (Echo Medical Systems LLC, Houston, TX, USA).

### **3.2.4 Glucose and insulin tolerance tests**

Oral (OGTT) or intraperitoneal GTT (IPGTT) was used to determine the status of glucose tolerance in all groups. IPGTT examines the effects of PAC feeding downstream of intestinal absorption factors because the glucose is introduced into the peripheral circulation, bypassing the gut. Seven days before tissue collection, after overnight fasting, all the rats were weighed and

baseline blood glucose concentration was measured with a glucometer (Accu-Check Compact Plus, Roche Diagnostics, Laval, Québec, Canada) in whole blood taken from the tail vein. Then they received a standard dose of glucose (1g/kg; oral: 40% w/v, in ddH<sub>2</sub>O; ip: 20% w/v, in saline), blood glucose was measured at 10, 20, 30, 60, 120 min. Additional blood samples were collected at the same time points to obtain plasma and stored at -80°C until assayed for insulin and glucagon. Incremental area under the curve (IAUC) was calculated as described [217].

Insulin tolerance tests (ITT) were conducted 1 day before the day of tissue collection. After 4-hour fasting, all the rats were weighed and baseline blood glucose level was measured in whole blood with a glucometer. After receiving insulin (0.5 U/kg, ip), blood glucose was measured at 15, 30, 60, 90, 120 min.

### **3.2.5 Tissue collection**

Fed or 16-hour fasted rats were euthanized under anaesthesia (pentobarbital sodium 60 mg/kg, ip) by exsanguination. Blood (5-10 ml) was obtained from the abdominal aorta and divided for preparation of plasma and serum, which were frozen at -80°C. The epididymal fat pad was extracted and weights recorded. Pancreatic islets were isolated and cultured overnight for insulin secretion studies as previous described [218,219]; an additional pancreas sample just adjacent to the spleen was fixed in formalin overnight for embedding in paraffin by standard techniques.

### **3.2.6 Soluble PAC and anthocyanin quantitation**

The total extractable PAC content of the native 'Solido' PSC fraction was determined by the butanol-HCl-Fe<sup>3+</sup> method [215]. Approximately 25 mg subsamples of seed coat tissue (lyophilized and ground to a fine powder using a Retsch ZM 200 mill (PA, USA) with 0.5 mm screen filter) were weighed into 15 mL Falcon tubes. The samples were extracted with 10 ml of 80% methanol for 24 h with shaking. After vortexing the slurry and centrifuging for 5 min at

4000 rpm, the supernatants were used for PAC analysis using the method of Porter et al. [215]. In brief, 2 mL of the butanol:HCl reagent and 66.75  $\mu$ L of iron reagent were added into a 15 mL glass culture tube. Then, 0.5 mL of clear sample extract was added to the tube and the mixture was vortexed. Two 350  $\mu$ L aliquots of this solution were removed for use as sample blanks, and the remaining solution was placed into a 95°C water bath. After 40 min, the solution was allowed to cool at room temperature for 30 min. The reaction products, sample blanks, and a PAC standard curve dilution series were monitored for absorbance at 550 nm using a 96 well UV plate reader (Spectra Max 190, Molecular Devices, CA, USA). The PAC standard solution used was an extract from 'CDC Acer' PSC purified as described by Jin [204]. The HPLC-photodiode array detection method of Zifkin et al. [220] was used to quantify anthocyanidins in the HPAC fraction.

### **3.2.7 Analysis of PAC-derived compounds in PSC and serum samples**

PSC (25mg, PAC or HPAC) were extracted in 1mL methanol for 4 h at -20 °C. The supernatant was collected and injected into a hydrophilic interaction liquid chromatography (HILIC) column (TSKgel Amide-80) for separation. The continuous gradient segments for HILIC (A: 10 mM NH<sub>4</sub>AC in H<sub>2</sub>O; B: 10 mM NH<sub>4</sub>AC in acetonitrile) were: t = 0 min, 90% B; t = 5 min, 10% B; t = 10 min, 10% B; t = 30 min, 90% B. The flow rate was 100  $\mu$ L/min. The flow was directed to the electrospray ionization (ESI) source of a Bruker Impact HD quadrupole time-of-flight (Q-TOF) mass spectrometer (MS). Parameters for analysis were set using HILIC-negative ion mode with spectra acquired over a mass range from m/z 50 to 800. The optimum values of the ESI-MS parameters were: collision energy, 22 eV for catechin derivatives and 25 eV for delphinidin derivatives; collision RF, 700.0 Vpp; transfer time, 30.0  $\mu$ s; pre-pulse storage, 8.0  $\mu$ s. The MS data were checked by Bruker's DataAnalyst 4.2.

Proteins in the serum samples were precipitated with 100% methanol (1:3, v/v) at room temperature, and the supernatant was collected and analyzed using Q-TOF MS linked to an HILIC column as described above.

### **3.2.8 Analysis of plasma insulin and glucagon**

Plasma samples obtained during the GTT and tissue collection were analysed in duplicate for insulin and glucagon by enzyme-linked immunosorbent assay (ELISA) using commercial assay kits according to the manufacturer's instructions (rat insulin ELISA, Alpco Diagnostics, Salem, NH; glucagon EIA kit, SCETI K.K., Tokyo, Japan).

### **3.2.9 Immunohistochemistry**

Immunohistochemical (IHC) staining was performed as previously described for determination of  $\alpha$ - and  $\beta$ -cell areas [214]. Primary antibodies and their dilutions were as follows: guinea pig anti-insulin, 1:200 (Dako, Burlington, Canada) and rabbit anti-glucagon, 1:200 (Millipore, Billerica, MA). Secondary antibodies were HRP-conjugated rabbit anti-guinea pig, 1:200 (Sigma) and goat anti-rabbit, 1:200 (Sigma), respectively. Positive immunoreactivity was visualized by diaminobenzidine plus hydrogen peroxide. Slides were then dehydrated and mounted for photography using an Axiovert microscope equipped with Axiovision 4.7 software (Carl Zeiss Microscopy GmbH, Jena, Germany). The total pancreatic area (excluding large ducts and veins), the insulin- and glucagon-positive areas were quantified using ImageJ [214].

### **3.2.10 Glucose stimulated insulin secretion from isolated islets**

To measure insulin release, duplicate samples of 3 islets/vial were incubated in Dulbecco's Modified Eagle's medium (Gibco, Burlington, Canada) with low or high glucose concentrations (2.8, 16.5 mM) for 2 h at 37°C. Supernatants were retained and insulin remaining in the islets was extracted with 3% acetic acid, then stored at -20°C for future insulin radioimmunoassay (RIA) [218]. Total islet insulin content was calculated by adding insulin secreted into

supernatant plus that remaining in the islet pellet, as determined by RIA. From this, the percentage of total insulin secreted was calculated for each data point to eliminate variance caused by islet size. Insulin stimulation index was calculated as the ratio of insulin percentage release in response to 16.5 mM glucose versus 2.8mM glucose.

### **3.2.11 Statistical analyses**

All data were expressed as means  $\pm$  standard error of the mean (SEM), and n represented the number of rats. Multiple groups were analyzed by one-way or two-way analysis of variance (ANOVA) followed by Bonferroni's multiple comparison, as appropriate. Nonparametric analyses were used for data with non-normal distribution. At  $P \leq 0.05$ , differences were considered significant. Statistical analyses were performed using GraphPad Prism for Windows version 6.0 (GraphPad Software, San Diego, CA, USA).

### 3.3 Results

#### 3.3.1 Hydrolysis depolymerized PAC and increased metabolites in serum

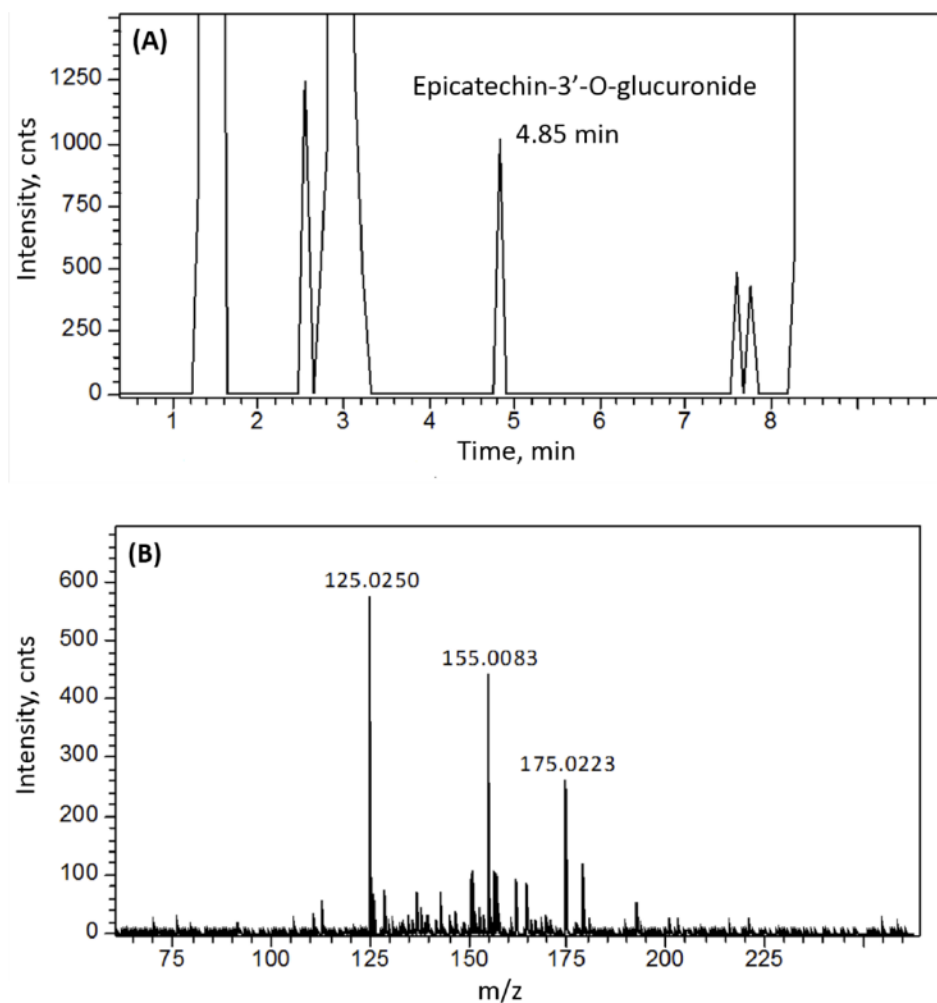
The total PAC content of the native ‘Solido’ PSC was  $264.1 \pm 14.6$  mg/100 g dry weight of PSC (n=3) as determined by the butanol-HCl-Fe<sup>3+</sup> method. Jin [204] found that in the PSC of ‘Solido’ the PAC flavan-3-ol extension units were nearly exclusively prodelphinidin, while epigallocatechin was the most abundant flavan-3-ol extension subunit followed by galocatechin. The PAC terminal subunits of this pea cultivar also mainly consisted of galocatechin and epigallocatechin. Upon acid hydrolysis, the epigallocatechin and galocatechin were converted to the anthocyanidin delphinidin with a yield of  $43 \pm 4.9$  mg/100g dry weight (n=3; HPAC fraction delphinidin content). Further characterization of the PAC and HPAC fractions by ESI-MS/MS found that PAC dimers were not present in the HPAC fraction (Table 3-2), showing that the acid hydrolysis procedure had effectively cleaved the PAC dimers to monomers.

**Table 3-2. PAC-derived compounds in pea seed coats and rat serum.**

		Compound	Retention Time (min)	[M-H] (m/z)	MS <sup>2</sup> Ions (m/z)
Standard		Epicatechin	1.85	289.067	125.026, 136.026, 151.041, 203.071
		Galocatechin	2.89	305.065	125.026, 139.042, 167.038, 179.035
		Delphinidin	12.23	301.034	125.026, 137.026, 147.010, 163.005
Pea seed coat	PAC	Prodelphinidin A1	5.98	607.109	125.026, 137.027, 147.011, 163.005
		Prodelphinidin B	6.31	609.125	125.025, 177.021
		Delphinidin	11.82	301.034	125.026, 137.027, 177.020
	HPAC	Delphinidin	12.65	301.034	125.026, 137.026, 147.010, 163.005
Serum	HPAC	Epicatechin-3'-O-glucuronide	4.85	465.1038	125.025, 155.013, 175.027
		4'-O-Methyl-epigallocatechin	1.85	319.0823	139.116, 167.111, 179.111, 207.106

Note: [M-H], precursor ion; MS<sup>2</sup>, product ion; m/z, mass-to-charge ratio.

High DP is the main factor limiting the absorption of PAC. Therefore, it was expected that PAC-hydrolyzed products would be readily absorbed into the body. To determine and compare the bioavailability between PAC and HPAC, PAC-related metabolites in non-fasted serum samples were analyzed using LC-MS/MS. Epicatechin-3'-O-glucuronide and 4'-O-methyl-epigallocatechin were detected in serum samples from HPAC but not PAC (Table 3-2 and Figure 3-1). The 4'-O-methyl-epigallocatechin PAC metabolite could have been derived from the flavan-3-ol epigallocatechin terminal units of the hydrolyzed PAC. The structures of the detected PAC-derived compounds in PSC and serum are shown Figure 3-2.





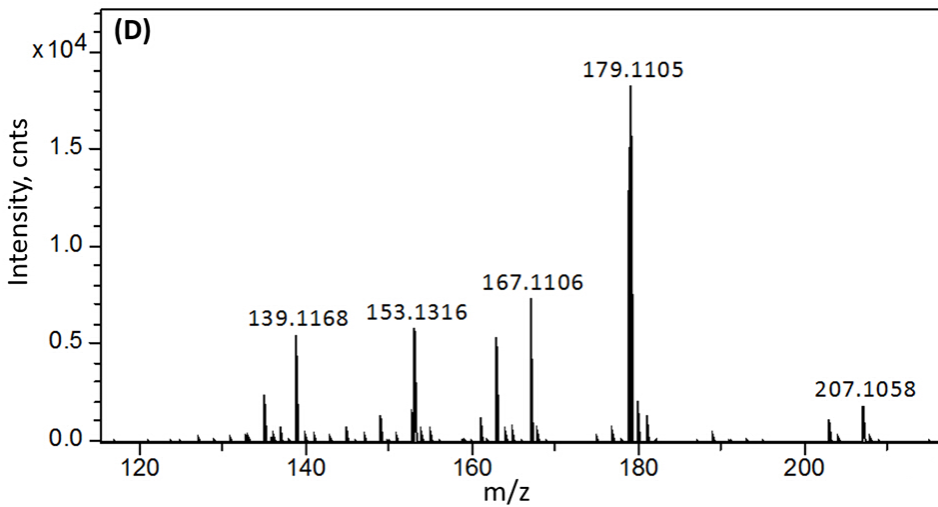
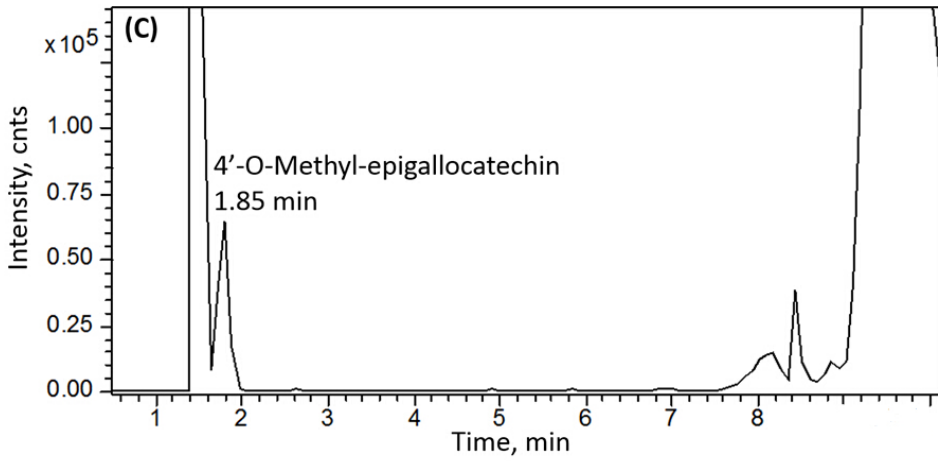
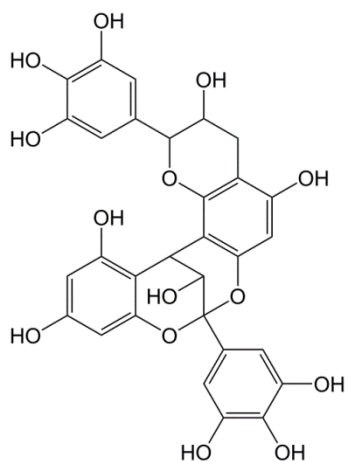
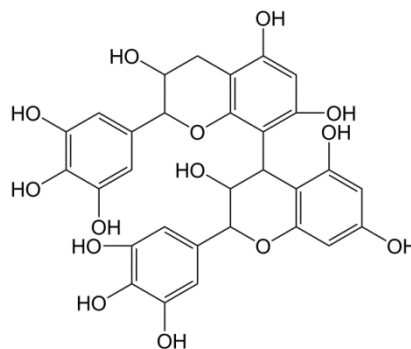


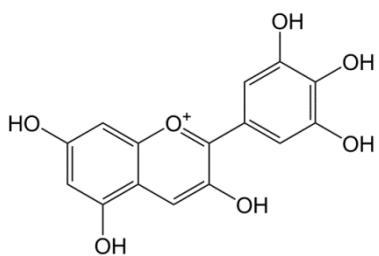
**Figure 3-1. ESI-MS spectrum of the HPAC serum extract showing the epicatechin-3'-O-glucuronide (A, B) and 4'-O-methyl-epigallocatechin (C, D).**



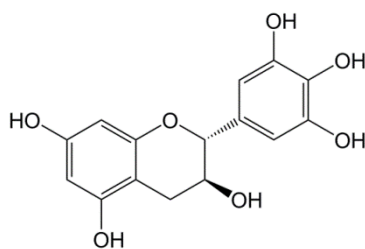
**Prodelphinidin A1**



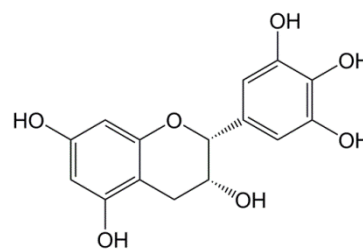
**Prodelphinidin B**



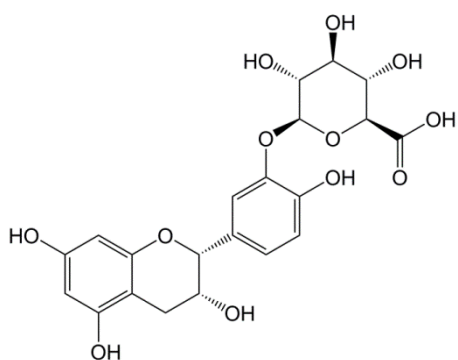
**Delphinidin**



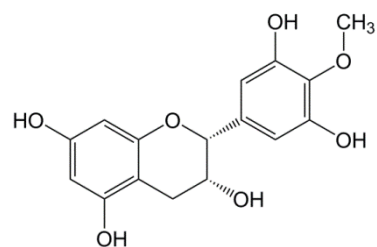
**Gallocatechin**



**Epigallocatechin**



**Epicatechin 3'-O-glucuronide**



**4'-O-Methyl-epigallocatechin**

**Figure 3-2. Structures of PAC-derived compounds**

### 3.3.2 HPAC improved body composition without affecting food intake

All the rats had similar body weights at both baseline and prior to diet change. Differences in body weights among groups became apparent after switching to the experimental diets (Figure 3-3). At the end of the feeding trial, rats in the HPAC group had approximately 18% less weight gain compared to HFD group (HPAC,  $139.3 \pm 17.0$ ; HFD,  $156.9 \pm 12.0$ , %,  $P < 0.05$ ). HPAC group percentage of body fat was ~6% lower versus HFD ( $P < 0.05$ , Table 3-3). In contrast, although rats fed PAC-supplemented diet gained ~10% less weight, their body composition was similar to HFD (Table 3-3). Lean mass was similar in all groups. We also measured epididymal fat pad mass in a subset of rats ( $n=8$  for each group), HPAC had significantly lower epididymal fat pad mass than HFD (HPAC:  $1.75 \pm 0.18$ , HFD:  $2.40 \pm 0.13$ , mean $\pm$ SEM, % of body weight,  $P < 0.05$ ), while no differences were found between PAC and HFD (PAC:  $2.39 \pm 0.38$ , mean $\pm$ SEM, % of body weight).

PAC contribute to the bitter and astringent tastes of food [5], which may affect food intake of the different experimental groups. However, PAC or HPAC supplementation did not affect food or energy intake compared with HFD (Table 3-3). Based on food consumption, the estimated PAC and HPAC intake was 17.5 mg/day. LFD rats achieved similar energy intake via increased food consumption (Table 3-3).

**Table 3-3. Food intake and body composition**

	HFD	PAC	HPAC	LFD
Food Intake (g/rat/d)	$31.25 \pm 1.14$	$41.63 \pm 2.86$	$39.81 \pm 3.34$	$42.50 \pm 2.82^*$
Energy Intake (kcal/rat/d)	$134.40 \pm 4.91$	$179.0 \pm 12.30$	$171.2 \pm 14.37$	$153.0 \pm 10.15$
Fat mass/Final Wt, %	$16.8 \pm 1.2$	$15.0 \pm 1.2$	$11.3 \pm 0.9^*$	$13.8 \pm 1.4$
Lean mass/Final Wt, %	$67.0 \pm 1.0$	$69.2 \pm 1.0$	$70.8 \pm 0.9^*$	$69.4 \pm 0.6$
Fat mass/Lean mass	$0.26 \pm 0.02$	$0.21 \pm 0.02$	$0.16 \pm 0.01^*$	$0.19 \pm 0.02$

Note: Values are means  $\pm$  standard error, N = 8 for all groups. \*  $P < 0.05$ , compared to HFD, Bonferroni's multiple comparison.

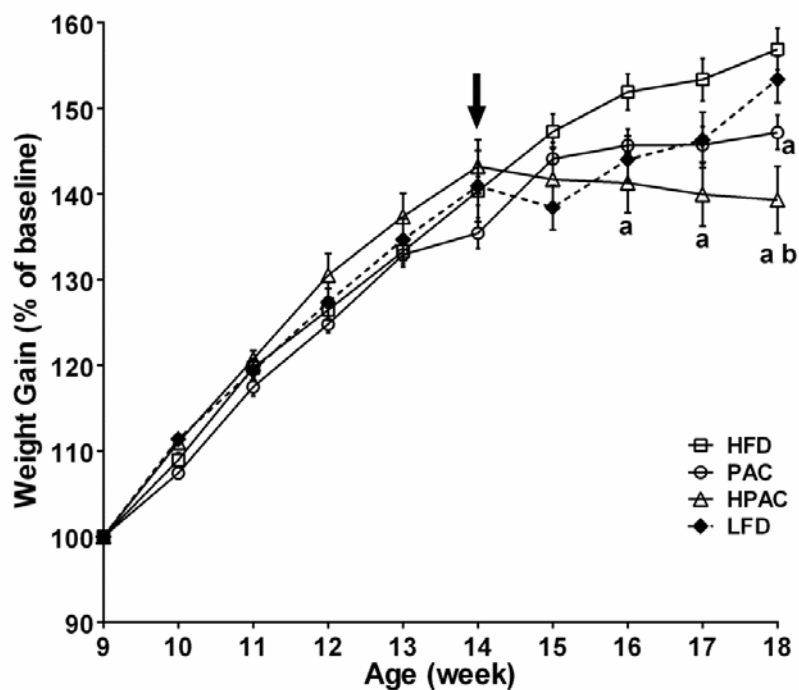


**Figure 3-3. Effects of diet on body weight change during the feeding trial.**

Male Sprague Dawley rats were fed 20% w/w high fat diet (HFD) for 6 weeks, then were randomly assigned [arrow] to HFD (n=23), 0.8% w/w proanthocyanidin + HFD (PAC, n=22), or 0.8% w/w hydrolyzed proanthocyanidin + HFD (HPAC, n=19) and maintained for 4 weeks. Additional rats were fed 6% w/w low fat diet (LFD, n=20) for 10 weeks as a normal control. Body weight was recorded weekly. Data are presented as percentage of the baseline weights. <sup>a</sup>P < 0.05 compared with HFD, <sup>b</sup>P < 0.05 compared with LFD, Bonferroni's multiple comparison.

### **3.3.3 HPAC diet improved insulin resistance induced by HFD**

Seven days prior to tissue collection, IPGTT was performed to compare the effects of different diets on glucose homeostasis. Data are shown as the glucose and insulin responses at each time point (Figure 3-4A and 3-4C) and as incremental area under the curve (IAUC, Figure 3-4B and 3-4D). In response to a standard dose of glucose, LFD group had overall lower glucose excursion compared to HFD, with ~50% decrease in IAUC of blood glucose ( $P < 0.01$ ). HPAC had significantly lower blood glucose than HFD at 10 min ( $P < 0.05$ ) and an approximately 25% reduction in IAUC, such that the overall glucose excursion was similar to LFD. Insulin responses in HPAC were much lower at 20 and 30 min, resulting in a significantly lower IAUC ( $P < 0.05$ ) than HFD. Those results indicate improved glucose disposal in HPAC. In contrast, PAC showed similar glucose and insulin responses compared with HFD, suggesting little improvement in glucose intolerance.

Insulin-glucose IAUC index is the product of IAUCs of insulin and glucose response curves and is an index for insulin resistance (IR) in which a higher value suggests higher degree of insulin resistance [221,222]. HPAC and LFD both had lower values of insulin-glucose IAUC index compared with HFD (Figure 3-4E,  $P < 0.05$ ), whereas PAC was similar to HFD.

ITT was also used to assess the degree of insulin resistance. Results from ITT (Figure 3-5) also support that HPAC were less insulin resistant than HFD rats. Although glucose levels (present as percentage of baseline glucose) responding to insulin administration (Figure 3-5A) were similar among all groups during the first 30 min, HPAC had significantly ( $P < 0.05$ ) lower glucose concentrations from 90 to 120 min. PAC also tended to have a slower glucose recovery rate, with a significantly lower glucose concentration at 120 min compared to HFD. Slopes of ITT for 60-120 min were calculated [223] as a direct measurement of glucose recovery rate. Both of the pea seed coat-supplemented groups, especially HPAC, had smaller slopes than HFD, suggesting slower glucose recovery rate (Figure 3-5B).

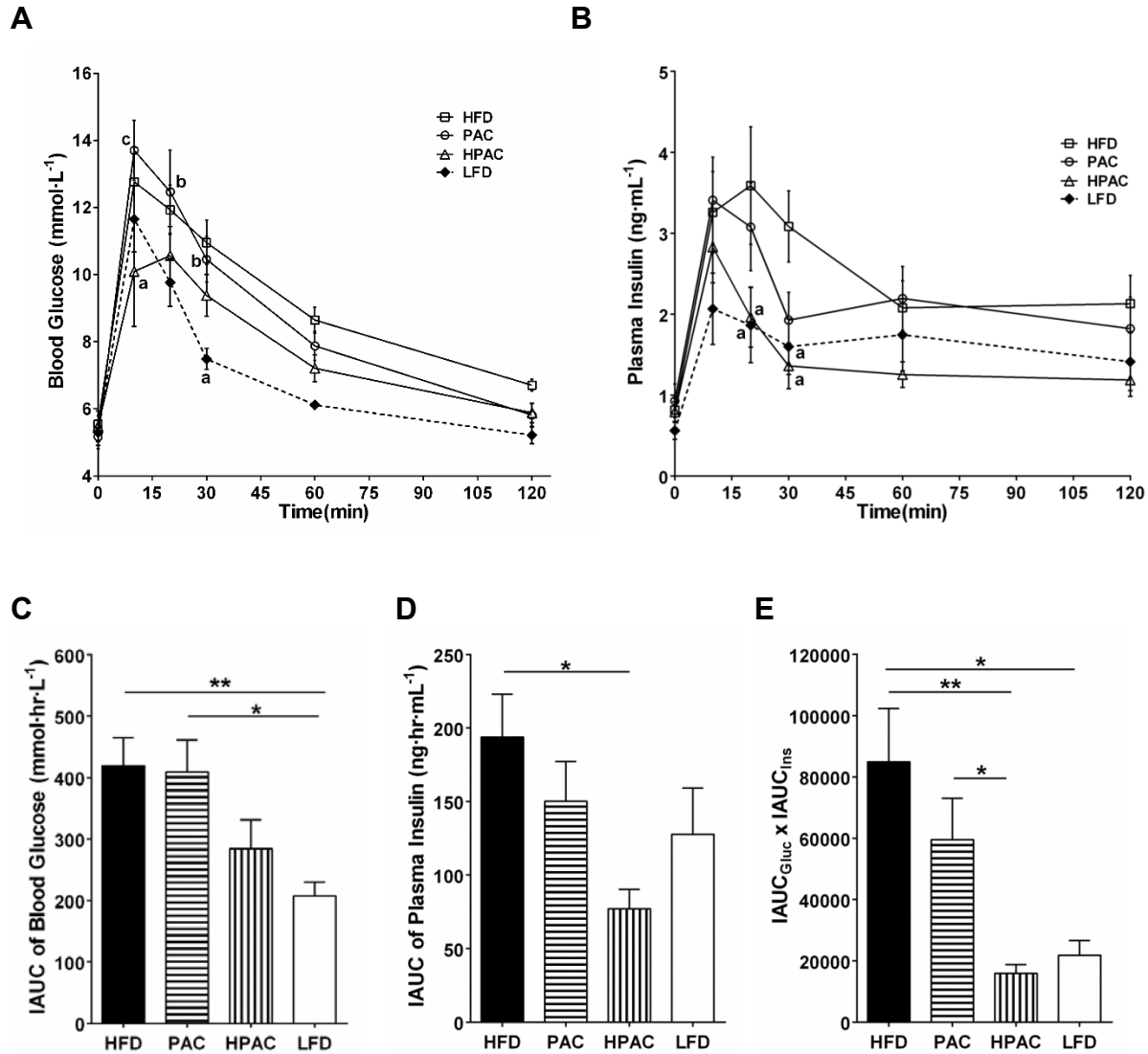


**Figure 3-4. Blood glucose concentrations and insulin release after glucose challenge.**

Intraperitoneal glucose tolerance tests were performed at week 11. After overnight fasting, blood glucose (A) and plasma insulin (B) were measured at 0, 10, 20, 30, 60, 120 min after intraperitoneal administration of 1 g/kg body weight glucose. <sup>a</sup>P < 0.05 compared with HFD, <sup>b</sup>P < 0.05 compared with LFD, <sup>c</sup>P < 0.05 compared with PAC. Incremental area under the curve (IAUC) of glucose response (C) and insulin secretion (D) were calculated from A and B, respectively. (E) Insulin-glucose AUC index calculated from the product of glucose and insulin AUC, where a lower value indicates increased insulin sensitivity [221]. HFD, n=11; LFD, n=10; PAC, n=10; HPAC, n=8. \*P < 0.05, \*\*P < 0.01, Bonferroni's multiple comparison.

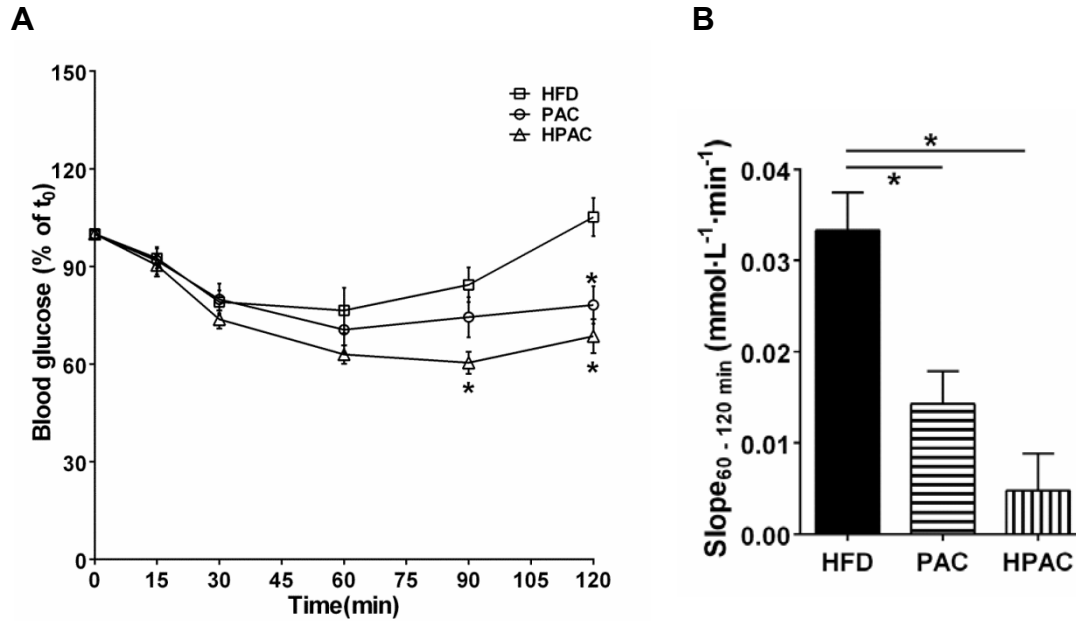


**Figure 3-5. Blood glucose responses after insulin challenge.**

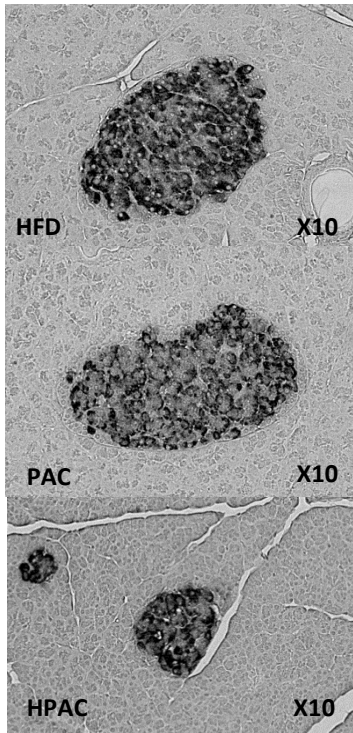
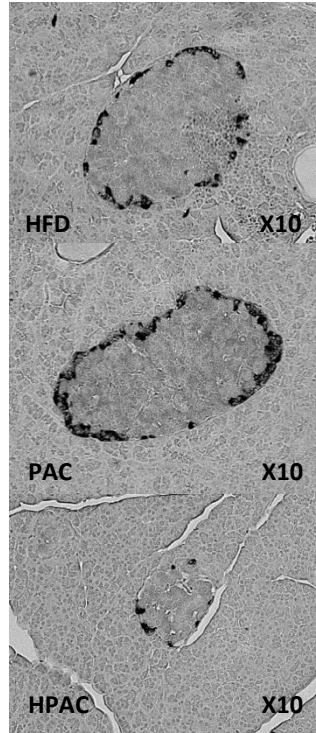
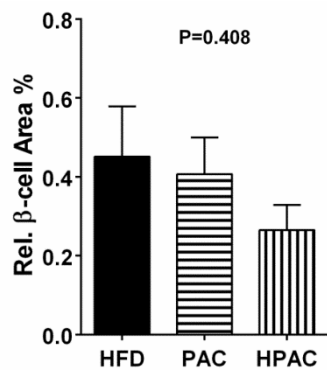
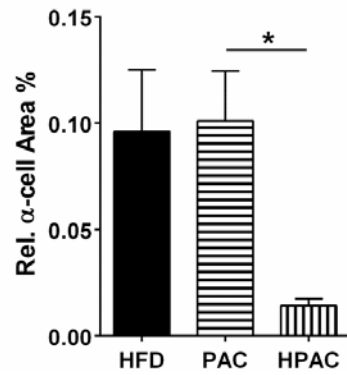
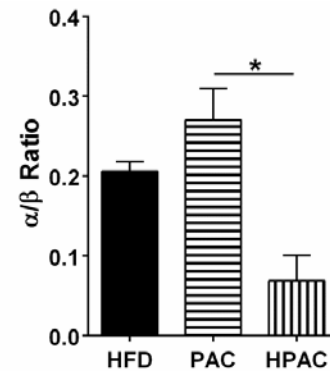
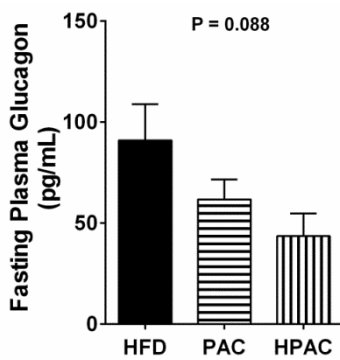
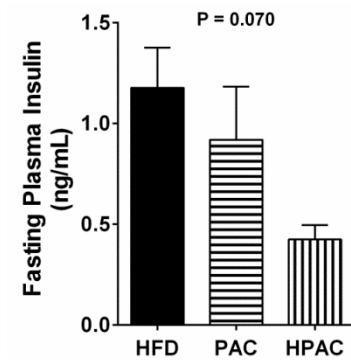
Insulin tolerance tests were performed before the day of tissue collection. After 4h fasting, blood glucose levels was measured at 0, 15, 30, 60, 90, 120 min after intraperitoneal administration of 0.5 U/kg body weight insulin. Changes in blood glucose (A) are expressed as percent of 4h-fasted glucose and (B) slopes for 60-120 min were calculated as a direct measurement of glucose recovery rate [223]. N=8 for all groups. \*P < 0.05, Bonferroni's multiple comparison.

### **3.3.4 HPAC preserved pancreatic islet morphology and function**

The lowered insulin responses in HPAC during IPGTT might be the result of a smaller  $\beta$ -cell mass. Therefore  $\beta$ -cell and  $\alpha$ -cell areas were quantified as an estimate of islet cell mass. Representative photomicrographs are shown in Figure 3-6A and 3-6B. Pancreatic  $\beta$ -cell area was not different between groups ( $P=0.4$ , Figure 3-6C). A  $\sim 80\%$  decrease ( $P < 0.05$ ) in pancreatic  $\alpha$ -cell areas in HPAC was found (Figure 3-6D), which contributed to significantly different cell composition ( $\alpha/\beta$  cell ratio) in pancreatic islets of HPAC (Figure 3-6E,  $P < 0.05$ ). Fasting plasma insulin and glucagon concentrations were not different among groups (Figure 3-6F,  $P=0.070$ ; Figure 3-6G,  $P=0.088$ ).

To further examine the effects of PAC and HPAC on pancreatic islet function, and to exclude the possibility that the lower insulin response during IPGTT was caused by impaired insulin secretion from pancreatic islets, GSIS was conducted on isolated islets. As shown in Figure 3-7A, insulin secretion in response to 2.8mM glucose was similar among all groups. When stimulated with 16.5mM glucose, % release of insulin in HPAC was increased  $\sim 3$ -fold compared to both HFD and PAC. Insulin stimulation indices were significantly different among all groups (Figure 3-7B,  $P=0.047$ ), and HPAC had the highest mean value, indicating ameliorated pancreatic islet function in HPAC. Also there was a trend (Figure 3-7C,  $P=0.126$ ) towards lower insulin content in HPAC.



**A****B****C****D****E****F****G**

**Figure 3-6. Effects of different diets on pancreatic morphology, fasted insulin and glucagon.**

Immunohistochemical staining of insulin and glucagon (n=5 for all groups) was shown in panel A and B, respectively. The percentages of insulin (C) - or glucagon (D)-positive area versus the total pancreas areas were calculated as estimates of pancreatic  $\beta$ - or  $\alpha$ -cell mass. The ratio of  $\alpha$ - to  $\beta$ -cell area (E) was calculated to reflect cell composition of pancreatic islets. Fasted plasma insulin (F, n=8 for all groups) and glucagon (G, n=6 for all groups) were also measured. \*P < 0.05, Bonferroni's multiple comparison.

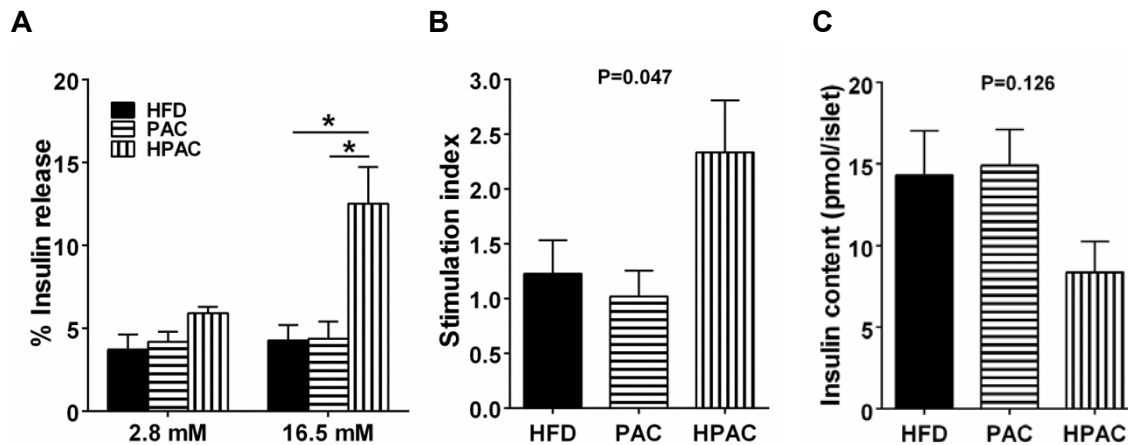


**Figure 3-7. Effects of different diets on glucose-stimulated insulin secretion from isolated islets.**

Isolated islets were cultured in fresh medium plus 2.8 and 16.5 mmol/L glucose for 2 h. Insulin secretion (A) is presented as percent of total content. Insulin content (B) and insulin stimulation index (C) were calculated as described above. N=5 for all groups. \*P < 0.05, Bonferroni's multiple comparison.

### 3.4 Discussion

The main objective of this study was to evaluate the bioavailability and compare effects on glucose homeostasis of PAC and HPAC pea seed coat fractions. Our results show that PAC's biological functions are clearly determined by its bioavailability *in vivo*. In the HPAC group, PAC-related metabolites detected in serum were significantly increased compared with PAC and this was associated with a more pronounced beneficial effect of HPAC on body weight gain, glucose tolerance and pancreatic  $\beta$ -cell function.

PAC bioavailability is profoundly affected by its degree of polymerization (DP). PAC with DP <3 are believed to be absorbed from the small intestine, whereas PAC with DP >3 reach the colon, where they are subjected to microbial metabolism, and the degraded products either get absorbed or excreted in the feces [33]. The absorbed compounds are extensively metabolised in the enterocytes and liver by phase II enzymes into conjugated derivatives, such as glucuronides, sulfate conjugates and methyl derivatives; these either persist in the circulation or are rapidly eliminated in urine [33]. Furthermore, in fibre-rich plant samples such as were used in this diet study, non-extractable PAC is found associated with fibre, which makes it even less bioavailable [63,64]. Acid hydrolysis of PAC can break the interflavan bonds [5,224]. It is also possible that acid hydrolysis can break the association of non-extractable PAC with fibre, although this was not explicitly evaluated. As shown in this study, hydrolysis of PAC (HPAC) significantly increased its bioavailability reflected by higher concentrations of metabolites in serum samples. This is in accordance with the findings of previous bioavailability studies showing that the small molecular weight PAC (monomers and dimers) can be absorbed and metabolized [30,40,225]. Because PAC has growth-inhibitory effects on bacteria [226] and some "tannin-resistant" species are candidates for PAC metabolism [71,227], it is also possible that hydrolysis reduced PAC growth-inhibitory effects on gut microbes and therefore more microbial metabolites were produced and absorbed in HPAC-treated rats.

Prolonged HFD feeding is well known to induce insulin resistance and glucose intolerance in rats. Hyperplasia of  $\beta$ -cells develops to adapt to changes in metabolic status and maintain glucose homeostasis [228,229]. Incorporating HPAC into HFD led to correction of glucose intolerance: both glucose excursion and insulin secretion of HPAC was similar to LFD in the IPGTT, while there was prolonged suppression of blood glucose in the ITT. Therefore, HPAC was able to reduce the demand for insulin compensation caused by HFD.

Insulin secretion from the islets in response to high glucose (16mM) stimulation was significantly enhanced in HPAC vs HFD. There may be two explanations for this improvement. Firstly, PAC may act as an insulin secretagogue. INS-1 cells pre-cultured with PAC-rich cranberry powder had increased basal and stimulated insulin secretion [195]. Jayaprakasam et al. [191] tested the effects of a series of anthocyanins from fruits on insulin secretion *in vitro*. They found delphinidin-3-glucoside was the most effective stimulant of GSIS. However, neither the forms nor the concentrations (cranberry powder: 0.25 and 0.5 mg/mL; anthocyanins: 50 g/mL) of compounds used in their studies is likely to exist in physiological post-absorptive conditions. According to our findings, catechin-related compounds (epicatechin-3'-O-glucuronide, 4'-O-methyl-epigallocatechin) were identified and increased significantly in the serum of HPAC in the current study. These compounds existing in nanomolar quantities in the circulation are likely candidates for the bioactive substances that regulate GSIS. On the other hand, improved GSIS may be the indirect result of the improved insulin sensitivity in HPAC. The demand for insulin secretion in HPAC was lower than the HFD group, thus creating less stressful condition for  $\beta$ -cells leading to better pancreatic function. These possibilities will be tested in future *in vitro* assays designed to assess direct effects on  $\beta$ -cells or insulin-sensitive tissues.

We also observed a striking reduction in  $\alpha$ -cell area and  $\alpha/\beta$  cell ratio in HPAC pancreas, while plasma glucagon concentrations were reduced by 50% in HPAC vs HFD ( $p < 0.07$ ). In type 2

diabetes, increased relative or absolute mass of  $\alpha$ -cells has been proposed to play a role in the pathology in addition to  $\beta$ -cell loss and dysfunction [230,231]. Elevated plasma glucagon concentration relative to insulin is believed to cause hyperglycemia and dysregulated glucose metabolism [146,232]. Therefore, in addition to improved insulin sensitivity, the glucagon secreting capacity may also contribute to the better glycemic control in HPAC group, as exemplified by the slower glucose rebound after ITT. The 60-120 minute phase of the ITT reflects the counter-regulatory response, the strength of which is dictated, in part, by the suppressive effect of insulin versus the positive effect of glucagon on hepatic glucose production [233].

Another interesting finding is that HPAC group exerted a favorable effect on body composition without altered energy intake. It has been suggested that catechins and PAC metabolites are able to cross the blood-brain barrier [36,37,234]. Wang et al. reported that the metabolite concentrations were about 300 pmol/gram of brain tissue after 10-day treatment, and basal synaptic transmission was significantly improved when using a biosynthetic brain-targeted PAC metabolite at a physiologically relevant concentration (300 nM) [234]. Thus, catechins and PAC metabolites may also have the potential to modulate neuropeptides involved in energy expenditure in hypothalamus. Yet studies examining the central nervous system (CNS) effects of PAC in regulating neuropeptides and neurohormones are scarce. In the study by Okuda et al., green tea extract (GTE) was able to reduce HFD-induced hypothalamic inflammation in rats, which was suggested to lead to well-controlled energy expenditure [235]. They also determined protein content of receptors and transporter of serotonin in serotonergic system, which induces anorexia in both humans and rodents [236], however it was not affected by the treatment [235]. Lu et al. found that after a 4-month GTE treatment, HFD-induced changes in gene expression related to energy expenditure were restored in SD rats [237]. Collectively, these studies indicate that PAC appears to have the potential to modulate hypothalamic neuropeptides involved in energy expenditure. Another mechanism may relate to changes in fatty acid

oxidation and metabolism. However, the available data are inconclusive [238–240]. These areas merit further investigation.

In summary, acid hydrolysis improved the limited bioavailability of PAC fractions, resulting in a significant increase in the concentrations of PAC-related metabolites in HPAC serum. This was associated with enhanced improvement in glucose handling in glucose intolerant rats.

Beneficial effects on pancreatic islet composition and insulin secretion were also elicited by HPAC treatment.

## Chapter 4

### **Epicatechin potentiates glucose-stimulated insulin secretion in INS-1 cells through CaMKII activation**

#### **4.1 Introduction**

Epicatechin (EC) belongs to a subgroup of flavonoids called flavan-3-ols. It is a plant secondary metabolite, and hence a ubiquitous constituent of various plants [13]. Dietary EC is mainly from tea and cocoa products, grains such as beans and peas, and fruits such as grape, berries and apples [5]. As a bioactive substance, the actions of EC are dependent on its bioavailability at target tissues. Studies *in vitro* have demonstrated that EC can be taken up and metabolised in enterocytes and hepatocytes [34,241]. Evidence from both animal and human studies shows that monomeric flavanols can be metabolized extensively to glucuronides, sulphates, and O-methylated forms by phase II enzymes in the intestine and liver [27,40,54,225]. Their metabolites are found not only in plasma, but also are accumulated in different tissues such as brain, liver, heart, intestine and kidney [36,38]. As a result, it is most likely EC could affect some functions of those tissues.

EC is well-known for its antioxidant ability. However, the concentrations of EC accumulated *in vivo* are lower than the effective concentrations of EC as an antioxidant. *In vivo* studies show that in plasma EC metabolites peak at ~40  $\mu\text{M}$ , whereas in different tissues they are about 0.1 – 0.3  $\mu\text{M}$  [36,38,234]. In contrast, EC's half maximal inhibitory concentration ( $\text{IC}_{50}$ ) as a protective antioxidant is about 200 – 400  $\mu\text{M}$  *in vitro* [242]. Therefore, it's debatable whether EC acts as an antioxidant *in vivo*.

Lately, it has been suggested that EC may interact with signaling proteins or enzymes, thus modulating cell signaling pathways. For example, EC may exert antioxidant effects indirectly by

modulation of redox enzymes. It can inhibit nicotinamide adenine dinucleotide phosphate (NADPH) oxidase activity effectively at a concentration of 10  $\mu\text{M}$  in human umbilical vein endothelial cells [243]. In tert-butylhydroperoxide (t-BOOH) treated INS-1E beta-cells, 20  $\mu\text{M}$  of cocoa EC prevents glutathione (GSH) depletion, recovers the activity of glutathione peroxidase and glutathione reductase, and reduces reactive oxygen species (ROS) [190]. EC also modulates the mitogen-activated protein kinase (MAPK) signaling pathway. In cortical neurons, EC and its metabolite 3'-O-methyl-(-)-EC stimulate the phosphorylation of extracellular signal-regulated kinase (ERK), an enzyme of the MAPK pathway, at concentrations ranging from 0.1 – 0.3  $\mu\text{M}$ , meanwhile showing inhibition of phosphorylation at higher (1 – 30  $\mu\text{M}$ ) concentrations [112]. EC-rich cocoa extract can protect HepG2 cells from oxidative stress induced by either t-BOOH or high glucose-high insulin treatment via upregulation of ERK phosphorylation [244,245].  $\text{Ca}^{2+}$ / calmodulin-dependent protein kinase (CaMK) II pathway is also reported to be modulated by EC in several studies. In the presence of  $\text{Ca}^{2+}$ , EC (1  $\mu\text{M}$ ) induces the synthesis of NO through endothelial nitric oxide synthase (eNOS) activation via CaMKII pathway in human coronary artery endothelial cells [246]. Improved basal synaptic transmission and long-term potentiation in hippocampus slices are revealed after 0.3  $\mu\text{M}$  EC metabolite treatment [234]. The underlying mechanism is associated with the activation of cAMP response element binding protein (CREB) signaling via CaMKII pathway [234]. Overall, current evidence suggests that the interaction of EC with molecular targets could in part explain its bioactivities; although the exact cellular signaling cascades of EC need to be further characterized, and also be specified in different cell types.

Many studies have looked into EC's effects on pancreatic  $\beta$ -cells. EC is able to enhance glucose-stimulated insulin secretion (GSIS) from healthy  $\beta$ -cell lines and isolated islets [192,193]. In oxidizing agent-treated models, including cell lines, isolated islets or animals, recovery of  $\beta$ -cell mass and function is observed in response to EC treatment [100,189,190]. Nonetheless, the mechanisms of these phenomena are less understood. Although not reported yet, the



concentrations of EC and its metabolites accessible to pancreatic  $\beta$ -cells are most likely similar to that of the other organs (0.1 – 0.3  $\mu$ M) [36,38,234]. That being the case, at those concentrations EC and its metabolites may as well act as a cellular signaling modulatory compound in pancreatic  $\beta$ -cells. In addition, studies have suggested an important role of CaMKII in insulin secretion from  $\beta$ -cells. CaMKII is a key  $Ca^{2+}$  sensor that controls  $Ca^{2+}$  homeostasis in pancreatic  $\beta$ -cells [129]. Elevated intracellular  $Ca^{2+}$  activates CaMKII thereby enhancing GSIS, whereas inhibition of CaMKII reduces GSIS [129]. Increases in intracellular  $Ca^{2+}$  can also activate ERK to promote  $\beta$ -cell survival [247]. Considering EC's intracellular targets found in other cell types, it's possible that EC modulates the  $Ca^{2+}$ /CaMKII pathway in pancreatic  $\beta$ -cells.

In our previous study (Chapter 3), we have demonstrated that glucose-intolerant rats fed oligomeric flavan-3-ols had improved pancreatic islet function suggested by enhanced GSIS from isolated islets. Correspondingly, there was an increase in serum metabolites derived from flavan-3-ols, including EC. Thus, we are curious whether EC's modulation of the CaMKII pathway in pancreatic  $\beta$ -cells would be the underlying mechanism. In addition, existing evidence suggests EC's concentration at organ level is about 0.3  $\mu$ M [234]. Therefore, we investigated EC's effects at a physiological concentration (0.3  $\mu$ M) on INS-1 cells stressed by treatment with saturated fatty acid (SFA). We hypothesized that EC at low concentration can recover insulin secretion and promote cell survival via activation of  $Ca^{2+}$ /CaMKII pathway in SFA-treated pancreatic  $\beta$ -cells. In addition, we also adopted a high (30  $\mu$ M) concentration of EC to test whether EC at high concentration could affect ROS production in response to different stimuli.

## **4.2 Materials and methods**

### **4.2.1 Cell culture**

The rat insulinoma  $\beta$ -cell line INS-1 (clone 832/13) (a gift from Dr. Peter Light, Alberta Diabetes Institute, Canada) were maintained in a humidified incubator containing 5% CO<sub>2</sub> at 37 °C. It was grown in Roswell Park Memorial Institute (RPMI)-1640 medium with 2 mM L-glutamine (Gibco, Burlington, ON, Canada), supplemented with 10% FBS (Sigma, Oakville, ON, Canada), 10 mM 4-(2-hydroxyethyl)-1-piperazineethanesulfonic acid (HEPES; Fisher, NJ, USA), 1 mM sodium pyruvate (Gibco, Burlington, ON, Canada), 50  $\mu$ M  $\beta$ -mercaptoethanol (Sigma, Oakville, ON, Canada) and 1X antibiotic antimycotic solution (Sigma, Oakville, ON, Canada).

### **4.2.2 Measurement of EC modulation of glucose-induced ROS production**

Cellular ROS were quantified using the DCFDA Cellular ROS Detection Assay Kit (Abcam, Cambridge, MA, USA). INS-1 cells ( $5 \times 10^5$  cells per well) were seeded in 96-well clear-bottom black-side plates and allowed to grow until 70% confluent. Cells were then cultured for 24 hours in medium containing vehicle, 0.3  $\mu$ M N-acetyl cysteine (NAC, Sigma, Oakville, ON, Canada) or 0.3  $\mu$ M Epicatechin (EC; purity > 98%; Sigma, Oakville, ON, Canada). Then medium was changed with Krebs–Ringer bicarbonate buffer (KRB: 116 mM NaCl, 24 mM NaHCO<sub>3</sub>, 4.4 mM KCl, 1.5 mM KH<sub>2</sub>PO<sub>4</sub>, 1.2 mM MgSO<sub>4</sub>·7H<sub>2</sub>O, 2.5 mM CaCl<sub>2</sub>) supplemented with 10 mM HEPES, 0.1% BSA and 2.8 mM glucose for a quiescent period of 30 min. Then, cells were incubated in KRB-HEPES containing 2.8 or 16.5 mM glucose, the latter with vehicle, 0.3  $\mu$ M or 30  $\mu$ M EC, or 0.3  $\mu$ M or 30  $\mu$ M NAC for 3 hours. After that, medium was removed and 100  $\mu$ l of 5  $\mu$ M 2',7' – dichlorofluorescein diacetate (DCFDA) in Hanks' Balanced salt solution (HBSS) without phenol red (Sigma, Oakville, ON, Canada) was added to the wells for 30 min at 37 °C. After diffusion into the cell, DCFDA is deacetylated by cellular esterases to a non-fluorescent compound, which is later oxidized by ROS into 2', 7' –dichlorofluorescein (DCF) and emits fluorescence. ROS generation was evaluated in a fluorescent microplate reader (Infinite 200 PRO Multimode

Reader, Tecan Group Ltd., Germany) at an excitation wavelength of 485 nm and an emission wavelength of 535 nm. Results were expressed in arbitrary units of fluorescence emission at 535 nm. Six or eight independent experiments were run in which each condition was tested in quadruplicate wells.

#### **4.2.3 Measurement of EC modulation of H<sub>2</sub>O<sub>2</sub>-induced ROS production**

Cellular ROS were quantified by the DCFDA Cellular ROS Detection Assay Kit (Abcam, Cambridge, MA, USA). INS-1 cells were seeded and then cultured in medium containing vehicle, 0.3 μM or 30 μM EC, or 0.3 μM or 30 μM NAC as described above. Medium was then removed and 100 μl of 5 μM DCFDA in HBSS without phenol red (Sigma, Oakville, ON, Canada) was added to the wells for 30 min at 37 °C. The antioxidant status of the cells was determined by adding 50 μM hydrogen peroxide (H<sub>2</sub>O<sub>2</sub>; 30%, w/w; Sigma, Oakville, ON, Canada) to each well and intracellular ROS immediately measured in the microplate reader as an endpoint assay as described earlier. Results were expressed in arbitrary units of fluorescence emission at 535 nm. Six or seven independent experiments were run in which each condition was tested in quadruplicate wells.

#### **4.2.4 Evaluation of cell viability**

Cell viability was determined using the TACS® MTT Cell proliferation assay (Trevigen, Gaithersburg, Maryland, USA). INS-1 cells were seeded at a density of 5x10<sup>5</sup> cells per well in 96-well plates. After cells reached 70% confluence, treatment media: RPMI, RPMI + 0.2 mM or 0.4 mM stearic acid (SFA; Sigma, Oakville, ON, Canada), RPMI + SFA + 0.3 μM EC or NAC, were added to cells for 24 hours, and then 10 μl/well 12 mM 3-(4,5-dimethylthiazol-2-yl)-2,5-diphenyltetrazolium bromide (MTT) was added for 4 hours, followed by overnight incubation with the addition of 100 μl/well detergent reagent [0.01M HCl with 0.1% sodium dodecyl sulfate (SDS)]. The absorbance of each well was measured using a microplate reader (SpectraMax 190, Molecular Devices, LLC., Sunnyvale, CA, USA) at 570 nm with a reference wavelength at 690

nm. Four independent experiments were run in which each condition was tested in quadruplicate wells.

#### **4.2.5 Glucose stimulated insulin secretion**

To determine GSIS, INS-1 cells after 24-hour treatments (RPMI, RPMI + 0.4 mM SFA, RPMI + 0.4 mM SFA + 0.3  $\mu$ M EC or NAC, RPMI + 0.4 mM SFA + 30  $\mu$ M EC or NAC) were washed and incubated in KRB-HEPES with 0.1% BSA for a quiescent period of 90 min. Then, cells were incubated in KRB-HEPES-BSA containing 2.8 or 16.5 mM glucose for 90 min. Insulin secreted into the medium was evaluated by radioimmunoassay (RIA). Total cell insulin content was calculated by adding insulin secreted into supernatant plus that remaining in the cells, as determined by RIA. From this, the percentage of total insulin secreted was calculated for each data point to eliminate variance caused by cell number. Five independent experiments were run in which each condition was tested in triplicate wells.

#### **4.2.6 Western blot analysis**

INS-1 cells were seeded at a density of  $1 \times 10^6$  cells per well in 24-well plates. After cells reached 70% confluence, treatment medium: RPMI, RPMI + 0.4 mM SFA, RPMI + 10  $\mu$ M KN-93 (a CaMKII inhibitor; Sigma, Oakville, ON, Canada), RPMI + 0.4 mM SFA + 0.3  $\mu$ M EC or NAC, RPMI + 0.4 mM SFA + 0.3  $\mu$ M EC or NAC + 10  $\mu$ M KN-93, were added to cells for 24 hours and GSIS assay conducted as described earlier. Supernatant was collected and assayed for insulin using RIA. Cells were lysed in a radioimmunoprecipitation assay (RIPA) buffer (150 mM NaCl; 1.0% NP-40; 0.5% sodium deoxycholate; 0.1% SDS; 50 mM Tris, pH 8.0) with 2  $\mu$ g/ml aprotinin, 10  $\mu$ l/ml protease inhibitor cocktail, and 1 mM NaF. All of the chemicals were from Sigma (Oakville, ON, Canada). Total protein was measured using a Lowry protein assay (Thermo Scientific, Pierce Biotechnology, Rockford, IL, USA). Insulin release was expressed as per  $\mu$ g protein. Five independent experiments were run in which each condition was tested in triplicate wells.

Protein samples (20 µg) were subjected to SDS-PAGE followed by blotting onto nitrocellulose membranes. The membranes were blocked in 3% BSA–0.1% Tween–Tris-buffered saline for 1 hour followed by overnight incubation at 4°C with primary antibodies diluted 1:1000 in the blocking solution. Primary antibodies included anti-Ca<sup>2+</sup>/calmodulin-dependent protein kinase II (CaMKII), antiphospho-CaMKII (p-CaMKII), anti-extracellular regulated kinases (ERKs), antiphospho-ERKs (p-ERKs), anti-protein kinase A (PKA) and antiphospho-PKA (p-PKA), all from Cell Signaling Technology (Danvers, MA, USA). Membranes were subsequently incubated with the appropriate HRP-conjugated secondary antibodies (1:5000; Sigma, Saint Louis, MO, USA) for 1 hour at room temperature. Labelling of each phosphorylated protein was compared with its total protein, respectively. Membranes were developed using ECL Prime (GE Healthcare Bio-Sciences Corp., Piscataway, NJ, USA) and digital images captured using a ChemiDoc MP™ imaging system (Bio-Rad Laboratories, Inc., Mississauga, ON, Canada). Band intensity was quantified using Quantity One v4.6.2 (Bio-Rad Laboratories, Inc., Hercules, CA, USA).

#### **4.2.7 Statistical analysis**

Results are presented in bar charts, with the top line indicating the mean and the whiskers the standard error of the mean (SEM). ANOVA followed by Bonferroni's post hoc test, with the p-value adjusted for the number of comparisons, was used to assess differences between different conditions using GraphPad Prism 6 (GraphPad Software, Inc. San Diego, CA, USA).

Nonparametric analyses were used for data with non-normal distribution. Values of  $P < 0.05$  were considered statistically significant.

## **4.3 Results**

### **4.3.1 EC (30 $\mu$ M) protects against high glucose-induced ROS in INS-1 cells**

Prolonged exposure to high glucose leads to ROS accumulation in pancreatic  $\beta$ -cells, which can eventually lead to  $\beta$ -cell dysfunction [248,249]. Incubation of INS-1 cells with high glucose for 3 h significantly increased ROS compared with cells treated in low glucose ( $P < 0.01$ ; Figure 4-1). Treatment with 30  $\mu$ M EC significantly reduced high glucose induced ROS production to a level comparable to low glucose ( $P < 0.0001$  vs high glucose). In contrast, 0.3  $\mu$ M EC had no effect on ROS production induced by high glucose. Similar results were found when using the same concentrations of NAC to treat INS-1 cells: a concentration of 30  $\mu$ M significantly ( $P < 0.01$ ) decreased ROS in high glucose treated cells while 0.3  $\mu$ M showing no improvement.

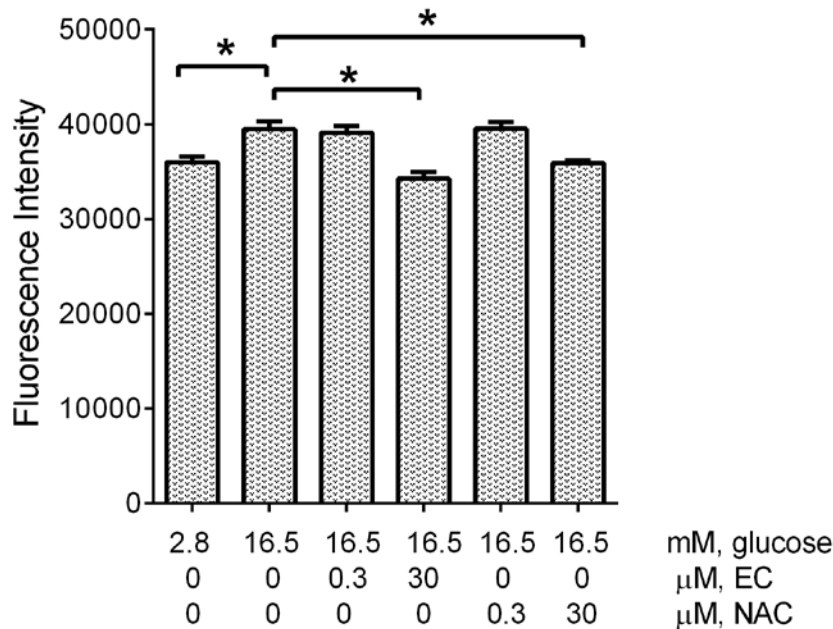


**Figure 4-1. EC at 30 μM protects against high glucose-induced ROS in INS-1 cells.**

INS-1 cells incubated 24 hours with or without EC or NAC were exposed to low or high glucose medium for 3 h in the continuous presence or absence of EC or NAC. Antioxidant status of the cells was then determined by measuring intracellular ROS accumulation after loading the cells with 5 μM of the ROS dye DCFDA for 30 min. Results were expressed in arbitrary units of fluorescence emission at 535 nm. Six to eight independent experiments were run in which each condition was tested in quadruplicate wells. \* indicates  $P < 0.05$ .

#### 4.3.2 EC at 30 μM protects against H<sub>2</sub>O<sub>2</sub>-induced ROS in INS-1 cells

We then tested whether EC treatment could reduce H<sub>2</sub>O<sub>2</sub>-induced ROS in INS-1 cells. It has been shown that H<sub>2</sub>O<sub>2</sub> treatment for 10 min can lead to impaired insulin secretion in β-cells [250]. Therefore, we measured ROS concentrations immediately after exposing cells to H<sub>2</sub>O<sub>2</sub>. ROS production was significantly increased in cells after short term exposure in H<sub>2</sub>O<sub>2</sub> compared with untreated cells ( $P < 0.001$ , Figure 4-2). Cells pretreated with 30 μM EC had significantly lower levels of ROS ( $P < 0.001$ ). Again, no significant reduction in H<sub>2</sub>O<sub>2</sub>-induced ROS was found

in cells treated with 0.3  $\mu\text{M}$  EC. When using antioxidant NAC at the same concentrations, 30  $\mu\text{M}$  NAC was effective in decreasing  $\text{H}_2\text{O}_2$ -induced ROS whereas 0.3  $\mu\text{M}$  was not.

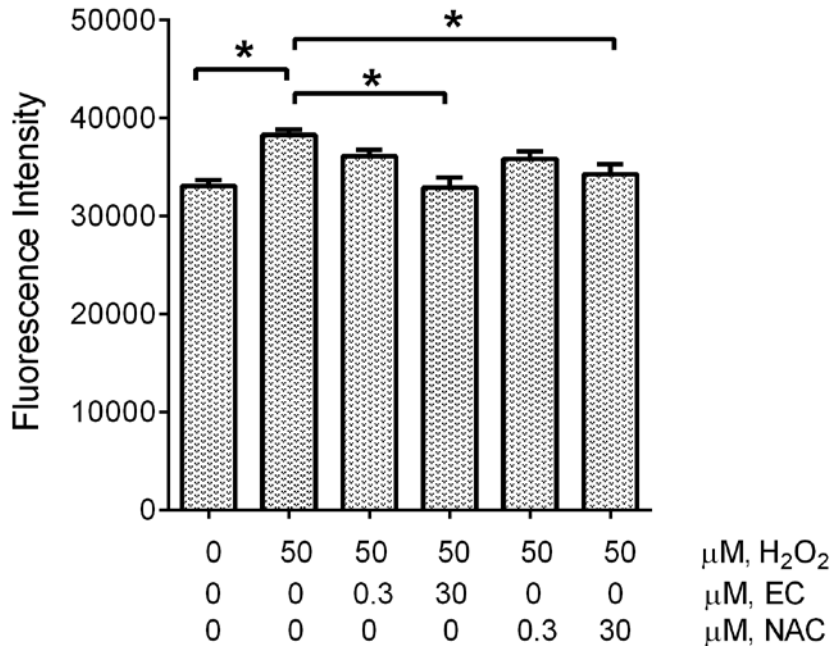


**Figure 4-2. EC at 30  $\mu\text{M}$  protects against  $\text{H}_2\text{O}_2$ -induced ROS in INS-1 cells.**

INS-1 cells incubated 24 hours with or without EC or NAC were loaded for 30 min with 5  $\mu\text{M}$  of the fluorescent ROS dye DCFDA. Cells were then exposed to 50  $\mu\text{M}$   $\text{H}_2\text{O}_2$  to increase intracellular ROS. Results were expressed in arbitrary units of fluorescence emission at 535 nm. Six or seven independent experiments were run in which each condition was tested in quadruplicate wells. \* indicates  $P < 0.05$ .

#### **4.3.3 EC at 0.3 $\mu\text{M}$ is not effective in improving cell viability of INS-1 cells treated with SFA**

Chronically exposing pancreatic  $\beta$ -cells to SFA is associated with increased cell apoptosis [130]. Consistent with this, 0.2 and 0.4 mM SFA reduced INS-1 cell viability by 40-50%. When cells were treated with either 0.2 mM or 0.4 mM SFA, addition of 0.3  $\mu\text{M}$  EC showed modest ( $P <$



0.05) or no improvement in cell viability (Figure 4-3A). Cell viability was not changed when adding 0.3  $\mu\text{M}$  NAC to SFA treated cells (Figure 4-3B).

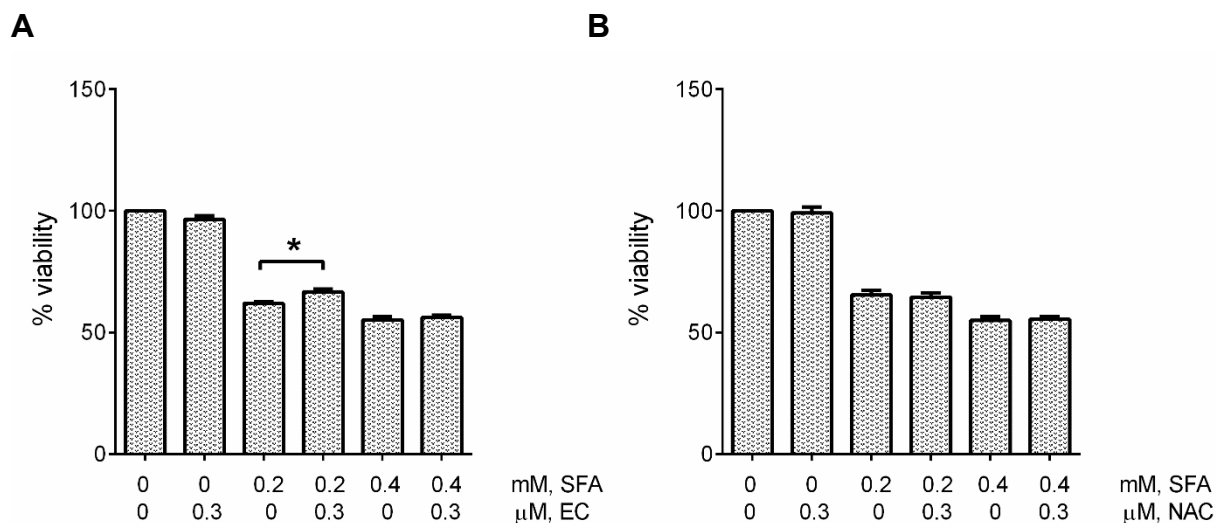


**Figure 4-3. EC (A) and NAC (B) at 0.3  $\mu\text{M}$  is not effective in improving cell viability of INS-1 cells treated with SFA.**

INS-1 cells were incubated 24 hours with or without EC or NAC in the continuous presence or absence of SFA. Cell viability was determined by an MTT assay. Four independent experiments were run in which each condition was tested in quadruplicate wells. \* indicates  $P < 0.05$ .

#### **4.3.4 EC at 0.3 $\mu\text{M}$ enhances insulin secretion from INS-1 cells treated with SFA**

Insulin secretion can be impaired by long-term SFA exposure [251]. We thus studied whether a low concentration of EC could affect insulin secretion in  $\beta$ -cells. Mean insulin secretion in response to high glucose was reduced by 30% ( $p > 0.05$ ) by treatment with 0.4 mM SFA for 24 hours (Figure 4-4). EC (0.3  $\mu\text{M}$ ) significantly increased GSIS when compared with SFA treated cells ( $P < 0.05$ ). On the contrary, SFA-impaired insulin secretion was not increased by a high concentration of EC (30  $\mu\text{M}$ ), remaining comparable to SFA treated cells. EC alone was not able

to stimulate insulin secretion as shown in cells incubated with 2.8 mM glucose and treated with 0.3  $\mu$ M EC (Figure 4-4). Thus, EC-enhanced insulin secretion is dependent on the presence of high glucose stimulation.

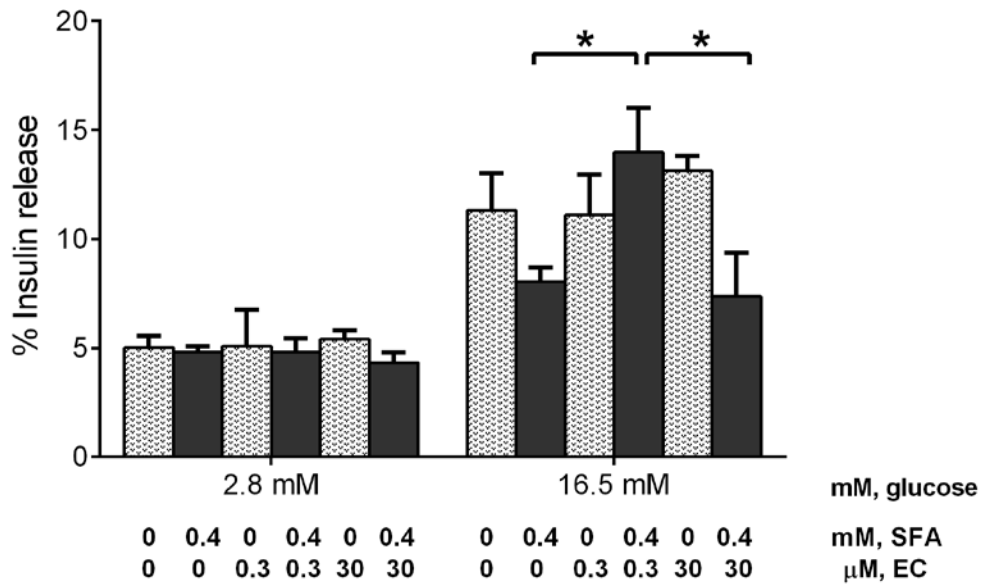


**Figure 4-4. EC at 0.3  $\mu$ M enhances insulin secretion from INS-1 cells treated with SFA.**

INS-1 cells were incubated 24 hours with or without EC in the continuous presence or absence of SFA. Then cells were exposed to low or high glucose medium for 90 min in the continuous presence or absence of EC after a quiescent period of 90 min. Total and secreted insulin was measured by RIA. Insulin release was expressed as the percentage of total insulin secreted. Five independent experiments were run in which each condition was tested in triplicate wells. \* indicates  $P < 0.05$ .

The reversed insulin secretion seen in 0.3  $\mu$ M EC-treated cells could be caused by increases in either cell numbers or secretory capacity. To clarify this question, we also calculated the total insulin content. As shown in Figure 4-5, SFA-treated cells had an ~30% decrease ( $P > 0.05$ ) in the insulin content, and EC treatment was not effective in reversing total insulin synthesized in

these cells, suggesting 0.3  $\mu$ M EC reverses insulin secretion via modulation of cell secretory capacity.

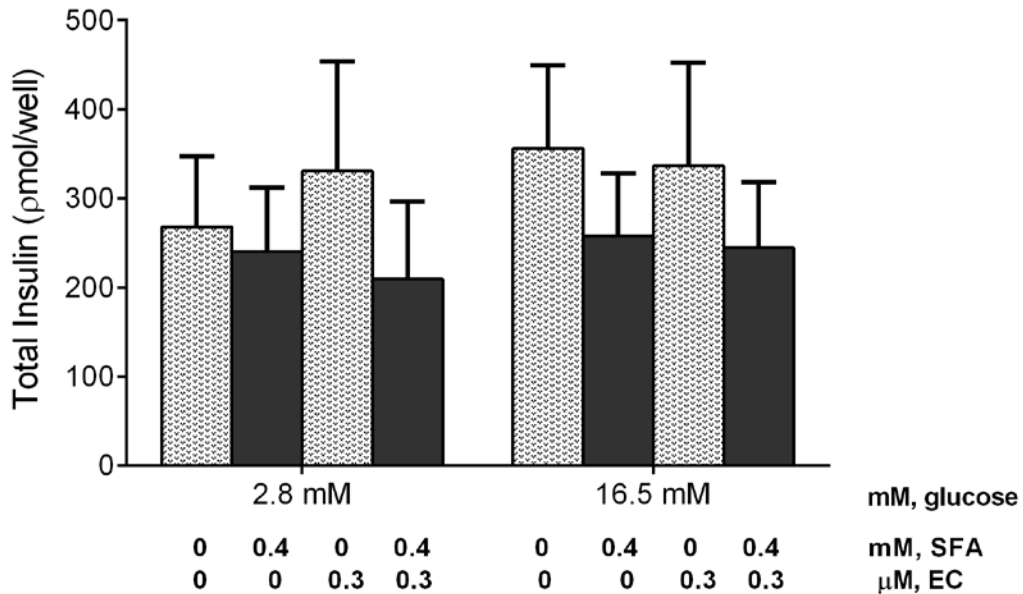


**Figure 4-5. EC and SFA's effects on total insulin synthesized in GSIS from INS-1 cells.**

INS-1 cells were incubated 24 hours with or without EC in the continuous presence or absence of SFA. Then cells were exposed to low or high glucose medium for 90 min in the continuous presence or absence of EC after a quiescent period of 90 min. Insulin secreted into the medium and remaining in the cells were measured by RIA. Total insulin synthesized was calculated as the sum of insulin secreted and remaining in the cells. Five independent experiments were run in which each condition was tested in triplicate wells.

### 4.3.5 CaMKII inhibitor KN-93 reverses EC-enhanced GSIS from INS-1 cells treated with SFA

CaMKII is considered to be a Ca<sup>2+</sup> sensor and regulator to promote insulin secretion in pancreatic β-cells [252]. EC may potentiate insulin secretion by activating CaMKII. We tested this hypothesis by blocking CaMKII using KN-93 and measuring insulin secretion in the presence of 0.3 μM EC. As expected, KN-93 decreased GSIS in normal cells to a similar level as SFA-treated cells. Furthermore, EC-enhanced GSIS was attenuated by adding 10 μM KN-93 although statistical significance was not reached (P=0.06, Figure 4-6).

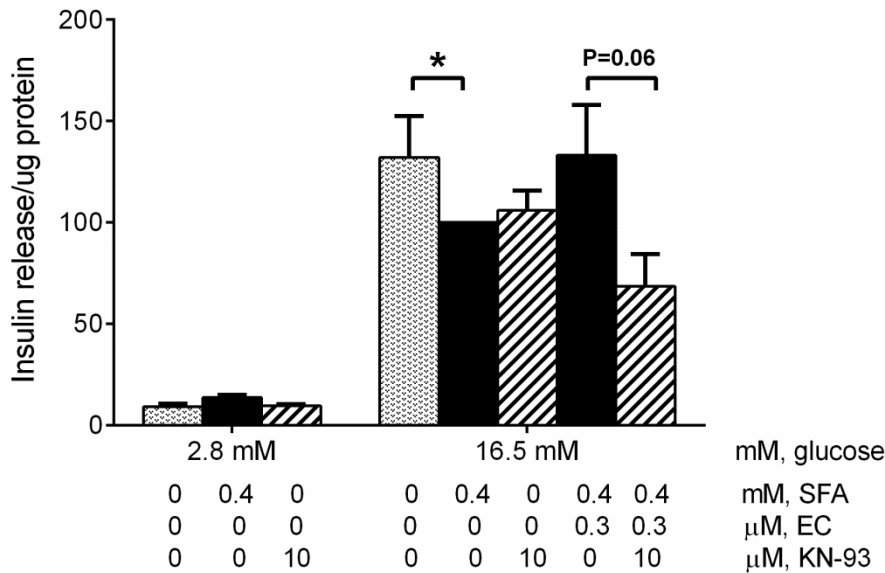


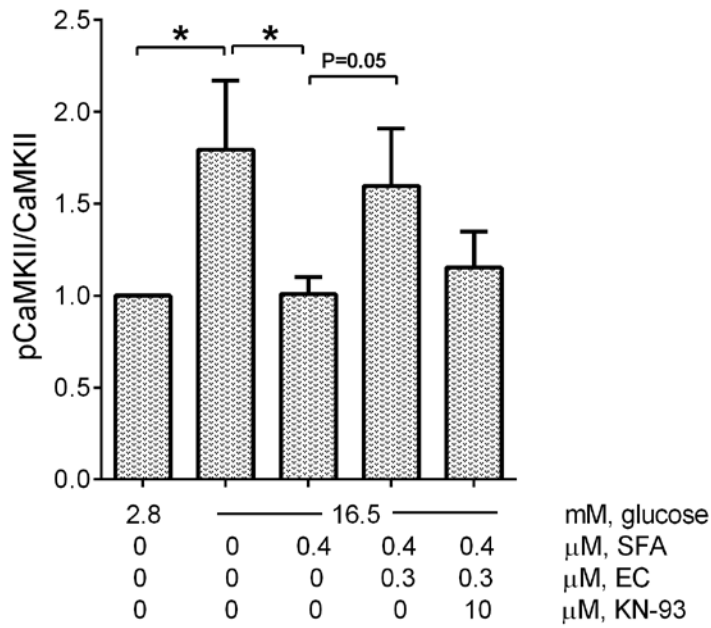
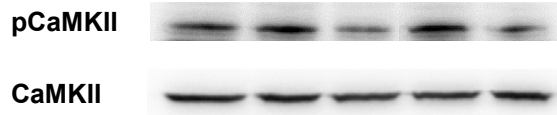
**Figure 4-6 CaMKII inhibitor KN-93 reverses EC-enhanced GSIS from INS-1 cells treated with SFA.**

INS-1 cells were incubated 24 hours with or without EC in the continuous presence or absence of SFA and KN-93. Then cells were exposed to low or high glucose medium in the continuous presence or absence of EC and KN-93 for 90 min after a quiescent period of 90 min. Insulin secreted into the medium were measured by RIA. Cells were lysed and quantified for total protein. Insulin release was expressed as per μg protein. Five independent experiments were run in which each condition was tested in triplicate wells. \* indicates P < 0.05.

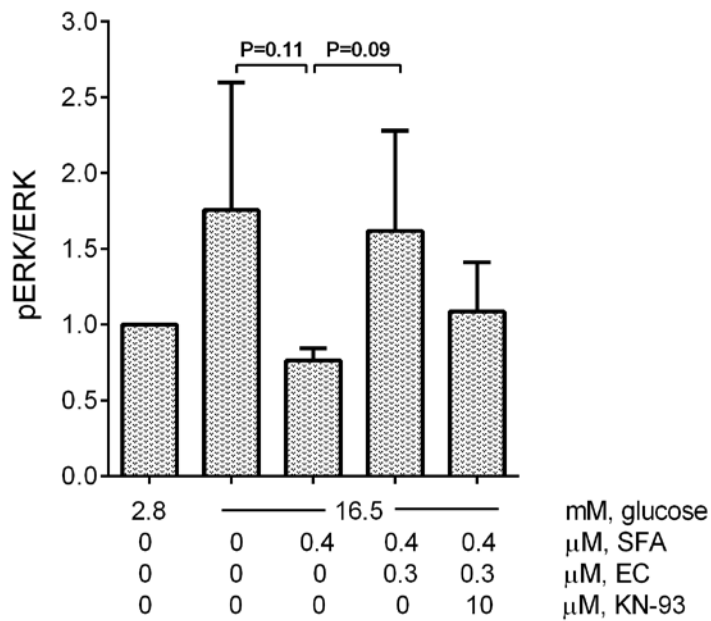
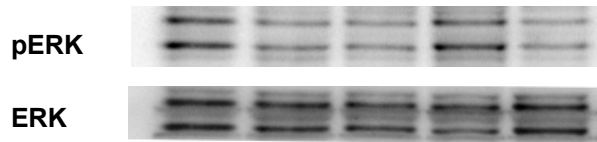
#### **4.3.6 CaMKII phosphorylation is normalized by EC in INS-1 cells treated with SFA**

To further characterize the EC-induced activation of intracellular signaling pathways, we examined the extent of phosphorylation/activation of CaMKII, ERK and PKA in INS-1 cells using inhibitor KN-93, which blocks the activation of CaMKII. As shown in Figure 4-7A, adding SFA to 16.5 mM glucose decreased phosphorylation of CaMKII to basal levels. The addition of 0.3  $\mu$ M EC was able to block SFA-mediated inhibition of CaMKII phosphorylation ( $P = 0.05$ ). EC-induced phosphorylation of CaMKII was partially blocked by preincubation of cells with 10  $\mu$ M KN-93 to a level similar to non-stimulated cells. In similar experiments to examine the effects of CAMKII antagonism by KN-93 on downstream phosphorylation of ERK, a similar pattern was detected as form CAMKII, however no significant differences were found among all the treatment groups (Figure 4-7B). PKA phosphorylation was reduced by SFA treatment, yet it was not improved in EC treated cells (Figure 4-7C).

**A**



**B**



C

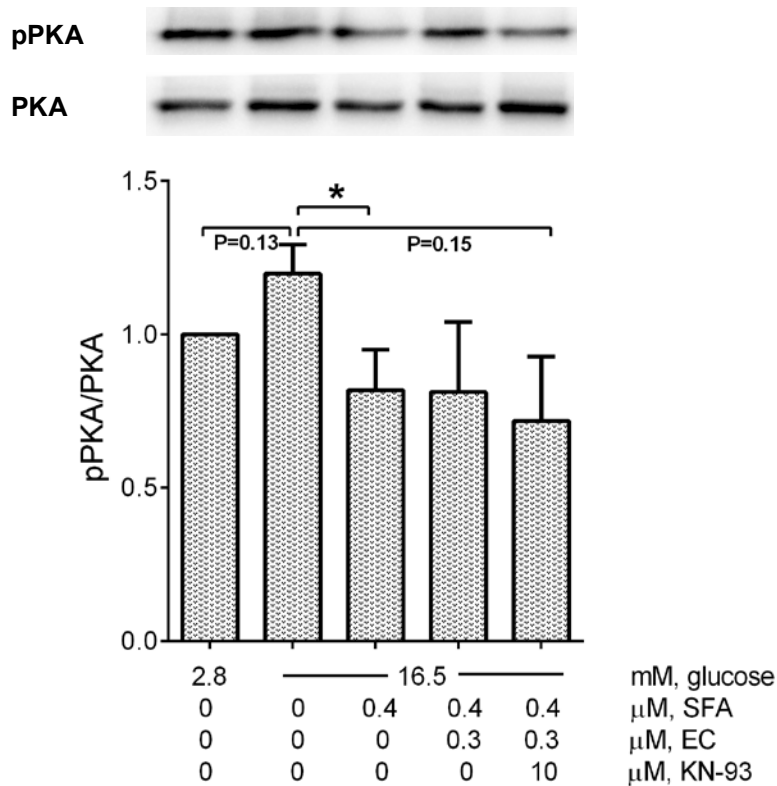


**Figure 4-7 Expression of proteins involved in EC-enhanced GSIS from INS-1 cells treated with SFA.**

INS-1 cells were incubated 24 hours with or without EC in the continuous presence or absence of SFA and KN-93. Then cells were exposed to low or high glucose medium in the continuous presence or absence of EC and KN-93 for 90 min after a quiescent period of 90 min, after which protein was harvested. Western blots were probed with specific antibodies for CaMKII, phosphorylated (p) CaMKII, ERK, pERK, PKA, pPKA and glyceraldehyde-3-phosphate dehydrogenase (GAPDH). Phosphorylation of CaMKII (A), ERK (B) and PKA (C) was normalized to total density of each respective enzyme, which was normalized to GAPDH. Four or five independent experiments were run in which each condition was tested in triplicate wells. \* indicates  $P < 0.05$ .

#### 4.4 Discussion

There is an abundance of studies investigating EC-rich foods or extracts' effect on glucose homeostasis in humans and animal models. Although controversy exists, quite a few studies have reported the effectiveness of EC in improving glucose handling and insulin sensitivity in both health and diabetes [100,173,176,178,179,187,193,195,198,199]. It has been of great interest to understand how EC exert their beneficial effects. One of the theories suggests that EC interacts with intracellular molecules to modulate cell signaling pathways [10]. In this study, we showed that a concentration (0.3  $\mu\text{M}$ ) of EC achievable via dietary intake of flavonoid-rich foods such as PAC-containing pea seed coats (Chapter 3) was able to modulate insulin secretion from pancreatic  $\beta$ -cells. The results suggest that EC enhances insulin secretion by activating CaMKII in the presence of high glucose.

Chronic elevation of free saturated fatty acids (FSFA) in plasma plays a key role in the pathology of insulin resistance and T2D [253]. FSFA also represents a crucial link between insulin resistance and  $\beta$ -cell dysfunction [254]. *In vitro* studies have found that SFA at 0.25 mM are able to blunt insulin secretion in response to glucose in isolated islets treated for 72 hours [255], and induce apoptosis in INS-1 cells and human islets after 24 hours' exposure [256]. Long-term exposure ( $\geq 48$  h) of insulin-secreting  $\beta$ -cell lines in palmitic acid (0.4 mM), another FSFA leads to impaired glucose-stimulated insulin secretion (GSIS) from the cells [130,251]. In this study, we used 0.4 mM SFA treating INS-1 cells for 24 hours to impair insulin secretion in cells. Our results showed a 30% reduction in percent insulin secretion from cells treated with SFA. Whereas adding 0.3  $\mu\text{M}$  EC potentiated insulin secretion in SFA-treated cells.

CaMKII is a multifunctional serine/threonine kinase that plays an important role in regulating nutrient metabolism, gene expression, membrane excitability, cell cycle, and neuronal communication [257]. CaMKII is expressed in pancreatic  $\beta$ -cells and several  $\beta$ -cell lines, such as INS-1, MIN6, and HIT T5 cells [258–260]. Insulin secretagogues induce the elevation of



cytosolic  $\text{Ca}^{2+}$ , which activates CaMKII and leads to autophosphorylation of the kinase. The autophosphorylation of CaMKII is thought to be crucial in extending the activation period and maintaining activity in the absence of  $\text{Ca}^{2+}$ /calmodulin [257,261]. Studies found that the activation of CaMKII is closely correlated with insulin secretion [127,128]. Overexpression of CaMKII in  $\beta$ -cells potentiates insulin secretion upon stimulation [260], whereas inhibition of the kinase impairs  $\text{Ca}^{2+}$  entry and insulin secretion during glucose stimulation [129,130]. Long-term palmitate exposure is reported to blunt the activation of CaMKII, which results in reduction in glucose or amino acid induced insulin release [130]. In our study, we also found decreases in insulin secretion (Figure 4-4 & 4-6) and that correlated with reduced CaMKII phosphorylation (Figure 4-7A) in SFA-treated cells. EC at 0.3  $\mu\text{M}$  was able to reverse this reduction. CaMKII inhibitor KN-93 alone decreased insulin release and CaMKII phosphorylation to a similar level as SFA, and it totally blocked EC's effects in SFA-treated cells (Figure 4-4 & 4-7A). Therefore, our results suggest that EC may promote insulin secretion by reversing the inactivation of CaMKII by SFA. Furthermore, EC's effect on insulin secretion is likely structure-related (Figure 4-8). Ramirez-Sanchez et al. report that catechin, a stereoisomer of EC fails to mimic EC's effects in inducing the synthesis of NO in human coronary artery endothelial cells, which is thought to be through endothelial nitric oxide synthase (eNOS) activation via CaMKII pathway [246].

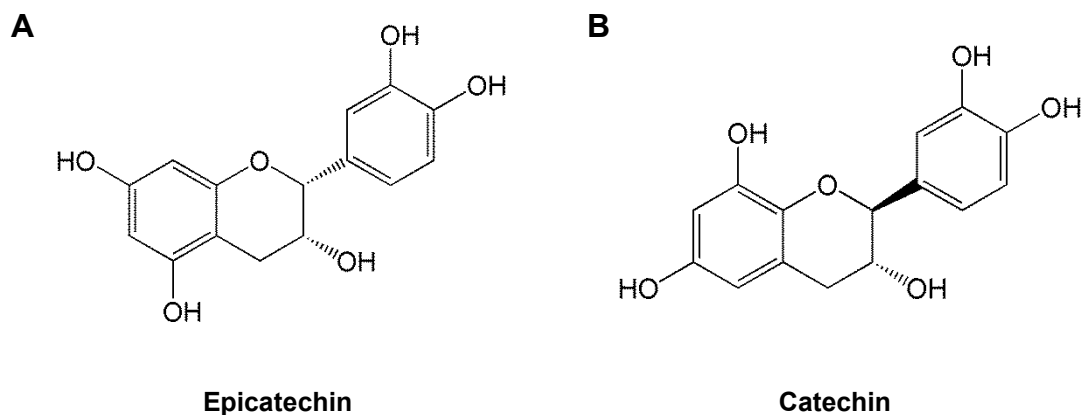


**Figure 4-8. Structure of epicatechin (EC, A) and catechin (B)**

Another interesting finding in this study is the differences in the effects of EC on ROS reduction at low and high concentrations. We found that at 30  $\mu\text{M}$  EC was effective in inhibiting ROS production induced by high glucose and acute exposure to  $\text{H}_2\text{O}_2$ , which was similar to the action of NAC at the same concentration. Neither EC nor NAC at 0.3  $\mu\text{M}$  was able to reverse the increase in ROS (Figure 4-1, 4-2). Pancreatic  $\beta$ -cells are highly sensitive to ROS mainly due to their low expression and activity of antioxidant enzymes [262]. Glucose stimulation results in endogenous  $\text{H}_2\text{O}_2$  accumulation in  $\beta$ -cells, which is thought to be necessary for insulin secretion [263], while excessive and/or sustained ROS production causes oxidative stress and leads to deterioration of  $\beta$ -cell function [249,250]. When using 3-hour high glucose stimulation or immediate  $\text{H}_2\text{O}_2$  exposure in  $\beta$ -cells, intracellular ROS presumably increase only moderately above the physiological level. Therefore it's possible that 30  $\mu\text{M}$  EC is capable of neutralizing increased ROS in our experimental settings, even though the suggested concentration of EC as an antioxidant is at least 10 times higher than 30  $\mu\text{M}$  [242]. Indeed, Martín et al. have reported that 5 – 20  $\mu\text{M}$  EC is effective in reducing ROS induced by 50  $\mu\text{M}$  t-BOOH in INS-1E cells [190]. Overall, with EC and NAC showing effects in a similar fashion, we assume that the inhibitory effect on ROS reduction observed after high EC exposure is due to their direct antioxidant ability.

On the other hand, when we compared the effects of EC on insulin secretion at low and high concentrations, 30  $\mu\text{M}$  EC was unsuccessful in enhancing SFA-impaired insulin secretion, which contradicts our initial hypothesis that 30  $\mu\text{M}$  EC can reduce oxidative stress to promote insulin secretion from  $\beta$ -cells, and suggests EC may exert other effects in  $\beta$ -cells aside from being an antioxidant. It's possible that EC inhibits protein phosphorylation at 30  $\mu\text{M}$ , as suggested by Schroeter et al [112]. That being the case, SFA-impaired CaMKII activation (phosphorylation) would not be rescued by 30  $\mu\text{M}$  EC so as to improve insulin secretion.

In pancreatic  $\beta$ -cells, glucose induced increase in cytosolic  $\text{Ca}^{2+}$  activates CaMKII, and activation of CaMKII is coincided with insulin secretion [127,128,261]. Meanwhile, studies also indicate that PKA can be activated by glucose via increase in intracellular  $\text{Ca}^{2+}$  and cyclic adenosine monophosphate (cAMP), and PKA activity correlates closely with  $\text{Ca}^{2+}$  spikes [264] and potentiates both acute and sustained insulin release [265]. In addition, activation of both CaMKII and PKA are related to ERK phosphorylation [126,130]. In this study, we failed to detect significant changes in the phosphorylation of PKA and ERK by EC treatment, although the pattern of ERK phosphorylation was similar to that of CAMKII. It has been reported that in hypothalamus, cAMP activated PKA is essential in CaMKII signaling in long-term potentiation (LTP) by inhibiting protein phosphatase-1 (PP1), which specifically dephosphorylates CaMKII [266–268]. Likewise, PKA may have a similar effect on CaMKII in pancreatic  $\beta$ -cells. As a result, EC treatment may only specifically affect CaMKII phosphorylation but not PKA. The schematic diagram is shown in Figure 4-9.

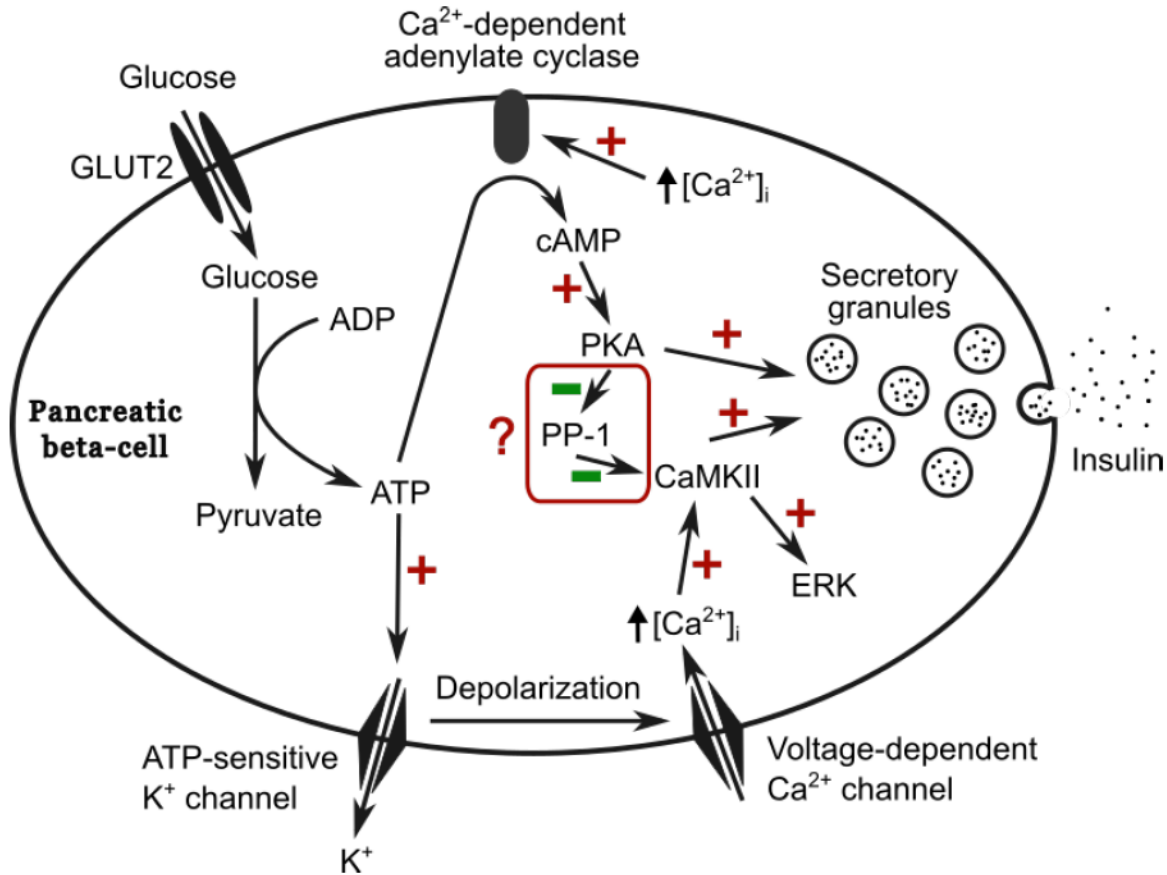


**Figure 4-9 Schematic diagram of the possible pathways of CaMKII and PKA in insulin secretion in pancreatic  $\beta$ -cells.**

Increase in cellular adenosine triphosphate (ATP)/adenosine diphosphate (ADP) ratio by glycolysis closes ATP-sensitive K<sup>+</sup> channels, which, in turn, causes membrane depolarization and opening of voltage-dependent Ca<sup>2+</sup> channels, leading to increased cytosolic [Ca<sup>2+</sup>]<sub>i</sub>. The increased [Ca<sup>2+</sup>]<sub>i</sub> activates Ca<sup>2+</sup>/calmodulin-dependent protein kinase II (CaMKII), which serves as the triggering signal in glucose-induced insulin secretion and increases extracellular signal-regulated kinase (ERK) phosphorylation. The increased [Ca<sup>2+</sup>]<sub>i</sub> also leads to activation of the Ca<sup>2+</sup>-dependent adenylate cyclase, which raises the cyclic adenosine monophosphate (cAMP) level leading to protein kinase A (PKA) activation. Activated PKA then prevents dephosphorylation of CaMKII by inhibiting protein phosphatase-1 (PP1), which specifically dephosphorylates CaMKII.

Although our results indicate a role of CaMKII in EC-enhanced insulin secretion in pancreatic  $\beta$ -cells, how EC activates CaMKII is still unknown. Moreno-Ulloa et al. suggest there may be an EC receptor that exists on cell membranes in endothelial cells [269], which could also be the case in pancreatic  $\beta$ -cells. We also didn't convincingly identify the downstream targets of CaMKII. It has been reported that CaMKII's substrates in  $\beta$ -cells includes microtubule-associated protein 2 (MAP-2) and synapsin I [252,261], hence, it's conceivable that CaMKII may also play a role in the transport of insulin granules to exocytosis sites in  $\beta$ -cells.

EC treatment has been reported to promote pancreatic  $\beta$ -cell regeneration in diabetic animal models *in vivo* [100,189,199]. Martín et al. also found EC from cocoa can increase viability in t-BOOH-treated INS-1E cells [190]. In contradiction to their findings, this study found that EC at 0.3  $\mu$ M didn't enhance cell viability of INS-1 cells treated with 0.2 or 0.4 mM SA. This is not surprising since in comparison with their cell model induced by 2-hour 50  $\mu$ M t-BOOH treatment, we used a 24-hour SFA incubation to impair cells, which is associated elevated ROS, disrupted lipid metabolism, mitochondrial dysfunction, alternations in  $\beta$ -cell gene expression and signaling, impaired insulin secretion, upregulated inflammatory responses and apoptosis [254,270]. In addition, we adopted a much lower but physiologically relevant concentration of EC at 0.3  $\mu$ M, whereas their effective concentrations of EC ranging from 5 to 20  $\mu$ M, which is about 20 – 60 times higher. Most importantly, the improved GSIS reported by Martín et al. could be due to increased cell numbers. In contrast, in this study, the insulin content in SFA treated cells decreased by ~30% (Figure 4-5) consistent with the reduction in viability (Figure 4-3A), while EC-treatment was able to increase insulin secretion by ~40% compared with SFA-treated cells (Figure 4-4,  $P < 0.05$ ). Therefore, we proved that 0.3  $\mu$ M EC potentiated insulin secretion via modulation of cellular signaling rather than enhanced cell viability.

Taken all together, our data support that EC at a physiological level (0.3  $\mu$ M) can act as a signaling molecule to stimulate insulin secretion via activation of CaMKII. EC at 30  $\mu$ M has

similar effects as NAC on ROS reduction, while having no effect on promoting insulin secretion. Due to its different actions at different concentrations, application of EC as a nutraceutical would have to be with careful evaluation of the dose according to specific conditions. Meanwhile, further investigation is needed to characterize the signaling pathways of EC in  $\beta$ -cells.

## Chapter 5

### **Flavan-3-ols improvement of insulin sensitivity and modulation of hepatic glucose production is associated with suppression of PEPCK expression in glucose intolerant rats**

#### **5.1 Introduction**

The liver plays a central role in the control of glucose homeostasis as a major depot for glucose uptake and storage. After a meal, up to one-third of glucose intake is disposed of in the liver [271,272], while in the post-absorptive state, approximately 80% of circulating glucose is produced by the liver via glycogenolysis and gluconeogenesis [116]. It is also the site of clearance of ~80% of endogenously secreted insulin [273].

Insulin signaling is crucial in modulating glucose metabolism in hepatocytes. Insulin's action in liver is through activation of the insulin receptor tyrosine kinase to initiate Akt/PKB signaling pathway. It promotes glucose utilization and storage as glycogen, meanwhile inhibiting hepatic glucose production (HGP) via down-regulation of phosphoenolpyruvate carboxykinase (PEPCK) and glucose-6-phosphatase (G6Pase) [136]. Disrupting insulin signaling by knocking out insulin receptor specifically in mouse liver leads to severely impaired glucose tolerance, insulin clearance, and aberrant hepatocyte morphology and function [274]. Impaired hepatic insulin sensitivity causes unsuccessful suppression of HGP, which is considered to be one of the causes of hyperglycemia in type 2 diabetes (T2D) [275].

Glucagon acts on the liver directly to enhance HGP. In the short term, glucagon stimulates glycogenolysis to increase glucose output from the liver, whereas in the longer term, it upregulates expression of PEPCK and G6Pase to enhance gluconeogenesis [147]. Studies in T2D

patients have reported that irregular glucagon concentration/release in both fasting and postprandial state leads to increased HGP, contributing to hyperglycemia [233,276–278].

To control hyperglycemia caused by increased HGP in T2D, 5' adenosine monophosphate (AMP)-activated protein kinase (AMPK) has been considered as a possible therapeutic target. AMPK is a serine/threonine protein kinase that acts as a sensor of cellular energy status. It can be activated by several modulatory molecules, such as increased AMP:adenosine triphosphate (ATP) ratio, Ca<sup>2+</sup>/calmodulin-dependent protein kinase kinase  $\beta$  (CaMKK  $\beta$ ), and liver kinase B1 (LKB1) [139]. Activation of AMPK in general stimulates catabolic pathways that generate ATP (e.g. glucose uptake, glycolysis), while inhibiting anabolic pathways that consume ATP (e.g. synthesis of glycogen, fatty acids, cholesterol and protein) [140]. As a result, in hepatocytes, AMPK activation is able to suppress glucose production from gluconeogenesis by decreasing gene transcription of PEPCK and G6Pase [142].

Plant polyphenols undergo phase II metabolism in the liver to enter the systemic circulation [279] but also exert biological effects on hepatocytes. Specifically, flavan-3-ols including catechin and proanthocyanidins (PAC) have the ability to activate AMPK [182]. Flavan-3-ols are a subgroup of flavonoids. They exist in a variety of plants, such as tea, wines, fruits, beans and peas [5]. Their structures are characterized by different degrees of polymerization (DP) of catechin and epicatechin [5]. Flavan-3-ols with small molecular weight (up to trimers), are suggested to be absorbed and metabolized in enterocytes and hepatocytes [32,280], hence are bioavailable to the body. Due to their low concentrations in both blood and tissues, it's likely they exert their effects as cellular signaling molecules to modulate cell signaling pathways [10].

Epigallocatechin-3-gallate (EGCG), a main catechin from green tea shows an inhibitory effect on gluconeogenesis from hepatocytes; this effect is mediated by activation of AMPK via CaMKK  $\beta$ , because a CaMKK  $\beta$  inhibitor blocks EGCG-induced phosphorylation of both AMPK and CaMKK  $\beta$  [184]. Mice fed a dietary bilberry extract have a decrease in HGP as a result of significantly



activated AMPK and down-regulated PEPCK and G6Pase in the liver [183]. Likewise, PAC-rich black soybean extract improves insulin sensitivity in T2D mice and down-regulates gluconeogenesis in the liver via activation of AMPK [181]. Yogalakshmi et al. report that grape seed PAC activates AMPK in the liver, but to a lesser extent compared with metformin, whereas using grape seed PAC with metformin potentiates AMPK activation [186]. In contrast, the insulin signaling pathway, in addition to AMPK, is reported to be activated when HepG2 cells are treated with a cocoa epicatechin [185]. Taken all together, the existing evidence suggests flavan-3-ols are able to act as cellular signaling molecules, however, bioavailability of the experimental compounds used in those studies has not systematically been taken into consideration. Besides, there is still no conclusive answer regarding whether PAC's target in the cells is AMPK, the insulin signaling pathway, or both.

Findings from our previous study revealed a slower glucose recovery rate during the last 60 min of an insulin tolerance test (ITT) in PAC-treated groups compared with high fat diet (HFD) group. Given that hepatic glucose production (HGP) contributes mostly to the last phase glucose recovery of ITT [223], those results indicated that PAC treatments suppress HGP under the fasting state, implying a role of PAC in improving hepatic insulin sensitivity. Therefore, we aimed to further examine PAC's effects on the liver and investigate the mechanisms underlying the effects of PAC on hepatic glucose homeostasis. A PAC-rich pea seed coat 'Solido' was used to prepare two kinds of diet supplements: a raw ground pea seed coat with high DP ( $DP \geq 5$ , PAC), and a hydrolyzed ground pea seed coat with low DP ( $DP \leq 3$ , HPAC). They were supplemented to high fat diet for rats; thus, by doing so we would be able to distinguish the difference caused by bioavailability of flavan-3-ols. We hypothesized that flavan-3-ols could improve hepatic insulin sensitivity and modulate hepatic glucose homeostasis by activating the AMPK pathway, and that flavan-3-ols with low DP (HPAC) would be more effective than high DP (PAC).

## 5.2 Methods

### 5.2.1 Preparation of pea seed coat diets

Seed coats of pea (*Pisum sativum L.*) cultivar ‘Solido’ were obtained from Mountain Meadows Food Processing Ltd. (Legal, Alberta, Canada). Pea seed coat fractions were processed as described in Chapter 3. PAC and HPAC fractions were added to a high fat diet (Table 5-1) such that the final concentration of both was 0.8% (w/w).

**Table 5-1. Experimental diet formulas.**

Ingredient (g)	HFD	PAC	HPAC
Canola stearine *	99.5	99.5	99.5
Flaxseed oil †	6	6	6
Sunflower oil ‡	94.5	94.5	94.5
Casein §	270	254	254
L-Methionine ¶	2.5	2.5	2.5
Dextrose §	189	189	189
Corn Starch ‡	169	169	169
Cellulose §	100	0	0
‘Solido’ seed coat (raw or hydrolyzed)	0	193	193
Mineral mix Bernhart & Tomarelli §	51	51	51
Vitamin mix AIN-93-VX §	10	10	10
Inositol ¶	6.3	6.3	6.3
Choline Chloride ¶	2.8	2.8	2.8

Note: To avoid other dietary factors’ effects on the outcomes, the nutrient contents of both raw and hydrolyzed pea seed coats (PSC) were analyzed (data not shown). The amount of added PSC was calculated to ensure diets were equal in total fat (20.0% w/w), protein (27.9% w/w), carbohydrate (35.8% w/w) and fibre (10.0% w/w) and thus were equal in caloric density. PAC content was  $264.1 \pm 14.6$  mg/100 g unprocessed PSC [204] as determined by the butanol-HCl-Fe<sup>3+</sup> method.

\* Richardson Oilseed, † Shoppers Drug Mart, ‡ Canada Safeway, § Harlan, ¶ MP Biomedicals.

### **5.2.2 Animal feeding trial**

The guidelines of the Canadian Council on Animal Care and the International Guide and Care of Laboratory Animals were followed in all animal experiments. Protocols were approved by the Animal Care and Use Committee of the University of Alberta. Male Sprague-Dawley rats (n=24) were obtained from Charles River Canada (St. Constant, QC) at 8 weeks of age and housed 2 per cage. All the animals had 1 week of acclimatization with access to standard chow and water *ad libitum*. Then they were randomized into 3 groups, i.e. high fat diet (HFD), PAC-supplemented HFD (PAC), and HPAC-supplemented HFD (HPAC). All the groups were introduced to a 6-week HFD regimen to induce glucose intolerance, which was confirmed using an oral glucose tolerance test (see below). Then they were switched to the experimental diets (Table 5-1) for 4 weeks. Body weights were measured weekly and food intake was recorded daily. At the end of the feeding, rats' lean and fat mass was determined by an EchoMRI Whole Body Composition Analyzer (Echo Medical Systems LLC, Houston, TX, USA).

### **5.2.3 Glucose and insulin tolerance tests**

Oral glucose tolerance test (OGTT) and insulin tolerance tests (ITT) were conducted as described in Chapter 3.

### **5.2.4 Tissue collection**

Fed rats were euthanized under anaesthesia (pentobarbital sodium 60 mg/kg, ip) by exsanguination. Blood (5-10 ml) was obtained from the abdominal aorta and divided for preparation of plasma and serum, which were frozen at -80°C. The liver and epididymal fat pad was extracted and weights recorded. Samples of the liver were snap-frozen in liquid N<sub>2</sub> and stored at 80°C.

### **5.2.5 Analysis of plasma insulin and glucagon**

Plasma samples obtained during the OGTT and tissue collection were analysed as described in Chapter 3. Briefly, samples were assayed in duplicate for insulin and glucagon by ELISA using commercial assay kits according to the manufacturer's instructions (rat insulin ELISA, Alpco Diagnostics, Salem, NH, USA; glucagon EIA kit, SCETI K.K., Tokyo, Japan).

### **5.2.6 Antioxidant assay**

The total antioxidant capacity (TAC) in serum was measured using an Antioxidant Assay Kit (Sigma, Saint Louis, MO, USA) following manufacturer's instruction. The specific assay is based on the formation of a ferryl myoglobin radical from myoglobin and hydrogen peroxide, which oxidizes ABTS [2,2'-azino-bis(3-ethylbenzthiazoline-6-sulfonic acid)] to produce a radical cation ABTS<sup>+</sup>, a soluble green color chromogen that can be determined spectrophotometrically at 405 nm (A<sub>405</sub>). In the presence of antioxidants the radical cation is suppressed to an extent dependent on the activity of the antioxidant and the color intensity is decreased proportionally (A<sub>405</sub> decreases). Trolox (6-hydroxy-2,5,7,8-tetramethylchroman-2-carboxylic acid), a water-soluble vitamin E analogue, serves as a standard or a control antioxidant [25]. In a 96-well plate, serum samples were mixed with 1X myoglobin working solution, ABTS working solution from the Kit, and 3% hydrogen peroxide and allowed to incubate at room temperature for 30 min. Stop solution was added to each well, and the absorbance of each well was measured using a microplate reader (SpectraMax 190, Molecular Devices) at 405 nm. The results were calibrated using a reference curve based on the soluble antioxidant Trolox as a standard and TAC was expressed in Trolox concentration (mM).

### **5.2.7 Total glutathione (tGSH) assay**

Total glutathione (tGSH) in the liver was measured colorimetrically using a Total Glutathione (tGSH) Microplate Assay kit (Eagle Biosciences; Boston, MA, USA). Briefly, liver samples were homogenised in 5% metaphosphoric acid (MPA) on ice to prepare a 0.5 mg/ml lysate. Standards and samples (50 µl/well) were added to the assay plate. Next, 5,5'-dithiobis(2-nitrobenzoic acid)

(DTNB) and glutathione oxidoreductase (50  $\mu$ l/well, respectively ) were added and incubated for 10 min at room temperature, allowing glutathione to reduce DTNB and form a mixed disulfide and a colored ion. This mixed disulfide then reacted with glutathione that is present in the sample to form glutathione disulfide (GSSG) and another colored ion. GSSG re-enters this cycle once it is reduced enzymatically. The absorbance of each well was measured using a microplate reader (SpectraMax 190, Molecular Devices) at 405nm at one-minute intervals for 10 minutes after the addition of  $\beta$ -NADPH<sub>2</sub> (50  $\mu$ l/well). Absorbance values were then used to determine the concentration of total glutathione (GSH and GSSG) present in the sample.

### **5.2.8 Measurement of hepatic glycogen concentrations**

Glycogen content was determined by an acid-hydrolysis method [281]. Basically, glucose, the hydrolysis product of glycogen, was converted into glucose-6-phosphate (G-6-P) by hexokinase in the presence of ATP. With a supply of NADP<sup>+</sup>, G-6-P was further converted into 6-phosphogluconic acid by glucose-6-phosphate dehydrogenase (G-6-PDH), while parallel production of NADPH was measured spectrophotometrically. Liver samples were boiled in ddH<sub>2</sub>O for 5 min, and centrifuged at 13000 rpm for 10 min. Supernatant was collected and hydrolyzed at 100°C in 3M HCl for 3 h. Then samples were neutralized with an equal volume of 3M NaOH. Glucose concentration of the hydrolysis product was determined using the Glucose (hexokinase, HK) assay reagent according to the manufacturer's instructions (Sigma-Aldrich, Saint Louis, MO, USA). Free glucose was measured in samples without hydrolysis. The absorbance of each well was measured using a microplate reader (SpectraMax 190, Molecular Devices, CA, USA) at 340 nm.

### **5.2.9 Western blot analysis**

Frozen liver samples were thawed on ice and homogenised in radioimmunoprecipitation assay (RIPA) buffer as previously described (Chapter 4). Total protein was measured using a Lowry protein assay (Sigma-Aldrich, Saint Louis, MO, USA). Samples (20  $\mu$ g protein) were subjected to

SDS-PAGE followed by blotting onto nitrocellulose membranes. The membranes were blocked in 5% skimmed milk–0.1% Tween–Tris-buffered saline for 60 min followed by overnight incubation at 4°C with primary antibodies diluted in blocking buffer. Primary antibodies were anti-AMPK $\alpha$  (1:1000), anti-phospho-Thr172-AMPK  $\alpha$  (pAMPK $\alpha$ , 1:1000), anti-Akt (1:1500), anti-phospho-Thr308-Akt (pAkt Thr308, 1:1500) and anti-phospho-Ser473-Akt (pAkt Ser473, 1:1500) from Cell Signaling Technology, Inc. (Danvers, MA, USA); and pyruvate carboxykinase (PEPCK; 1:1000) from Cayman Chemical (Ann Arbor, MI, USA). Membranes were subsequently incubated with the appropriate peroxidase-conjugated secondary antibodies (1:5000; Sigma, Saint Louis, MO, USA) for 1 h at room temperature. Labelling of specific proteins was compared with  $\beta$ -actin (Sigma) used as loading control. Membranes were developed using ECL Prime (GE Healthcare Bio-Sciences Corp., Piscataway, NJ, USA) and digital images captured using a ChemiDoc MP™ imaging system (Bio-Rad Laboratories, Inc., Mississauga, ON, Canada). Band intensity was quantified by Quantity One v4.6.2 (Bio-Rad Laboratories, Inc., Hercules, CA, USA).

#### **5.2.10 Statistical analysis**

Results are presented in bar charts, with the top line indicates the mean and the whiskers the standard error of the mean (SEM). Analysis of variance (ANOVA) followed by Bonferroni's post hoc test was used to assess differences between different conditions using GraphPad Prism 6 (GraphPad Software, Inc., San Diego, CA, USA). Non-normal distributed data were  $\log_{10}$  transformed firstly; depending on whether the transformed data were normal or non-normal distributed, either parametric or nonparametric analyses were used, respectively. Values of  $P < 0.05$  were considered statistically significant.

## 5.3 Results

### 5.3.1 PAC- and HPAC-feeding decrease body weight gain induced by HFD

Body weight gain was significantly decreased in HPAC compared to HFD (Table 5-2,  $P < 0.05$ , see also in Chapter 3, Figure 3-3), despite that HFD had the lowest energy intake among all groups. The total fat and epididymal fat mass in HPAC was significantly lower than that in HFD ( $P < 0.05$ , see also in Chapter 3, Table 3-3), whereas total lean mass was not different among all groups. PAC had reduced body weight gain even with the highest energy intake ( $P < 0.05$ , see also in Chapter 3, Table 3-3). There was a significant decrease in liver weight in PAC compared with HFD ( $P < 0.05$ ).

**Table 5-2. Energy Intake, body weight and tissue weights.**

	HFD	PAC	HPAC	P value
Energy Intake (kcal/rat/d)	134.4 ± 4.9	179.0 ± 12.3*	171.2 ± 14.4	0.045
Δ Body Weight (%)	63.1 ± 3.0	54.7 ± 2.8*	47.6 ± 4.1*	0.0002
Total Fat/Final Wt, %	16.8 ± 1.2	15.0 ± 1.2	11.3 ± 0.9*	0.039
Total Lean/Final Wt, %	67.0 ± 1.0	69.2 ± 1.0	70.8 ± 0.9	0.079
Liver/Final Wt, %	3.12 ± 0.04	2.84 ± 0.08*	3.15 ± 0.05	0.002
Epididymal Fat/Final Wt, %	2.40 ± 0.13	2.39 ± 0.38	1.75 ± 0.18*	0.043

Values are means ± standard error; one-way ANOVA P values are shown in the last column; N = 8 for all groups. \*  $P < 0.05$ , compared to HFD, Bonferroni's multiple comparison.

### 5.3.2 HPAC has marginally decreased fasting plasma insulin and glucagon

Concentrations of fasting plasma insulin in HPAC were significantly decreased compared to HFD (Table 5-3,  $P < 0.05$ ). However, fasting glucagon in HPAC decreased by about 50% but failed to be statistically significant (Table 5-3, compared with HFD,  $P = 0.08$ ). Fasting blood glucose had no differences among groups. Calculation of homeostasis model assessment-

estimated insulin resistance index (HOMA-IR) showed that HPAC had the lowest score compared with other groups (P=0.04), suggesting improvements in fasting insulin sensitivity. Serum antioxidant concentrations were similar in all groups.

**Table 5-3. Antioxidant, glucose, insulin, glucagon in blood and HOMA-IR.**

	HFD	PAC	HPAC	P value
Serum Antioxidant Concentration (mmol/L)	0.21 ± 0.02	0.20 ± 0.02	0.21 ± 0.02	NS
Fasting Glucose (mmol/L)	5.53 ± 0.27	5.58 ± 0.27	5.21 ± 0.09	NS
Fasting Insulin (ng/mL)	1.18 ± 0.20	0.92 ± 0.26	0.42 ± 0.07*	0.04†
Fasting Glucagon (pg/mL)	90.96 ± 17.85	61.64 ± 9.96	43.5 ± 11.18	0.08
HOMA-IR	1.38 ± 0.25	1.54 ± 0.37	0.48 ± 0.08*	0.04†
ITT Slope <sub>60-120min</sub> (mmol/L/min)	0.033 ± 0.004	0.014 ± 0.004*	0.005 ± 0.004*	0.0002

Values are means ± standard error, one-way ANOVA P values are shown in the last column; N = 8 for all groups. \* P<0.05, compared to HFD, Bonferroni's multiple comparison. † indicates data analyzed after log<sub>10</sub> transformation.

### 5.3.3 PAC increases hepatic glutathione and glycogen content

It has been suggested that low concentration of flavan-3-ols in tissues can modulate redox enzymes. We found that hepatic tGSH concentration was significantly increased in PAC but not in HPAC, compared with HFD (Figure 5-1, P < 0.05). PAC also had increased glycogen content in the liver compared with HFD (Figure 5-2, P < 0.05).



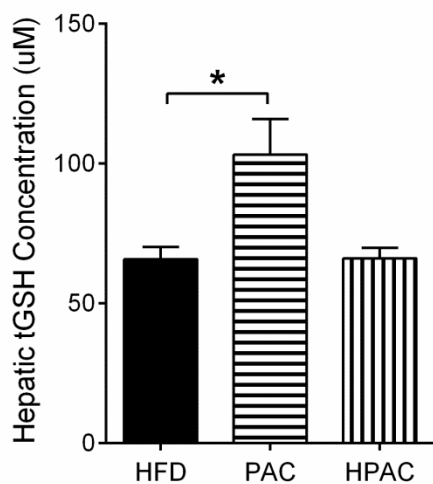


**Figure 5-1. Effects of PAC and HPAC on total glutathione concentrations in the liver.**

Liver samples were assayed for total glutathione (tGSH) concentrations as described. N=8 for all groups. \*P < 0.05, Bonferroni's multiple comparison.

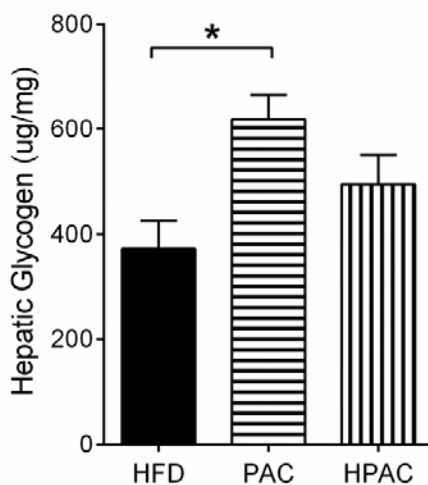


**Figure 5-2 Effects of PAC and HPAC on hepatic glycogen content.**

Liver samples were assayed for glycogen content as described. N=8 for all groups. \*P < 0.05, Bonferroni's multiple comparison.

#### **5.3.4 HPAC reverses glucose intolerance induced by HFD**

During oral glucose challenge, blood glucose at each time point was not different among all groups (Figure 5-3A), however, HPAC had a decreased overall glucose response suggested by a significantly lower AUC compared with HFD (Figure 5-3C,  $P < 0.05$ ). Insulin secretion in HPAC during OGTT was significantly reduced by about 50% compared to HFD (Figure 5-3B and 5-3D,  $P < 0.05$ ). Insulin-glucose AUC index is calculated as the product of AUCs of insulin and glucose response curves, in which a higher value suggests higher degree of insulin resistance [221]. As a result of decrease in both glucose and insulin response during OGTT, HPAC had the lowest score of insulin-glucose AUC index, indicating alleviated insulin resistance. In contrast, the improvement in insulin sensitivity in PAC was moderate and not significantly different from HFD.

#### **5.3.5 HPAC affects hepatic glucose output during insulin challenge**

Upon insulin challenge, glucose typically falls and then climbs back towards baseline upon degradation of the injected insulin. The rate of decline in the initial phase indicates insulin sensitivity in peripheral tissues, while the rate of the recovery phase indicates hepatic glucose output [217]. As reported in Chapter 3, we didn't detect any difference during the first 30 min after insulin injection. However, HPAC had lower glucose at 90 min and 120 min (Chapter 3), and a smaller slope of glucose recovery during 60-120 min compared with HFD (Table 5-3), suggesting attenuated hepatic glucose production (HGP). Similar results were also found in PAC, indicating less glucose production from the liver.

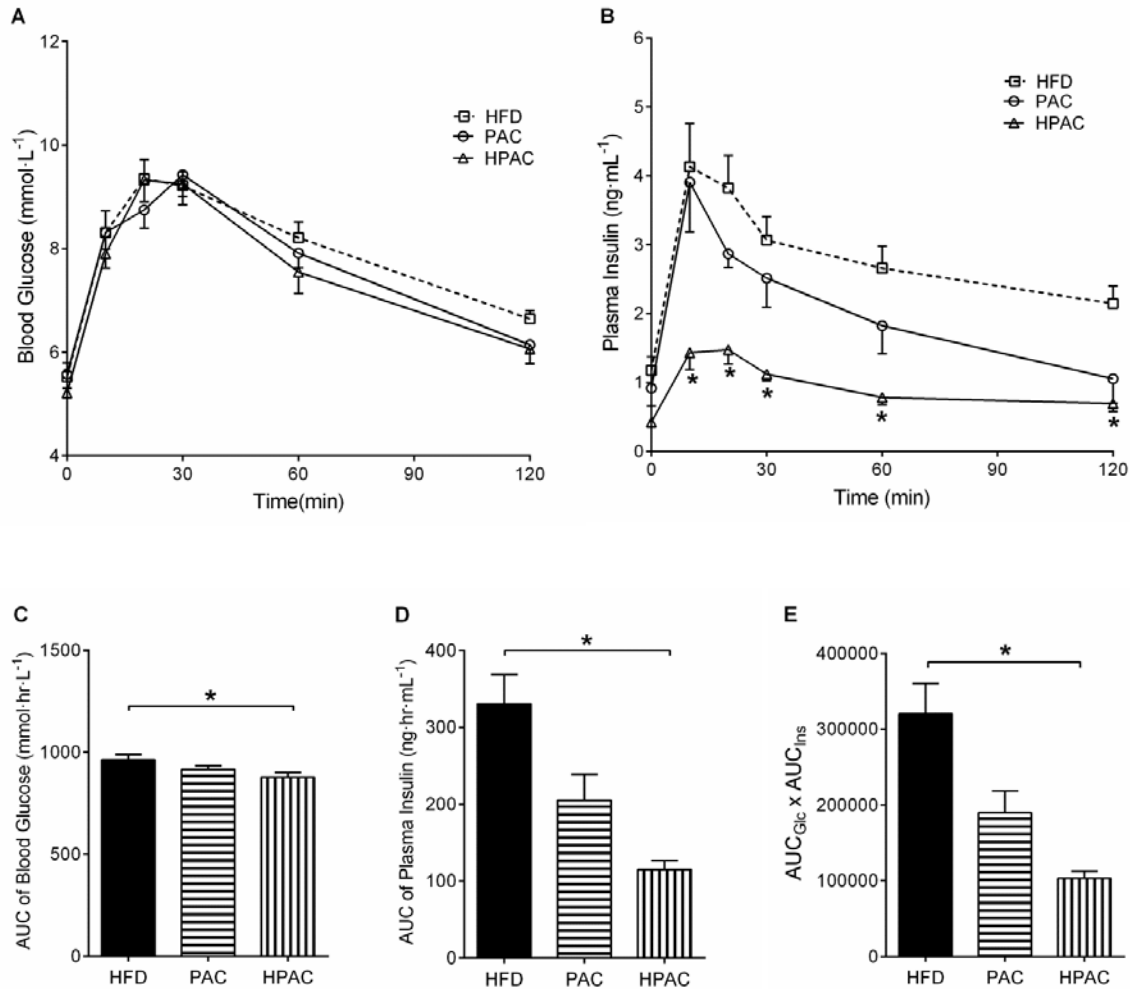


**Figure 5-3 Glucose and insulin responses after oral glucose challenge.**

Oral glucose tolerance tests were performed at week 11. After overnight fasting, blood glucose (A) and plasma insulin (B) were measured at 0, 10, 20, 30, 60, 120 min after oral administration of 1 g/kg body weight glucose. Area under the curve (AUC) of glucose response (C) and insulin secretion (D) were calculated from A and B, respectively. (E) Insulin-glucose AUC index calculated from the product of glucose and insulin AUC, where a lower value indicates increased insulin sensitivity [221]. N=8 for all groups. \*P < 0.05, Bonferroni's multiple comparison.

### **5.3.6 Effects of PAC and HPAC on the expression of hepatic enzymes**

HGP can be suppressed by activation of both insulin dependent (Akt) and independent (AMPK) pathways. Activation of both pathways will lead to a decrease in PEPCK expression thus inhibiting gluconeogenesis. To understand how PAC and HPAC suppressed HGP, we measured protein expression and phosphorylation of AMPK, Akt and PEPCK. Total AMPK and total Akt expression were not different among all groups (data not shown). Phosphorylation of AMPK in HPAC was similar to HFD, whereas PAC had 40% lower pAMPK compared with HFD (Figure 5-4A,  $P < 0.05$ ). Phosphorylation of Akt at either Serine 473 or Threonine 308 was not different among all groups (Figure 5-4B and 5-4C). Nonetheless, PEPCK expression in PAC was significantly reduced compared with HFD (Figure 5-4D,  $P < 0.05$ ).

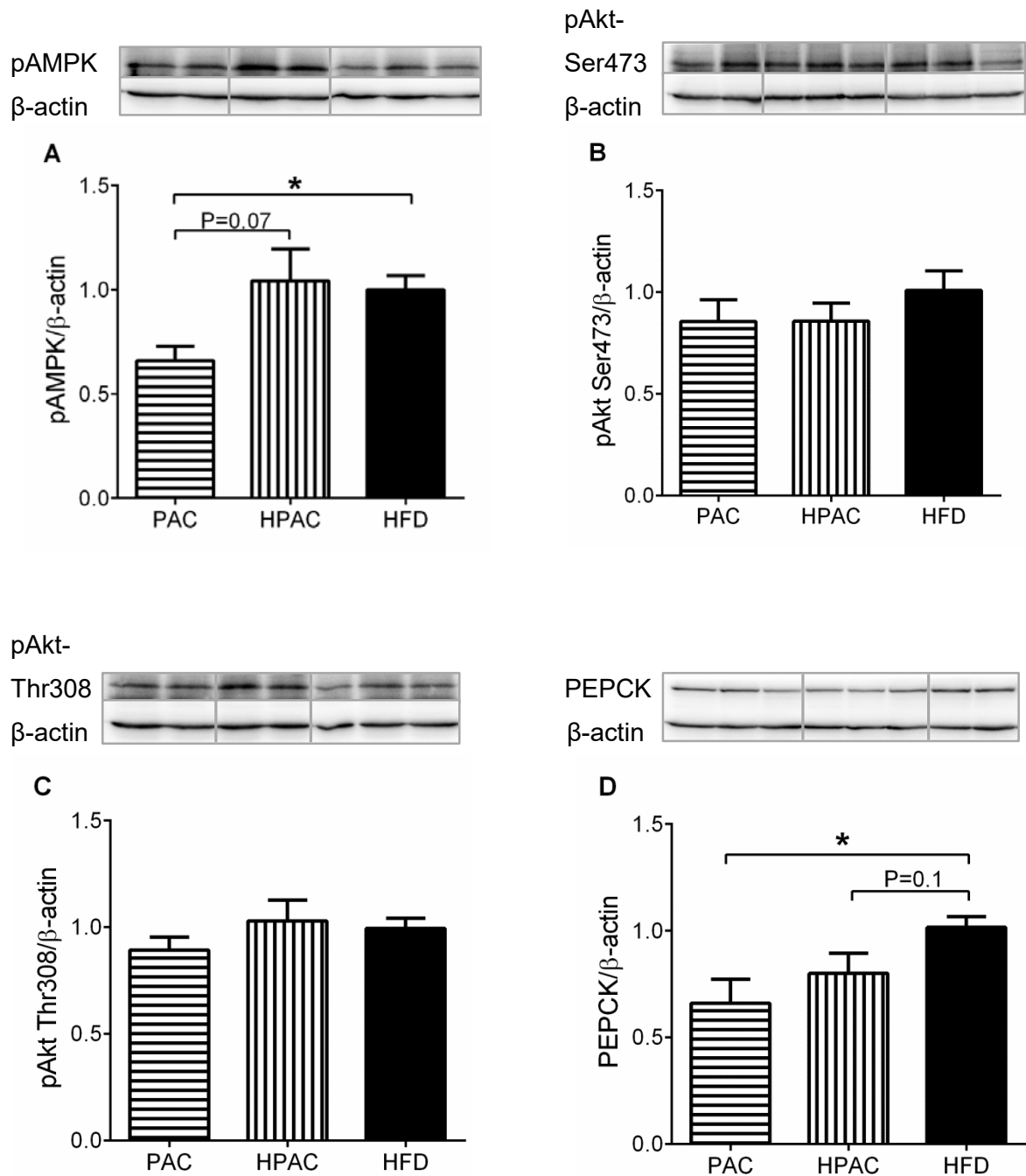


**Figure 5-4. Effects of PAC and HPAC on the expression of hepatic enzymes**

Immunoblot analysis of the levels of phosphorylated AMPK (pAMPK, A), PEPCK (B), and phosphorylated Akts – pAkt Ser473 (C) and pAkt Thr308 (D) were measured, and band intensity was compared with  $\beta$ -actin as loading controls. The protein levels are expressed as fold of control (HFD). N=8 for all groups. \* $P < 0.05$ , Bonferroni's multiple comparison.

## 5.4 Discussion

In an effort to identify and compare the effects of flavan-3-ols with different DP on hepatic glucose homeostasis, and to identify relevant intracellular signaling pathways in the liver, we assayed PAC- and HPAC action in diet-supplemented glucose-intolerant rats. Our results in Chapter 3 show that compared with PAC, HPAC are more effective in reversing HFD-induced insulin resistance and modulating hepatic glucose production (HGP) after insulin challenge. Paradoxically, however, PAC had a greater influence on hepatic metabolic and signalling pathways that we studied, including glutathione production, glycogen storage and PEPCK content.

Insulin resistance in the liver is one of the underlying causes of T2D. Disrupted hepatic insulin signaling causes incomplete suppression of HGP [136], and leads to severe dysregulation of whole-body metabolic homeostasis. During HFD feeding, insulin resistance in the liver is induced by day 3, prior to muscle insulin resistance [282]. *In vivo* characterization of the animals from which tissues were harvested for the current study was consistent with development of hepatic insulin resistance (Chapter 3). Specifically, the second phase of the ITT (minutes 60-120) revealed longer and stronger suppression of blood glucose in both PAC and HPAC animals, since the second phase of the ITT represents primarily HGP [223]. Studies using tissue specific insulin receptor knockout animals show that deletion of insulin receptor in the liver causes severe whole-body insulin resistance [274]; in contrast, normal glucose tolerance is maintained in animals with insulin receptor knockout in skeletal muscle [283] or adipose tissue [284]. Therefore, targeting hepatic insulin signaling and reducing HGP is important in control of the progression of T2D.

Flavan-3-ols, i.e. catechins and PAC have previously been shown to modulate HGP both in cultured cells and in animal models; and the effect is suggested to be mediated by either Akt or AMPK [181,184,185,285]. Here we confirmed that both PAC and HPAC are inhibitory to HGP.

However, our results show that Akt is not activated by either PAC or HPAC and, furthermore, that other indicators of reduced HGP were of greater magnitude in PAC than HPAC. For example, suppression of PEPCK expression, which is normally mediated by long-term modulation to suppress gluconeogenesis, suggests the possible role of AMPK activation by PAC more than HPAC. Activation of AMPK may have been blunted by the non-fasting state in which we collected the tissues but nevertheless was significantly reduced in PAC but not HPAC livers. Furthermore, glycogen content of PAC livers was significantly elevated in PAC but not HPAC, suggesting that enzymes regulating glycogen synthesis or breakdown (e.g. glycogen synthase and glycogen phosphorylase) may have been differentially regulated by PAC vs HPAC. This is also suggestive for improved insulin sensitivity in PAC, as the significantly different glycogen contents in PAC and HFD are induced by similar postprandial insulin concentrations of PAC and HFD, indicated by peak plasma insulin in OGTT.

We observed an increase in hepatic tGSH content in PAC, which suggests an indirect role of PAC in alleviating oxidative stress in hepatocytes, in order to improve hepatic insulin sensitivity. Glutathione (GSH) is an antioxidant in cells that scavenges free radicals and other reactive species, and modulates intracellular redox status [286]. GSH deficiency is related to increased cellular oxidative stress, which plays a key role in the pathogenesis of T2D [287]. Plant polyphenols, especially green tea catechins have been suggested to modulate GSH by induction of phase II detoxifying enzymes via activation of nuclear factor-erythroid (NF-E) 2-related factor 2 (Nrf2) [288,289]. Unexpectedly, GSH concentration in HPAC was not increased. However, we observed an overall improved glucose handling during OGTT and the slowest glucose recovery rate during ITT in HPAC group, as well as reduced whole-body fat percentage. With these findings we speculate that their hepatocytes might have improved insulin sensitivity and probably less oxidative stress than PAC. That being the case, an increase in GSH would not be necessary in HPAC.

Another possibility suggested by the data is that reduced feed efficiency (weight gain divided by energy intake) leading to reduced weight gain and body fat might be a more important factor governing improved glucose homeostasis. According to studies examining the effect of PAC on energy expenditure, a single dose of flavan-3-ols is able to increase resting energy expenditure during a 20 hours period in mice [290]. Two hours after ingestion, upregulated expression of uncoupling protein-1 (UCP-1) and peroxisome proliferator-activated receptor gamma coactivator-1 $\alpha$  (PGC-1 $\alpha$ ) are found in brown adipose tissue (BAT), meanwhile, plasma adrenaline level was significantly increased [290]. Whereas supplementing grape seed PAC for 21 days results in less weight gain and improved mitochondrial function in BAT in Wistar rats [291]. These findings indicate that PAC may be able to affect energy expenditure. In addition, even though there are quite limited numbers of studies available, considering PAC and/or metabolites' accumulation in the brain, they may have the potential to modulate neuropeptides involved in energy expenditure as well as food intake and satiety [292]. Unfortunately, in the present study, we were unable to measure energy expenditure of the rats due to the size limitation of the metabolic cages. Although it's possible that HPAC with improved bioavailability accumulated in the brain and had an influence on energy expenditure and eating behaviour, which requires further investigation to confirm.

We initially hypothesized that lower DP of HPAC, which we previously showed to increase bioavailability (Chapter 3) would lead to enhanced effects on liver insulin signalling that would explain superior suppression of HGP. However, this was not the case, as explained above. HPAC reduced body weight gain mainly by decreasing fat mass, and significantly improved whole-body insulin sensitivity and HGP, whereas PAC had no effect or moderate effect. HPAC also had an impact on pancreatic islet cellular composition, with lower numbers of glucagon-secreting  $\alpha$ -cells relative to insulin-secreting  $\beta$ -cells and trends to lower fasting insulin and glucagon secretion that suggest reduced islet stress, while no changes in islet morphology were found in PAC compared to HFD (Chapter 3). On the other hand, PAC had increased GSH and



glycogen concentrations and lowered PEPCK expression in the liver than HPAC, which nonetheless, only results in moderately improved glucose handling and suppressed HGP. This suggests that PAC and/or its metabolites might be able to improve some aspects of hepatic insulin resistance, however, these improvements might just be the results of compensation to the impaired hepatic insulin sensitivity, since they didn't lead to enhanced whole-body glucose homeostasis to the extent HPAC achieved.

In summary, our results suggest that non-hydrolyzed flavan-3-ol treatment is related with improvements in insulin sensitivity and suppress HGP by downregulation of PEPCK expression. They may also improve hepatocyte insulin sensitivity via relief of oxidative stress. Although the findings show that flavan-3-ols with high DP ( $DP \geq 5$ ) are more effective than low DP ( $DP \leq 3$ ) in these effects, it does not correspond precisely with *in vivo* investigations of HGP. This is indicative of the compensation rather than reversion of hepatic insulin resistance. Further investigation in the mechanism by which non-hydrolyzed and hydrolyzed flavan-3-ols suppresses hepatic gluconeogenesis may provide new therapeutic approaches for the management of diabetes.

## **Chapter 6**

### **General Discussion**

#### **6.1 Summary of hypotheses and results**

This thesis research set out to explore the effects of proanthocyanidins (PAC) on glucose homeostasis in a state of glucose intolerance and insulin resistance. PAC-rich pea seed coats (PSC) were used as the source of PAC in this study, and two means of preparation provided PAC with either high degree of polymerization (DP) or low DP. By doing so, the study sought to understand whether the DP of PAC can affect their bioavailability, and thus have an impact on their effects. Furthermore, this study investigated the mechanisms of action underlying PAC's modulation of glucose homeostasis.

The overall hypothesis is that hydrolyzed PAC (HPAC) with reduced DP has increased bioavailability thus exerts enhanced benefits towards glucose homeostasis.

In Chapter 3, the bioavailability of PAC and HPAC, and effects on pancreatic islets were investigated, with the hypothesis being that HPAC are more bioavailable than PAC, therefore HPAC is more effective in improving HFD-impaired insulin sensitivity and pancreatic islet function in glucose intolerant rats.

In Chapter 4, a PAC-derived compound epicatechin (EC) was studied for its direct effects on insulin-secreting INS-1 cell line. The hypotheses were: (1) EC can act as a cellular signaling molecule at a physiological relevant concentration (0.3  $\mu\text{M}$ ) to promote insulin secretion via activation of CaMKII pathway; (2) EC with high concentration (30  $\mu\text{M}$ ) can protect INS-1 cells against oxidative stress and improve cell viability.

In Chapter 5, the main focus was PAC and HPAC's effects on hepatic insulin sensitivity and glucose production (HGP). The hypothesis was that, compared with PAC, HPAC can effectively suppress hepatic glucose production (HGP), and this is associated with activation of AMPK or Akt signaling pathways to limit gluconeogenesis via reducing the key rate-limiting enzyme PEPCK content.

A schematic diagram of the findings and possible mechanisms of the current thesis research is shown in Figure 6-3. The investigations undertaken in the current study demonstrate that HPAC is more bioavailable than PAC. HPAC is able to reverse some aspects of HFD-induced insulin resistance, particularly the inability to suppress hepatic glucose production (HGP) (Chapter 3). HPAC or its metabolite EC affects pancreatic islet morphology and functions favorably (Chapter 3) and promotes insulin secretion via CaMKII pathway (Chapter 4). Conversely, the mechanisms by which HPAC correct the dysregulated HGP remain largely undetermined because downregulation of PEPCK expression and increased glycogen storage is greater in PAC than HPAC livers (Chapter 5). In contrast, PAC also has significant improvements in insulin-sensitive suppression of HGP (Chapter 3). It plays a role in improving hepatic insulin sensitivity and reducing PEPCK expression to limit HGP (Chapter 5). However, it shows no impact on pancreatic islets morphology or function (Chapter 3). These results will be discussed in detail in the following subsections.

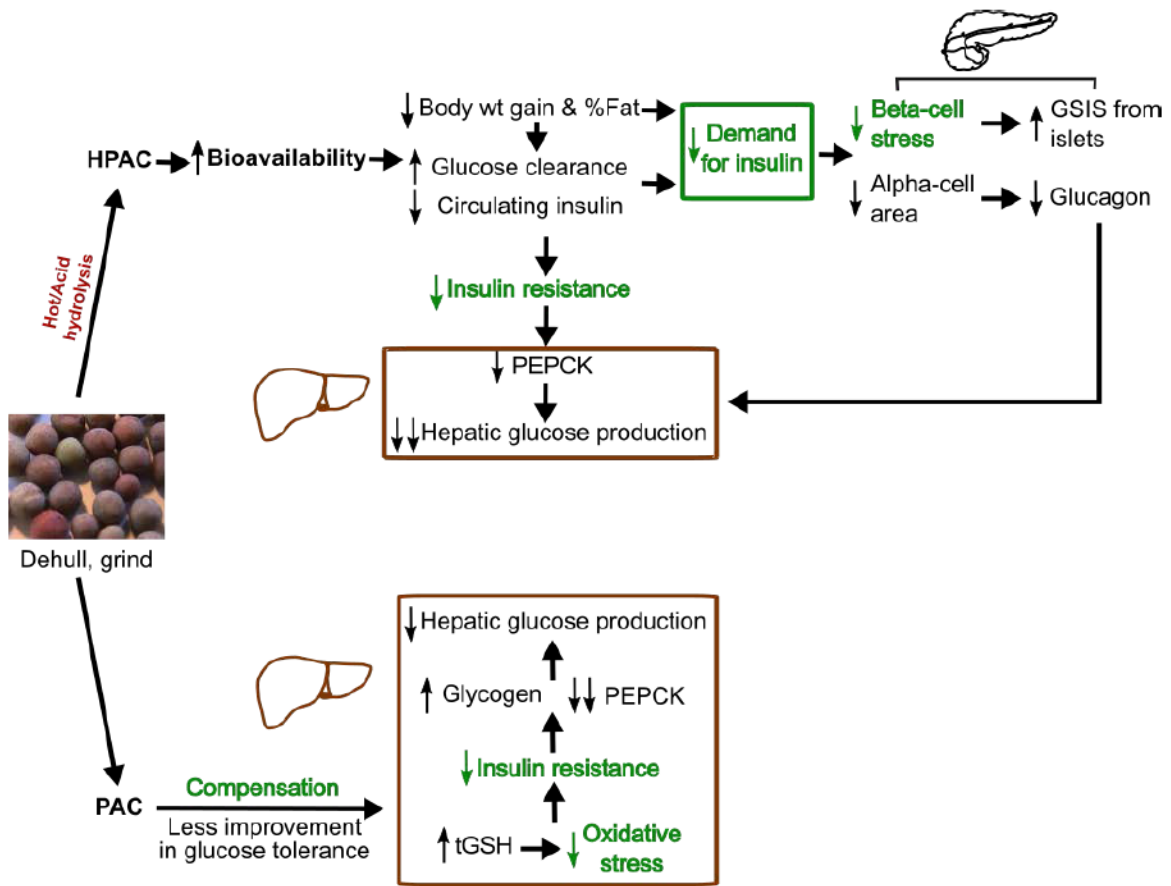


**Figure 6-1 Schematic diagram of the effects and possible mechanisms of PAC and HPAC on improving disrupted glucose homeostasis under glucose intolerant condition.**

## 6.2 Impact of DP on the bioavailability of PAC

As shown in Chapter 3, depolymerisation of PAC by hot acid hydrolysis decreased structural complexity of compounds, leading to increased bioavailability as indicated by detectable metabolites in serum. In particular, epicatechin-3'-O-glucuronide and 4'-O-methyl-epigallocatechin, which are derived from phase II metabolism in the body, were abundant, suggesting the absorption of PAC to be highly dependent on the DP. This is consistent with existing bioavailability studies in both rodents and humans, which report that PAC with low DP are absorbed more easily in the digestive tract than those with high DP [40], and glucuronidated and methylated forms of monomeric PAC (e.g. epicatechin, epigallocatechin) are found in serum after either single or repeated doses of PAC consumption [27,40,42]. However, due to the limited availability standards and quantity of samples, we were not able to quantify the concentrations of identified metabolites, or to further investigate some other metabolites, such as PAC dimers and trimers, which are thought to be present in the circulation after direct absorption from the upper intestine as suggested by a number of studies [30,39,41,225]. In spite of that, our results support the importance of DP in the bioavailability of PAC, particularly in their absorption in the digestive tract.

In consideration of PAC catabolism by colonic microbiota, we also determined the relative abundance of metabolites derived from microbial metabolism in both serum and urine (Table 6-1). Most of the PAC reaching the colon can be degraded into phenylvalerolactones and phenolic acids by microbiota; especially phenylvalerolactones are thought to be the biomarkers of PAC microbial metabolism [32]. Unfortunately, we didn't identify any phenylvalerolactones either in serum or urine. On the other hand, the relative concentrations of phenolic acids found in serum were comparable among all groups, while in urine, the metabolite profiles showed different patterns – for example, compared with HFD, protocatechuic acid, trans-ferulic acid and gallic acid were increased in HPAC group (Table 6-1,  $P < 0.05$ ), meanwhile 3-hydroxyhippuric acid

and 3-hydroxyphenylpropionic acid were increased in PAC group (Table 6-1,  $P < 0.05$ ). Those outcomes may be the result of differences in DP of PAC affecting metabolites produced by microbes and/or the profile of microbial species. Further investigations, such as characterization of the effects of PAC and HPAC on the distribution of gut microbiota genera are required to address this question.

As reported in other studies, serum metabolites generated from phase II metabolism peak 1-4 hours after PAC ingestion, whereas microbial metabolites usually reach maximum concentrations in urine 24 hours after consumption of PAC [30,40,47,48]. Therefore, collecting samples at peak hours and/or in a time-course are often adopted to study metabolites profile even more accurately. In our experimental setting, PAC was supplemented into food and rats were fed *ad libitum*, therefore it would be hard to precisely control the time of food ingestion. In addition, due to the high demands of time-course sampling and different peak times of the metabolites, in current study we only collected non-fasting serum and urine samples at a single time point in order to characterize postprandial PAC metabolite profile. This would reflect the state that animals are under for most of the day, although this might also be the reason we detected fewer metabolites in serum than in some other studies [38,225].

**Table 6-1. PAC-derived metabolites from microbial metabolism in serum and urine.**

	Metabolite	HFD	PAC	HPAC	P-value
Serum	Vanillic acid	0.757 ± 0.200	0.712 ± 0.109	0.619 ± 0.203	0.4738
	3-hydroxyphenylpropionic acid	0.391 ± 0.285	2.707 ± 0.511	0.122 ± 0.017	< 0.0001
	Homovanillic acid	1.504 ± 0.354	1.437 ± 0.289	1.318 ± 0.337	0.6709
	Hydroxybenzoic acid	0.477 ± 0.148	2.032 ± 1.437	0.971 ± 0.640	0.0529
	Hydroxyphenylacetic acid	1.049 ± 0.031	0.831 ± 0.026*	1.077 ± 0.043†	< 0.0001
	Protocatechuic Acid	0.74 ± 0.22	1.21 ± 0.58	2.82 ± 0.96*	0.0067
	Vanillic acid	ND	2.20 ± 0.16	2.42 ± 1.00	0.9000‡
	Trans-ferulic acid	1.17 ± 0.21	1.08 ± 0.42	4.23 ± 2.48*†	0.0043
	3-Hydroxybenzoic acid	ND	1.78 ± 0.48	2.00 ± 0.76	0.9000‡
	3-Hydroxyhippuric acid	0.45 ± 0.08	2.24 ± 0.91	0.74 ± 0.54*†	0.0055
Urine	Homovanillic acid	0.96 ± 0.26	1.25 ± 0.32	2.52 ± 1.93	0.2147
	2-(3,4-dihydroxyphenyl)acetic acid	ND	0.80 ± 0.66	1.38 ± 0.50	0.2286‡
	3,4-Dihydroxyphenylpropionic acid	ND	0.71 ± 0.57	1.99 ± 1.44	0.0952‡
	3,4-Dihydroxyphenylvaleric acid	ND	1.94 ± 0.92	ND	NA
	3-Hydroxyphenyl-valeric acid	1.29 ± 0.62	1.47 ± 0.70	1.69 ± 0.22	0.8286
	3-hydroxyphenylpropionic acid	0.21 ± 0.11	2.48 ± 0.77*	0.18 ± 0.10†	0.0037
	m-Coumaric acid	0.53 ± 0.21	2.12 ± 0.74*	3.78 ± 0.17*	0.0009
	3-Hydroxyphenylacetic acid	1.18 ± 0.56	0.92 ± 0.25	1.91 ± 1.08	0.1064
	Gallic acid	ND	0.88 ± 0.33	4.23 ± 1.54	0.0286‡

ND, not detected; NA, not applicable; \* P < 0.05, compared to HFD and † P < 0.05, compared to PAC, Bonferroni's multiple comparisons; ‡ Mann-Whitney test.

### **6.3 PAC's effects on glucose handling**

Knowing that there were differences in the bioavailability of HPAC and PAC, we were curious whether that would result in different outcomes in glucose handling between the two groups. We then conducted glucose tolerance tests (GTT) to measure and compare the effects. As discussed in Chapter 3, upon the challenge with intraperitoneal or oral administration of glucose (IPGTT or OGTT), the HPAC-treated group revealed relatively faster glucose clearance, correspondingly, a reduction in peak insulin secretion when compared with HFD. In contrast, there was little change in the glucose and insulin responses to PAC versus HFD during GTTs. This inability of PAC to influence GTT is similar to our previous findings [214]. These findings suggest improved glucose tolerance and insulin sensitivity by HPAC, which is consistent with their increased bioavailability.

Due to the fact that HPAC and PAC were supplemented in the context of pea seed coats (PSC), it's possible that PSC may cause some of the changes we found in the treatment groups. To control for this possibility, we also prepared PSC containing minimal PAC in the same ways as PAC and HPAC to better understand the effects of PAC compounds alone. As shown in Figure 6-1, feeding PSC that contained very low concentrations of PAC (nonPAC, or RP from Hashemi et al. [293]) elicited similar glucose responses as PAC ( $p > 0.05$ ). Thus, it seems that PAC had minimal additional benefits towards glucose handling in comparison with nonPAC PSC. On the other hand, after performing the hydrolysis procedure on nonPAC PSC, dietary supplementation led to a similar glucose excursion as HPAC, whereas insulin secretion during IPGTT resembled HFD (Figure 6-2), which indicated that HPAC is more beneficial overall possibly because of reduced stress on pancreatic  $\beta$ -cells.



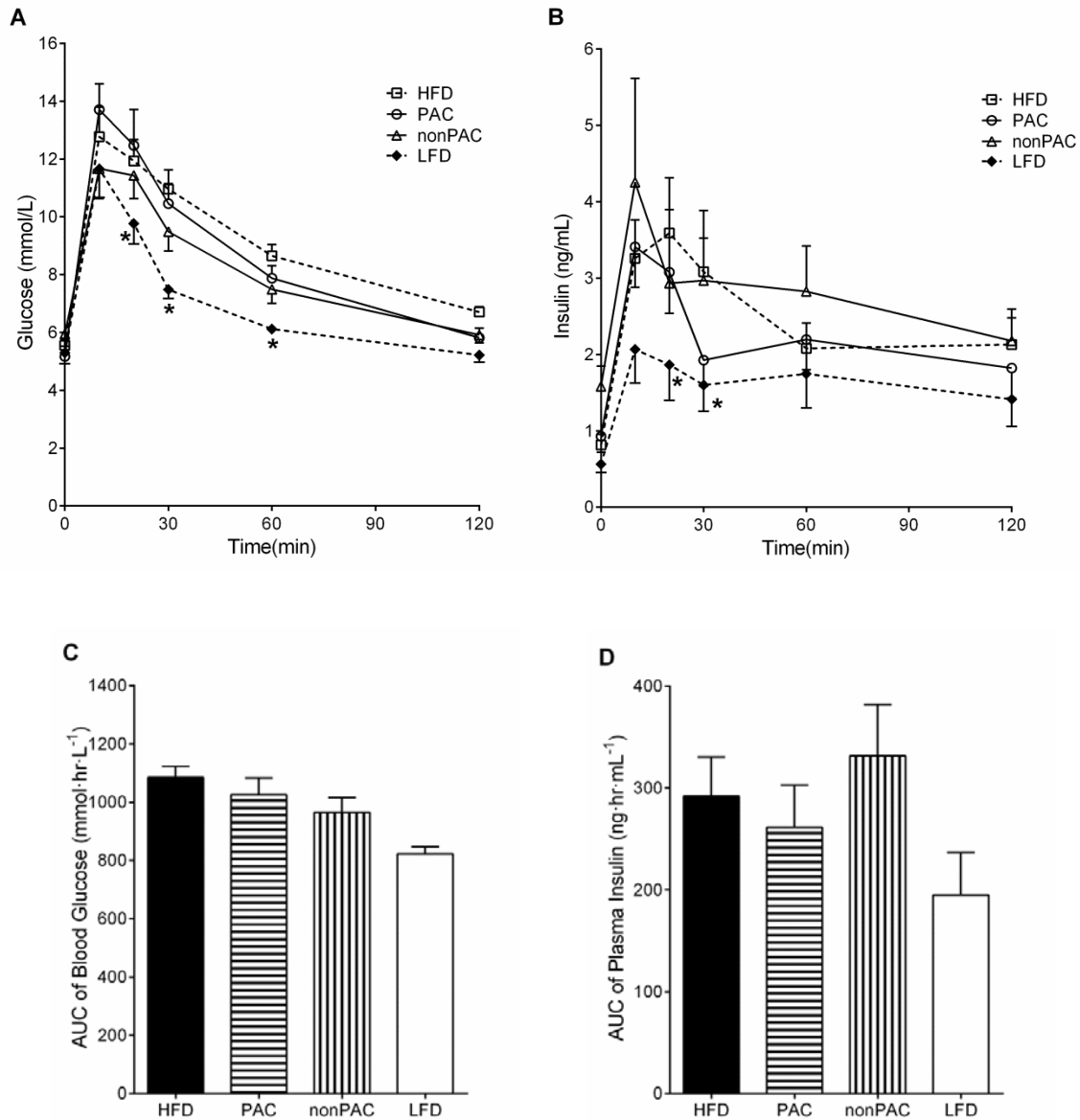


**Figure 6-2 Comparison of PAC and nonPAC during intraperitoneal glucose tolerance test (IPGTT).**

IPGTT were performed at week 11. After overnight fasting, blood glucose (A) and plasma insulin (B) were measured at 0, 10, 20, 30, 60, 120 min after intraperitoneal administration of 1 g/kg body weight glucose. Incremental area under the curve (IAUC) of glucose response (C) and insulin secretion (D) were calculated from A and B, respectively. HFD, n=11; LFD, n=10; PAC, n=10; nonPAC, n=10. \*P < 0.05, Bonferroni's multiple comparison.

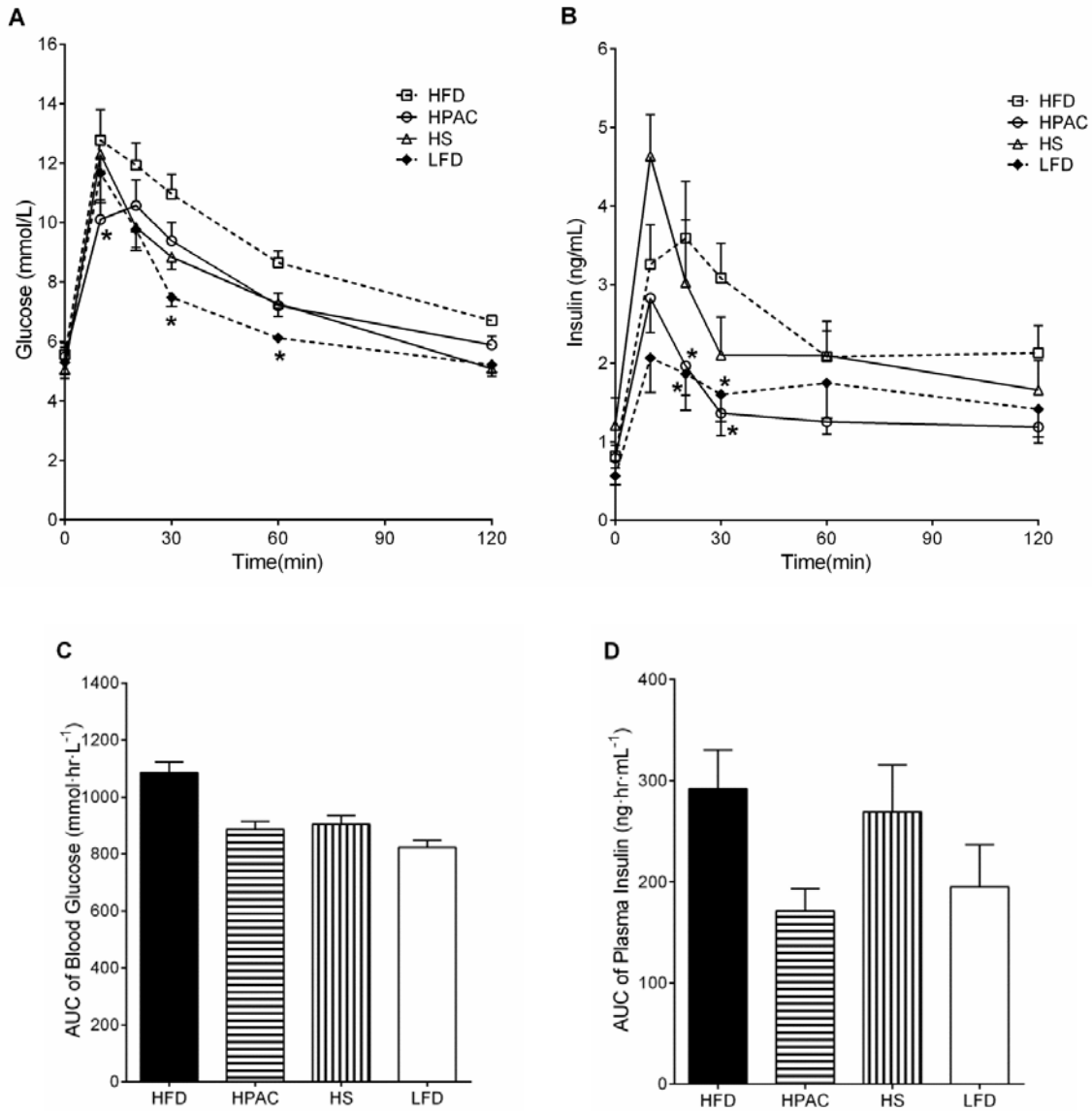


**Figure 6-3 Comparison of PAC and HS during intraperitoneal glucose tolerance test (IPGTT)**

IPGTT were performed at week 11. After overnight fasting, blood glucose (A) and plasma insulin (B) were measured at 0, 10, 20, 30, 60, 120 min after intraperitoneal administration of 1 g/kg body weight glucose. Incremental area under the curve (IAUC) of glucose response (C) and insulin secretion (D) were calculated from A and B, respectively. HFD, n=11; LFD, n=10; PAC, n=10; HS, n=8. \*P < 0.05, Bonferroni's multiple comparison.

There are several possible explanations for HPAC's effects that we developed and prioritized, based on known physiological responses to insulin resistance. **One** hypothesis is that HPAC may cause a reduction in pancreatic  $\beta$ -cell mass, perhaps secondary to relief of insulin resistance in other tissues. It is known that HFD-induced insulin resistance can lead to  $\beta$ -cell hyperplasia in order to meet increased demands for insulin to maintain glucose homeostasis [228,229]. In this study, evidence for reduction of insulin resistance included improved glucose tolerance after HPAC treatment. In addition, HPAC rats had much less total body fat and epididymal fat mass compared to HFD (Chapter 5), which would lead to improved whole-body metabolic status. Adiposity, particular visceral adiposity is associated with a pro-inflammatory state that contributes to the development of insulin resistance [294,295]. Hence, HPAC may reverse HFD-caused  $\beta$ -cell hyperplasia, resulting in smaller  $\beta$ -cell mass. **Secondly**, HPAC could have inhibitory effects on insulin secretion from pancreatic  $\beta$ -cells, leading to low insulin responses during GTTs. However, the rationale for this is not strong because a primary effect observed, a suppression of glucose-stimulated insulin secretion would be predicted to worsen glucose tolerance. **Thirdly**, evidence from the continued suppression of glucose in the second phase of the insulin tolerance test (ITT) led to a hypothesis that HPAC treatment created conditions to reduce the counter-regulatory response to hypoglycemia, such as reduced glucagon secretion, or down-regulation of genes involved in HGP. **Finally**, we hypothesized that HPAC could enhance insulin sensitivity in peripheral tissues (e.g., skeletal muscle), thus glucose clearance would be promoted less increase in insulin. However, this was not the case for present study, as the results of insulin tolerance test (ITT) showed no differences in glucose reduction in the first 30 minutes (Chapter 3), which is usually considered as an indication for peripheral tissue insulin sensitivity [223]. The first three of these possibilities were investigated and will be discussed in the following sections.

## **6.4 PAC/HPAC effects on pancreatic islets and insulin secreting $\beta$ -cells**

### **6.4.1 PAC/HPACs effects on the morphology of pancreatic islets**

To determine whether PAC or HPAC could have an impact on pancreatic islets, we measured relative pancreatic  $\alpha$ - and  $\beta$ -cell areas as an estimation of cell mass (Chapter 3). Counter to our hypothesis, we didn't detect significant changes in pancreatic  $\beta$ -cell areas after either PAC or HPAC supplementation, which is similar to our previously published study of PAC-containing PSC [214]. In other studies, PAC-rich extracts given *in vivo* have been reported to increase  $\beta$ -cell mass and reduce the frequency of apoptotic cells within islets [187,195,198]. A main difference from our study is that in the experimental settings of the cited studies, animal models had already been subjected to reduction in pancreatic  $\beta$ -cell mass, either induced by  $\beta$ -cell toxic agents or aging. Thus, if PAC is beneficial for  $\beta$ -cell integrity, a recovery of  $\beta$ -cell is expected. Whereas in our study, HFD induces  $\beta$ -cell hyperplasia along with increased apoptosis in the worst scenario; therefore HPAC's beneficial effects towards  $\beta$ -cells could be both reducing  $\beta$ -cell hyperplasia and decreasing apoptotic cells, which may explain the nonsignificant finding in  $\beta$ -cell areas. Moreover, effects of HPAC on  $\beta$ -cell mass could be both the direct effects of metabolites (as explored in Chapter 4 and discussed further below in Section 6.4.2) or the indirect effects of reduced insulin resistance of liver and other peripheral tissues (discussed below).

Unexpectedly, in HPAC group there was a profound decrease in  $\alpha$ -cell areas, consequently causing a reduction in  $\alpha$ -/ $\beta$ -cell ratio, suggesting that HPAC may correct dysregulated glucose homeostasis through modulation of pancreatic  $\alpha$ - and  $\beta$ -cell composition. Pancreatic  $\alpha$ - and  $\beta$ -cells are essential in the regulation of whole-body glucose metabolism, as the glucagon and insulin they secrete, respectively, are the key glucose-regulating hormones in the body [146,296]. In T2D, the decrease in  $\beta$ -cell mass

together with the increase in  $\alpha$ -cell proportion is thought to contribute to alterations in their secretion of hormones [121,297,298]. Elevated fasting glucagon is now considered as the main cause of fasting hyperglycemia seen in glucose intolerant and T2D patients [146,232]. Thus we determined fasting glucagon concentrations. Our results showed a trend ( $p=0.088$ ) towards a decrease in circulating glucagon in HPAC. Taken together, our findings suggest that, instead of predominantly affecting  $\beta$ -cells, HPAC acts on pancreatic islet composition by reducing  $\alpha$ -/ $\beta$ -cell ratio. A marginal decrease in fasting glucagon seen in HPAC suggests a role of HPAC in the inhibition of gluconeogenesis under the postabsorptive state.

#### **6.4.2 PAC/HPAC effects on insulin secretion from pancreatic islets and $\beta$ -cell lines**

Regarding the decrease in peak insulin secretion during GTTs in HPAC-treated animals, we deemed it possible that the decrease might be due to a decline in pancreatic islet function. However, our data suggest otherwise (Chapter 3). Isolated islets from HPAC group showed highly enhanced insulin secretion under high (16.5 mM) glucose stimulation, whereas islets from PAC and HFD were not so responsive to stimulation. This suggests that HPAC supplementation enhances the health of  $\beta$ -cells; therefore, the reduced secretion of insulin *in vivo* is more likely due to reduced demand as a result of improved whole body insulin sensitivity.

We then sought to look into the direct effects of PAC metabolites on  $\beta$ -cell insulin secretion and viability. Existing studies have found accumulation of PAC metabolites in many tissues, such as liver, intestine, kidney, heart and brain [36,38]. Although not reported yet, pancreatic islets probably are exposed to PAC and their metabolites, considering their highly vascularized structure [121,299]. As mentioned previously (Chapter 3), PAC metabolites, epicatechin-3'-O-glucuronide and 4'-O-methyl-

epigallocatechin were detected in the serum of HPAC rats. It's very likely that HPAC and/their metabolites affect  $\beta$ -cell function directly. Therefore it was of interest to conduct an *in vitro* study to characterize their direct effects on  $\beta$ -cells. Among various of compounds, epicatechin (EC) is considered a potent bioactive component of tea, grape seeds and other plant extracts [13]. Meanwhile, in the present study, EC-3'-O-glucuronide was detected in serum. Because it is not commercially available we selected non-glucuronidated EC as the compound to be tested.

A long-chain saturated fatty acid, stearic acid (SFA, 0.4 mM) was used to induce cell dysfunction in INS-1 cells, an insulin-secreting cell line. Elevated free fatty acids in plasma are thought to play a key role in the pathology of insulin resistance and T2D [253]. Palmitic acid (PA) at 0.4 mM can inhibit GSIS from  $\beta$ -cell lines after long-term exposure ( $\geq 48$  h) [130,251]. Whereas SFA at 0.25 mM is able to blunt insulin secretion in response to glucose in isolated islets [255] and induce apoptosis in INS-1 cells and human islets [256]. In the current work, SFA at 0.4 mM impaired GSIS from INS-1 cells by about 30% as shown in Chapter 4. Incubation of SFA-treated cells with 0.3  $\mu$ M EC significantly improved insulin secretion, while 30  $\mu$ M EC showed no effects. This finding is consistent with a previous study by Schroeter et al.. They show that EC at 0.1 – 0.3  $\mu$ M stimulates protein phosphorylation dose dependently, while stimulation is no longer apparent after exceeding 1  $\mu$ M, and 30  $\mu$ M inhibits protein phosphorylation [112].

Whereas when we examined ROS production induced by either long-term hyperglycemia or acute H<sub>2</sub>O<sub>2</sub>, 30  $\mu$ M of EC was able to attenuate the increase in ROS, although 0.3  $\mu$ M EC was not. This effect of high-concentration EC on ROS was similar to that of equimolar N-acetyl cysteine (NAC), a strong antioxidant. On the basis of these results, it is reasonable to suggest that EC's effects may be dependent on its concentration – it can act as an antioxidant at high concentration, while at low concentrations it demonstrates

the potential to modulate cellular signaling pathways. Since it is unlikely that high concentrations of EC would be achieved from dietary sources we focused on identifying a signalling pathway modulated by EC in  $\beta$ -cells.

### **6.4.3 The mechanism of EC effects on insulin secretion**

To further address the effects of EC as a cellular signaling molecule, the mechanism of EC restoration of insulin secretion after SFA insult was investigated (Chapter 4). Our results suggest a role of  $\text{Ca}^{2+}$ /calmodulin-dependent protein kinase II (CaMKII) in EC-restored insulin secretion. CaMKII is considered a  $\text{Ca}^{2+}$  sensor in the cell, and is essential in maintaining cytoplasmic  $\text{Ca}^{2+}$  homeostasis [252]. In pancreatic  $\beta$ -cells, GSIS is dependent on the activation of CaMKII, and impaired insulin secretion induced by long-term PA exposure is associated with decreased in phosphorylation/activation of CaMKII [130]. Inhibition of CaMKII by pharmacological agents leads to reduced insulin secretion upon stimulation [129,130].

As reported in Chapter 4, impaired insulin secretion in SFA-treated cells was restored after incubation with EC, paralleled by increased phosphorylation of CaMKII, whereas KN-93, an inhibitor of CaMKII, caused dephosphorylation of CaMKII and resulted in blunted insulin secretion. All of those findings indicated that EC could restore GSIS via activation of CaMKII. Indeed, EC has been shown to act on CaMKII in other cell types previously. Wang et al. have shown that activation of cAMP response element binding protein (CREB) signaling in hypothalamus by a biosynthetic EC metabolite is mediated via CaMKII pathway [234]. What's more, it's suggested that EC is involved in endothelial nitric oxide synthase (eNOS)-mediated nitric oxide production in endothelial cells, which is mediated via CaMKII pathway as well [246]. Thus, CaMKII is a potential target of EC in modulation of cellular signaling pathways.

The results from current study do not precisely define the signaling cascades of EC in pancreatic  $\beta$ -cells. Further *in vitro* investigation in  $\beta$ -cells is needed for the identification of up-stream modulators and down-stream targets of EC. In addition, there are many other mechanistic possibilities that will need to be explored. There is evidence in endothelial cells that EC rather than EC metabolites can be taken up by the cells [300]. Studies by Ramirez-Sanchez et al. and Moreno-Ulloa et al. suggest the possibility of a cell membrane receptor existing for EC to mediate its effects in endothelial cells [246,269]. Thus it would be interesting to work on the possibilities as to whether: 1) EC can be taken up into pancreatic  $\beta$ -cells, 2) it is EC or EC metabolites exerting effects on  $\beta$ -cells, and 3) there is a receptor/molecule on cell membranes that can react with EC in  $\beta$ -cells. However, our studies did establish a signalling pathway for further characterization and was able to rule out an effect of low, potentially achievable concentrations of EC on  $\beta$ -cell ROS production and viability. Furthermore, our results also imply a potential role in modulation of cellular signaling by PAC-derived compounds, which probably is not only limited to EC itself, but also applicable to other bioavailable compounds. Consequently, the effects of PAC we observed *in vivo* would be the results of all/some bioavailable compounds present in serum, which would need to be interpreted with caution.

### **6.5 PAC/HPAC effects on liver function and glucose production**

Upon insulin challenge, glucose typically falls and then climbs back towards baseline upon degradation of the circulating insulin and induction of the counter-regulatory response. The rate of decline in the initial phase indicates insulin sensitivity in peripheral tissues, while the rate of the recovery phase indicates hepatic glucose production (HGP) [217]. As mentioned briefly in section 6.3, during insulin tolerance test (ITT, Chapter 3) all diet groups showed similar glucose clearance in the first 30 minutes. Thus we presumed that insulin sensitivity was unchanged by PAC/HPAC in



peripheral tissues. Differences appeared after 60 min following insulin administration. Glucose concentrations in HFD quickly returned to baseline, whereas both PAC and HPAC revealed slower glucose recovery rates compared with HFD, which suggested suppressed HGP in both groups. It is known that absorbed PAC are firstly metabolized in the liver through phase II metabolism [32], hence the liver is exposed to considerable amount of those compounds. It would be expected that PAC could influence hepatic function. Therefore we explored how PAC and HPAC might suppress HGP (Chapter 5). Firstly, we suspected that HGP could be suppressed through interaction of PAC/HPAC with insulin signaling in hepatocytes. In hepatocytes, insulin binds to insulin receptors (IR) on cell membrane and activates Akt signaling to inhibit HGP [136]. *In vitro* studies have shown that EC increases phosphorylation of IR and insulin receptor substrate-1 (IRS-1) to activate Akt signaling pathway (although at a lower kinetics than insulin [285]), and thus reduce gene expression of PEPCK in hepatoma cells [185,285]. In Chapter 5, we found a trend to increased hepatic fasting insulin sensitivity indicated by HOMA-IR ( $p=0.1$ ) in HPAC. However, analysis of the expression of both phosphorylated and total Akt showed no differences among all groups. Thus, it appears that suppression of HGP by PAC and HPAC is not mediated by insulin signaling.

Then we determined whether AMPK pathway could be activated by PAC and HPAC. AMPK pathway is insulin-independent and is activated by elevated AMP/ATP ratio or intracellular  $Ca^{2+}$  to switch on catabolic pathways that generate ATP [139]. Most of *in vivo* studies have reported that instead of affect insulin signaling, activation of AMPK is contributed to PAC extract's suppression on HGP [181,184], although one of the *in vitro* study mentioned previously by Cordero-Herrera et al. show that both Akt and AMPK pathways are activated in HepG2 cells (hepatoma cells) by cocoa PAC [185]. In the present study, hepatic AMPK were measured in liver samples from non-fasting animals,

it's likely that activation of AMPK was blunted by high glucose under the postprandial state. Nonetheless, phosphorylation of AMPK in PAC but not HPAC was significantly suppressed when compared with HFD, which, on the other hand, may indicate improved insulin sensitivity in PAC livers. As discussed above, those results were insufficient to conclude whether or not PAC/HPAC activated hepatic AMPK pathway. Analysis of AMPK activation under fasting state will be required to clarify the effects of PAC/HPAC on AMPK pathway.

In spite of the results regarding Akt and AMPK, we were curious about whether PAC and HPAC would have any effect on hepatic PEPCK, which is a key enzyme mediating gluconeogenesis to promote glucose output from the liver. As reported in Chapter 5, there was a significant reduction in PEPCK content in PAC, whereas PEPCK content in HPAC was reduced but not significantly different compared with HFD ( $P=0.1$ ). These results indicate that both PAC and HPAC's suppression of HGP is associated with downregulated PEPCK content, yet PAC suppressed HGP to a lesser extent with lower PEPCK levels than HPAC. Studies have shown that oxidative stress in hepatocytes enhances PEPCK gene expression, while balancing redox state suppresses it [301–303]. Hence, oxidative stress status in hepatocytes in PAC and HPAC might affect PEPCK expression. Moreover, since HGP are attributable to glycogenolysis by up to ~50% in addition to gluconeogenesis [137], it's possible that glycogen metabolism was also affected by PAC and HPAC differently. Thus, we explored these possibilities which are discussed as follows.

GSH is a cellular antioxidant that is important in modulating redox states and relieving oxidative stress [34]. We measured total glutathione (tGSH) concentration in the liver as an indicator for oxidative stress. Compared with HFD, higher tGSH concentrations were found in PAC but not in HPAC. Although the unchanged tGSH in HPAC is unexpected,

given the results from Chapter 3 that HPAC had improved glucose and insulin responses in GTTs, suppressed HGP significantly in the last phase of ITT and reduced body fat especially epididymal fat mass, it is reasonable to suggest that HPAC had overall improved metabolic state, thus alleviating oxidative stress in hepatocytes, leading to relatively low tGSH. In contrast, considering the fact that PAC only had mild improvement in GTTs and ITT, their hepatocytes would be relatively more stressed than HPAC, hence a higher tGSH is needed so as to compensate cellular stress. Elevated tGSH in PAC might, to some extent, contribute to the reduced PEPCK content.

Hepatic glycogen content in the fed state was measured. In PAC-fed rat livers, there was more glycogen compared with HFD whereas in HPAC-fed rat livers, glycogen stores were unchanged. On the aspect of glycogen breakdown, the high glycogen content in PAC may result in relatively more glycogenolysis for HGP in ITT than HPAC. As for glycogen synthesis, when taking into account the postprandial insulin concentrations as indicated in OGTT, lower insulin in HPAC led to similar glycogen content as HFD, whereas increased glycogen content in PAC were induced by similar insulin as HFD, suggesting improved insulin sensitivity in the liver of PAC and HPAC. Overall, it is plausible to conclude that compared with HFD, PAC and HPAC improve insulin sensitivity and reduce oxidative stress in hepatocytes.

In this study, PEPCK was the single indicator used to assess hepatic gluconeogenesis. It would also be interesting to determine the other direct indicator for HGP, glucose 6-phosphatase (G6Pase)/glucokinase (GK) ratio, in which G6Pase indicates glucose uptake whereas GK indicates glucose output in the liver [304], therefore G6Pase/GK ratio would better reflect the control of HGP than PEPCK alone. In consideration of liver's role in both insulin clearance and PAC metabolism, there is a possibility that HPAC/PAC might

affect insulin degradation by the liver, which may lead to prolonged effects on glucose uptake and HGP seen *in vivo*.

## **6.6 Contributions and implications of present thesis research**

Findings from this thesis research provide evidence on PAC bioavailability and beneficial effects towards improvements in glucose homeostasis. Most of all, an association between PAC bioavailability and effects is presented, showing that improved bioavailability of PAC leads to enhanced benefits on glucose regulation and other metabolic events. Meanwhile, our results suggest that PAC with different bioavailability can modulate the functions of target tissues such as pancreatic islets and liver through different mechanisms. In addition, by using an *in vitro* study design (Chapter 4), we were able to differentiate the effects of a compound of interest (epicatechin) at different concentrations, confirming the role of PAC metabolites in cellular signaling, and suggesting a novel signaling pathway as the target of PAC in pancreatic  $\beta$ -cells. A part of this thesis research (Chapter 3) has contributed to a Report of Invention as a prelude to a full patent application: 'Pea (*Pisum Sativum L.*) Seed Coats and Seed Coat Fractions', by OZGA, Jocelyn; CHAN, Catherine; JIN, Alena; HAN, Yang; HASHEMI, Seyede; YANG, Kaiyuan. United States Provisional Patent Application Serial No. 62/041,277. The methodology developed to hydrolyze the PAC and enhance its benefits on glucose homeostasis could have interest for companies looking to develop ingredients to increase the healthful benefits of food products.

One of the aspects not being investigated in present study is PAC's effects on colonic microbiota. Tabulation of microbial-derived metabolites in this study showed different catabolism patterns of PAC with different DP, suggesting differences in microbial species. Other studies have shown that PAC has selective inhibitory effects on bacteria, resulting in modulation of the species in colonic microbiota [71,226,227]. The

preparation method we used may have an impact on the selective inhibitory effects of PAC, which could lead to either an altered or just simply reduced inhibition of microbiota. At the time of tissue collection, we did collect fecal samples and colonic scrapings from the rats so that these possibilities can be further explored in the future.

Even though there are many aspects left to be studied, the potent effects of PAC from pea seed coats on improving whole-body glucose homeostasis is worthwhile to further test in a setting of a clinical trial. PAC-rich pea seed coats or even whole peas could be incorporated into the experimental foods. Compared with other studies using PAC-rich extracts, PAC from peas may have additional benefits for the participants due to the other nutrients in peas and might also be less expensive to prepare. Being able to demonstrate similar beneficial effects in humans is important for establishing health claims and marketing the product to the food industry.

The pea seed coat (PSC) used in this thesis research is from a pea (*Pisum Sativum L.*) cultivar 'Solido'. 'Solido' is a local crop in Alberta with brown seed coats containing a high concentration of PAC ( $264.1 \pm 14.6$  mg/100 g dry weight of PSC) with a mean DP of 5 [204]. Given the fact that peas are Canada's largest pulse crop, they are inexpensive and accessible. Meanwhile peas can provide significant amounts of protein, carbohydrates, dietary fiber, vitamins, minerals and phytochemicals to our diet [305]. Therefore, 'Solido' (or other cultivars containing PAC) is an excellent healthy food choice that would help in promoting people's health. What's more, considering the potential market of 'Solido', it is reasonable for the pulse industry in Canada to provide additional opportunities for 'Solido' cultivar in both planting and marketing. However currently, 'Solido' is usually dehulled and used to produce pea butter [306,307], leaving those seed coats as a by-product. As a great source of both fiber and PAC, 'Solido' pea seed coats can

be collected and incorporated in appropriate food products as supplementation of fiber and PAC. They can also be used to obtain PAC extracts.

## **6.7 Conclusions**

The results presented in this thesis confirmed the importance of DP in the bioavailability of PAC, showing that a decrease in the structural complexity of PAC by reducing DP results in enhanced bioavailability evidenced by increased metabolites derived from phase II metabolism. HPAC significantly improved glucose tolerance and insulin sensitivity with PAC's effects being more modest. HPAC treatment revealed beneficial effects on pancreatic islet composition and insulin secretion. The underlying mechanism of enhanced insulin secretion was contributed to by the activation of CaMKII by EC. Furthermore, both PAC and HPAC suppressed HGP in fasting state, which was associated with down-regulation of hepatic PEPCK content. In addition, PAC might compensate for improved insulin sensitivity in the liver through alleviating oxidative stress, however was not able to further improve whole-body glucose homeostasis as HPAC. Findings from current study also indicated that PAC's effects may be concentration dependent and tissue specific. All in all, this thesis research supports the role of bioavailable PAC in promoting whole-body glucose homeostasis.

## Bibliography

- [1] Ross JA, Kasum CM. Dietary flavonoids: bioavailability, metabolic effects, and safety. *Annu Rev Nutr* 2002;22:19–34.
- [2] Middleton E, Kandaswami C, Theoharides TC. The effects of plant flavonoids on mammalian cells: implications for inflammation, heart disease, and cancer. *Pharmacol Rev* 2000;52:673–751.
- [3] Croft KD. The chemistry and biological effects of flavonoids and phenolic acids. *Ann N Y Acad Sci* 1998;854:435–42.
- [4] Heim KE, Tagliaferro AR, Bobilya DJ. Flavonoid antioxidants: chemistry, metabolism and structure-activity relationships. *J Nutr Biochem* 2002;13:572–84.
- [5] Guyot S. Flavan-3-Ols and Proanthocyanidins. In: Nollet LML, Toldrá F, editors. *Handb. Anal. Act. Compd. Funct. Foods*, CRC Press; 2012, p. 317–48.
- [6] Kennedy J. Proanthocyanidins: Extraction, Purification, and determination of subunit composition by HPLC. *Curr Protoc Food Anal Chem* 2002:1–11.
- [7] Vidal S, Francis L, Guyot S, Marnet N, Kwiatkowski M, Gawel R, et al. The mouth-feel properties of grape and apple proanthocyanidins in a wine-like medium. *J Sci Food Agric* 2003;83:564–73.
- [8] Lea AGH, Arnold GM. The phenolics of ciders: bitterness and astringency. *J Sci Food Agric* 1978;29:478–83.
- [9] Santos-Buelga C, Scalbert A. Proanthocyanidins and tannin-like compounds – nature, occurrence, dietary intake and effects on nutrition and health. *J Sci Food Agric* 2000;80:1094–117.
- [10] Williams RJ, Spencer JPE, Rice-Evans C. Flavonoids: antioxidants or signalling molecules? *Free Radic Biol Med* 2004;36:838–49.
- [11] Laks PE. Chemistry of the Condensed Tannin B-ring. In: Hemingway RW, Karchesy JJ, Branham SJ, editors. *Chem. Significance Condens. Tann.*, Boston, MA: Springer US; 1989, p. 249–63.
- [12] Xu Z, Du P, Meiser P, Jacob C. Proanthocyanidins: oligomeric structures with unique biochemical properties and great therapeutic promise. *Nat Prod Commun* 2012;7:381–8.
- [13] Aron PM, Kennedy JA. Flavan-3-ols: nature, occurrence and biological activity. *Mol Nutr Food Res* 2008;52:79–104.
- [14] Dixon RA, Xie D-Y, Sharma SB. Proanthocyanidins--a final frontier in flavonoid research? *New Phytol* 2005;165:9–28.

- [15] Lesschaeve I, Noble AC. Polyphenols: factors influencing their sensory properties and their effects on food and beverage preferences. *Am J Clin Nutr* 2005;81:330S – 335S.
- [16] Gu L, Kelm MA, Hammerstone JF, Beecher G, Holden J, Haytowitz D, et al. Concentrations of proanthocyanidins in common foods and estimations of normal consumption. *J Nutr* 2004;134:613–7.
- [17] Prior RL, Gu L. Occurrence and biological significance of proanthocyanidins in the American diet. *Phytochemistry* 2005;66:2264–80.
- [18] Zamora-Ros R, Andres-Lacueva C, Lamuela-Raventós RM, Berenguer T, Jakszyn P, Barricarte A, et al. Estimation of dietary sources and flavonoid intake in a Spanish adult population (EPIC-Spain). *J Am Diet Assoc* 2010;110:390–8.
- [19] Pérez-Jiménez J, Fezeu L, Touvier M, Arnault N, Manach C, Hercberg S, et al. Dietary intake of 337 polyphenols in French adults. *Am J Clin Nutr* 2011;93:1220–8.
- [20] Ovaskainen M-L, Törrönen R, Koponen JM, Sinkko H, Hellström J, Reinivuo H, et al. Dietary intake and major food sources of polyphenols in Finnish adults. *J Nutr* 2008;138:562–6.
- [21] Wu X, Gu L, Prior RL, McKay S. Characterization of anthocyanins and proanthocyanidins in some cultivars of *Ribes*, *Aronia*, and *Sambucus* and their antioxidant capacity. *J Agric Food Chem* 2004;52:7846–56.
- [22] Feo V De, Quaranta E, Fedele V. Flavonoids and terpenoids in goat milk in relation to forage intake. *Ital J Food Sci* 2006;18:85–92.
- [23] Wang Y, Chung S, Song WO, Chun OK. Estimation of daily proanthocyanidin intake and major food sources in the U.S. diet. *J Nutr* 2011;141:447–52.
- [24] Wedick NM, Pan A, Cassidy A, Rimm EB, Sampson L, Rosner B, et al. Dietary flavonoid intakes and risk of type 2 diabetes in US men and women. *Am J Clin Nutr* 2012;95:925–33.
- [25] USDA. USDA database for proanthocyanidin content of selected foods. Beltsville, MD US Dep Agric Agric Res Serv Nutr Data Lab 2004.
- [26] Bravo L. Polyphenols: chemistry, dietary sources, metabolism, and nutritional significance. *Nutr Rev* 1998;56:317–33.
- [27] Stalmach A, Mullen W, Steiling H, Williamson G, Lean MEJ, Crozier A. Absorption, metabolism, and excretion of green tea flavan-3-ols in humans with an ileostomy. *Mol Nutr Food Res* 2010;54:323–34.



- [28] Serra A, Macià A, Romero M-P, Valls J, Bladé C, Arola L, et al. Bioavailability of procyanidin dimers and trimers and matrix food effects in in vitro and in vivo models. *Br J Nutr* 2010;103:944–52.
- [29] Williamson G, Manach C. Bioavailability and bioefficacy of polyphenols in humans. II. Review of 93 intervention studies. *Am J Clin Nutr* 2005;81:243S – 255S.
- [30] Stoupi S, Williamson G, Viton F, Barron D, King LJ, Brown JE, et al. In vivo bioavailability, absorption, excretion, and pharmacokinetics of [<sup>14</sup>C]procyanidin B2 in male rats. *Drug Metab Dispos* 2010;38:287–91.
- [31] Rios LY, Bennett RN, Lazarus SA, Rémésy C, Scalbert A, Williamson G. Cocoa procyanidins are stable during gastric transit in humans. *Am J Clin Nutr* 2002;76:1106–10.
- [32] Ou K, Gu L. Absorption and metabolism of proanthocyanidins. *J Funct Foods* 2014;7:43–53.
- [33] Monagas M, Urpi-Sarda M, Sánchez-Patán F, Llorach R, Garrido I, Gómez-Cordovés C, et al. Insights into the metabolism and microbial biotransformation of dietary flavan-3-ols and the bioactivity of their metabolites. *Food Funct* 2010;1:233–53.
- [34] Deprez S, Mila I, Huneau JF, Tome D, Scalbert A. Transport of proanthocyanidin dimer, trimer, and polymer across monolayers of human intestinal epithelial Caco-2 cells. *Antioxid Redox Signal* 2001;3:957–67.
- [35] Rio D Del, Calani L, Brighenti F. *Tea in Health and Disease Prevention*. Elsevier; 2013.
- [36] Abd El Mohsen MM, Kuhnle G, Rechner AR, Schroeter H, Rose S, Jenner P, et al. Uptake and metabolism of epicatechin and its access to the brain after oral ingestion. *Free Radic Biol Med* 2002;33:1693–702.
- [37] Janle EM, Lila MA, Grannan M, Wood L, Higgins A, Yousef GG, et al. Pharmacokinetics and tissue distribution of <sup>14</sup>C-labeled grape polyphenols in the periphery and the central nervous system following oral administration. *J Med Food* 2010;13:926–33.
- [38] Serra A, Macià A, Romero M-P, Anglès N, Morelló JR, Motilva M-J. Distribution of procyanidins and their metabolites in rat plasma and tissues after an acute intake of hazelnut extract. *Food Funct* 2011;2:562–8.
- [39] Appeldoorn MM, Vincken J, Gruppen H, Hollman PCH. Procyanidin dimers A1, A2, and B2 are absorbed without conjugation or methylation from the small intestine of rats. *J Nutr* 2009;139:1469–73.

- [40] Shoji T, Masumoto S, Moriichi N, Akiyama H, Kanda T, Ohtake Y, et al. Apple procyanidin oligomers absorption in rats after oral administration: analysis of procyanidins in plasma using the porter method and high-performance liquid chromatography/tandem mass spectrometry. *J Agric Food Chem* 2006;54:884–92.
- [41] Sano A, Yamakoshi J, Tokutake S, Tobe K, Kubota Y, Kikuchi M. Procyanidin B1 is detected in human serum after intake of proanthocyanidin-rich grape seed extract. *Biosci Biotechnol Biochem* 2003;67:1140–3.
- [42] Spencer JP, Schroeter H, Shenoy B, Srail SK, Debnam ES, Rice-Evans C. Epicatechin is the primary bioavailable form of the procyanidin dimers B2 and B5 after transfer across the small intestine. *Biochem Biophys Res Commun* 2001;285:588–93.
- [43] Baba S, Osakabe N, Natsume M, Terao J. Absorption and urinary excretion of procyanidin B2 [epicatechin-(4beta-8)-epicatechin] in rats. *Free Radic Biol Med* 2002;33:142–8.
- [44] Donovan JL, Manach C, Faulks RM, Kroon PA. Absorption and metabolism of dietary plant secondary metabolites. In: Crozier A, Clifford MN, Ashihara H, editors. *Plant Second. Metab. Occur. Struct. Role Hum. Diet*, Oxford, UK: Blackwell Publishing Ltd; 2006.
- [45] Serrano J, Puupponen-Pimiä R, Dauer A, Aura A-M, Saura-Calixto F. Tannins: current knowledge of food sources, intake, bioavailability and biological effects. *Mol Nutr Food Res* 2009;53 Suppl 2:S310–29.
- [46] Manach C, Scalbert A, Morand C, Rémésy C, Jiménez L. Polyphenols: food sources and bioavailability. *Am J Clin Nutr* 2004;79:727–47.
- [47] Roowi S, Stalmach A, Mullen W, Lean MEJ, Edwards CA, Crozier A. Green tea flavan-3-ols: colonic degradation and urinary excretion of catabolites by humans. *J Agric Food Chem* 2010;58:1296–304.
- [48] Déprez S, Brezillon C, Rabot S, Philippe C, Mila I, Lapiere C, et al. Polymeric proanthocyanidins are catabolized by human colonic microflora into low-molecular-weight phenolic acids. *J Nutr* 2000;130:2733–8.
- [49] Green RJ, Murphy AS, Schulz B, Watkins BA, Ferruzzi MG. Common tea formulations modulate in vitro digestive recovery of green tea catechins. *Mol Nutr Food Res* 2007;51:1152–62.
- [50] Van der Burg-Koorevaar MCD, Miret S, Duchateau GSMJE. Effect of milk and brewing method on black tea catechin bioaccessibility. *J Agric Food Chem* 2011;59:7752–8.
- [51] Van het Hof KH, Kivits GA, Weststrate JA, Tijburg LB. Bioavailability of catechins from tea: the effect of milk. *Eur J Clin Nutr* 1998;52:356–9.

- [52] Kyle JAM, Morrice PC, McNeill G, Duthie GG. Effects of infusion time and addition of milk on content and absorption of polyphenols from black tea. *J Agric Food Chem* 2007;55:4889–94.
- [53] Henning SM, Niu Y, Lee NH, Thames GD, Minutti RR, Wang H, et al. Bioavailability and antioxidant activity of tea flavanols after consumption of green tea, black tea, or a green tea extract supplement. *Am J Clin Nutr* 2004;80:1558–64.
- [54] Auger C, Mullen W, Hara Y, Crozier A. Bioavailability of polyphenon E flavan-3-ols in humans with an ileostomy. *J Nutr* 2008;138:1535S – 1542S.
- [55] Schramm DD, Karim M, Schrader HR, Holt RR, Kirkpatrick NJ, Polagruto J a, et al. Food effects on the absorption and pharmacokinetics of cocoa flavanols. *Life Sci* 2003;73:857–69.
- [56] Rodriguez-Mateos A, Oruna-Concha MJ, Kwik-Urbe C, Vidal A, Spencer JPE. Influence of sugar type on the bioavailability of cocoa flavanols. *Br J Nutr* 2012;108:2243–50.
- [57] Roura E, Andrés-Lacueva C, Estruch R, Lourdes Mata Bilbao M, Izquierdo-Pulido M, Lamuela-Raventós RM. The effects of milk as a food matrix for polyphenols on the excretion profile of cocoa (-)-epicatechin metabolites in healthy human subjects. *Br J Nutr* 2008;100:846–51.
- [58] Neilson AP, Sapper TN, Janle EM, Rudolph R, Matusheski N V, Ferruzzi MG. Chocolate matrix factors modulate the pharmacokinetic behavior of cocoa flavan-3-ol phase II metabolites following oral consumption by Sprague-Dawley rats. *J Agric Food Chem* 2010;58:6685–91.
- [59] Neilson AP, George JC, Janle EM, Mattes RD, Rudolph R, Matusheski N V, et al. Influence of chocolate matrix composition on cocoa flavan-3-ol bioaccessibility in vitro and bioavailability in humans. *J Agric Food Chem* 2009;57:9418–26.
- [60] Mullen W, Borges G, Donovan JL, Edwards CA, Serafini M, Lean MEJ, et al. Milk decreases urinary excretion but not plasma pharmacokinetics of cocoa flavan-3-ol metabolites in humans. *Am J Clin Nutr* 2009;89:1784–91.
- [61] Serafini M, Bugianesi R, Maiani G, Valtuena S, De Santis S, Crozier A. Plasma antioxidants from chocolate. *Nature* 2003;424:1013.
- [62] Goldberg D. Absorption of three wine-related polyphenols in three different matrices by healthy subjects. *Clin Biochem* 2003;36:79–87.
- [63] Mateos-Martín ML, Pérez-Jiménez J, Fuguet E, Torres JL. Non-extractable proanthocyanidins from grapes are a source of bioavailable (epi)catechin and derived metabolites in rats. *Br J Nutr* 2012;108:290–7.

- [64] Saura-Calixto F, Pérez-Jiménez J, Touriño S, Serrano J, Fuguet E, Torres JL, et al. Proanthocyanidin metabolites associated with dietary fibre from in vitro colonic fermentation and proanthocyanidin metabolites in human plasma. *Mol Nutr Food Res* 2010;54:939–46.
- [65] Hatano T, Miyatake H, Natsume M, Osakabe N, Takizawa T, Ito H, et al. Proanthocyanidin glycosides and related polyphenols from cacao liquor and their antioxidant effects. *Phytochemistry* 2002;59:749–58.
- [66] Bouhamidi R, Prévost V, Nouvelot A. High protection by grape seed proanthocyanidins (GSPC) of polyunsaturated fatty acids against UV-C induced peroxidation. *C R Acad Sci III* 1998;321:31–8.
- [67] Carini M, Maffei Facino R, Aldini G, Calloni MT, Bombardelli E, Morazzoni P. The protection of polyunsaturated fatty acids in micellar systems against UVB-induced photo-oxidation by procyanidins from *Vitis vinifera* L., and the protective synergy with vitamin E. *Int J Cosmet Sci* 1998;20:203–15.
- [68] Devi A, Jolitha A, Ishii N. Grape Seed Proanthocyanidin Extract (GSPE) and antioxidant defense in the brain of adult rats. *Med Sci Monit* 2006;12:124–30.
- [69] Löhr G, Beikler T, Podbielski A, Standar K, Redanz S, Hensel A. Polyphenols from *Myrothamnus flabellifolia* Welw. inhibit in vitro adhesion of *Porphyromonas gingivalis* and exert anti-inflammatory cytoprotective effects in KB cells. *J Clin Periodontol* 2011;38:457–69.
- [70] Mayer R, Stecher G, Wuerzner R, Silva RC, Sultana T, Trojer L, et al. Proanthocyanidins: target compounds as antibacterial agents. *J Agric Food Chem* 2008;56:6959–66.
- [71] Smith AH, Mackie RI. Effect of condensed tannins on bacterial diversity and metabolic activity in the rat gastrointestinal tract. *Appl Environ Microbiol* 2004;70:1104–15.
- [72] Kylli P, Nohynek L, Puupponen-Pimiä R, Westerlund-Wikström B, Leppänen T, Welling J, et al. Lingonberry (*Vaccinium vitis-idaea*) and European cranberry (*Vaccinium microcarpon*) proanthocyanidins: isolation, identification, and bioactivities. *J Agric Food Chem* 2011;59:3373–84.
- [73] Ouédraogo M, Charles C, Ouédraogo M, Guissou IP, Stévigny C, Duez P. An overview of cancer chemopreventive potential and safety of proanthocyanidins. *Nutr Cancer* 2011;63:1163–73.
- [74] Pierini R, Kroon PA, Guyot S, Ivory K, Johnson IT, Belshaw NJ. Procyanidin effects on oesophageal adenocarcinoma cells strongly depend on flavan-3-ol degree of polymerization. *Mol Nutr Food Res* 2008;52:1399–407.

- [75] Kim Y-J, Park H-J, Yoon S-H, Kim M-J, Leem K-H, Chung J-H, et al. Anticancer effects of oligomeric proanthocyanidins on human colorectal cancer cell line, SNU-C4. *World J Gastroenterol* 2005;11:4674–8.
- [76] Maldonado-Celis ME, Bousserouel S, Gossé F, Lobstein A, Raul F. Apple procyanidins activate apoptotic signaling pathway in human colon adenocarcinoma cells by a lipid-raft independent mechanism. *Biochem Biophys Res Commun* 2009;388:372–6.
- [77] Valko M, Rhodes CJ, Moncol J, Izakovic M, Mazur M. Free radicals, metals and antioxidants in oxidative stress-induced cancer. *Chem Biol Interact* 2006;160:1–40.
- [78] Oikawa S, Yamada K, Yamashita N, Tada-Oikawa S, Kawanishi S. N-acetylcysteine, a cancer chemopreventive agent, causes oxidative damage to cellular and isolated DNA. *Carcinogenesis* 1999;20:1485–90.
- [79] Sakano K, Mizutani M, Murata M, Oikawa S, Hiraku Y, Kawanishi S. Procyanidin B2 has anti- and pro-oxidant effects on metal-mediated DNA damage. *Free Radic Biol Med* 2005;39:1041–9.
- [80] Oikawa S, Furukawa A, Asada H, Hirakawa K, Kawanishi S. Catechins Induce Oxidative Damage to Cellular and Isolated DNA through the Generation of Reactive Oxygen Species. *Free Radic Res* 2003;37:881–90.
- [81] Ebadi M, Swanson S. The status of zinc, copper, and metallothionein in cancer patients. *Prog Clin Biol Res* 1988;259:161–75.
- [82] Chun OK, Chung S-J, Claycombe KJ, Song WO. Serum C-reactive protein concentrations are inversely associated with dietary flavonoid intake in U.S. adults. *J Nutr* 2008;138:753–60.
- [83] Landberg R, Sun Q, Rimm EB, Cassidy A, Scalbert A, Mantzoros CS, et al. Selected dietary flavonoids are associated with markers of inflammation and endothelial dysfunction in U.S. women. *J Nutr* 2011;141:618–25.
- [84] Ceriello A, Taboga C, Tonutti L, Quagliaro L, Piconi L, Bais B, et al. Evidence for an independent and cumulative effect of postprandial hypertriglyceridemia and hyperglycemia on endothelial dysfunction and oxidative stress generation: effects of short- and long-term simvastatin treatment. *Circulation* 2002;106:1211–8.
- [85] Fernandez-Panchon MS, Villano D, Troncoso AM, Garcia-Parrilla MC. Antioxidant activity of phenolic compounds: from in vitro results to in vivo evidence. *Crit Rev Food Sci Nutr* 2008;48:649–71.
- [86] Crozier A, Jaganath IB, Clifford MN. Dietary phenolics: chemistry, bioavailability and effects on health. *Nat Prod Rep* 2009;26:1001–43.

- [87] Prior RL, Gu L, Wu X, Jacob RA, Sotoudeh G, Kader AA, et al. Plasma antioxidant capacity changes following a meal as a measure of the ability of a food to alter in vivo antioxidant status. *J Am Coll Nutr* 2007;26:170–81.
- [88] Natella F, Belevi F, Gentili V, Ursini F, Scaccini C. Grape seed proanthocyanidins prevent plasma postprandial oxidative stress in humans. *J Agric Food Chem* 2002;50:7720–5.
- [89] Kay CD, Holub BJ. The effect of wild blueberry (*Vaccinium angustifolium*) consumption on postprandial serum antioxidant status in human subjects. *Br J Nutr* 2002;88:389–98.
- [90] Kar P, Laight D, Rooprai HK, Shaw KM, Cummings M. Effects of grape seed extract in Type 2 diabetic subjects at high cardiovascular risk: a double blind randomized placebo controlled trial examining metabolic markers, vascular tone, inflammation, oxidative stress and insulin sensitivity. *Diabet Med* 2009;26:526–31.
- [91] Karlsen A, Retterstøl L, Laake P, Paur I, Kjølrsrud-Bøhn S, Sandvik L, et al. Anthocyanins Inhibit Nuclear Factor- $\kappa$ B Activation in Monocytes and Reduce Plasma Concentrations of Pro-Inflammatory Mediators in Healthy Adults. *J Nutr* 2007;137:1951–4.
- [92] Naruszewicz M, Laniewska I, Millo B, Dłuzniewski M. Combination therapy of statin with flavonoids rich extract from chokeberry fruits enhanced reduction in cardiovascular risk markers in patients after myocardial infraction (MI). *Atherosclerosis* 2007;194:e179–84.
- [93] Basu A, Du M, Sanchez K, Leyva MJ, Betts NM, Blevins S, et al. Green tea minimally affects biomarkers of inflammation in obese subjects with metabolic syndrome. *Nutrition* 2011;27:206–13.
- [94] Terra X, Montagut G, Bustos M, Llopiz N, Ardèvol A, Bladé C, et al. Grape-seed procyanidins prevent low-grade inflammation by modulating cytokine expression in rats fed a high-fat diet. *J Nutr Biochem* 2009;20:210–8.
- [95] Vendrame S, Daugherty A, Kristo AS, Riso P, Klimis-Zacas D. Wild blueberry (*Vaccinium angustifolium*) consumption improves inflammatory status in the obese Zucker rat model of the metabolic syndrome. *J Nutr Biochem* 2013;24:1508–12.
- [96] Bose M, Lambert JD, Ju J, Reuhl KR, Shapses SA, Yang CS. The major green tea polyphenol, (-)-epigallocatechin-3-gallate, inhibits obesity, metabolic syndrome, and fatty liver disease in high-fat-fed mice. *J Nutr* 2008;138:1677–83.
- [97] Terra X, Pallarés V, Ardèvol A, Bladé C, Fernández-Larrea J, Pujadas G, et al. Modulatory effect of grape-seed procyanidins on local and systemic inflammation in diet-induced obesity rats. *J Nutr Biochem* 2011;22:380–7.

- [98] Song X, Xu H, Feng Y, Li X, Lin M, Cao L. Protective effect of grape seed proanthocyanidins against liver ischemic reperfusion injury: particularly in diet-induced obese mice. *Int J Biol Sci* 2012;8:1345–62.
- [99] Coskun O, Kanter M, Korkmaz A, Oter S. Quercetin, a flavonoid antioxidant, prevents and protects streptozotocin-induced oxidative stress and beta-cell damage in rat pancreas. *Pharmacol Res* 2005;51:117–23.
- [100] Kim M-J, Ryu GR, Chung J-S, Sim SS, Min DS, Rhie D-J, et al. Protective effects of epicatechin against the toxic effects of streptozotocin on rat pancreatic islets: in vivo and in vitro. *Pancreas* 2003;26:292–9.
- [101] El-Alfy AT, Ahmed AAE, Fatani AJ. Protective effect of red grape seeds proanthocyanidins against induction of diabetes by alloxan in rats. *Pharmacol Res* 2005;52:264–70.
- [102] Sakurai T, Kitadate K, Nishioka H, Fujii H, Kizaki T, Kondoh Y, et al. Oligomerized grape seed polyphenols attenuate inflammatory changes due to antioxidative properties in coculture of adipocytes and macrophages. *J Nutr Biochem* 2010;21:47–54.
- [103] Letenneur L, Proust-Lima C, Le Gouge A, Dartigues JF, Barberger-Gateau P. Flavonoid intake and cognitive decline over a 10-year period. *Am J Epidemiol* 2007;165:1364–71.
- [104] Checkoway H, Powers K, Smith-Weller T, Franklin GM, Longstreth WT, Swanson PD. Parkinson's disease risks associated with cigarette smoking, alcohol consumption, and caffeine intake. *Am J Epidemiol* 2002;155:732–8.
- [105] Dai Q, Borenstein AR, Wu Y, Jackson JC, Larson EB. Fruit and vegetable juices and Alzheimer's disease: the Kame Project. *Am J Med* 2006;119:751–9.
- [106] Balu M, Sangeetha P, Murali G, Panneerselvam C. Age-related oxidative protein damages in central nervous system of rats: modulatory role of grape seed extract. *Int J Dev Neurosci* 2005;23:501–7.
- [107] Asha Devi S, Sagar Chandrasekar BK, Manjula KR, Ishii N. Grape seed proanthocyanidin lowers brain oxidative stress in adult and middle-aged rats. *Exp Gerontol* 2011;46:958–64.
- [108] Balu M, Sangeetha P, Haripriya D, Panneerselvam C. Rejuvenation of antioxidant system in central nervous system of aged rats by grape seed extract. *Neurosci Lett* 2005;383:295–300.
- [109] Joseph JA, Shukitt-Hale B, Casadesus G. Reversing the deleterious effects of aging on neuronal communication and behavior: beneficial properties of fruit polyphenolic compounds. *Am J Clin Nutr* 2005;81:313S – 316S.

- [110] Wang J, Ho L, Zhao W, Ono K, Rosensweig C, Chen L, et al. Grape-derived polyphenolics prevent Abeta oligomerization and attenuate cognitive deterioration in a mouse model of Alzheimer's disease. *J Neurosci* 2008;28:6388–92.
- [111] Maher P, Akaishi T, Abe K. Flavonoid fisetin promotes ERK-dependent long-term potentiation and enhances memory. *Proc Natl Acad Sci* 2006;103:16568–73.
- [112] Schroeter H, Bahia P, Spencer JPE, Sheppard O, Rattray M, Cadenas E, et al. (-)Epicatechin stimulates ERK-dependent cyclic AMP response element activity and up-regulates GluR2 in cortical neurons. *J Neurochem* 2007;101:1596–606.
- [113] Ho L, Ferruzzi MG, Janle EM, Wang J, Gong B, Chen T-Y, et al. Identification of brain-targeted bioactive dietary quercetin-3-O-glucuronide as a novel intervention for Alzheimer's disease. *FASEB J* 2013;27:769–81.
- [114] Youdim K a, Qaiser MZ, Begley DJ, Rice-Evans C a, Abbott NJ. Flavonoid permeability across an in situ model of the blood-brain barrier. *Free Radic Biol Med* 2004;36:592–604.
- [115] Saltiel AR, Kahn CR. Insulin signalling and the regulation of glucose and lipid metabolism. *Nature* 2001;414:799–806.
- [116] Shrayyef MZ, Gerich JE. Normal Glucose Homeostasis. In: Poretzky L, editor. *Princ. Diabetes Mellit.*, Boston, MA: Springer US; 2010, p. 19–35.
- [117] Ferrannini E, Bjorkman O, Reichard GA, Pilo A, Olsson M, Wahren J, et al. The disposal of an oral glucose load in healthy subjects. A quantitative study. *Diabetes* 1985;34:580–8.
- [118] Hers HG. Mechanisms of blood glucose homeostasis. *J Inherit Metab Dis* 1990;13:395–410.
- [119] Langerhans P, Morrison H. Contributions to the microscopic anatomy of the pancreas, by Paul Langerhans <Berlin, 1869> Reprint of the German original with an English translation and an introductory essay by H. Morrison, M. D. Baltimore, The Johns Hopkins press, 1937.; 1937.
- [120] Jain R, Lammert E. Cell-cell interactions in the endocrine pancreas. *Diabetes Obes Metab* 2009;11 Suppl 4:159–67.
- [121] Bosco D, Armanet M, Morel P, Niclauss N, SgROI A, Muller YD, et al. Unique arrangement of alpha- and beta-cells in human islets of Langerhans. *Diabetes* 2010;59:1202–10.
- [122] Wiederkehr A, Wollheim CB. Mitochondrial signals drive insulin secretion in the pancreatic  $\beta$ -cell. *Mol Cell Endocrinol* 2012;353:128–37.
- [123] Rorsman P. The pancreatic beta-cell as a fuel sensor: an electrophysiologist's viewpoint. *Diabetologia* 1997;40:487–95.



- [124] Ashcroft FM, Gribble FM. ATP-sensitive K<sup>+</sup> channels and insulin secretion: their role in health and disease. *Diabetologia* 1999;42:903–19.
- [125] Wollheim CB, Sharp GW. Regulation of insulin release by calcium. *Physiol Rev* 1981;61:914–73.
- [126] Briaud I, Lingohr MK, Dickson LM, Wrede CE, Rhodes CJ. Differential activation mechanisms of Erk-1/2 and p70(S6K) by glucose in pancreatic beta-cells. *Diabetes* 2003;52:974–83.
- [127] Wenham RM, Landt M, Easom RA. Glucose activates the multifunctional Ca<sup>2+</sup>/calmodulin-dependent protein kinase II in isolated rat pancreatic islets. *J Biol Chem* 1994;269:4947–52.
- [128] Easom RA, Filler NR, Ings EM, Tarpley J, Landt M. Correlation of the activation of Ca<sup>2+</sup>/calmodulin-dependent protein kinase II with the initiation of insulin secretion from perfused pancreatic islets. *Endocrinology* 1997;138:2359–64.
- [129] Dadi PK, Vierra NC, Ustione A, Piston DW, Colbran RJ, Jacobson D a. Inhibition of pancreatic  $\beta$ -cell ca<sup>2+</sup>/calmodulin-dependent protein kinase ii reduces glucose-stimulated calcium influx and insulin secretion, impairing glucose tolerance. *J Biol Chem* 2014;289:12435–45.
- [130] Watson ML, Macrae K, Marley AE, Hundal HS. Chronic effects of palmitate overload on nutrient-induced insulin secretion and autocrine signalling in pancreatic MIN6 beta cells. *PLoS One* 2011;6.
- [131] Henquin JC. Regulation of insulin secretion: a matter of phase control and amplitude modulation. *Diabetologia* 2009;52:739–51.
- [132] Moore MC, Cherrington AD, Wasserman DH. Regulation of hepatic and peripheral glucose disposal. *Best Pract Res Clin Endocrinol Metab* 2003;17:343–64.
- [133] Kahn CR, White MF. The insulin receptor and the molecular mechanism of insulin action. *J Clin Invest* 1988;82:1151–6.
- [134] Cross DA, Alessi DR, Cohen P, Andjelkovich M, Hemmings BA. Inhibition of glycogen synthase kinase-3 by insulin mediated by protein kinase B. *Nature* 1995;378:785–9.
- [135] Postic C, Dentin R, Girard J. Role of the liver in the control of carbohydrate and lipid homeostasis. *Diabetes Metab* 2004;30:398–408.
- [136] Klover PJ, Mooney RA. Hepatocytes: critical for glucose homeostasis. *Int J Biochem Cell Biol* 2004;36:753–8.
- [137] Roden M, Bernroider E. Hepatic glucose metabolism in humans—its role in health and disease. *Best Pract Res Clin Endocrinol Metab* 2003;17:365–83.

- [138] Taniguchi CM, Emanuelli B, Kahn CR. Critical nodes in signalling pathways: insights into insulin action. *Nat Rev Mol Cell Biol* 2006;7:85–96.
- [139] Towler MC, Hardie DG. AMP-activated protein kinase in metabolic control and insulin signaling. *Circ Res* 2007;100:328–41.
- [140] Lage R, Diéguez C, Vidal-Puig A, López M. AMPK: a metabolic gauge regulating whole-body energy homeostasis. *Trends Mol Med* 2008;14:539–49.
- [141] Hardie DG. AMPK: positive and negative regulation, and its role in whole-body energy homeostasis. *Curr Opin Cell Biol* 2015;33:1–7.
- [142] Viollet B, Guigas B, Leclerc J, Hébrard S, Lantier L, Mounier R, et al. AMP-activated protein kinase in the regulation of hepatic energy metabolism: from physiology to therapeutic perspectives. *Acta Physiol* 2009;196:81–98.
- [143] Viollet B, Lantier L, Devin-Leclerc J, Hébrard S, Amouyal C, Mounier R, et al. Targeting the AMPK pathway for the treatment of Type 2 diabetes. *Front Biosci* 2009;14:3380–400.
- [144] Steinberg GR, Kemp BE. AMPK in Health and Disease. *Physiol Rev* 2009;89:1025–78.
- [145] Jiang G, Zhang BB. Glucagon and regulation of glucose metabolism. *Am J Physiol Endocrinol Metab* 2003;284:E671–8.
- [146] Quesada I, Tudurí E, Ripoll C, Nadal A. Physiology of the pancreatic alpha-cell and glucagon secretion: role in glucose homeostasis and diabetes. *J Endocrinol* 2008;199:5–19.
- [147] Ramnanan CJ, Edgerton DS, Kraft G, Cherrington a D. Physiologic action of glucagon on liver glucose metabolism. *Diabetes Obes Metab* 2011;13 Suppl 1:118–25.
- [148] WHO; International Diabetes Foundation. Definition and diagnosis of diabetes mellitus and intermediate hyperglycemia: report of a WHO/IDF consultation. Geneva World Heal Organ 2006.
- [149] American Diabetes Association. Diagnosis and classification of diabetes mellitus. *Diabetes Care* 2012;35 Suppl 1:S64–71.
- [150] International Diabetes Federation. *IDF Diabetes Atlas. Sixth.* 2013.
- [151] Nathan DM, Davidson MB, DeFronzo RA, Heine RJ, Henry RR, Pratley R, et al. Impaired fasting glucose and impaired glucose tolerance: implications for care. *Diabetes Care* 2007;30:753–9.
- [152] DeFronzo RA, Tripathy D. Skeletal muscle insulin resistance is the primary defect in type 2 diabetes. *Diabetes Care* 2009;32 Suppl 2:S157–63.

- [153] Shulman GI, Rothman DL, Jue T, Stein P, DeFronzo RA, Shulman RG. Quantitation of muscle glycogen synthesis in normal subjects and subjects with non-insulin-dependent diabetes by  $^{13}\text{C}$  nuclear magnetic resonance spectroscopy. *N Engl J Med* 1990;322:223–8.
- [154] Cline GW, Petersen KF, Krssak M, Shen J, Hundal RS, Trajanoski Z, et al. Impaired glucose transport as a cause of decreased insulin-stimulated muscle glycogen synthesis in type 2 diabetes. *N Engl J Med* 1999;341:240–6.
- [155] Pendergrass M, Bertoldo A, Bonadonna R, Nucci G, Mandarino L, Cobelli C, et al. Muscle glucose transport and phosphorylation in type 2 diabetic, obese nondiabetic, and genetically predisposed individuals. *Am J Physiol Endocrinol Metab* 2007;292:E92–100.
- [156] Morino K, Petersen KF, Dufour S, Befroy D, Frattini J, Shatzkes N, et al. Reduced mitochondrial density and increased IRS-1 serine phosphorylation in muscle of insulin-resistant offspring of type 2 diabetic parents. *J Clin Invest* 2005;115:3587–93.
- [157] Krook A, Björnholm M, Galuska D, Jiang XJ, Fahlman R, Myers MG, et al. Characterization of signal transduction and glucose transport in skeletal muscle from type 2 diabetic patients. *Diabetes* 2000;49:284–92.
- [158] Weyer C, Bogardus C, Pratley RE. Metabolic characteristics of individuals with impaired fasting glucose and/or impaired glucose tolerance. *Diabetes* 1999;48:2197–203.
- [159] Festa A, D’Agostino R, Hanley AJG, Karter AJ, Saad MF, Haffner SM. Differences in insulin resistance in nondiabetic subjects with isolated impaired glucose tolerance or isolated impaired fasting glucose. *Diabetes* 2004;53:1549–55.
- [160] Butler AE, Janson J, Bonner-Weir S, Ritzel R, Rizza RA, Butler PC. Beta-cell deficit and increased beta-cell apoptosis in humans with type 2 diabetes. *Diabetes* 2003;52:102–10.
- [161] Del Guerra S, Lupi R, Marselli L, Masini M, Bugliani M, Sbrana S, et al. Functional and molecular defects of pancreatic islets in human type 2 diabetes. *Diabetes* 2005;54:727–35.
- [162] Tripathy D, Eriksson KF, Orho-Melander M, Fredriksson J, Ahlqvist G, Groop L. Parallel manifestation of insulin resistance and beta cell decompensation is compatible with a common defect in Type 2 diabetes. *Diabetologia* 2004;47:782–93.
- [163] Kanat M, Mari A, Norton L, Winnier D, DeFronzo RA, Jenkinson C, et al. Distinct  $\beta$ -cell defects in impaired fasting glucose and impaired glucose tolerance. *Diabetes* 2012;61:447–53.

- [164] Abdul-Ghani MA, Tripathy D, DeFronzo RA. Contributions of beta-cell dysfunction and insulin resistance to the pathogenesis of impaired glucose tolerance and impaired fasting glucose. *Diabetes Care* 2006;29:1130–9.
- [165] Meyer C, Pimenta W, Woerle HJ, Van Haeften T, Szoke E, Mitrakou A, et al. Different mechanisms for impaired fasting glucose and impaired postprandial glucose tolerance in humans. *Diabetes Care* 2006;29:1909–14.
- [166] Hanefeld M, Koehler C, Fuecker K, Henkel E, Schaper F, Temelkova-Kurktschiev T. Insulin secretion and insulin sensitivity pattern is different in isolated impaired glucose tolerance and impaired fasting glucose: the risk factor in Impaired Glucose Tolerance for Atherosclerosis and Diabetes study. *Diabetes Care* 2003;26:868–74.
- [167] Consortium TI. Tea consumption and incidence of type 2 diabetes in Europe: the EPIC-InterAct case-cohort study. *PLoS One* 2012;7:e36910.
- [168] Huxley R, Lee CMY, Barzi F, Timmermeister L, Czernichow S, Perkovic V, et al. Coffee, decaffeinated coffee, and tea consumption in relation to incident type 2 diabetes mellitus: a systematic review with meta-analysis. *Arch Intern Med* 2009;169:2053–63.
- [169] Törrönen R, Sarkkinen E, Niskanen T, Tapola N, Kilpi K, Niskanen L. Postprandial glucose, insulin and glucagon-like peptide 1 responses to sucrose ingested with berries in healthy subjects. *Br J Nutr* 2011;1–7.
- [170] Törrönen R, Sarkkinen E, Tapola N, Hautaniemi E, Kilpi K, Niskanen L. Berries modify the postprandial plasma glucose response to sucrose in healthy subjects. *Br J Nutr* 2010;103:1094–7.
- [171] Hlebowicz J, Darwiche G, Björgell O, Almér L-O. Effect of cinnamon on postprandial blood glucose, gastric emptying, and satiety in healthy subjects. *Am J Clin Nutr* 2007;85:1552–6.
- [172] Hlebowicz J, Hlebowicz A, Lindstedt S, Björgell O, Höglund P, Holst JJ, et al. Effects of 1 and 3 g cinnamon on gastric emptying, satiety, and postprandial blood glucose, insulin, glucose-dependent insulinotropic polypeptide, glucagon-like peptide 1, and ghrelin concentrations in healthy subjects. *Am J Clin Nutr* 2009;89:815–21.
- [173] Khan A, Safdar M, Ali Khan MM, Khattak KN, Anderson RA. Cinnamon improves glucose and lipids of people with type 2 diabetes. *Diabetes Care* 2003;26:3215–8.
- [174] Bryans JA, Judd PA, Ellis PR. The effect of consuming instant black tea on postprandial plasma glucose and insulin concentrations in healthy humans. *J Am Coll Nutr* 2007;26:471–7.
- [175] Sapwarobol S, Adisakwattana S, Changpeng S, Ratanawachirin W, Tanruttanawong K, Boonyarit W. Postprandial blood glucose response to grape

seed extract in healthy participants: A pilot study. *Pharmacogn Mag* 2012;8:192–6.

- [176] Grassi D, Desideri G, Necozione S, Lippi C, Casale R, Properzi G, et al. Blood pressure is reduced and insulin sensitivity increased in glucose-intolerant, hypertensive subjects after 15 days of consuming high-polyphenol dark chocolate. *J Nutr* 2008;138:1671–6.
- [177] Liu X, Zhou H-J, Rohdewald P. French maritime pine bark extract Pycnogenol dose-dependently lowers glucose in type 2 diabetic patients. *Diabetes Care* 2004;27:839.
- [178] Liu X, Wei J, Tan F, Zhou S, Würthwein G, Rohdewald P. Antidiabetic effect of Pycnogenol French maritime pine bark extract in patients with diabetes type II. *Life Sci* 2004;75:2505–13.
- [179] Törrönen R, Kolehmainen M, Sarkkinen E, Poutanen K, Mykkänen H, Niskanen L. Berries reduce postprandial insulin responses to wheat and rye breads in healthy women. *J Nutr* 2013;143:430–6.
- [180] Zhang H-J, Ji B-P, Chen G, Zhou F, Luo Y-C, Yu H-Q, et al. A combination of grape seed-derived procyanidins and gypenosides alleviates insulin resistance in mice and HepG2 cells. *J Food Sci* 2007;74:H1–7.
- [181] Kurimoto Y, Shibayama Y, Inoue S, Soga M, Takikawa M, Ito C, et al. Black soybean seed coat extract ameliorates hyperglycemia and insulin sensitivity via the activation of AMP-activated protein kinase in diabetic mice. *J Agric Food Chem* 2013;61:5558–64.
- [182] Hwang J-T, Kwon DY, Yoon SH. AMP-activated protein kinase: a potential target for the diseases prevention by natural occurring polyphenols. *N Biotechnol* 2009;26:17–22.
- [183] Takikawa M, Inoue S, Horio F, Tsuda T. Dietary anthocyanin-rich bilberry extract ameliorates hyperglycemia and insulin sensitivity via activation of AMP-activated protein kinase in diabetic mice. *J Nutr* 2010;140:527–33.
- [184] Collins QF, Liu H-Y, Pi J, Liu Z, Quon MJ, Cao W. Epigallocatechin-3-gallate (EGCG), a green tea polyphenol, suppresses hepatic gluconeogenesis through 5'-AMP-activated protein kinase. *J Biol Chem* 2007;282:30143–9.
- [185] Cordero-Herrera I, Martín MA, Bravo L, Goya L, Ramos S. Cocoa flavonoids improve insulin signalling and modulate glucose production via AKT and AMPK in HepG2 cells. *Mol Nutr Food Res* 2013;57:974–85.
- [186] Yogalakshmi B, Bhuvaneshwari S, Sreeja S, Anuradha CV. Grape seed proanthocyanidins and metformin act by different mechanisms to promote insulin signaling in rats fed high calorie diet. *J Cell Commun Signal* 2013;6:13–22.

- [187] Ding Y, Zhang Z, Dai X, Jiang Y, Bao L, Li Y, et al. Grape seed proanthocyanidins ameliorate pancreatic beta-cell dysfunction and death in low-dose streptozotocin- and high-carbohydrate/high-fat diet-induced diabetic rats partially by regulating endoplasmic reticulum stress. *Nutr Metab (Lond)* 2013;10:51.
- [188] Andrali SS, Sampley ML, Vanderford NL, Ozcan S. Glucose regulation of insulin gene expression in pancreatic beta-cells. *Biochem J* 2008;415:1–10.
- [189] Chakravarthy BK, Gupta S, Gode KD. Functional beta cell regeneration in the islets of pancreas in alloxan induced diabetic rats by (-)-epicatechin. *Life Sci* 1982;31:2693–7.
- [190] Martín MÁ, Fernández-Millán E, Ramos S, Bravo L, Goya L. Cocoa flavonoid epicatechin protects pancreatic beta cell viability and function against oxidative stress. *Mol Nutr Food Res* 2013:1–10.
- [191] Jayaprakasam B, Vareed SK, Olson LK, Nair MG. Insulin secretion by bioactive anthocyanins and anthocyanidins present in fruits. *J Agric Food Chem* 2005;53:28–31.
- [192] Chemler JA, Lock LT, Koffas MAG, Tzanakakis ES. Standardized biosynthesis of flavan-3-ols with effects on pancreatic beta-cell insulin secretion. *Appl Microbiol Biotechnol* 2007;77:797–807.
- [193] Hii CS, Howell SL. Effects of epicatechin on rat islets of Langerhans. *Diabetes* 1984;33:291–6.
- [194] Pinent M, Castell A, Baiges I, Montagut G, Arola L, Ardévol A. Bioactivity of Flavonoids on Insulin-Secreting Cells. *Compr Rev Food Sci Food Saf* 2008;7:299–308.
- [195] Zhu M, Hu J, Perez E, Phillips D, Kim W, Ghaedian R, et al. Effects of long-term cranberry supplementation on endocrine pancreas in aging rats. *Journals Gerontol* 2011;66A:1139–51.
- [196] Castell-Auví A, Cedó L, Pallarès V, Blay MT, Pinent M, Motilva MJ, et al. Procyanidins modify insulinemia by affecting insulin production and degradation. *J Nutr Biochem* 2012:<http://dx.doi.org/10.1016/j.jbbr.2011.03.031>.
- [197] Cedó L, Castell-Auví A, Pallarès V, Ubaida Mohien C, Baiges I, Blay M, et al. Pancreatic islet proteome profile in Zucker fatty rats chronically treated with a grape seed procyanidin extract. *Food Chem* 2012;135:1948–56.
- [198] Ansarullah, Bharucha B, Dwivedi M, Laddha NC, Begum R, Hardikar AA, et al. Antioxidant rich flavonoids from *Oreocnide integrifolia* enhance glucose uptake and insulin secretion and protects pancreatic  $\beta$ -cells from streptozotocin insult. *BMC Complement Altern Med* 2011;11:126.

- [199] Fernández-Millán E, Cordero-Herrera I, Ramos S, Escrivá F, Alvarez C, Goya L, et al. Cocoa-rich diet attenuates beta cell mass loss and function in young Zucker diabetic fatty rats by preventing oxidative stress and beta cell apoptosis. *Mol Nutr Food Res* 2015;n/a – n/a.
- [200] Cedó L, Castell-Auví A, Pallarès V, Blay M, Ardévol A, Arola L, et al. Grape seed procyanidin extract modulates proliferation and apoptosis of pancreatic beta-cells. *Food Chem* 2013;138:524–30.
- [201] Walpole SC, Prieto-Merino D, Edwards P, Cleland J, Stevens G, Roberts I. The weight of nations: an estimation of adult human biomass. *BMC Public Health* 2012;12:439.
- [202] Bhattacharya S, Oksbjerg N, Young JF, Jeppesen PB. Caffeic acid, naringenin and quercetin enhance glucose-stimulated insulin secretion and glucose sensitivity in INS-1E cells. *Diabetes, Obes Metab* 2014;16:602–12.
- [203] Fernández-Millán E, Ramos S, Alvarez C, Bravo L, Goya L, Martín MÁ. Microbial phenolic metabolites improve glucose-stimulated insulin secretion and protect pancreatic beta cells against tert-butyl hydroperoxide-induced toxicity via ERKs and PKC pathways. *Food Chem Toxicol* 2014;66:245–53.
- [204] Jin L. *Flavonoids in Saskatoon Fruits, Blueberry Fruits, and Legume Seeds*. University of Alberta, 2011.
- [205] Craig W, Beck L. *Phytochemicals: Health Protective Effects*. *Can J Diet Pract Res* 1999;60:78–84.
- [206] Scalbert A, Williamson G. Dietary Intake and Bioavailability of Polyphenols. *J Nutr* 2000;130:2073S – 2085S.
- [207] Chen ZY, Chan PT, Ho KY, Fung KP, Wang J. Antioxidant activity of natural flavonoids is governed by number and location of their aromatic hydroxyl groups. *Chem Phys Lipids* 1996;79:157–63.
- [208] Rice-Evans CA, Miller NJ, Paganga G. Structure-antioxidant activity relationships of flavonoids and phenolic acids. *Free Radic Biol Med* 1996;20:933–56.
- [209] Evans JL. Oxidative Stress and Stress-Activated Signaling Pathways: A Unifying Hypothesis of Type 2 Diabetes. *Endocr Rev* 2002;23:599–622.
- [210] Kirkham S, Akilen R, Sharma S, Tsiami A. The potential of cinnamon to reduce blood glucose levels in patients with type 2 diabetes and insulin resistance. *Diabetes Obes Metab* 2009;11:1100–13.
- [211] Stalmach A, Troufflard S, Serafini M, Crozier A. Absorption, metabolism and excretion of Choladi green tea flavan-3-ols by humans. *Mol Nutr Food Res* 2009;53:S44–53.

- [212] Kahle K, Kraus M, Scheppach W, Ackermann M, Ridder F, Richling E. Studies on apple and blueberry fruit constituents: do the polyphenols reach the colon after ingestion? *Mol Nutr Food Res* 2006;50:418–23.
- [213] Halliwell B, Rafter J, Jenner A. Health promotion by flavonoids, tocopherols, tocotrienols, and other phenols: direct or indirect effects? Antioxidant or not? *Am J Clin Nutr* 2005;81:268S – 276S.
- [214] Whitlock KA, Koziicky L, Jin A, Yee H, Ha C, Morris J, et al. Assessment of the mechanisms exerting glucose-lowering effects of dried peas in glucose-intolerant rats. *Br J Nutr* 2012;108 Suppl:S91–102.
- [215] Porter LJ, Hrstich LN, Chan BG. The conversion of procyanidins and prodelphinidins to cyanidin and delphinidin. *Phytochemistry* 1985;25:223–30.
- [216] Quinn R. Comparing rat's to human's age: How old is my rat in people years? *Nutrition* 2005;21:775–7.
- [217] Heikkinen S, Argmann CA, Champy M-F, Auwerx J. Evaluation of glucose homeostasis. *Curr Protoc Mol Biol* 2007;Chapter 29:Unit 29B.3.
- [218] Chan CB, MacPhail RM, Mitton K. Evidence for defective glucose sensing by islets of fa/fa obese Zucker rats. *Can J Physiol Pharmacol* 1993;71:34–9.
- [219] Chan CB, De Leo D, Joseph JW, McQuaid TS, Ha XF, Xu F, et al. Increased Uncoupling Protein-2 Levels in beta-cells Are Associated With Impaired Glucose-Stimulated Insulin Secretion: Mechanism of Action. *Diabetes* 2001;50:1302–10.
- [220] Zifkin M, Jin A, Ozga JA, Zaharia LI, Schernthaner JP, Gesell A, et al. Gene expression and metabolite profiling of developing highbush blueberry fruit indicates transcriptional regulation of flavonoid metabolism and activation of abscisic acid metabolism. *Plant Physiol* 2012;158:200–24.
- [221] Sutherland LN, Capozzi LC, Turchinsky NJ, Bell RC, Wright DC. Time course of high-fat diet-induced reductions in adipose tissue mitochondrial proteins: potential mechanisms and the relationship to glucose intolerance. *Am J Physiol Endocrinol Metab* 2008;295:E1076–83.
- [222] Thrush AB, Chabowski A, Heigenhauser GJ, McBride BW, Or-Rashid M, Dyck DJ. Conjugated linoleic acid increases skeletal muscle ceramide content and decreases insulin sensitivity in overweight, non-diabetic humans. vol. 32. 2007.
- [223] Borai A, Livingstone C, Ferns GAA. The biochemical assessment of insulin resistance. *Ann Clin Biochem* 2007;44:324–42.
- [224] Hemingway RW, McGraw GW. Kinetics of Acid-Catalyzed Cleavage of Procyanidins. *J Wood Chem Technol* 1983;3:421–35.



- [225] Tsang C, Auger C, Mullen W, Bornet A, Rouanet J-M, Crozier A, et al. The absorption, metabolism and excretion of flavan-3-ols and procyanidins following the ingestion of a grape seed extract by rats. *Br J Nutr* 2005;94:170–81.
- [226] Smith AH, Zoetendal E, Mackie RI. Bacterial Mechanisms to Overcome Inhibitory Effects of Dietary Tannins. *Microb Ecol* 2005;50:197–205.
- [227] Yamakoshi J, Tokutake S, Kikuchi M, Kubota Y, Konishi H, Mitsuoka T. Effect of Proanthocyanidin-Rich Extract from Grape Seeds on Human Fecal Flora and Fecal Odor. *Microb Ecol Health Dis* 2001;13:25–31.
- [228] Cerf ME, Chapman CS, Louw J. High-fat programming of hyperglycemia, hyperinsulinemia, insulin resistance, hyperleptinemia, and altered islet architecture in 3-month-old wistar rats. *ISRN Endocrinol* 2012;2012:627270.
- [229] Ahrén B, Gudbjartsson T, Al-Amin AN, Mårtensson H, Myrsén-Axcróna U, Karlsson S, et al. Islet perturbations in rats fed a high-fat diet. *Pancreas* 1999;18:75–83.
- [230] Deng S, Vatamaniuk M, Huang X, Doliba N, Lian M-MM-M, Frank A, et al. Structural and functional abnormalities in the islets isolated from type 2 diabetic subjects. *Diabetes* 2004;53:624–32.
- [231] Clark A, Wells CA, Buley ID, Cruickshank JK, Vanhegan RI, Matthews DR, et al. Islet amyloid, increased A-cells, reduced B-cells and exocrine fibrosis: quantitative changes in the pancreas in type 2 diabetes. *Diabetes Res* 1988;9:151–9.
- [232] Ehses JA, Ellingsgaard H, Böni-Schnetzler M, Donath MY. Pancreatic islet inflammation in type 2 diabetes: from alpha and beta cell compensation to dysfunction. *Arch Physiol Biochem* 2009;115:240–7.
- [233] Dinneen S, Alzaid A, Turk D, Rizza R. Failure of glucagon suppression contributes to postprandial hyperglycaemia in IDDM. *Diabetologia* 1995;38:337–43.
- [234] Wang J, Ferruzzi MG, Ho L, Blount J, Janle EM, Gong B, et al. Brain-targeted proanthocyanidin metabolites for Alzheimer’s disease treatment. *J Neurosci* 2012;32:5144–50.
- [235] Okuda MH, Zemdegs JCS, de Santana AA, Santamarina AB, Moreno MF, Hachul ACL, et al. Green tea extract improves high fat diet-induced hypothalamic inflammation, without affecting the serotonergic system. *J Nutr Biochem* 2014;25:1084–9.
- [236] Ward AS, Comer SD, Haney M, Fischman MW, Foltin RW. Fluoxetine-maintained obese humans: effect on food intake and body weight. vol. 66. 1999.
- [237] Lu C, Zhu W, Shen CL, Gao W. Green tea polyphenols reduce body weight in rats by modulating obesity-related genes. *PLoS One* 2012;7:1–11.

- [238] Venables MC, Hulston CJ, Cox HR, Jeukendrup AE. Green tea extract ingestion, fat oxidation, and glucose tolerance in healthy humans. *Am J Clin Nutr* 2008;87:778–84.
- [239] Hodgson AB, Randell RK, Jeukendrup AE. The effect of green tea extract on fat oxidation at rest and during exercise: evidence of efficacy and proposed mechanisms. *Adv Nutr* 2013;4:129–40.
- [240] Randell RK, Hodgson AB, Lotito SB, Jacobs DM, Boon N, Mela DJ, et al. No effect of 1 or 7 d of green tea extract ingestion on fat oxidation during exercise. *Med Sci Sports Exerc* 2013;45:883–91.
- [241] van't Slot G, Humpf HU. Degradation and metabolism of catechin, epigallocatechin-3-gallate (EGCG), and related compounds by the intestinal microbiota in the pig cecum model. *J Agric Food Chem* 2009;57:8041–8.
- [242] Halliwell B, Zhao K, Whiteman M. The gastrointestinal tract: a major site of antioxidant action? *Free Radic Res* 2000;33:819–30.
- [243] Steffen Y, Schewe T, Sies H. (-)-Epicatechin elevates nitric oxide in endothelial cells via inhibition of NADPH oxidase. *Biochem Biophys Res Commun* 2007;359:828–33.
- [244] Martín MÁ, Serrano ABG, Ramos S, Pulido MI, Bravo L, Goya L. Cocoa flavonoids up-regulate antioxidant enzyme activity via the ERK1/2 pathway to protect against oxidative stress-induced apoptosis in HepG2 cells. *J Nutr Biochem* 2010;21:196–205.
- [245] Cordero-herrera I, Martín MA, Goya L. Cocoa flavonoids protect hepatic cells function against high glucose-induced oxidative stress . Relevance of MAPKs. *Mol Nutr Food Res* 2014:1–32.
- [246] Ramirez-Sanchez I, Maya L, Ceballos G, Villarreal F. (-)-Epicatechin activation of endothelial cell endothelial nitric oxide synthase, nitric oxide, and related signaling pathways. *Hypertension* 2010;55:1398–405.
- [247] Frödin M, Sekine N, Roche E, Filloux C, Prentki M, Wollheim CB, et al. Glucose, other secretagogues, and nerve growth factor stimulate mitogen-activated protein kinase in the insulin-secreting  $\beta$ -cell line, INS-1. *J Biol Chem* 1995;270:7882–9.
- [248] Fujimoto S, Mukai E, Inagaki N. Role of endogenous ROS production in impaired metabolism-secretion coupling of diabetic pancreatic  $\beta$ -cells. *Prog Biophys Mol Biol* 2011;107:304–10.
- [249] Li N, Brun T, Cnop M, Cunha D a., Eizirik DL, Maechler P. Transient oxidative stress damages mitochondrial machinery inducing persistent  $\beta$ -cell dysfunction. *J Biol Chem* 2009;284:23602–12.

- [250] Maechler P. Hydrogen Peroxide Alters Mitochondrial Activation and Insulin Secretion in Pancreatic Beta Cells. *J Biol Chem* 1999;274:27905–13.
- [251] Hoppa MB, Collins S, Ramracheya R, Hodson L, Amisten S, Zhang Q, et al. Chronic Palmitate Exposure Inhibits Insulin Secretion by Dissociation of Ca<sup>2+</sup> Channels from Secretory Granules. *Cell Metab* 2009;10:455–65.
- [252] Easom RA. CaM kinase II: A protein kinase with extraordinary talents germane to insulin exocytosis. *Diabetes* 1999;48:675–84.
- [253] Boden G. Role of fatty acids in the pathogenesis of insulin resistance and NIDDM. *Diabetes* 1997;46:3–10.
- [254] Boden G, Shulman GI. Free fatty acids in obesity and type 2 diabetes: defining their role in the development of insulin resistance and beta-cell dysfunction. *Eur J Clin Invest* 2002;32 Suppl 3:14–23.
- [255] Ayvaz G, Balos Törüner F, Karakoç A, Yetkin I, Cakir N, Arslan M. Acute and chronic effects of different concentrations of free fatty acids on the insulin secreting function of islets. *Diabetes Metab* 2002;28:3S7–12; discussion 3S108–12.
- [256] El-Assaad W, Buteau J, Peyot ML, Nolan C, Roduit R, Hardy S, et al. Saturated fatty acids synergize with elevated glucose to cause pancreatic beta-cell death. *Endocrinology* 2003;144:4154–63.
- [257] Braun AP, Schulman H. The multifunctional calcium/calmodulin-dependent protein kinase: from form to function. *Annu Rev Physiol* 1995;57:417–45.
- [258] Wang Z, Ramanadham S, Ma ZA, Bao S, Mancuso DJ, Gross RW, et al. Group VIA phospholipase A2 forms a signaling complex with the calcium/calmodulin-dependent protein kinase IIbeta expressed in pancreatic islet beta-cells. *J Biol Chem* 2005;280:6840–9.
- [259] Niki I, Okazaki K, Saitoh M, Niki A, Niki H, Tamagawa T, et al. Presence and possible involvement of Ca<sup>2+</sup>/calmodulin-dependent protein kinases in insulin release from the rat pancreatic beta cell. *Biochem Biophys Res Commun* 1993;191:255–61.
- [260] Tabuchi H, Yamamoto H, Matsumoto K, Ebihara K, Takeuchi Y, Fukunaga K, et al. Regulation of insulin secretion by overexpression of Ca<sup>2+</sup>/calmodulin-dependent protein kinase II in insulinoma MIN6 cells. *Endocrinology* 2000;141:2350–60.
- [261] Norling LL, Colca JR, Kelly PT, McDaniel ML, Landt M. Activation of calcium and calmodulin dependent protein kinase II during stimulation of insulin secretion. *Cell Calcium* 1994;16:137–50.

- [262] Lenzen S, Drinkgern J. Low antioxidant enzyme gene expression in pancreatic islets compared with various other mouse tissues. *Free Radic Biol Med* 1996;20:463–6.
- [263] Pi J, Bai Y, Zhang Q, Wong V, Floering LM, Daniel K, et al. Reactive Oxygen Species as a Signal in Glucose- Stimulated Insulin Secretion. *Diabetes* 2007;56:1783–91.
- [264] Ni Q, Ganesan A, Aye-Han N-N, Gao X, Allen MD, Levchenko A, et al. Signaling diversity of PKA achieved via a Ca<sup>2+</sup>-cAMP-PKA oscillatory circuit. *Nat Chem Biol* 2011;7:34–40.
- [265] Kaihara KA, Dickson LM, Jacobson DA, Tamarina N, Roe MW, Philipson LH, et al.  $\beta$ -cell-specific protein kinase A activation enhances the efficiency of glucose control by increasing acute-phase insulin secretion. *Diabetes* 2013;62:1527–36.
- [266] Munton RP, Vizi S, Mansuy IM. The role of protein phosphatase-1 in the modulation of synaptic and structural plasticity. *FEBS Lett.*, vol. 567, 2004, p. 121–8.
- [267] Blitzer RD, Connor JH, Brown GP, Wong T, Shenolikar S, Iyengar R, et al. Gating of CaMKII by cAMP-regulated protein phosphatase activity during LTP. *Science* (80- ) 1998;280:1940–2.
- [268] Lisman J, Schulman H, Cline H. The molecular basis of CaMKII function in synaptic and behavioural memory. *Nat Rev Neurosci* 2002;3:175–90.
- [269] Moreno-Ulloa A, Romero-Perez D, Villarreal F, Ceballos G, Ramirez-Sanchez I. Cell membrane mediated (-)-epicatechin effects on upstream endothelial cell signaling: Evidence for a surface receptor. *Bioorganic Med Chem Lett* 2014;24:2749–52.
- [270] McGarry JD. Banting lecture 2001: dysregulation of fatty acid metabolism in the etiology of type 2 diabetes. *Diabetes* 2002;51:7–18.
- [271] Taylor R, Magnusson I, Rothman DL, Cline GW, Caumo A, Cobelli C, et al. Direct assessment of liver glycogen storage by <sup>13</sup>C nuclear magnetic resonance spectroscopy and regulation of glucose homeostasis after a mixed meal in normal subjects. *J Clin Invest* 1996;97:126–32.
- [272] Petersen KF, Cline GW, Gerard DP, Magnusson I, Rothman DL, Shulman GI. Contribution of net hepatic glycogen synthesis to disposal of an oral glucose load in humans. *Metabolism* 2001;50:598–601.
- [273] Ferrannini E, Wahren J, Faber OK, Felig P, Binder C, DeFronzo RA. Splanchnic and renal metabolism of insulin in human subjects: a dose-response study. *Am J Physiol* 1983;244:E517–27.

- [274] Michael MD, Kulkarni RN, Postic C, Previs SF, Shulman GI, Magnuson MA, et al. Loss of insulin signaling in hepatocytes leads to severe insulin resistance and progressive hepatic dysfunction. *Mol Cell* 2000;6:87–97.
- [275] Consoli A. Role of Liver in Pathophysiology of NIDDM. *Diabetes Care* 1992;15:430–41.
- [276] Consoli A, Nurjhan N, Capani F, Gerich J. Predominant role of gluconeogenesis in increased hepatic glucose production in NIDDM. *Diabetes* 1989;38:550–7.
- [277] Shah P, Vella A, Basu A, Basu R, Schwenk WF, Rizza RA. Lack of suppression of glucagon contributes to postprandial hyperglycemia in subjects with type 2 diabetes mellitus. *J Clin Endocrinol Metab* 2000;85:4053–9.
- [278] Gastaldelli A, Baldi S, Pettiti M, Toschi E, Camastra S, Natali A, et al. Influence of obesity and type 2 diabetes on gluconeogenesis and glucose output humans. A quantitative study. *Diabetes* 2000;49:1367–73.
- [279] Walle T. Absorption and metabolism of flavonoids. *Free Radic Biol Med* 2004;36:829–37.
- [280] Donovan JL, Crespy V, Manach C, Morand C, Besson C, Scalbert A, et al. Catechin is metabolized by both the small intestine and liver of rats. *J Nutr* 2001;131:1753–7.
- [281] Passonneau J V, Lauderdale VR. A Comparison of Three Measurement in Tissues. *Anal Biochem* 1974;60:405–12.
- [282] Kraegen EW, Clark PW, Jenkins AB, Daley EA, Chisholm DJ, Storlien LH. Development of muscle insulin resistance after liver insulin resistance in high-fat-fed rats. *Diabetes* 1991;40:1397–403.
- [283] Brüning JC, Michael MD, Winnay JN, Hayashi T, Hörsch D, Accili D, et al. A muscle-specific insulin receptor knockout exhibits features of the metabolic syndrome of NIDDM without altering glucose tolerance. *Mol Cell* 1998;2:559–69.
- [284] Blüher M, Michael MD, Peroni OD, Ueki K, Carter N, Kahn BB, et al. Adipose tissue selective insulin receptor knockout protects against obesity and obesity-related glucose intolerance. *Dev Cell* 2002;3:25–38.
- [285] Waltner-Law ME, Wang XL, Law BK, Hall RK, Nawano M, Granner DK. Epigallocatechin gallate, a constituent of green tea, represses hepatic glucose production. *J Biol Chem* 2002;277:34933–40.
- [286] Sies H. Glutathione and its role in cellular functions. *Free Radic Biol Med* 1999;27:916–21.
- [287] Wu G, Fang Y-Z, Yang S, Lupton JR, Turner ND. Glutathione metabolism and its implications for health. *J Nutr* 2004;134:489–92.

- [288] Lee SF, Liang YC, Lin JK. Inhibition of 1,2,4-benzenetriol-generated active oxygen species and induction of phase II enzymes by green tea polyphenols. *Chem Biol Interact* 1995;98:283–301.
- [289] Na HK, Surh YJ. Modulation of Nrf2-mediated antioxidant and detoxifying enzyme induction by the green tea polyphenol EGCG. *Food Chem Toxicol* 2008;46:1271–8.
- [290] Matsumura Y, Nakagawa Y, Mikome K, Yamamoto H, Osakabe N. Enhancement of Energy Expenditure following a Single Oral Dose of Flavan-3-Ols Associated with an Increase in Catecholamine Secretion. *PLoS One* 2014;9:e112180.
- [291] Pajuelo D, Quesada H, Díaz S, Fernández-Iglesias A, Arola-Arnal A, Bladé C, et al. Chronic dietary supplementation of proanthocyanidins corrects the mitochondrial dysfunction of brown adipose tissue caused by diet-induced obesity in Wistar rats. *Br J Nutr* 2012;107:170–8.
- [292] Panickar KS. Effects of dietary polyphenols on neuroregulatory factors and pathways that mediate food intake and energy regulation in obesity. *Mol Nutr Food Res* 2013;57:34–47.
- [293] Hashemi Z, Yang K, Yang H, Jin A, Ozga J, Chan CB. Cooking enhances beneficial effects of pea seed coat consumption on glucose tolerance, incretin and pancreatic hormones in high fat diet-fed rats. *Appl Physiol Nutr Metab* n.d.;0:null.
- [294] Gil A, Olza J, Gil-Campos M, Gomez-Llorente C, Aguilera CM. Is adipose tissue metabolically different at different sites? *Int J Pediatr Obes* 2011;6 Suppl 1:13–20.
- [295] Després J-P, Lemieux I. Abdominal obesity and metabolic syndrome. *Nature* 2006;444:881–7.
- [296] Kahn SE, Zraika S, Utzschneider KM, Hull RL. The beta cell lesion in type 2 diabetes: There has to be a primary functional abnormality. *Diabetologia* 2009;52:1003–12.
- [297] Henquin JC, Rahier J. Pancreatic alpha cell mass in European subjects with type 2 diabetes. *Diabetologia* 2011;54:1720–5.
- [298] Yoon KH, Ko SH, Cho JH, Lee JM, Ahn YB, Song KH, et al. Selective beta-cell loss and alpha-cell expansion in patients with type 2 diabetes mellitus in Korea. *J Clin Endocrinol Metab* 2003;88:2300–8.
- [299] Kim A, Miller K, Jo J, Kilimnik G, Wojcik P, Hara M. Islet architecture: A comparative study. *Islets* 2009;1:129–36.
- [300] Rodriguez-Mateos A, Toro-Funes N, Cifuentes-Gomez T, Cortese-Krott M, Heiss C, Spencer JPE. Uptake and metabolism of (-)-epicatechin in endothelial cells. *Arch Biochem Biophys* 2014;559:17–23.

- [301] Ito Y, Oumi S, Nagasawa T, Nishizawa N. Oxidative stress induces phosphoenolpyruvate carboxykinase expression in H4IIE cells. *Biosci Biotechnol Biochem* 2006;70:2191–8.
- [302] Davies GF, Khandelwal RL, Wu L, Juurlink BHJ, Roesler WJ. Inhibition of phosphoenolpyruvate carboxykinase (PEPCK) gene expression by troglitazone: a peroxisome proliferator-activated receptor- Catalyzes the O-methylation of the hydroxy group of the hydroxymycolate to form methoxymycolate.  $\gamma$  (PPAR $\gamma$ )-independent,. *Biochemical Pharmacology* 2001;62:1071–9.
- [303] Kumashiro N, Tamura Y, Uchida T, Ogihara T, Fujitani Y, Hirose T, et al. Impact of oxidative stress and peroxisome proliferator-activated receptor gamma coactivator-1 alpha in hepatic insulin resistance. *Diabetes* 2008;57:2083–91.
- [304] Oakes ND, Cooney GJ, Camilleri S, Chisholm DJ, Kraegen EW. Mechanisms of liver and muscle insulin resistance induced by chronic high-fat feeding. *Diabetes* 1997;46:1768–74.
- [305] Oomah BD, Patras A, Rawson A, Singh N, Compos-Vega R. *Chemistry of Pulses*. 1st ed. Elsevier Ltd; 2011.
- [306] Lawson M. Hey Skippy, Spread the Word. *Natl Post* 2006.
- [307] Kanters J. No Pea butter and jam, anyone? *Food Thought* 2002.

## **Appendix A**

### **U.S. Provisional Patent Application**

**For**

**Pea (*Pisum sativum* L.) Seed Coats and Seed Coat Fractions**

Inventors: Jocelyn OZGA

Catherine CHAN

Alena JIN

Han YANG

Seyede HASHEMI

Kaiyuan YANG

Assignee: University of Alberta



## **FIELD**

The present disclosure relates to pulse grains and methods and compositions for improving health and/or beneficial effects in a human and/or animal diet.

## **INTRODUCTION**

Plant-based foods provide a significant amount of phytochemicals in our diet. Phytochemicals are non-nutrient compounds that have biological activity in the body [1]. Among them, flavonoids have been extensively studied because they exhibit a variety of physiological effects [2]. A subgroup of flavonoids, proanthocyanidins (PAC, or condensed tannins) are the oligomers and polymers of flavan-3-ols [3]. They exist in a variety of foods such as peas, beans, nuts, spices, fruits, wine and tea, and contribute the most to total flavonoid intake in the diet [4]. The estimated average dietary intake of PAC varies from 95 – 227 mg/d in different populations [5–9].

The availability of the phenolic hydrogens as hydrogen-donating radical scavengers and singlet oxygen quenchers predicts PAC antioxidant activity [10,11]. PAC as well as their monomeric flavan-3-ol subunits and hydrolysis-derived anthocyanin products can scavenge free radicals and reactive oxygen species (ROS) such as hydroxyl and peroxy radicals [10,11], which play a significant role in inducing oxidative stress [12], hence, research has been focused on their effects on alleviating oxidative stress.

Evidence is emerging to support consumption of PAC-rich foods to improve glycemic control. Black tea [13] and berries [14] reduced postprandial glycemia and moderately increased plasma glucagon-like peptide-1 in healthy subjects. Improvement in insulin sensitivity and lowered fasting blood glucose were observed in randomized clinical trials that evaluated the therapeutic potential of cinnamon amongst diabetic and insulin-resistant patients [15].

Animal studies suggest that PAC may exert effects on the endocrine pancreas. Grape seed PAC extracts alleviated oxidative stress in alloxan-induced diabetic rats by increasing pancreatic glutathione concentrations and reducing of lipid peroxidation [16]. Green tea epicatechin preserved pancreatic islet morphology and function against streptozotocin (STZ) toxicity both *in vivo* and *in vitro* [17]. Grape seed PAC extracts favorably modulated proteins involved in insulin

synthesis and secretion [18]. PAC also prevented  $\beta$ -cell loss caused by aging and apoptosis [18–20].

Thus, findings from studies both *in vivo* and *in vitro* indicate PAC's physiological role in modulating glucose homeostasis in the body, potentially by acting on cell signalling pathways to improve pancreatic  $\beta$ -cell function. However, plant-derived PAC are polymeric structures with a wide degree of polymerization (DP) range; therefore, the absorption and bioavailability of native PAC is limited [21]. Many *in vitro* PAC mechanistic studies tested concentrations not relevant to dietary intake and absorption, whereas the amount of PAC absorbed into the body was not quantified in most *in vivo* studies. Other obstacles included lack of knowledge of the metabolism of PAC in humans, lack of biomarkers specific for PAC intake and insufficiently sensitive analytical methods for PAC and metabolites. The existing bioavailability studies only detect trace amounts of PAC with  $DP < 2$ , usually pmol/L or nmol/L, in the urine and plasma [22–25]. This concentration range of PAC is not likely to have antioxidant actions in the body [26].

### **SUMMARY**

Disclosed is a method for improving health and/or other beneficial effects in a subject, comprising administering pea seed coat fractions to said subject. In some embodiments, said subject is a human or animal. In some embodiments, said health and/or beneficial effect is selected from retained PAC bioavailability, retained PAC bioactivity, improved insulin sensitivity, reduced glycemia, increased satiety, improved glucose tolerance, improved glucose control, improved glucose homeostasis, beneficial effects on pancreatic islet composition and insulin secretion. In some embodiments, said health and/or beneficial effect is selected from PAC-derived products that have increased bioavailability, improved insulin sensitivity, reduced glycemia, increased satiety, improved glucose tolerance, improved glucose control, improved glucose homeostasis, beneficial effects on pancreatic islet composition and insulin secretion.

Disclosed is a composition comprising pea seed coat fractions. In some embodiments, said composition is selected from a food, animal feed, flour, fibre, and ingredient.

Disclosed is a method for improving health and/or other beneficial effects in a subject, comprising administering cooked pea seed coat fractions to said subject.

Disclosed is a method for improving health and/or other beneficial effects in a subject, comprising administering pea seed coat fractions processed by cooking followed by freeze-drying to said subject.

Disclosed is method for increasing the bioavailability of proanthocyanidins (PAC), comprising hydrolyzing pea seed coat-derived PACs.

### **BRIEF DESCRIPTION OF THE DRAWINGS**

#### **FIGURE 1: Effects of diet on body weight change during the PAC/HPAC feeding trial.**

Male Sprague Dawley rats were fed 20% w/w high fat diet (HFD) for 6 weeks, then were randomly assigned [arrow] to HFD (n=23), 0.8% w/w proanthocyanidin + HFD (PAC, n=22), or 0.8% w/w hydrolyzed proanthocyanidin + HFD (HPAC, n=19) and maintained for 4 weeks. Additional rats were fed 6% w/w low fat diet (LFD, n=20) for 10 weeks as a normal control. Body weight was recorded weekly. Data are presented as percentage of the baseline weights. <sup>a</sup>P < 0.05 compared with HFD, <sup>b</sup>P < 0.05 compared with LFD, Bonferroni's multiple comparison.

**FIGURE 2: Blood glucose concentrations and insulin release after glucose challenge in rats fed PAC or HPAC.** Intraperitoneal glucose tolerance tests were performed at week 11. After overnight fasting, blood glucose (A) and plasma insulin (B) were measured at 0, 10, 20, 30, 60, 120 min after intraperitoneal administration of 1 g/kg body weight glucose. <sup>a</sup>P < 0.05 compared with HFD, <sup>b</sup>P < 0.05 compared with LFD, <sup>c</sup>P < 0.05 compared with PAC. Incremental area under the curve (IAUC) of glucose response (C) and insulin secretion (D) were calculated from A and B, respectively. (E) Insulin-glucose AUC index calculated from the product of glucose and insulin AUC, where a lower value indicates increased insulin sensitivity (Sutherland et al., 2008; Thrush et al., 2007). HFD, n=11; LFD, n=10; PAC, n=10; HPAC, n=8. \*P < 0.05, \*\*P < 0.01, Bonferroni's multiple comparison.

#### **FIGURE 3: Blood glucose responses after insulin challenge in rats fed PAC or HPAC.**

Insulin tolerance tests were performed before the day of tissue collection. After 4h fasting, blood glucose levels was measured at 0, 15, 30, 60, 90, 120 min after intraperitoneal administration of 5 U/kg body weight insulin. Changes in blood glucose (A) are expressed as percent of 4h-fasted glucose and (B) slopes for 60-120 min were calculated as a direct measurement of glucose recovery rate (Borai et al., 2007). N=8 for all groups. \*P < 0.05, Bonferroni's multiple comparison.

**FIGURE 4: Effects of different diets on pancreatic morphology, fasted insulin and glucagon in rats fed PAC or HPAC.** Immunohistochemical staining of insulin and glucagon (n=5 for all groups) was shown in panel A and B, respectively. The percentages of insulin (C)- or glucagon (D)-positive area versus the total pancreas areas were calculated as estimates of pancreatic  $\beta$ - or  $\alpha$ -cell mass. The ratio of  $\alpha$ - to  $\beta$ -cell area (E) was calculated to reflect cell composition of pancreatic islets. Fasted plasma insulin (F, n=8 for all groups) and glucagon (G, n=6 for all groups) were also measured. \*P < 0.05, Bonferroni's multiple comparison.

**FIGURE 5: Effects of different diets on glucose-stimulated insulin secretion from isolated islets of rats fed PAC or HPAC.** Isolated islets were cultured in fresh medium plus 2.8 and 16.5 mmol/L glucose for 2 h. Insulin secretion (A) is presented as percent of total content. Insulin content (B) and insulin stimulation index (C) were calculated as described above. N=5 for all groups. \*P < 0.05, Bonferroni's multiple comparison.

**FIGURE 6A: Structures of pea seed coat PAC dimers, the acid hydrolyzed PAC-derived compound delphinidin, PAC subunit flavan-3-ols epigallocatechin and epicatechin, and serum-derived metabolites.**

**Figure 6B: ESI-MS spectrum of the HPAC serum extract identifying epicatechin-3'-O-glucuronide and 4'-O-methyl-epigallocatechin.** (A) Total ion chromatogram in negative MS/MS mode with precursor ion mass 465.1038; (B) Product ion spectrum of the 4.85 min peak which belongs to epicatechin-3'-O-glucuronide; (C) Total ion chromatogram in negative MS/MS mode with precursor ion mass 319.0823; (D) Product ion spectrum of the 1.85 min peak which belongs to 4'-O-methyl-epigallocatechin.

**FIGURE 7: Plasma gastric inhibitory polypeptide (GIP) concentrations measured during oGTT at fasting (t=0 min), and following administration of 1g/kg glucose (t=30 min) in rats fed raw or cooked pea seed coats.** The bars are the mean  $\pm$  SEM, n=4-7. \* indicates significant difference compared to HFD (\*P<0.05).

**FIGURE 8: Effect of feeding PSC on oral and intraperitoneal glucose tolerance in rats fed raw or cooked pea seed coats.** (A, C) Effect of 4 weeks of feeding a high fat diet (HFD, 20% w/w) supplemented with raw (RP) or cooked (CP) pea seed coats on blood glucose levels measured basally and following oral or intraperitoneal administration of 1g/kg glucose. (B, D) Incremental area under the curve (IAUC) was calculated for glucose during oral glucose

tolerance test (oGTT) and intraperitoneal glucose tolerance test (ipGTT). (E,G) Plasma insulin levels measured using the blood samples collected during oGTT and ipGTT (baseline and in response to administration of 1g/kg glucose). (F,H) Incremental area under the curve for insulin during oGTT and ipGTT. The data are means  $\pm$  SEM, n=4-14. Significant differences seen at different time points are explained in the text, while differences between incremental area under the curve (IAUC) are depicted here. Asterisks show significant difference compared to HFD (\*\*\*P<0.001, \*\* P<0.01, \*P<0.05).

**FIGURE 9: Insulin tolerance test was performed on rats fed raw or cooked pea seed coats after a 4 hour fast.** Blood glucose levels are shown as (A) % of basal glucose, and Area Under the Curve (AUC) from (B) t=0 to t= 30 min and (C) t=30 to t=120 min for blood glucose. A significant decrease in glucose for RP compared to HFD was observed at t=30-120 min (\*P<0.05). Data are means  $\pm$  SEM, n=8.

**FIGURE 10: Beta-cell (A) and alpha-cell (B) areas of rats fed a high fat diet (HFD), raw PSC (RP), cooked PSC (CP) and low fat diet (LFD) for 4 weeks, presented as percentage of pancreatic area.** (C) Estimated total islet area. Alpha-cell area was significantly different between the groups (P<0.05), where CP rats revealed a smaller alpha-cell area ( $\delta$  P<0.05) when compared to RP. Data are means  $\pm$  SEM, n=6-8. (D) Representative insulin- and glucagon-stained islets of all the groups.

**FIGURE 11: Number of K-cells (A) and L-cells (B) as detected using GIP and GLP-1 immunoreactivity in jejunum and ileum of rats fed raw or cooked pea seed coats,** presented as number of positive cells per villus. Data are means  $\pm$  SEM, n=4. No significant differences were observed.

**FIGURE 12: mRNA expression of Glut2 (A), SGLT1 (B) and Glut5 (C) (normalized to 18S rRNA expression) in jejunum of rats fed raw or cooked pea seed coats.** Data are means  $\pm$  SEM, n=5-12. Letter <sup>b</sup> indicates significant difference compared to LFD (<sup>b</sup>P<0.01).

### **DETAILED DESCRIPTION**

Pulse grains, including dried peas, provide rich sources of fibre with low glycemic indices. Their unique nutritional profile has led to many studies investigating different varieties of pulses in terms of their health benefits. Sievenpiper et al. (2009) found that consumption of

non-oil-seed pulses was associated with enhanced long-term glycemic control. Consumption of dried peas has specifically been linked with enhanced glycemic control in several human intervention studies. Type 2 diabetic patients consuming a mixed meal containing whole dried peas had a delayed increase in postprandial plasma glucose and insulin concentration compared with controls eating potato-based meals (Schafer et al., 2003) and whole pea flour muffins ameliorated insulin sensitivity in overweight subjects compared with wheat flour muffins (Marinangeli & Jones, 2011).

Most studies identifying beneficial effects of pulses on glycemia have used the whole grain (Sievenpiper et al., 2009) but recent studies consider pulse fractions. In an animal study, for example, feeding hamsters a hypercholesterolemic diet with partial substitution of cornstarch with pea hull flour resulted in significant decreases in circulating glucose and insulin levels (Marinangeli et al., 2011). Lunde et al. (2011) also showed that consumption of pea fibre-enriched breads resulted in improved post-prandial glucose tolerance and increased satiety in human subjects with a high risk of developing type 2 diabetes.

While these studies suggest seed coat fractions contribute beneficial effects, the data remains inconclusive because of inconsistent and variable preparations of the fractions. In humans, for example, fraction processing by gastric enzymes may reduce beneficial effects. There are also industrial processes that may reduce beneficial effects (e.g., spray drying), although this has not been systematically evaluated.

As described below, the present inventors developed methodology for preparing pea seed coat fractions conferring improved health and/or other beneficial effects, and such fractions may be used in a human and/or animal diet. In so doing, the present inventors developed methodology for preparing seed coat fractions with retained bioactivity. That is, and in one embodiment, the present inventors realized that seed coat PAC can be hydrolyzed to reduce the polymeric nature of PAC. In another embodiment, the present inventors determined that pea seed coat fractions can be ground, cooked, and then freeze dried, and that such pea seed coat fractions confer beneficial effects on glucose tolerance, incretin concentrations, and pancreatic hormones.

For example, and as described below, the seed coats of the pea (*Pisum sativum*) cultivar ‘Solido’, a marrowfat-type field pea with brown seed coats containing primarily prodelphinidin-

type PAC with B-type PAC linkages and a mean DP of 5, were acid hydrolyzed. In so doing, the bioavailability and effects of both PAC and hydrolyzed PAC (HPAC) PSC fractions were demonstrated by evaluating glucose homeostasis in rats. The hydrolyzed PAC (HPAC) fraction has enhanced bioavailability and therefore better effects on glycemic control.

Because the present inventors discovered that seed coat PAC can be acid-hydrolyzed to reduce the polymeric nature of PAC, and that the PAC (HPAC) fraction has enhanced bioavailability, such pea seed coat fractions can be used as or in a variety of products including but not limited to ingredients, food products, and animal feed.

In another embodiment, the present inventors determined that cooked pea seed coats confer health benefits, such as, for example, improved glucose tolerance.

Technical terminology in this description conforms to common usage in plant physiology, molecular biology, biochemistry, agriculture, and the like.

As used herein, **seed coat** refers to the seed hull and comprises mostly soluble and insoluble fibre. A **seed coat fraction** refers to the portion of a seed comprising the seed coat. The terms **seed coat fraction** and **fraction** are used interchangeably, as they both refer to the portion of the seed comprising the seed coat.

**Pulse grains**, also called **pulses** or **grain legumes**, belonging to the family *Leguminosae* (alternatively *Fabaceae*) and are grown primarily for their edible grains or seeds. Pulses, such as dried peas, provide rich sources of fibre with low glycemic indices. These seeds are harvested mature and marketed dry, and used as food or feed.

**Proanthocyanidins** (PAC, or condensed tannins) are the oligomers and polymers of flavan-3-ols. They exist in a variety of foods such as peas, beans, nuts, spices, fruits, wine and tea, and contribute the most to total flavonoid intake in the diet. PACs generally accumulate in the seed coat of some legume seeds, as evidenced by their brownish coloration due to oxidation by polyphenol oxidase.

**Bioavailability** or **PAC bioavailability** refers to the degree and rate at which a substance (as a drug, or PAC) is absorbed into a living system or made available at the site of physiological activity. PAC bioavailability is profoundly affected by its degree of polymerization (DP). For example, PAC with DP <3 are believed to be absorbed from the small intestine, whereas PAC

with DP >3 reach the colon, where they are subjected to microbial metabolism, and the degraded products either get absorbed or excreted in the feces. Furthermore, in fibre-rich plant samples such as those used herein, non-extractable PAC is found associated with fibre, which makes it even less bioavailable. Acid hydrolysis of PAC can break the interflavan bonds, which increases bioavailability. Hydrolysis of PAC (HPAC) significantly increased its bioavailability reflected by detection of PAC-derived metabolites only in the serum of HPAC-fed rats.

Improved health-beneficial effects refers to the ability of the instant methodology and/or compositions to confer health and/or other beneficial effects in a human and/or animal. For example, and in no way limiting, such improved health and/or beneficial effects include any of retained PAC and PAC component bioavailability, retained PAC and PAC component bioactivity, improved insulin sensitivity, reduced glycemia, increased satiety, improved glucose tolerance, improved glucose control, improved glucose homeostasis, beneficial effects on pancreatic islet composition and insulin secretion, improved incretin secretion, lower body weight, lower body fat content, and improved serum lipids.

#### **A. Pulses**

**Pulse grains**, also called **pulses** or **grain legumes**, belonging to the family *Leguminosae* (alternatively *Fabaceae*) and are grown primarily for their edible grains or seeds. Pulses, such as dried peas, provide rich sources of fibre with low glycemic indices. They are also good sources of protein. These seeds are harvested mature and marketed dry, and used as food or feed.

Illustrative pulses include but are not limited to adzuki beans (e.g., azuki, Adanka, danka), broad beans (e.g., faba bean, fava bean, bell bean), vetch, common beans (e.g., field bean, dry bean, kidney bean, navy), chick pea (e.g., bengal gram, garbanzo bean, yellow gram), cowpea (e.g., asparagus bean, black eyed pea, frijole), guar bean (e.g., cluster bean, gawaar), hycainth bean (e.g., bonavist, bataw, lablab), lentil (e.g., green lenti, yellow lentil, mungbean ), lima bean (e.g., butter bean), lupin (e.g., lupine, sweet lupin), mung bean (e.g., black dahl, urd, chop suey), pea (e.g., dry pea, field pea, Chinese pea), ), peanut (e.g., ground nut, earth nut, Virginia peanut), pigeon pea (e.g., kadios), soybean (e.g., soya, edamame ), and tepary bean (e.g., tepari bean).

The pea seed (*Pisum sativum* L.) consists of an embryo (cotyledons and an embryo axis), which is enclosed in a seed coat (hull). The nutrient components of the embryo are mostly starch



and protein, while the seed coats are largely soluble and insoluble fibre (Whitlock et al., 2012; Guillon & Champ, 2002; Duenas et al., 2004). Many studies have shown that dietary fibre has positive effects on postprandial glucose control (reviewed by Babio et al., 2010). It was concluded that a high intake of soluble dietary fibre (SDF) is associated with reduced postprandial glucose levels. However, deeper insights into the mechanisms by which different sources of fibre affect glucose metabolism are yet to be elucidated. It is known that dietary fibre is fermented by colon microflora, producing short-chain fatty acids (SCFA) like acetate, propionate, and butyrate (Jenkins et al., 2000). Increased accumulation of SCFA has been linked with decreased production of glucose in the liver (Galisteo et al., 2008). Soluble fibre also dissolves in water to form a viscous slow-moving solution that results in slowed gastric emptying; however, the effect of this increased transit time on digestion and absorption is controversial (Haub & Lattimer, 2010).

Applicants previously showed that insulin-resistant rats fed a raw pea seed coat-supplemented diet had better glucose homeostasis compared to embryo-supplemented diet fed rats, suggesting that the beneficial effects are associated with the seed coat fraction (Whitlock et al., 2012). One limitation of that study was that raw pea seed coats incorporated into the diet were not suitable for human consumption. Some studies have suggested that processing reduces the effectiveness of pulses in improving glycemia (Jenkins et al., 1982). Therefore, this study was undertaken to examine the effects of grinding and cooking followed by freeze-drying on the ability of pea seed coat fractions to improve glucose control and to identify potential physiological mechanisms. Supplementing diets with pea seed coat fractions may ameliorate glucose tolerance by modulating glucose handling by the gut and reducing high fat diet-induced stress on pancreatic islets. Further, cooking should not destroy the beneficial effects of pea seed coat fibre consumption.

#### **B. Bioavailability and effects on glucose homeostasis of PAC and HPAC pea seed coat fractions**

A main objective of this study was to evaluate the bioavailability and compare effects on glucose homeostasis of PAC and HPAC pea seed coat fractions. As described below and in the Examples, the present inventors discovered that PAC's biological functions are clearly determined by its bioavailability in vivo. PAC-related metabolites were only detected in serum

of HPAC-fed rats, and this was associated with a more pronounced beneficial effect of HPAC on body weight gain, glucose tolerance and pancreatic  $\beta$ -cell function.

PAC bioavailability is profoundly affected by its degree of polymerization (DP). PAC with DP <3 are believed to be absorbed from the small intestine, whereas PAC with DP >3 reach the colon, where they are subjected to microbial metabolism, and the degraded products either get absorbed or excreted in the feces [38]. The absorbed compounds are extensively metabolised in the enterocytes and liver by phase II enzymes into conjugated derivatives, such as glucuronides, sulfate conjugates and methyl derivatives; these either persist in the circulation or are rapidly eliminated in urine [38]. Furthermore, in fibre-rich plant samples such as were used in this diet study, non-extractable PAC is found associated with fibre, which makes it even less bioavailable [39,40]. Acid hydrolysis of PAC can break the interflavan bonds [21,41]. It is also possible that acid hydrolysis can break the association of non-extractable PAC with fibre, although this was not explicitly evaluated.

As shown below, hydrolysis of PAC (HPAC) significantly increased its bioavailability reflected by detection of PAC-derived metabolites only in the serum of HPAC-fed rats. This is in accordance with the findings of previous bioavailability studies showing that the small molecular weight PAC (monomers and dimers) can be absorbed and metabolized [42–44]. Because PAC has growth-inhibitory effects on bacteria [45] and some “tannin-resistant” species are candidates for PAC metabolism [46,47], it is also possible that hydrolysis reduced PAC growth-inhibitory effects on gut microbes and therefore more microbial metabolites were produced and absorbed in HPAC-treated rats.

Prolonged HFD feeding is well known to induce insulin resistance and glucose intolerance in rats. Hyperplasia of  $\beta$ -cells develops to adapt to changes in metabolic status and maintain glucose homeostasis [48,49]. Incorporating HPAC to into HFD led to correction of glucose intolerance: both glucose excursion and insulin secretion of HPAC was similar to LFD in the IPGTT, while there was prolonged suppression of blood glucose in the ITT. Meanwhile, consistent with the reduced insulin response during IPGTT, pancreatic  $\beta$ -cell areas in HPAC was ~50% less than HFD ( $p=0.4$ ). Therefore, HPAC was able to reduce the demand for insulin compensation caused by HFD.

Insulin secretion from the islets in response to high glucose (16mM) stimulation was significantly enhanced in HPAC vs HFD. There may be two explanations for this improvement. Firstly, PAC may act as an insulin secretagogue. INS-1 cells pre-cultured with PAC-rich cranberry powder had increased basal and stimulated insulin secretion [20]. Jayaprakasam et al. [50] tested the effects of a series of anthocyanins from fruits on insulin secretion in vitro. They found delphinidin-3-glucoside was the most effective stimulant of GSIS. However, neither the forms nor the concentrations (cranberry powder: 0.25 and 0.5 mg/mL; anthocyanins: 50µg/mL) of compounds used in their studies is likely to exist in physiological post-absorptive conditions. According to the present inventors' findings, PAC-derived compounds (including 4'-O-methyl-epigallocatechin (main metabolite) and epicatechin-3'-O-glucuronide) were identified in the serum of HPAC-fed rats only (Table 2). These compounds existing in nanomolar quantities in the circulation are likely candidates for the bioactive substances that regulate GSIS.

On the other hand, improved GSIS may be the indirect result of the improved insulin sensitivity in HPAC. The demand for insulin secretion in HPAC was lower than the HFD group, thus creating less stressful condition for  $\beta$ -cells leading to better pancreatic function. These possibilities will be tested in future in vitro assays designed to assess direct effects on  $\beta$ -cells or insulin-sensitive tissues.

Additionally, the present disclosure shows a striking reduction in  $\alpha$ -cell area and  $\alpha/\beta$  cell ratio in HPAC pancreas, while plasma glucagon concentrations were reduced by 50% in HPAC vs HFD ( $p<0.07$ ). In type 2 diabetes, increased relative or absolute mass of  $\alpha$ -cells has been proposed to play a role in the pathology in addition to  $\beta$ -cell loss and dysfunction [51,52]. Elevated plasma glucagon concentration relative to insulin is believed to cause hyperglycemia and dysregulated glucose metabolism [53,54]. Therefore, in addition to improved insulin sensitivity, the glucagon secreting capacity may also contribute to the better glycemic control in HPAC group, as exemplified by the slower glucose rebound after ITT. The 60-120 minute phase of the ITT reflects the counter-regulatory response, the strength of which is dictated, in part, by the suppressive effect of insulin versus the positive effect of glucagon on hepatic glucose production [55].

Another interesting finding is that HPAC group exerted a favorable effect on body composition without altered energy intake. Dietary polyphenols such as catechins have the

potential to modulate neuropeptides involved in energy expenditure [56,57] and catechins and PAC metabolites are able to cross the blood-brain barrier [58–60]. Wang et al. reported that the metabolite concentrations were about 300 pmol/gram of brain tissue after 10-day treatment, and basal synaptic transmission was significantly improved when using a biosynthetic brain-targeted PAC metabolite at a physiologically relevant concentration (300 nM) [60]. Another mechanism may relate to changes in fatty acid oxidation and metabolism.

In summary, and in one embodiment, the present inventors determined that acid hydrolysis improved the limited bioavailability of PAC fractions, resulting in the detection of PAC-related metabolites in HPAC serum. This was associated with enhanced improvement in glucose handling in glucose intolerant rats. Beneficial effects on pancreatic islet composition and insulin secretion were also elicited by HPAC treatment.

### **C. Cooking enhances beneficial effects of pea seed consumption on glucose tolerance, incretin and pancreatic homeostasis of pea seed coat fractions**

The pea seed (*Pisum sativum* L.) consists of an embryo (cotyledons and an embryo axis), which is enclosed in a seed coat (hull). The nutrient components of the embryo are mostly starch and protein, while the seed coats are largely soluble and insoluble fibre (Whitlock et al., 2012; Guillon & Champ, 2002; Duenas et al., 2004). Many studies have shown that dietary fibre has positive effects on postprandial glucose control (reviewed by Babio et al., 2010). It was concluded that a high intake of soluble dietary fibre (SDF) is associated with reduced postprandial glucose levels. However, deeper insights into the mechanisms by which different sources of fibre affect glucose metabolism are yet to be elucidated. It is known that dietary fibre is fermented by colon microflora, producing short-chain fatty acids (SCFA) like acetate, propionate, and butyrate (Jenkins et al., 2000). Increased accumulation of SCFA has been linked with decreased production of glucose in the liver (Galisteo et al., 2008). Soluble fibre also dissolves in water to form a viscous slow-moving solution that results in slowed gastric emptying; however, the effect of this increased transit time on digestion and absorption is controversial (Haub & Lattimer, 2010).

Applicants previously showed that insulin-resistant rats fed a raw pea seed coat-supplemented diet had better glucose homeostasis compared to embryo-supplemented diet fed rats, suggesting that the beneficial effects are associated with the seed coat fraction (Whitlock et

al., 2012). One limitation of that study was that raw pea seed coats incorporated into the diet were not suitable for human consumption. Some studies have suggested that processing reduces the effectiveness of pulses in improving glycemia (Jenkins et al., 1982).

Herein, the present inventors examined the effects of grinding and cooking followed by freeze-drying on the ability of pea seed coat fractions to improve glucose control and to identify potential physiological mechanisms. In so doing, they discovered that supplementing diets with pea seed coat fractions may ameliorate glucose tolerance by modulating glucose handling by the gut and reducing high fat diet-induced stress on pancreatic islets. The beneficial effects of pea seed coat fibre consumption is not lost following cooking.

#### **D. Products**

The instant methodology and materials may be used for creating a product conferring novel health and/or beneficial effects in a human and/or animal diet. In no way limiting, illustrative products include foods, flours, fibres, pet foods, compositions, and other ingredients, any of which may comprise pea seed coat fractions.

\*\*\*\*\*

Specific Examples are provided below to demonstrate preparation of illustrative embodiments, including material and methodology. The Examples are illustrative and non-limiting.

Disclosed below are findings from two feeding trials examining different aspects of pea seed coat preparation, namely, hydrolysis of PAC versus cooking followed by freeze-drying of seed coats not containing PAC.

As evidenced below, Section I (Examples 1-14) demonstrates that hydrolysis enhances bioavailability and improves beneficial effects, and Section II (Examples 15-30) demonstrates that cooking and stabilization of cooking-induced changes by freeze-drying enhances the beneficial effects of PSC consumption.

#### **I. HYDROLYSIS ENHANCES BIOAVAILABILITY OF PAC**

##### **EXAMPLE 1: Preparation of Pea Seed Coat Diet**

Seed coats of pea (*Pisum sativum* L.) cultivar ‘Solido’ were obtained from Mountain Meadows Food Processing Ltd. (Legal, Alberta). The smaller seed fragments were removed from the bulk PSC sample using a 1.0 mm screen (Canadian Standard sieve series #18, W.S. Tyler Co. of Canada, St. Catherines, ON). The cleaned PSC were then ground into a powder using a standard electric coffee grinder for rat feeding studies. A portion of the ground samples were used unprocessed (PAC fraction) and a portion was subjected to acid hydrolysis (HPAC fraction).

For acid hydrolysis, a 2N HCl solution (1L total volume consisting of 170 mL food grade HCl, 330 mL deionized water and 500 mL ethanol) was added to ~200 g of ground ‘Solido’ PSC, making a slurry. Acid hydrolysis was performed by placing the PSC slurry into a 100°C water bath for 1 h (from the time the slurry came to a boil). After 1 h of slurry boiling, the mixture was cooled down to approximately room temperature using an ice bath. Saturated NaOH solution (approximately 78 g NaOH) was slowly added into the slurry to neutralize the excess HCl. After neutralization, the PSC slurry was lyophilized using a freeze dryer. PAC and HPAC fractions were added to a high fat diet (HFD ) (Table 1) such that the final concentration of both was 0.8% (w/w).

**Table 1. Experimental Diets Formula (g)**

Ingredient	HFD	PAC	HPAC	LFD
Stearine	99.5	99.5	99.5	29.85
Flaxseed oil	6	6	6	1.8
Sunflower oil	94.5	94.5	94.5	28.35
Casein	270	254	254	270
L-Methionine	2.5	2.5	2.5	2.5
Dextrose	189	189	189	255
Corn Starch	169	169	169	245
Cellulose	100	0	0	100
‘Solido’ seed coat	0	193	193	0

(raw or hydrolyzed)				
Mineral Mix	51	51	51	51
Vitamin Mix	10	10	10	7.6
Inositol	6.3	6.3	6.3	6.3
Choline Chloride	2.8	2.8	2.8	2.8

Note: To avoid other dietary factors' effects on the outcomes, the nutrient contents of both raw and hydrolyzed pea seed coats (PSC) were analyzed (data not shown). The amount of added PSC was calculated to ensure diets are equal in total fat (20.0% w/w), protein (27.9% w/w), carbohydrate (35.8% w/w) and fibre (10.0% w/w) and thus are equal in caloric density, except for LFD (total fat 6.0% w/w, protein 27.9% w/w, carbohydrate 49.9% w/w, and fibre 10.0% w/w). PAC content was 435.9 mg/100 g unprocessed PSC.

### **EXAMPLE 2: Animal Feeding Trial**

Male Sprague-Dawley rats (n=84) were obtained from Charles River Canada (St. Constant, QC) at 8 wk of age and housed 2 per cage. All the animals had 1 wk of acclimatization with access to standard chow and water *ad libitum*. Then they were randomized into 4 groups, i.e. high fat diet (HFD), low fat diet (LFD), PAC-supplemented HFD (PAC), and HPAC-supplemented HFD (HPAC). LFD group remained on standard chow. All the others were introduced to a 6-week HFD regimen to induce glucose intolerance, which was confirmed using an oral glucose tolerance test (GTT, see Example 3 below). The 4 groups of rats were switched to the experimental diets (Table 1) for 4 wk. Body weights were measured weekly and food intake was recorded daily.

### **EXAMPLE 3: Glucose and Insulin Tolerance Tests**

Oral (OGTT) or intraperitoneal GTT (IPGTT) was used to determine the status of glucose tolerance in all groups. IPGTT examines the effects of PAC feeding downstream of intestinal absorption factors because the glucose is introduced into the peripheral circulation, bypassing the gut. Seven days before tissue collection, after overnight fasting, all the rats were weighed and baseline blood glucose concentration was measured in whole blood taken from the

tail vein with a glucometer (Accu-Check Compact Plus, Roche Diagnostics). Then they received a standard dose of glucose (1g/kg; oral: 40% w/v, in ddH<sub>2</sub>O; ip: 20% w/v, in saline), blood glucose was measured at 10, 20, 30, 60, 120 min. Additional blood samples were collected at the same time points to obtain plasma and stored at -80°C until assayed for insulin and glucagon. Incremental area under the curve (IAUC) was calculated as described [30].

Insulin tolerance tests (ITT) were conducted 1-2 days before the day of tissue collection. After 4-hour fasting, all the rats were weighed and baseline blood glucose level was measured in whole blood with a glucometer. After receiving insulin (0.5 U/kg, ip), blood glucose was measured at 15, 30, 60, 90, 120 min.

#### **EXAMPLE 4: Tissue Collection**

Fed or 16-hour fasted rats were euthanized under anaesthesia (pentobarbital sodium 60 mg/kg, ip) by exsanguination. Blood (5-10 ml) was obtained from the abdominal aorta and divided for preparation of plasma and serum, which were frozen at -80°C. Pancreatic islets were isolated and cultured overnight for insulin secretion studies as previous described [31,32]; an additional pancreas sample just adjacent to the spleen was fixed in formalin overnight for embedding in paraffin by standard techniques.

#### **EXAMPLE 5: Soluble PAC and anthocyanin quantitation**

The total extractable PAC content of the native 'Solido' PSC fraction was determined by the butanol-HCl-Fe<sup>3+</sup> method [28]. Approximately 25 mg subsamples of seed coat tissue (lyophilized and ground to a fine powder using a Retsch ZM 200 mill (PA, USA) with 0.5 mm screen filter) were weighed into 15 mL Falcon tubes. The samples were extracted with 10 ml of 80% methanol for 24 h with shaking. After vortexing the slurry and centrifuging for 5 min at 4000 rpm, the supernatants were used for PAC analysis using the method of Porter et al. [28]. In brief, 2 mL of the butanol:HCl reagent and 66.75 µL of iron reagent were added into a 15 mL glass culture tube. Then, 0.5 mL of clear sample extract was added to the tube and the mixture was vortexed. Two 350 µL aliquots of this solution were removed for use as sample blanks, and the remaining solution was placed into a 95°C water bath. After 40 min, the solution was allowed to cool at room temperature for 30 min. The reaction products, sample blanks, and a PAC standard curve dilution series were monitored for absorbance at 550 nm using a 96 well UV



plate reader (Spectra Max 190, Molecular Devices, CA, USA). The PAC standard solution used was an extract from ‘CDC Acer’ PSC purified as described by Jin [29].

The high pressure liquid chromatography (HPLC)-photodiode array detection method of Zifkin et al. [33] was used to quantify anthocyanidins in the HPAC fraction.

### **EXAMPLE 6: Analysis of PAC-derived compounds in PSC and serum samples**

#### **A. Pea Seed Coats**

PSC (25mg, PAC or HPAC) were extracted in 1mL methanol for 4 h at -20 °C. The supernatant was collected and injected into a HILIC Column (TSKgel Amide-80) for separation. The continuous gradient segments for HILIC (A: 10 mM NH<sub>4</sub>AC in H<sub>2</sub>O; B: 10 mM NH<sub>4</sub>AC in acetonitrile) were: t = 0 min, 90% B; t = 5 min, 10% B; t = 10 min, 10% B; t = 30 min, 90% B. The flow rate was 100 µl/min. The flow was directed to the electrospray ionization (ESI) source of a Bruker Impact HD quadrupole time-of-flight (Q-TOF) mass spectrometer (MS). Parameters for analysis were set using HILIC-negative ion mode with spectra acquired over a mass range from m/z 50 to 800. The optimum values of the ESI-MS parameters were: collision energy, 22 eV for catechin derivatives and 25 eV for delphinidin derivatives; collision RF, 700.0 Vpp; transfer time, 30.0 µs; pre-pulse storage, 8.0 µs. The MS data were checked by Bruker’s DataAnalyst 4.2.

#### **B. Serum Samples**

Proteins in the serum samples were precipitated with 100% methanol (1:3, v/v) at room temperature, and the supernatant was collected and analyzed using Q-TOF MS linked to an HILIC column as described above.

### **EXAMPLE 7: Analysis of plasma insulin and glucagon**

Plasma samples obtained during the GTT and tissue collection were analysed in duplicate for insulin and glucagon by ELISA using commercial assay kits according to the manufacturer’s instructions (rat insulin ELISA, Alpco Diagnostics, Salem, NH; glucagon EIA kit, SCETI K.K., Tokyo, JP).

### **EXAMPLE 8: Immunohistochemistry**

Immunohistochemical staining (IHC) was performed as previously described for determination of  $\alpha$ - and  $\beta$ -cell areas [27]. Primary antibodies and their dilutions were as follows: guinea pig anti-insulin, 1:200 (Dako, Burlington, Canada) and rabbit anti-glucagon, 1:200 (Millipore, Billerica, MA). Secondary antibodies were HRP-conjugated rabbit anti-guinea pig, 1:200 (Sigma, Oakville, Canada) and goat anti-rabbit, 1:200 (Sigma), respectively. Positive immunoreactivity was visualized by diaminobenzidine plus hydrogen peroxide. Slides were then dehydrated and mounted for photography using an Axiovert microscope equipped with Axiovision 4.7 software (Zeiss). The total pancreatic area (excluding large ducts and veins), the insulin- and glucagon-positive areas were quantified using ImageJ [27].

#### **EXAMPLE 9: Glucose stimulated insulin secretion from isolated islets**

To measure insulin release, 3 islets/vial were incubated in Dulbecco's Modified Eagle's medium with low or high glucose concentrations (2.8, 16.5 mM) for 2 h at 37°C. Supernatants were retained and insulin remaining in the islets was extracted with 3% acetic acid, then stored at -20°C for future insulin radioimmunoassay (RIA) [34]. Total islet insulin content was calculated by adding insulin secreted into supernatant plus that remaining in the islet pellet, as determined by RIA. From this, the percentage of total insulin secreted was calculated for each data point to eliminate variance caused by islet size. Insulin stimulation index was calculated as the ratio of insulin percentage release in response to 16.5 mM glucose versus 2.8mM glucose.

#### **EXAMPLE 10: Statistical analyses**

All data were expressed as means  $\pm$  SE, and n represented the number of rats. Multiple groups were analyzed by one-way or two-way analysis of variance followed by Bonferroni's multiple comparison, as appropriate. At  $P \leq 0.05$ , differences were considered significant. Statistical analyses were performed using GraphPad Prism for Windows version 6.0 (GraphPad Software, San Diego, CA).

#### **EXAMPLE 11: Hydrolysis depolymerized PAC and increased metabolites in serum**

The total PAC content of the native 'Solido' PSC was  $4.51 \pm 0.05$  mg/100mg dry weight of sample, n=3) as determined by the butanol-HCl-Fe<sup>3+</sup> method. Jin [29] found that in the PSC of 'Solido' the PAC flavan-3-ol extension units were nearly exclusively prodelphinidin, while epigallocatechin was the most abundant flavan-3-ol extension subunit followed by galliccatechin.

The PAC terminal subunits of this pea cultivar also mainly consisted of gallicocatechin and epigallocatechin. Upon acid hydrolysis, the epigallocatechin and gallicocatechin were converted to the anthocyanidin delphinidin (Figure 6A) with a yield of  $43 \pm 4.9$  mg/100g dwt (n=3; HPAC fraction delphinidin content).

Further characterization of the PAC and HPAC fractions by ESI-MS/MS found that PAC dimers (prodelphinidin A1 and B; Figure 6) were present in the PAC fraction, but were not present in the HPAC fraction (Table 2), showing that the acid hydrolysis procedure had effectively cleaved the PAC dimers to monomers.

**Table 2. PAC-derived compounds in pea seed coats and rat serum** as detected by ESI-MS/MS.

Compound		Retention Time (min)	Precursor Ion Mass (Da)	Main Product Ion		
				Ion Mass (Da)	Absolute Intensity (cnts)	
					PAC	HPAC
Standards	Epicatechin	1.85	289.0673	125.0259	-	-
	Gallicocatechin	2.89	305.0649	179.1105	-	-
	Delphinidin	12.23	301.0335	125.0259	-	-
Pea Seed Coats	Prodelphinidin A1	5.98	607.1093	125.0256	704	ND
	Prodelphinidin B	6.31	609.1250	125.0256	1303	ND
	Delphinidin	12.24	301.0335	125.0261	893	6075
Serum	Epicatechin-3'-O-glucuronide	4.85	465.1038	125.0250	ND	573
	4'-O-Methyl-epigallocatechin	1.85	319.0823	179.1105	ND	18197

ND, not detected.

High DP is the main factor limiting the absorption of PAC. Therefore, it was expected that PAC-hydrolyzed products would be readily absorbed into the body. To determine and compare the bioavailability between PAC and HPAC, PAC-related metabolites in non-fasted serum samples were analyzed using ESI-MS/MS. 4'-O-methyl-epigallocatechin (the major metabolite) and epicatechin-3'-O-glucuronide were detected in serum samples from HPAC but not PAC (Table 2; for structures see Figure 6A and Figure 6B for ESI-MS spectrum). Using the data of 'Solido' PAC composition reported by Jin [29], we conclude that the 4'-O-methyl-epigallocatechin PAC-derived metabolite originated from the flavan-3-ol epigallocatechin extension/terminal units of the hydrolyzed PAC, and epicatechin-3'-O-glucuronide was derived from the terminal units of the hydrolyzed PAC.

#### **EXAMPLE 12: HPAC improved body composition without affecting food intake**

All the rats had similar body weights at both baseline and prior to diet change. Differences in body weights among groups became apparent after switching to the experimental diets as shown in Figure 1. At the end of the feeding trial, rats in the HPAC group had approximately 18% less weight gain compared to HFD group (HPAC,  $139.3 \pm 17.0$ ; HFD,  $156.9 \pm 12.0$ , %,  $P < 0.05$ ). HPAC group percentage of body fat was ~6% lower versus HFD ( $P < 0.05$ , Table 3). In contrast, although rats fed PAC-supplemented diet gained ~10% less weight, their body composition was similar to HFD (Table 3). Lean mass was similar in all groups.

PAC contribute to the bitter and astringent tastes of food [21], which may affect food intake of the different experimental groups. However, PAC or HPAC supplementation did not affect food or energy intake compared with HFD (Table 3). LFD rats achieved similar energy intake via increased food intake (Table 3).

**Table 3. Food intake and body composition**

	HFD	PAC	HPAC	LFD
Food Intake (g/rat/d)	31.25 ± 1.14	41.63 ± 2.86	39.81 ± 3.34	42.50 ± 2.82*
Energy Intake (kcal/rat/d)	134.40 ± 4.91	179.0 ± 12.30	171.2 ± 14.37	153.0 ± 10.15
Fat mass/Final Wt, %	16.8 ± 1.2	15.0 ± 1.2	11.3 ± 0.9*	13.8 ± 1.4
Lean mass/Final Wt, %	67.0 ± 1.0	69.2 ± 1.0	70.8 ± 0.9*	69.4 ± 0.6
Fat mass/Lean mass	0.26 ± 0.02	0.21 ± 0.02	0.16 ± 0.01*	0.19 ± 0.02

Values are means ± standard error, \* P<0.05, compared to HFD, Bonferroni's multiple comparison.

### **EXAMPLE 13: HPAC diet improved insulin resistance induced by HFD**

Seven days prior to tissue collection, IPGTT was performed to compare the effects of different diets on glucose homeostasis. Data are shown as the glucose and insulin responses at each time point (Figure 2A and 2C) and as incremental area under the curve (IAUC, Figure 2B and 2D). In response to a standard dose of glucose, LFD group had overall lower glucose excursion compared to HFD, with ~50% decrease in IAUC of blood glucose (P < 0.01). HPAC had significantly lower blood glucose than HFD at 10 min (P < 0.05) and an approximately 25% reduction in IAUC, such that the overall glucose excursion was similar to LFD. Insulin responses in HPAC were much lower at 20 and 30 min, resulting in a significantly lower IAUC (P < 0.05) than HFD. Those results indicate improved glucose disposal in HPAC. In contrast, PAC showed similar glucose and insulin responses compared with HFD, suggesting little improvement in glucose intolerance.

Insulin-glucose IAUC index is the product of IAUCs of insulin and glucose response curves and is an index for insulin resistance (IR) in which a higher value suggests higher degree of IR [35,36]. HPAC and LFD both had lower values of insulin-glucose IAUC index compared to HFD (P < 0.05), whereas PAC was similar to HFD.

ITT was also used to assess the degree of insulin resistance. Results from ITT (Figure 3) also support that HPAC were less insulin resistant than HFD rats. Although glucose levels (present as percentage of baseline glucose) responding to insulin administration (Figure 3A) were similar among all groups during the first 30 min, HPAC had significantly ( $P < 0.05$ ) lower glucose concentrations from 90 to 120 min. PAC also tended to have a slower glucose recovery rate, with a significantly lower glucose concentration at 120 min compared to HFD. Slopes of ITT for 60-120 min were calculated [37] as a direct measurement of glucose recovery rate. Both of the pea seed coat-supplemented groups, especially HPAC, had smaller slopes than HFD, suggesting slower glucose recovery rate (Figure 3B).

#### **EXAMPLE 14: HPAC preserved pancreatic islet morphology and function**

The lowered insulin responses in HPAC during IPGTT might be the result of a smaller  $\beta$ -cell mass. Therefore  $\beta$ -cell and  $\alpha$ -cell areas were quantified as an estimate of islet cell mass. Representative photomicrographs are shown in Figure 4A and 4B. Pancreatic  $\beta$ -cell area was not different between groups ( $P=0.4$ , Figure 4C). A ~80% decrease ( $P < 0.05$ ) in pancreatic  $\alpha$ -cell areas in HPAC was found (Figure 4D), which contributed to significantly different cell composition ( $\alpha / \beta$  cell ratio) in pancreatic islets of HPAC (Figure 4E,  $P < 0.05$ ). Fasting plasma insulin and glucagon concentrations were not different among groups (Figure 4F,  $P=0.070$ ; Figure 4G,  $P=0.088$ ).

To further examine the effects of PAC and HPAC on pancreatic islet function, and to exclude the possibility that the lower insulin response during IPGTT was caused by impaired insulin secretion from pancreatic islets, GSIS was conducted on isolated islets. As shown in Figure 5A, insulin secretion in response to 2.8mM glucose was similar among all groups. When stimulated with 16.5mM glucose, % release of insulin in HPAC was increased ~3-fold compared to both HFD and PAC. Insulin stimulation indices were significantly different among all groups (Figure 5B,  $P=0.047$ ), and HPAC had the highest mean value, indicating ameliorated pancreatic islet function in HPAC. Also there was a trend (Figure 5C,  $P=0.126$ ) towards lower insulin content in HPAC.

## **II. COOKING AND FREEZE-DRYING ENHANCES GLUCOSE-LOWERING EFFECTS OF PSC**

#### **EXAMPLE 15: Animals and Diets**

All animal care protocols comply with the guidelines of the Canadian Council on Animal Care. They were also reviewed and approved by the Health Sciences Animal Care and Use Committee at the University of Alberta. Eight-week old male Sprague Dawley rats were purchased from the Department of Biology, University of Alberta or Charles River Canada (St. Constant, QC). They were housed two per cage with *ad libitum* access to normal chow and water for one week. After acclimatization, rats received 6 weeks of high fat control diet (HFD, 20% w/w) to induce insulin resistance, except for the low fat diet (LFD) control group, which remained on chow. The HFD-fed rats were then randomly assigned to the following 3 diets: high fat diet (HFD), raw pea seed coat (RP, HFD supplemented with raw seed coats), cooked pea seed coat (CP, HFD supplemented with cooked seed coats). All these diet groups were isocaloric and maintained a macronutrient ratio of 40:40:20 for fat, carbohydrate and protein. The chow fed rats were put on low fat diet (LFD, 6% w/w), in which carbohydrate replaced the fat. In the treatment groups, the fibre source, which was 10% w/w cellulose in HFD and LFD, was replaced by prepared pea seed coat fractions so that the total fibre weight per gram of chow was identical (Table 4). The protein was adjusted as necessary to ensure the diets were isonitrogenous. The animals were on the pea seed coat diets for four weeks with *ad libitum* access to food and water.

**Table 4. Diet Composition (g/kg).**

	HFD	HFD+PSC	LFD
Canola Sterine	99.5	99.5	29.85
Flaxseed Oil	6	6	1.8
Sunflower Oil	94.5	94.5	28.35
Casein	270	263	270
Dextrose	189	189	255
Corn Starch	169	169	245
Cellulose	100	0	100
Pea seed coat	0	143	0
L-methionine	2.5	2.5	2.5
Essential Nutrients	70.1	70.1	67.7
Total weight (g)	1000.6	1036.6	1000.2
Carbohydrate %	35.7	34.6	50
Fat %	20	20	6
Protein %	27.8	27.8	27.8
Fibre %	10	10	10

HFD, high fat diet; HFD+PSC, high fat diet supplemented with pea seed coats; LFD, low fat diet.

#### **EXAMPLE 16: Pea Seed Coat Preparation and Analysis**

##### *Seed coat preparation*

The pea seed coat fractions used in this study were produced from the seeds of the pea (*Pisum sativum* L.) cultivar Canstar that were grown in Alberta, Canada. ‘Canstar’ is a yellow-seeded field pea cultivar with little to no proanthocyanidins present in its seed coats. The whole



pea seeds were dehulled (seed coats removed) using a mechanical dehuller at Agri-Food Discovery Place, University of Alberta. The smaller seed fragments were removed from the bulk seed coat sample using a 1.0 mm screen (Canadian Standard sieve series #18, W.S. Tyler Co. of Canada, St. Catharines, ON). The cleaned seed coats were then ground into a powder using a standard electric coffee grinder for rat feeding studies. A portion of the ground samples were used unprocessed (raw seed coat material) and a portion was subjected to a cooking treatment (cooked seed coat material) which consisted of boiling the samples at 100°C in deionized water (approximately 10 volumes of water to 1 volume of seed sample) for 30 min. After 30 min of cooking, the samples were cooled down to room temperature and stored at -20 °C until lyophilization of samples (using a freeze dryer; Virtis Ultra 35L Freeze Dryer, Stone Ridge, New York, United States) for 7 days. For starch, protein, and fibre analyses, both raw seed coat and cooked seed coat material were lyophilized for 7 days and further ground using a Retsch, ZM 200 (PA, USA) mill to produce finely ground powder that passed through a 0.5 mm screen.

#### *Starch and protein analysis*

The ground lyophilized samples were assayed for total starch content using the Total Starch Assay Procedure AA/AMG 11/01 (Megazyme International Ireland, Ltd, Bray, Ireland; AOAC Method 996.11). A nitrogen analyzer (LECO TruSpec CN Carbon/Nitrogen Determinator; Leco Corporation; St. Joseph, MI) was used to estimate the total protein content in the lyophilized ground seed coat samples. Total protein content of the seed coats was calculated by multiplying the nitrogen content with a conversion factor of 6.25 (AOAC method 968.06). Caffeine (150 mg) and EDTA (Ethylenediaminetetraacetic acid; 100 mg) were used as standards for instrument calibration.

#### *Non-starch polysaccharides (NSP) analysis (fibre)*

The total, water insoluble and soluble non-starch polysaccharide (fibre) components of seed coats were determined using the methods described in Englyst and Hudson (1987) and Englyst (1989). Briefly, for hydrolysis and removal of starch from the seed coat material, 45 to 50 mg of ground sample was incubated with DMSO (dimethyl sulphoxide; 0.25 mL) at 100°C in a water bath for 1 h. The sample was immediately transferred to a 42°C water bath, then sodium acetate buffer (1 mL; 0.1M, pH 5.2), aqueous pancreatin solution (100 µL; 25 mg/mL;

pancreatin from porcine pancreas; 8xU.S.P., Sigma Co.) and aqueous pullulanase solution (50  $\mu$  L; 0.0165 enzyme units) were added, vortexed, and incubated for 16 hours.

The resulting starch-free residue was processed for total and insoluble NSP determination in independent samples (two replicates per sample). For total NSP analysis, ethanol (95 %, 6 mL) was added to a starch-free residue sample, followed by vortexing and incubation for 1 h at room temperature. Subsequently, the solution was centrifuged at 1914 g for 20 min and the supernatant was removed by aspiration. The residue was washed twice with ethanol (85%; 5 mL) and then placed into a 65°C water bath until the residue was dry.

For insoluble NSP analysis, phosphate buffer (0.2 M, pH 7.0; 6 mL) was added to a starch-free residue sample, then the sample was vortexed and heated for 1 h in a 100°C water bath. Subsequently, the solution was centrifuged at 1914 g for 20 minutes and the supernatant was removed by aspiration. The residue was washed with ethanol (85%; 5 mL), then phosphate buffer (0.2 M, pH 7.0; 5 mL), and then placed into a 65°C water bath until the residue was dry.

The following steps were performed on the dry total NSP and insoluble NSP residue samples. The dried starch-free residue was dispersed in H<sub>2</sub>SO<sub>4</sub> (12 M; 0.5 mL) and incubated in a 35°C water bath for 1 h. Subsequently, distilled water (5.5 mL) was added to the sample slurry followed by vortexing, and the solution was placed in a 100°C water bath for 2 h. The resulting hydrolysate solution was then cooled to room temperature and aqueous myo-inositol (20 mg/mL; 0.1 mL) was added as an external standard. For conversion of the hydrolyzed sugars to their alditol acetates, the hydrolysate was vortexed and centrifuged at 2000g for 5 min. NH<sub>4</sub>OH (12 M 0.2 mL; 12 M) was added to a 1 mL aliquot of the hydrolysate and the mixture was vortexed, then freshly prepared NaBH<sub>4</sub> solution (0.1 mL; 100 mg NaBH<sub>4</sub> per mL of 3 M aq NH<sub>4</sub>OH solution) was added and the solution was incubated for 1 h in a 40°C water bath. Subsequently, glacial acetic acid (0.1 mL) was added to the solution, followed by vortexing. A 0.2 mL aliquot of the acidified solution was added to 0.3 mL 1-methylimidazole. Acetic anhydride (2 mL) was then added to this solution and vortexed continuously for 10 min. Distilled water (5 mL) was subsequently added to the solution to decompose excess acetic anhydride and aid in phase separation. After the solution was cooled to room temperature, dichloromethane (4 mL) was added and mixed for 15 sec. After centrifugation at 700 g for 5 min, the top layer was aspirated off and distilled water (5 mL) was added. The solution was again centrifuged at 700 g for 5

minutes, the top layer was aspirated off, and the bottom layer was dried in a 50°C evaporator. Dichloromethane (1mL) was added to the residue and a 0.5  $\mu$  L aliquot of the derivatized sample was injected onto a DB-17 fused silica capillary column (0.25 mm i.d. x 30m; J&W Scientific, Folsom, CA) connected to a Varian 3400 gas chromatograph equipped with a cool-on-column injector. Helium was used as the carrier gas with a flow rate of 1.5 mL/min. The injector temperature was increased from 60°C to 270°C at the rate of 150°C/min and maintained for 20 min. Oven temperature was raised from 50°C to 190°C at a rate of 30°C/min, and maintained for 3 min, then increased to 270°C at the rate of 5°C/min, and maintained for 5 min. The flame ionization detector (FID) temperature was set at 270°C. Peak area integration for carbohydrate analyses were according to a Shimadzu Ezchrom Data System (Shimadzu Scientific Instruments Inc., Columbia, MD). The soluble NSP values were estimated by subtracting the insoluble NSP value from the total NSP value for a given sample.

#### **EXAMPLE 17: Glucose and Insulin Tolerance Tests**

After 3 weeks of experimental diets (9 weeks in total on HFD), rats were appointed to either an oral glucose tolerance test (oGTT) or an intraperitoneal glucose tolerance test (ipGTT). The tests were performed following an overnight fast. Fasting blood glucose was measured and blood was collected from a tail vein for insulin determination. Then, each rat received 1g of glucose per kg of body weight via oral administration or intraperitoneal injections. Blood glucose values were obtained at 10, 20, 30, 60, and 120 minutes, using a glucometer (Accu-Check Compact Plus, Roche Diagnostics, Laval, QC). About 50  $\mu$ l of blood was taken at each time point during ipGTT and centrifuged to obtain serum, which was stored at -20°C. Dipeptidyl peptidase (DPP)-IV inhibitor (Millipore, Billerica, MA) was added to aliquots obtained at baseline and 30 minutes in order to assay gastric inhibitory polypeptide (GIP). Insulin tolerance test was conducted at the end of the fourth week, during which animal received an intraperitoneal injection of 20  $\mu$ g/kg dose of insulin, and blood glucose was determined at 0, 15, 30, 60, 90 & 120 minutes. Area under the curve (AUC) and incremental area under the curve (IAUC) were calculated in accordance with established methods (Wolever, 2004).

#### **EXAMPLE 18: Body Weight, Food Intake and Measurement of Body Composition**

Body weights were measured on a weekly basis. After introduction of the supplemented diets, food intake was measured for 24 hours twice during the 4-week period. In addition, one

day prior to tissue collection, magnetic resonance imaging (MRI) technique was applied to specify lean and fat mass body composition using an EchoMRI Whole Body Composition Analyzer (Echo Medical Systems LLC, Houston, TX).

#### **EXAMPLE 19: Tissue Collection**

At the end of the 10th week, animals were euthanized by an overdose of xylazine/ketamine via ip injection. A 3-5 mL blood sample was obtained by cardiac puncture and serum obtained following centrifugation, which was then stored at -80°C. Intestinal segments and pancreatic tissue were collected and fixed in buffered formalin, dehydrated in graded ethanol and embedded in paraffin. They were then cut to generate 5  $\mu$  m cross sections using a microtome, and adhered to glass slides.

#### **EXAMPLE 20: Assays of Serum**

Samples from the ipGTT were assayed for insulin using an ELISA kit (Alpco Diagnostics, Salem, NH). GIP was assayed by Meso Scale Discovery human total GIP kit (validated for use with rat samples). Serum obtained at euthanasia was assayed for triglyceride (Serum Triglyceride Determination Kit, Sigma-Aldrich) and free fatty acids (Waco Diagnostics, Richmond, VA) by colourimetric assays and active glucagon-like peptide-1 by ELISA (Millipore, Billerica, MA) according to manufacturers' instructions.

#### **EXAMPLE 21: Immunohistochemistry and Morphometric Tissue Analysis**

Tissue slides were rehydrated and endogenous peroxidases quenched using techniques described previously (Whitlock et al., 2012). Non-specific binding was reduced by blocking with appropriate non-immune sera (1:20 dilution in PBS) for twenty minutes at room temperature. For pancreas, rabbit anti-glucagon (Linco) and guinea pig anti-insulin primary antibodies (Dako) were diluted 1:100 in PBS, applied to the tissue sections and incubated overnight at 4°C. For jejunum and ileum, mouse anti-GIP (generously provided by University of British Columbia) and rabbit anti-GLP-1 (Epitomics, Burlingame, CA) were respectively diluted 1:1000 and 1:250 in PBS, then applied and incubated under the same conditions. Following washes, appropriate peroxidase-coupled secondary antibodies (1:200) were applied to the sections and the slides were incubated for 1 hour at room temperature. Positive reactions were identified by peroxidation of diaminobenzidine in the presence of H<sub>2</sub>O<sub>2</sub>. Imaging was performed using an Axiovert

microscope connected to an AxioCam MRm digital camera (Carl Zeiss, TO, Ontario, Canada), and controlled with AxioVision 4.6 software.

For pancreas, each section of the tissue was photographed under ten times magnification and then total pancreatic tissue area as well as alpha- and beta-cell areas were quantified by ImageJ software. The ratios of the alpha-cell and beta-cell to total pancreatic area were calculated for each rat. For jejunum and ileum, random sections of each tissue were selected and photographed under twenty times magnification, and total number of GIP-positive and GLP-1-positive cells were calculated. The number of positive cells was then normalized to the number of villus.

#### **EXAMPLE 22: Quantification of Glucose Transporter Gene Expression (Glut2, Glut5, SGLT1)**

Total RNA was isolated from ileal tissue using Trizol reagent and purified with an RNeasy Mini Kit (Qiagen, Valencia, CA) per manufacturer's instructions. The complementary DNA (cDNA) was generated from RNA samples using a cloned AMV first-strand cDNA synthesis kit (Invitrogen). The cDNA samples were amplified using primers synthesized by the IBD core at the University of Alberta and analyzed by quantitative reverse transcription polymerase chain reaction (qRT-PCR). Primer sequences used for amplifications were as follows: Glut2 (Accession Number NM\_012879) forward primer, 5'-GAC ACC CCA CTC ATA GTC ACA C-3', Glut2 reverse primer, 5'-CAG CAA TGA TGA GAG CAT GTG-3', Glut5 (Accession Number NM\_031741) forward primer, 5'-AAC TTT CCT AGC TGC CTT TGG CTC-3', Glut5 reverse primer, 5'-TAG CAG GTG GGA GGT CAT TAA GCT-3', SGLT-1 (Accession Number NM\_013033) forward primer, 5'-ATG GTG TGG TGG CCG ATT GG-3', SGLT-1 reverse primer, 5'-GTG TAG ATG TCC ATG GTG AAG AG-3'. The housekeeping gene 18S ribosomal RNA was used for normalization (forward primer 5'-AGC GAT TTG TCT GGT TAA TTC CGA TA-3', reverse primer 5'-CTA AGG GCA TCA CAG ACC TGT TAT TG-3'). All sample reactions were prepared using Evolution Eva Green qPCR mastermix (Montreal Biotech, Montreal, Canada) and run in duplicate on a Corbett Rotor-Gene 6000 cycler.

#### **EXAMPLE 23: Statistical Analysis**

Two-way repeated measures ANOVA was performed on the oGTT, ipGTT, and insulin ELISA data. One-way ANOVA and student t-test were used to compare the other data, as

appropriate. All data are expressed as means  $\pm$  SEM; Bonferroni post-test was performed to assess differences between diet groups and a p-value  $<0.05$  was considered to be significant.

#### **EXAMPLE 24: Fibre Analysis**

Analysis of the fibre constituents from raw and cooked pea seed coats is reported in Table 5. The total fibre (NSP) content of the raw seed coat fraction was 68% w/w, with 64-65% composed of insoluble fibre and 3-4% soluble fibre. The total fibre fraction was composed mainly of glucose moieties (52%), while the total and insoluble NSF fibre fraction was also rich in xylose. Arabinose (4%), and mannose (0.2%) were also present in the total fibre of pea seed coats, but at low levels. Consistently, the amount of rhamnose was enriched in the soluble fraction compared to the total and insoluble fibre fractions. Galactose, xylose and a small amount of fucose were also detected in the soluble fibre fraction. The cooking treatment did not affect the fibre classes of the pea seed coats.

**Table 5: Sugar components of raw, cooked and hydrolyzed seed coats of ‘Canstar’ by GC analysis**

	Rhamnose	Ribose	Fucose	Arabinose	Xylose	Mannose	Glucose	Galactose	Total
	mg/100 mg dwt (%)								
<hr/>									
Raw Seed Coat Fraction									
Total	0.73±0.01	0.05±0.01	0.27±0.02	3.73±0.33	10.59±0.87	0.19±0.01	51.81±1.11	0.77±0.03	68.13±2.04
Insoluble	0.43±0.05	0.02±0.01	0.14±0.00	2.02±0.12	9.99±0.56	0.17±0.01	52.07±0.65	0.43±0.02	65.28±0.17
Soluble	0.30±0.07	0.03±0.01	0.12±0.02	1.71±0.21	0.60±0.31	0.02±0.00	1.00±1.00	0.34±0.02	4.11±1.50
<hr/>									
Cooked Seed Coat Fraction									
Total	0.62±0.01	0.06±0.01	0.25±0.01	3.71±0.36	10.64±0.91	0.20±0.01	51.50±0.56	0.86±0.05	67.84±1.84
Insoluble	0.34±0.01	0.01±0.00	0.14±0.01	1.76±0.16	9.50±0.76	0.17±0.00	52.64±1.15	0.40±0.03	64.96±1.97
Soluble	0.28±0.02	0.04±0.01	0.11±0.01	1.95±0.21	1.14±0.15	0.03±0.00	0.30 ±0.30	0.46±0.07	4.33±0.31

\*Data are means ± standard error of the mean, n=3.

The total protein content of the raw pea seed coat fraction was 6-7% by weight, and the total starch content was less than 1% (Table 6). Again, the cooking treatment did not affect the total protein or starch content of the pea seed coat fraction.

**Table 6: Protein and total starch components of raw and cooked pea seed coats of ‘Canstar’.**

Pea seed coat	Protein (%)	Total starch (%)
Raw	6.65 ± 0.05	0.16 ± 0.01
Cooked <sup>a</sup>	6.91 ± 0.03	0.59 ± 0.02

<sup>a</sup> placed in boiling water for 30 minutes

% = mg/100 mg dry weight of sample.

Data are means ± SEM, n=3.

#### **EXAMPLE 25: Body Weight and Body Composition Analysis**

Rats in all groups gained the same amount of weight, calculated as % of baseline, at the end of the study (Table 7,  $P \geq 0.05$ ). Food intake data were also comparable between groups indicating that the palatability of the diets did not affect the results. MRI data revealed higher fat mass in RP compared with LFD when normalized to total body weight ( $P < 0.05$ , Table 7).



**Table 7. Metabolic profile of rats fed diets containing pea fractions.**

Diet group	HFD		RP		CP		LFD	
	Mean	SEM	Mean	SEM	Mean	SEM	Mean	SEM
BW (g) Baseline	401.1	11	402.2	10	394.2	14.1	397	13.3
BW (g) Final	627	12.3	649.3	13.9	660.3	16.1	608	14.07
Change (% of baseline BW)	65.84	3.79	67.61	3.12	74.52	3.33	62.54	3.91
Fat mass (% of final BW)	18.9	1.21	19.1	0.97	18.1	0.92	16.2	1.08
Food intake (Kcal/day)	134.4	4.9	138.1	8.4	143	14.5	153	10.2
Fasting blood glucose (mmol/l)	5.3	0.18	5.5 <sup>a</sup>	0.14	4.9	0.28	4.4	0.08
Fasting serum insulin (pmol/l)	1.04	0.13	1.24	0.19	0.49*	0.08	0.72	0.15
Serum TG (mg/dl)	52.2	2.3	45.3	8.7	30.4*	4.4	32.6	4.0
Serum NEFA (mmol/l)	0.5	0.1	0.49	0.07	0.37	0.09	0.37	0.08
Fasting serum glucagon (pg/ml)	308	32.31	286.6	12.28	167.5*	26.9	246.7	17.61
Fasting serum GLP-1 (pg/ml) <sup>‡</sup>	18.3	0.7	23.1	2.5	27.9*	1.6	23.4	1.5

BW, body weight; HFD, high fat diet; RP, raw pea seed coat (HFD supplemented with raw seed coats); CP, cooked pea seed coat (HFD supplemented with cooked seed coats); LFD, low fat diet; Data are means  $\pm$  standard error of the mean (SEM), n=4 to 25.

Asterisks show significant difference compared to HFD (\*P<0.05); Superscript letter indicates significant difference compared to LFD (<sup>a</sup>P <0.05); <sup>§</sup> Blood sampling was done at the end of the feeding trial during oral glucose tolerance test; Serum for TG, NEFA, glucagon and GLP-1 assessment was obtained from blood samples collected from fasted rats by cardiac puncture at the time of tissue collection.

### **EXAMPLE 26: Circulating Metabolites and Hormones**

Fasting blood glucose was significantly higher in RP than LFD ( $P < 0.05$ ; Table 7). Fasting serum insulin was significantly lower in CP than HFD ( $P < 0.05$ ; Table 8). Serum triglyceride concentrations were significantly higher ( $P < 0.05$ ) in HFD than CP or LFD, but no differences in serum NEFA were detected (Table 8). Serum GLP-1 was significantly higher only in CP compared with HFD ( $P < 0.05$ ; Table 7). As shown in Figure 7, in fasted rats, fasting serum GIP concentrations were 50% higher in RP and CP than HFD ( $P < 0.05$  for both). A similar trend was observed with GIP measured 30 min after glucose administration in the OGTT, in which RP was 2-fold higher than HFD (Figure 7A and 7B,  $P < 0.05$ ).

### **EXAMPLE 27: Glucose Tolerance Tests and Insulin Tolerance Test**

OGTT and ipGTT results are shown as responses over 120 minutes (Figure 8A and 8C), and as incremental area under the curve (IAUC; Figure 8B and 8D). As expected, LFD had lower glucose response compared to HFD at  $t = 10$  min ( $P < 0.05$ ), and  $t = 20, 30,$  and  $60$  min ( $P < 0.001$ ). CP but not RP rats had lower glucose response compared to the HFD group at  $t = 10$  ( $P < 0.05$ ),  $t = 20$  ( $P < 0.001$ ), and  $t = 30$  ( $P < 0.01$ ) min. IAUC during oGTT showed that both CP and LFD groups had glucose values that were significantly lower than HFD (Figure 2B;  $P < 0.05$  and  $P < 0.001$ , respectively). Although neither CP nor RP had different ipGTT from HFD group (Figure 8C), LFD had improved response at  $t = 20$  ( $P < 0.001$ ) and  $t = 30$  ( $P < 0.01$ ) min. Trends for LFD and CP to lower IAUC during ipGTT were attenuated and not statistically significant (Figure 8D).

During oGTT, RP rats had lower insulin concentrations than HFD rats at  $t = 10$  and  $20$  min (Figure 8E;  $P < 0.001$ ); CP group had decreased insulin concentrations compared to the HFD group at  $t = 10$  ( $P < 0.001$ ),  $t = 20$  ( $P < 0.001$ ),  $t = 30$  ( $P < 0.01$ ),  $t = 60$  ( $P < 0.01$ ) and  $t = 120$  ( $P < 0.05$ ) min. The LFD group had lower serum insulin than the HFD group at  $t = 10$  ( $P < 0.01$ ) min. Both RP and CP groups had smaller IAUC values when compared to HFD (Figure 8F;  $P < 0.05$  and  $P < 0.01$  respectively); LFD rats also had significantly lower IAUC ( $P < 0.01$ ). Insulin concentrations of CP and RP groups during ipGTT were not different than those of HFD (Figure 8G). However, LFD had decreased concentrations at  $t = 20$  and  $30$  min ( $P < 0.05$ ). IAUC data also only revealed a difference between HFD and LFD ( $P < 0.05$ ) (Figure 8H). Blood glucose levels during the glucose disappearance phase (0-30 min) of the ITT were comparable among the groups (Figure 3A,B).

During the recovery phase (60-120 min), HFD rats rebounded most quickly and this was significantly faster than for RP rats ( $P < 0.05$ ) (Figure 9C).

#### **EXAMPLE 28: Pancreatic Beta- and Alpha-cell Mass Analysis**

Pancreatic beta- and alpha-cell area at the end of the study are shown in Figure 10A and 10B. After four weeks of pea seed coat intervention, no significant difference in beta-cell area between diet groups was observed (Figure 10A;  $P > 0.05$ ). As shown in Figure 4B, alpha-cell area in the four diet groups followed a similar pattern with beta-cell area; however, significant differences were found between diet groups ( $P < 0.05$ ), with CP fed rats having a significantly smaller alpha-cell area compared with the RP fed rats ( $P < 0.05$ ). Total islet area was estimated by adding alpha- and beta-cell areas and are presented in Figure 10C ( $P = 0.16$ ; denoting trend to increased islet area in the RP group). Representative micrographs depicted in Figure 4D suggest that the increase in islet area of the RP group is due to an increase in the number of islets, rather than the size of individual islets.

#### **EXAMPLE 29: K- and L-cell Quantification**

There was no significant difference in the number of K-cells expressing GIP in the jejunum shown in Figure 11A ( $P > 0.05$ ). Similarly, the number of GLP-1 positive L-cells in the ileum was comparable between all the groups (Figure 11B;  $P > 0.05$ ).

#### **EXAMPLE 30: mRNA Expression of Glucose Transporters**

Jejunal mRNA expression of Glut2 and SGLT1 were similar between the groups (Figure 12A and 12B); however, Glut5 expression was significantly different between diet groups ( $P = 0.005$ ), with a higher expression in RP when compared to LFD (Figure 12C;  $P < 0.01$ ).

The present study demonstrated that supplementing a HFD with cooked pea seed coats improved glucose tolerance, whereas raw seed coat supplementation was not as beneficial. We also observed that the effect of the pea seed coat fibre on postprandial glucose excursions was only detectable when glucose was administered orally and not intraperitoneally. In other words, bypassing the gastrointestinal tract during ipGTT diminished the improved glycemic excursions in the pea fibre groups to a high degree. These divergent outcomes on oral versus ip glucose tolerance led us to consider mechanisms of action involving the gastrointestinal tract.

The total fibre fraction of pea seed coats was mainly composed of the monosaccharide glucose (Table 2), indicating that the most abundant polysaccharide present was cellulose (made up of linear chains of glucose). Because cellulose is a water-insoluble polysaccharide, the insoluble fibre component was also mainly made up of cellulose. The glucose content determined in the total NSP fibre of pea seed coats in this study is consistent with that of 58% reported by Weightman et al. (1994). The higher percentage of xylose (also consistent with Weightman et al. 1994), along with the occurrence of fucose, galactose, and glucose in the total and insoluble NSF fibre fraction is indicative of the presence of the cell wall cellulose microfibril cross-linking polysaccharide, fucogalacto-xyloglucan, commonly found in legume family members (Carpita and McCann, 2002). The presence of arabinose in the total fibre of pea seed coats (Weightman et al., 1994 reported 3.9% arabinose in this fraction) suggests the presence of glucuronoarabinoxylans and/or pectins (Carpita and McCann, 2002). Very low levels of mannose indicate minimal presence of glucomannans, galactoglucomannans, or galactomannans in interlocking microfibrils of the cell wall (Carpita and McCann, 2002). The major non-cellulosic neutral sugars, arabinose and xylose, detected in the soluble fibre pea seed coat fraction indicate the presence of pectin (Weightman et al., 1994; Carpita and McCann, 2002). Rhamnose, which is another constituent of pectins, was also enriched in the soluble fraction of pea seed coats. Galactose, xylose and the small amount of fucose also indicate the presence of fucogalacto-xyloglucans in the soluble fibre fraction.

Cooking treatment improved glucose homeostasis but did not alter the fibre classes of the pea seed coat fraction. One explanation is that the boiling process may have caused separation and/or hydration of the fibre components that were stabilized by the subsequent lyophilization. Our results are consistent with previous studies showing that cooking procedures did not affect the total dietary fibre (Goodlad & Mathers, 1992; Marconi et al., 2000). In another study, however, it was reported that cooking followed by freeze-drying resulted in increased insoluble dietary fibre (IDF) in whole legume seeds (Almeida Costa et al., 2006). Conversely, Kutos<sup>ˇ</sup> et al. (2003), found decreased IDF content when examining the effect of thermal processing on whole beans. Other thermal procedures such as autoclaving have also been shown to result in changes in the composition of wheat bran fibre that lead to less fat accumulation upon consumption (Jones et al., 2014). In addition, boiling may lead to partial solubilization and depolymerization of hemicelluloses and insoluble pectic substances (Marconi et al., 2000), which may change the

properties of the fibre with respect to gut fermentation. Altered microstructures of pea flour, as a result of thermal treatments in general, can promote its nutritional and functional characteristics, among which are increased fat and water absorption capacity, and emulsifying and gelling activity (Ma et al., 2011). In addition to higher nutritional value, the thermal processing-derived characteristics of pea flour have been suggested to improve its practicality for food application (Almeida Costa et al., 2006; Ma et al., 2011).

As shown here, enhanced glucose control occurred in the CP group during oGTT versus no improvement during ipGTT. This effect could be explained by several different mechanisms. SDF in general has been proposed to improve glycemic control and insulin sensitivity through mechanisms such as delayed gastric emptying and glucose absorption by increasing gastrointestinal viscosity (Galisteo et al., 2008). In this study however, insulin sensitivity did not appear to be affected by pea seed coat supplementation. SDF can also be fermented to SCFA in the colon, which are absorbed into the blood and are reported to suppress glucose production in the liver (Galisteo et al., 2008) and stimulate skeletal muscle uptake of glucose (Lu et al., 2004). A previous study by our group showed increased circulating 3-hydroxybutyrate believed to be derived from butyrate of dietary origin because butyrate dehydrogenase expression in the liver was suppressed (Chan et al., 2014). On the other hand IDF, in spite of lacking effects on viscosity, has also been shown to have a role in regulating glucose homeostasis (Schenk et al., 2003; Weickert et al., 2006). CP might improve oGTT by down-regulating the expression of intestinal glucose transporters; however, HFD appeared to be the main negative driver of glucose transporter expression, and there was no subsequent modulation upon addition of RP or CP. Contrary to our results, a study performed on dogs showed that a diet containing high fermentable dietary fiber resulted in increased jejunal SGLT1 and Glut2 mRNA abundance (Massimino et al., 1998), but that would not explain enhanced glucose tolerance.

Pea seed coat-supplemented diets significantly enhanced plasma incretin concentrations. GLP-1 has insulinotropic effects and acts directly on pancreatic islets to stimulate insulin secretion from beta-cells, promote beta-cell proliferation and suppress apoptosis (Seino et al., 2010) as well as noninsulinotropic effects such as inhibiting gastric emptying. GLP-1 also inhibits glucagon secretion, and decelerates endogenous production of glucose (Seino et al., 2010). In several animal studies, consumption of fermentable dietary fibres has been linked with elevated plasma GLP-1 (Grover et al., 2011; Wang et al., 2007; Massimino et al., 1998). In

addition, in both healthy (Tarini et al., 2010; Johansson et al., 2013) and hyperinsulinemic (Freeland et al., 2010) human subjects, diets high in SDF increased GLP-1 in plasma. In our study, we observed 50% higher fasting GLP-1 in CP group relative to HFD. This could be positive given that it has previously been reported that diabetic patients had significantly lower fasting serum GLP-1 when compared with non-diabetic overweight subjects (Legakis et al., 2003); however, the physiological significance of fasting GLP-1 levels remains elusive. Pannacciulli et al. (2006) examined the association between fasting plasma GLP-1 concentration and energy expenditure and fat oxidation, and reported a positive association between them. In another study, both in-vitro and in-vivo results showed that GLP-1 increased basal uptake of glucose in the muscle through a nitric oxide-dependent pathway, although the concentration of the GLP-1 used was higher than the fasting levels seen in our rats (Chai et al., 2012).

GIP is another incretin that is secreted in response to nutrient ingestion resulting in many similar actions as GLP-1 in the pancreas; however, outside the pancreas, GIP and GLP-1 seem to function differently from one another. GIP secretion has been reported by many studies to be normal or sometimes increased in the state of impaired glucose tolerance and T2D, whereas its insulinotropic effect is diminished in T2D (Kim & Egan, 2008). Studies of the effects of dietary fibre intake on circulating GIP have produced diverse results, with SDF suppressing and IDF augmenting GIP in diabetic and healthy human subjects (Weickert & Pfeiffer, 2008). In healthy adults, a whole barley kernel meal resulted in higher postprandial GIP in plasma (Johansson et al., 2013). In another human study, healthy subjects had lower GIP responses following a whole-kernel rye bread when compared to a white bread meal (Juntunen et al., 2002). In our study, we observed higher GIP responses in the pea fibre-fed rats before and post-glucose ingestion, independent of changes in K-cell number, suggesting increased sensitivity to stimulation. However, because GIP secretion changes were similar in RP and CP, this could not account for the differential effects on oGTT between the groups. Furthermore, improved glucose tolerance could not be accounted for by differences in body weight gain or body fat amongst the groups. In contrast, male Wistar rats, following a high fibre diet (21% wt/wt), composed of inulin and oligofructose, had a lower percentage of body fat (Reimer et al., 2012). In our study, we failed to detect a significant change in body composition, which may be related to the short length of our study (10 weeks) versus that of (21 weeks) Reimer et al (2012).

Finally, the present disclosure demonstrated that HFD supplementation with CP for 4 weeks resulted in almost 50% decrease in beta-cell area in insulin-resistant rats (non-significant). This observation was expected based on the oGTT results suggesting CP-fed rats had an improved glucose tolerance compared with those on the diets supplemented with either RP or cellulose. Given the well-documented beta-cell mass expansion as a major adaptation to insulin resistance (Ahren et al., 2010), the marginal decline in beta-cell mass shown here, in the absence of further elevation in plasma glucose concentrations, could be an indicator of a reversed progression of insulin resistance. A novel finding upon dietary intervention with PSC was the significant difference in alpha-cell mass between groups. Specifically, supplementation with CP decreased alpha-cell mass in glucose-intolerant rats to the level comparable to that seen in the LFD group. While it has been widely asserted that HFD-induced insulin resistance results in expansion in beta-cell area (Goodlad & Mathers, 1992; Pick et al., 1998; Marconi et al., 2000; Hull et al., 2005; Almeida Costa et al, 2006; Ahren et al., 2010), it is not very clear if it has the same impact on alpha-cells. Dysregulated glucagon secretion has been proposed as an early hallmark of type 2 diabetes (D'Alessio, 2011; Liu et al., 2011; Weiss et al., 2011). In diabetic mice increased number of alpha-cells and alpha-cell mass was reported as diabetes developed over time (Liu et al., 2011). In general, it has been suggested that alpha-cell proliferation is regulated by both insulin and glucagon. In response to insulin resistance, elevated intra-islet insulin concentration can originally inhibit glucagon secretion; however, consequently, as alpha-cells develop resistance to insulin, the regulation of glucagon secretion will be impaired. Elevated circulating glucagon then, independent of intra-islet insulin secretion, leads to excessive hepatic glucose production and aggravating hyperglycemia (Liu et al., 2011). In our study, increased alpha-cell area in HFD rats may be due to elevated insulin and glucagon levels in the plasma. At the same time, rats in the CP group had significantly lower plasma insulin concentrations compared to those in the RP and HFD groups, which could explain the smaller alpha-cell area and lower fasting glucagon in that group. In addition, lower glucagon secretion could result in downregulation of hepatic gluconeogenesis and hence reduced fasting plasma glucose concentration. A smaller beta-cell area observed in rats fed CP as compared to those fed RP or cellulose may thus be a result of reduced stress on pancreatic beta-cells.

Current Canadian guidelines (2013) recommend that the diabetic population increase its dietary fibre intake to 25-50 g/day; however, it is not specified what proportion of each fibre type

to include. In the present study, rats received 100 grams of pea fibre for almost every 1000 calories consumed, which was approximately 0.05% of their final body weight. This amount corresponds to a daily intake of 35 g fibre in a 70 kg human, which is within the range of the current recommendation of Canadian Diabetes Association for dietary intake in diabetic adults (CDA, 2013). Therefore, incorporating the corresponding amount of pea fibre into human diet may not only be beneficial for improving insulin-sensitivity, but also seems feasible from a practical standpoint.



What is claimed is:

1. A method for improving health and/or other beneficial effects in a subject, comprising administering pea seed coat fractions to said subject.
2. The method of claim 1, wherein said subject is a human or animal.
3. The method of claim 1, wherein said health and/or beneficial effect is selected from retained PAC bioavailability, retained PAC bioactivity, improved insulin sensitivity, reduced glycemia, increased satiety, improved glucose tolerance, improved glucose control, improved glucose homeostasis, beneficial effects on pancreatic islet composition and insulin secretion.
4. The method of claim 1, wherein said health and/or beneficial effect is selected from PAC-derived products that have increased bioavailability, improved insulin sensitivity, reduced glycemia, increased satiety, improved glucose tolerance, improved glucose control, improved glucose homeostasis, beneficial effects on pancreatic islet composition and insulin secretion.
5. A composition comprising pea seed coat fractions.
6. The composition of claim 4, wherein said composition is selected from a food, animal feed, flour, fibre, and ingredient.
7. A method for improving health and/or other beneficial effects in a subject, comprising administering cooked pea seed coat fractions to said subject.

8. A method for improving health and/or other beneficial effects in a subject, comprising administering pea seed coat fractions processed by cooking followed by freeze-drying to said subject.

9. A method for increasing the bioavailability of proanthocyanidins (PAC), comprising hydrolyzing pea seed coat-derived PACs.

## **ABSTRACT OF THE DISCLOSURE**

The present disclosure embraces methodology and compositions for preparing pea seed coat fractions conferring improved health and/or other beneficial effects, and such fractions may be used in a human and/or animal diet.

**FIGURE 1**

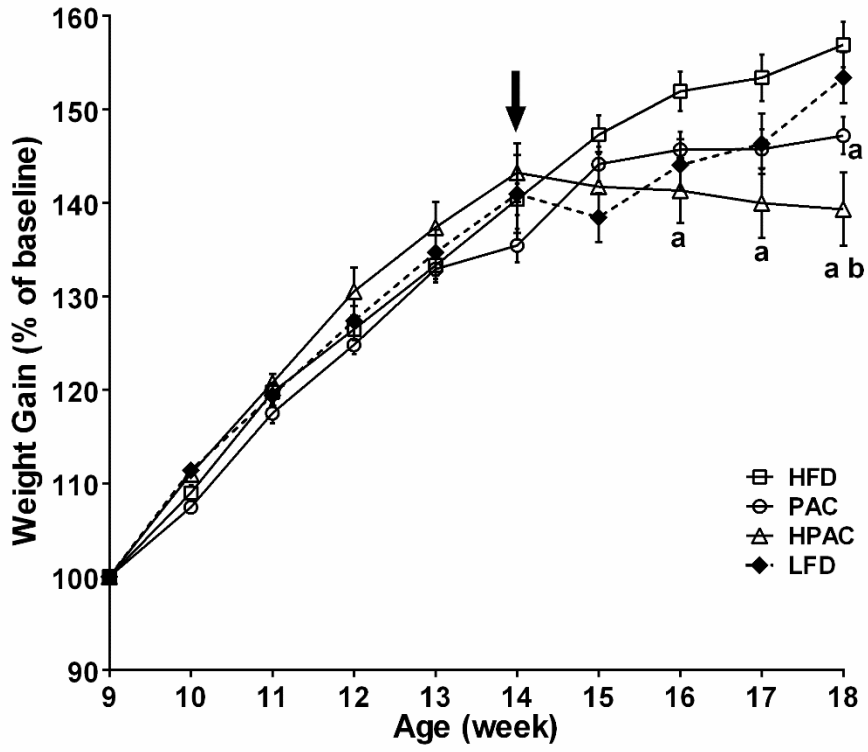
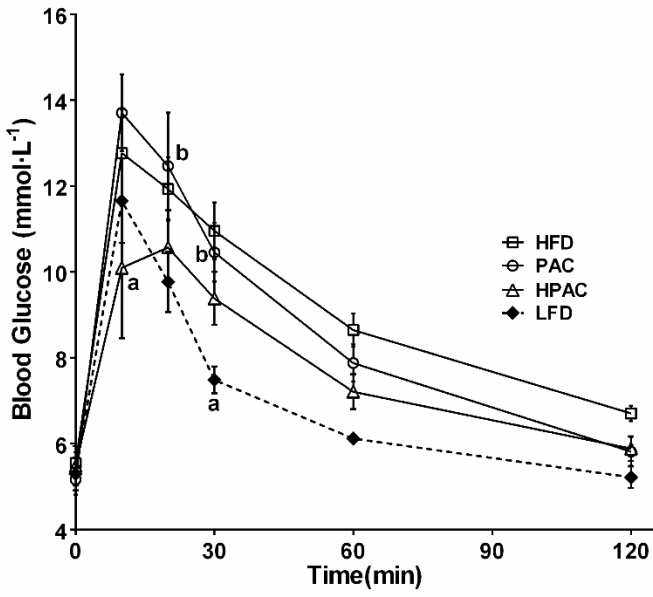
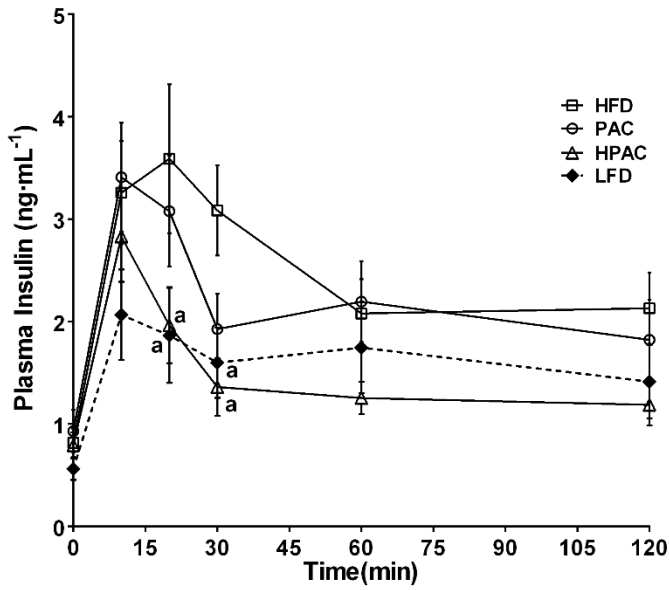


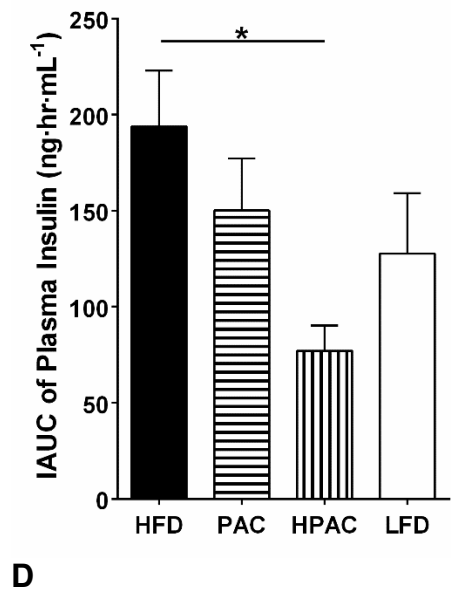
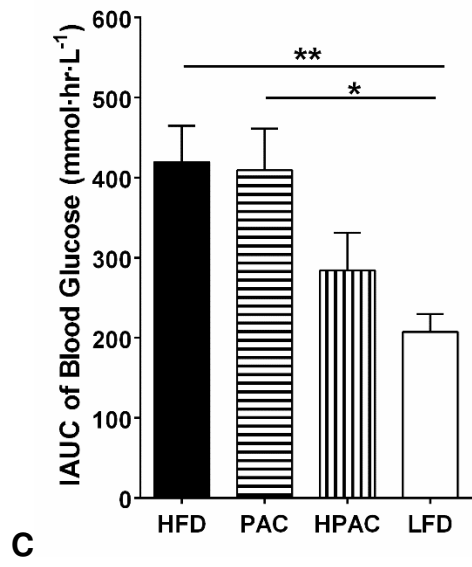
**FIGURE 2**



**A**



**B**



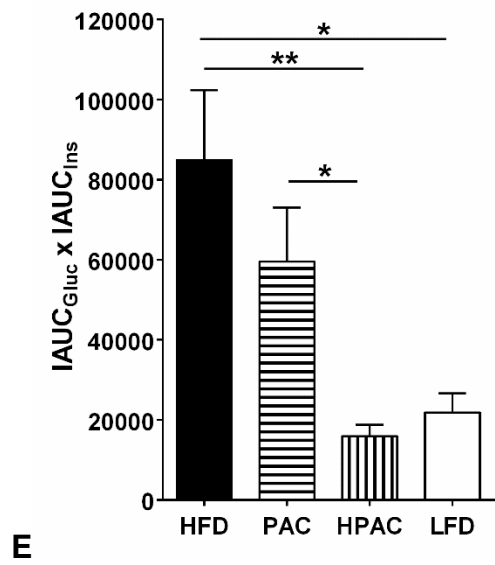
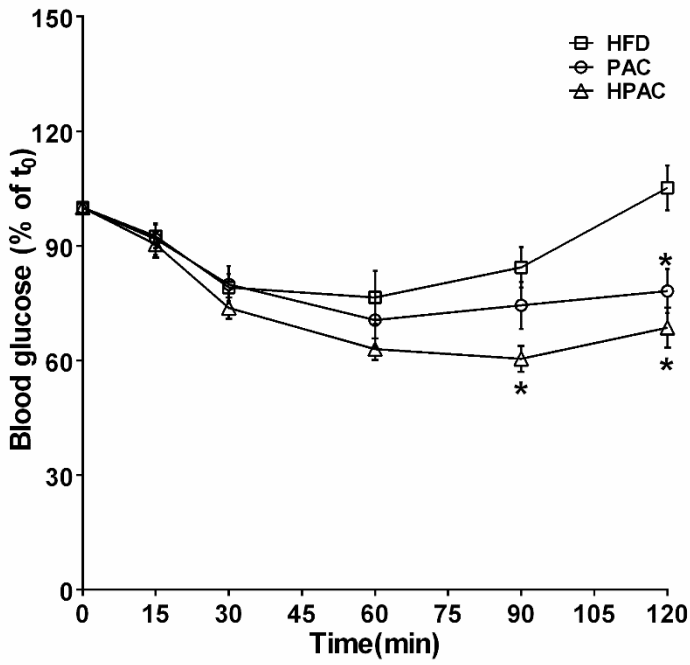
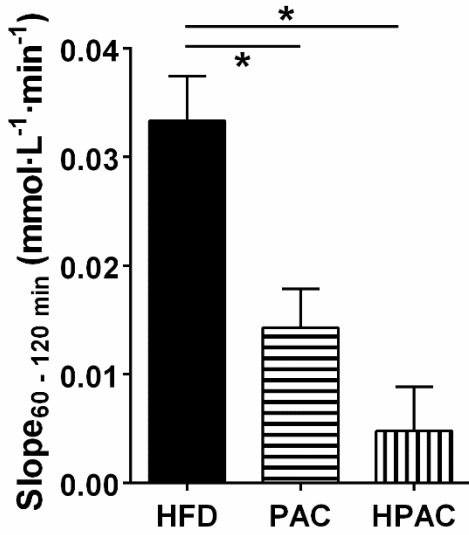


**FIGURE 3**



**A**



**B**



**Figure 4. Effects of diet on pancreatic morphology, fasted insulin and glucagon**

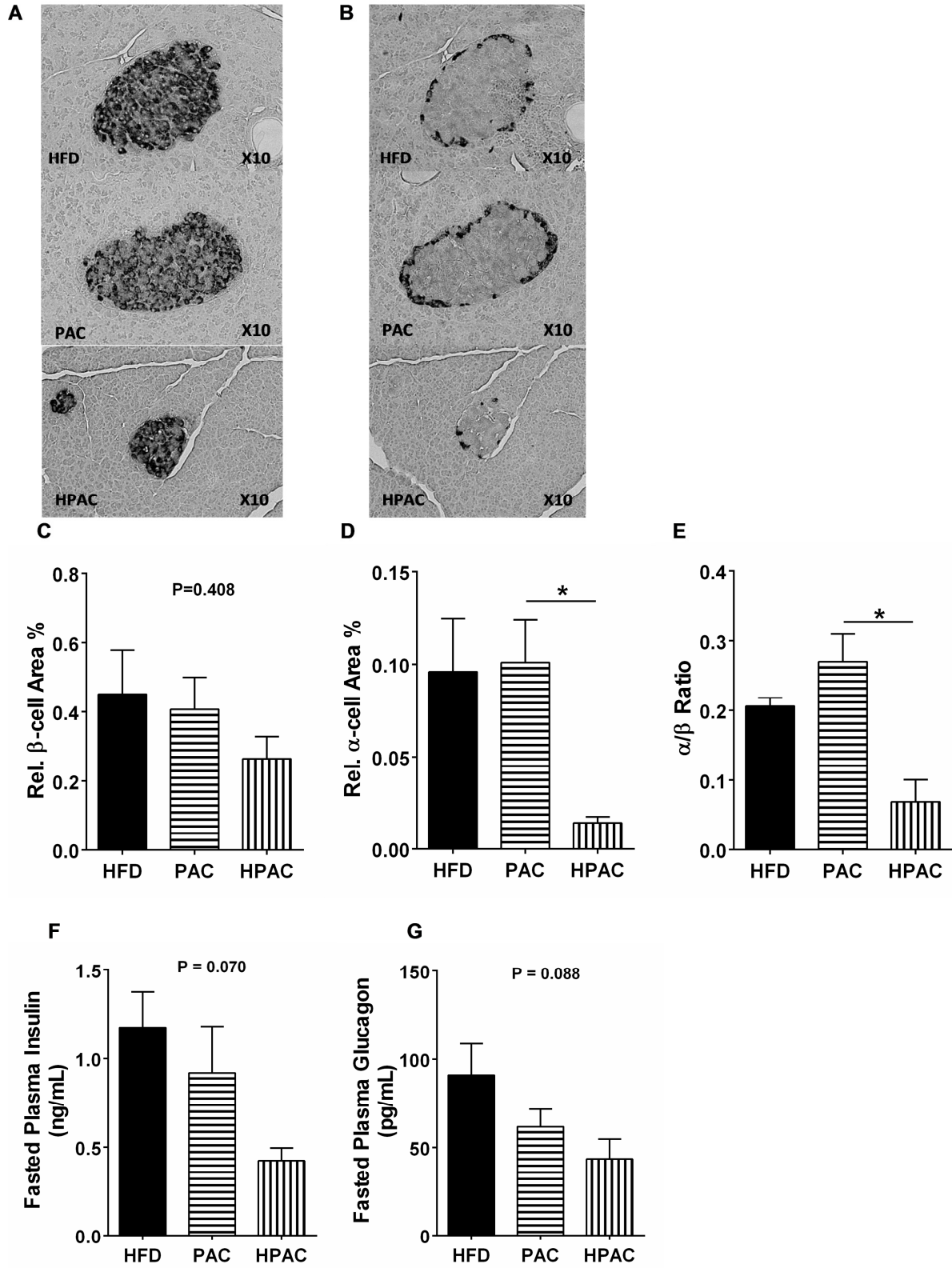
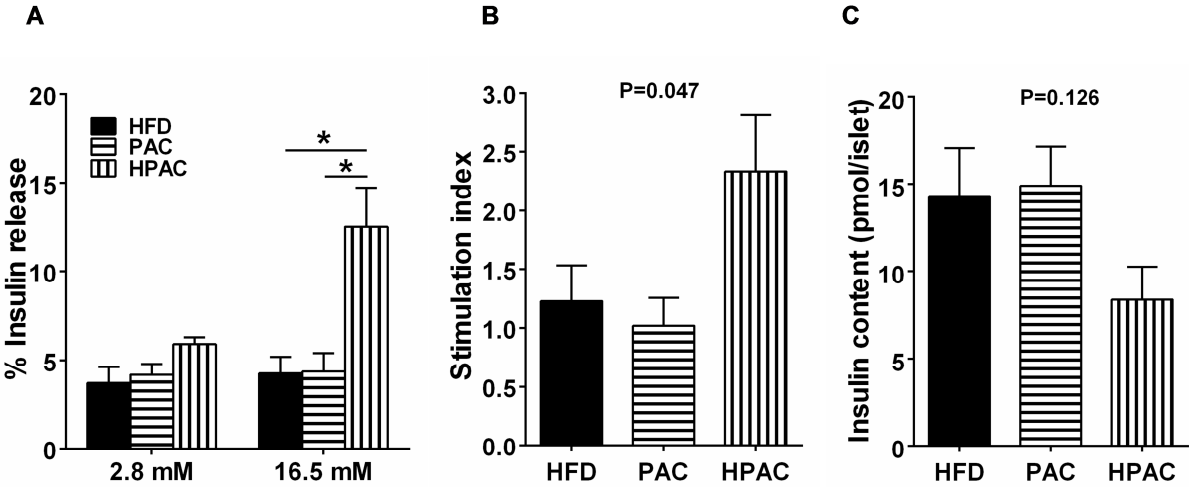
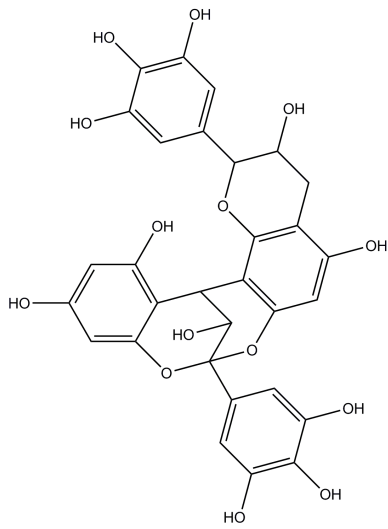


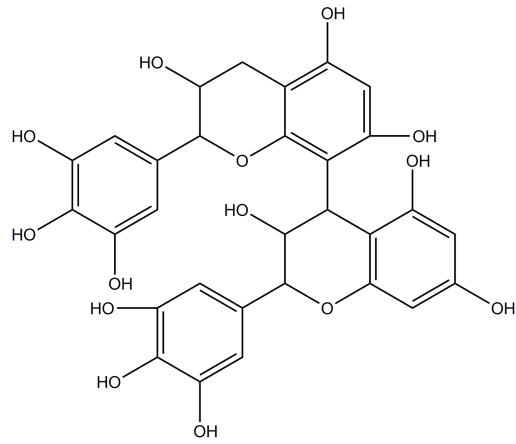
Figure 5. Effects of diet on glucose-stimulated insulin secretion from isolated islets



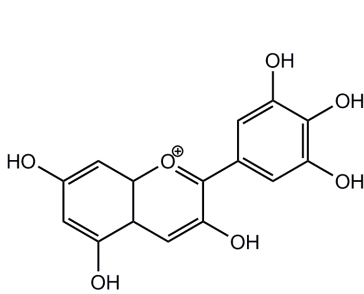
**FIGURE 6A**



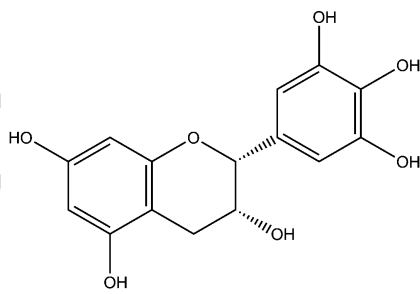
**Prodelphinidin A1**



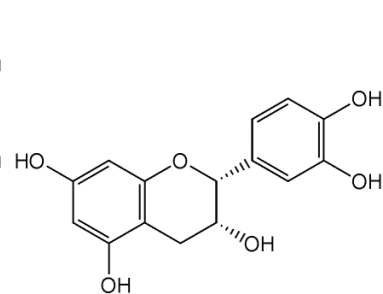
**Prodelphinidin B**



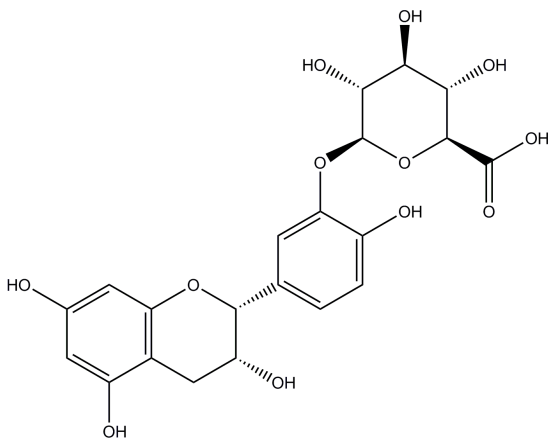
**Delphinidin**



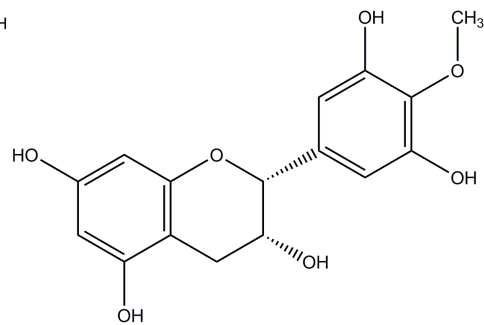
**(-)-Epigallocatechin**



**(-)-Epicatechin**



**Epicatechin 3'-O-glucuronide**



**4'-O-Methyl-epigallocatechin**

**FIGURE 6B**

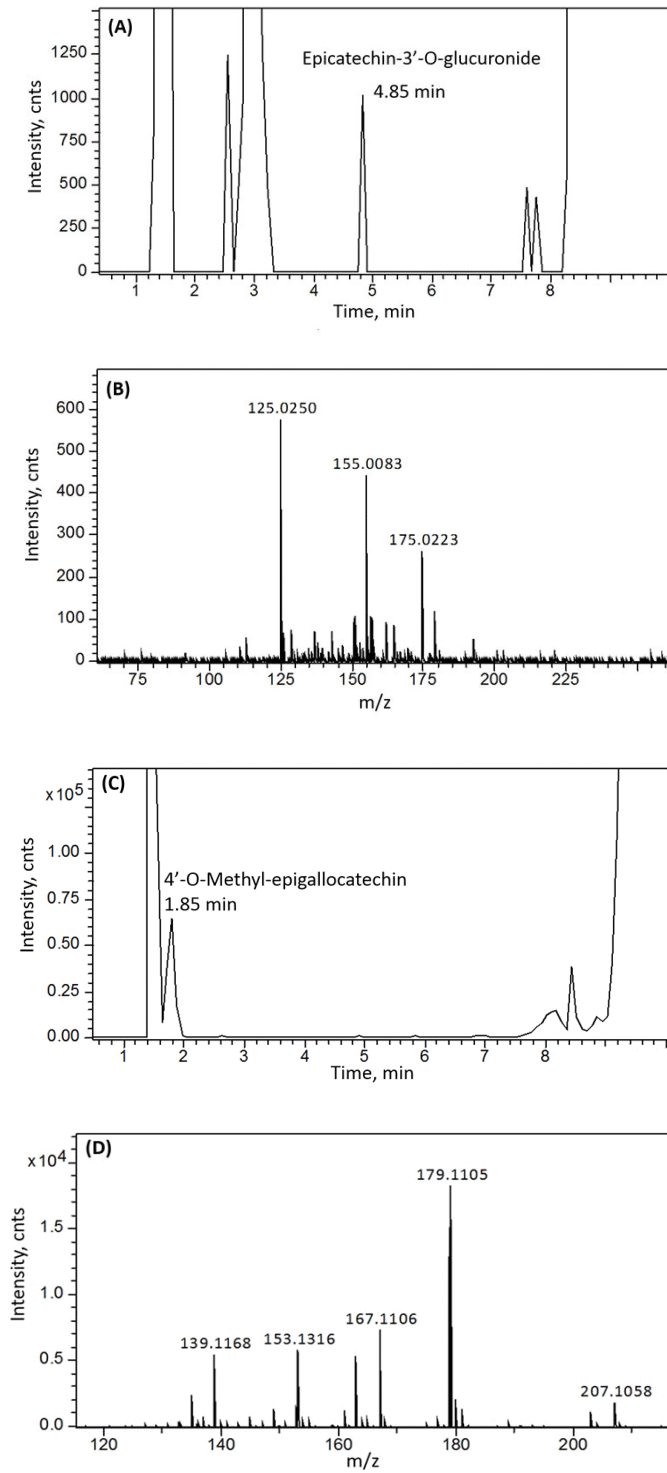


**FIGURE 7**

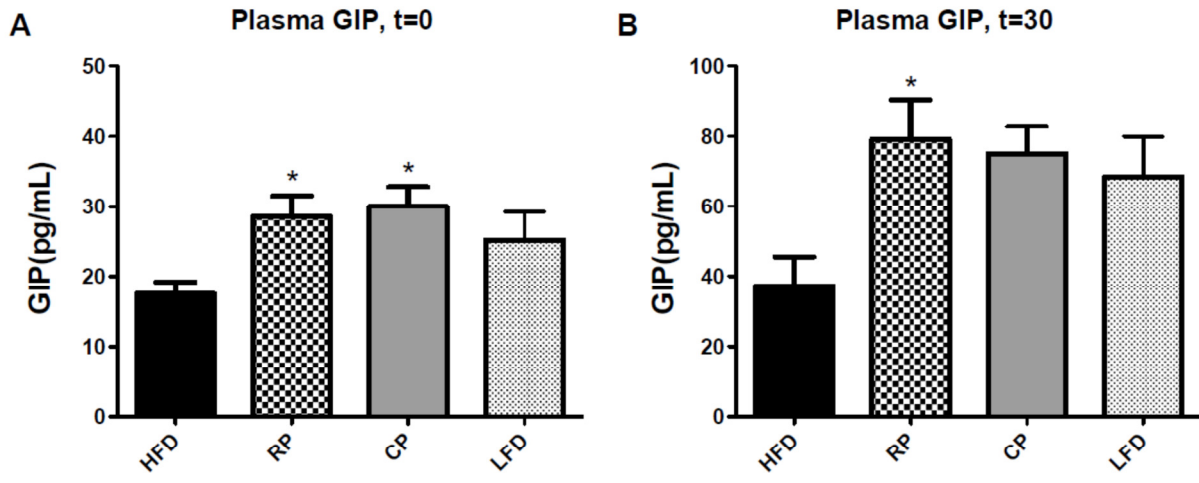


**FIGURE 8**

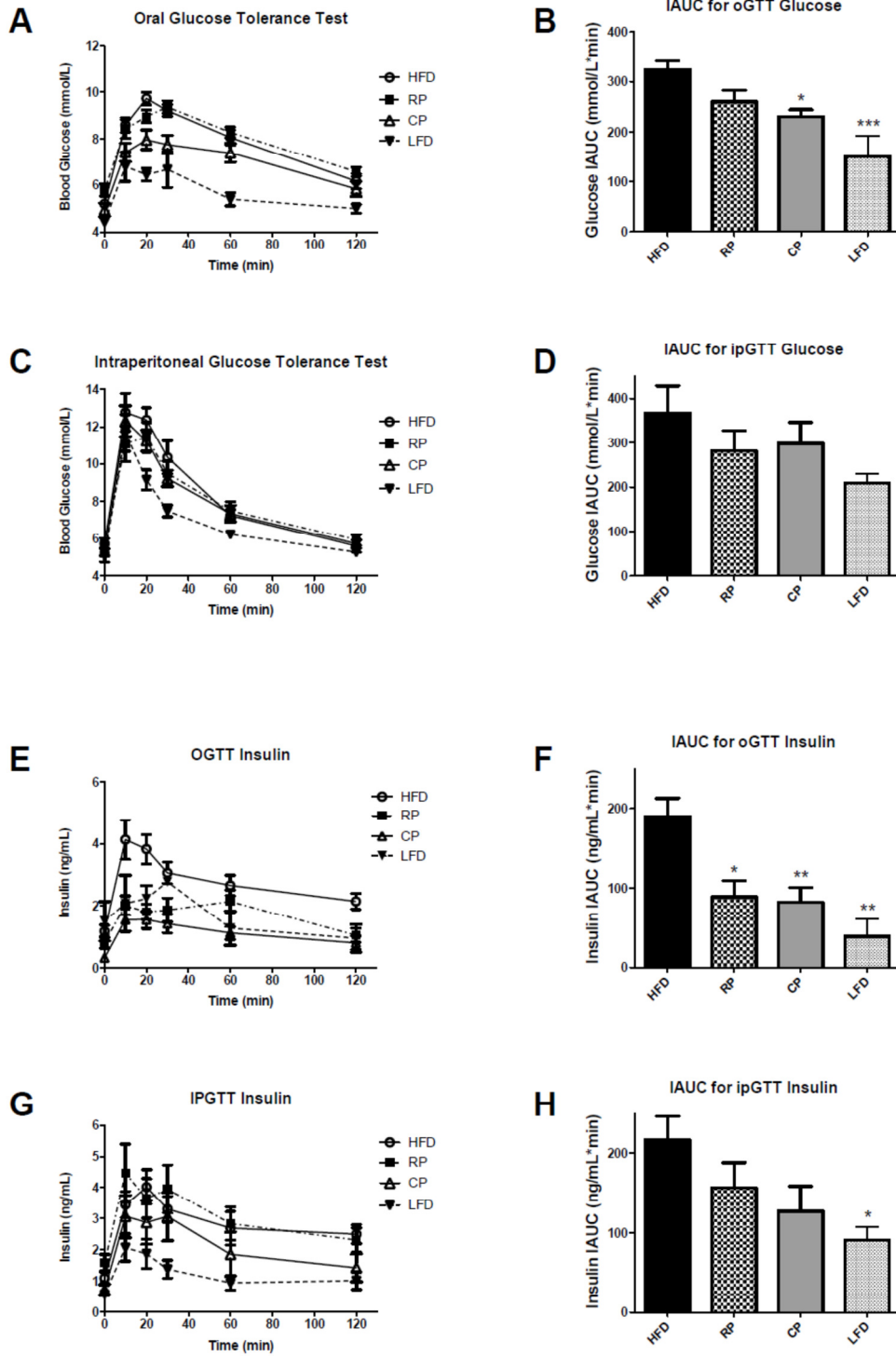


**FIGURE 9**

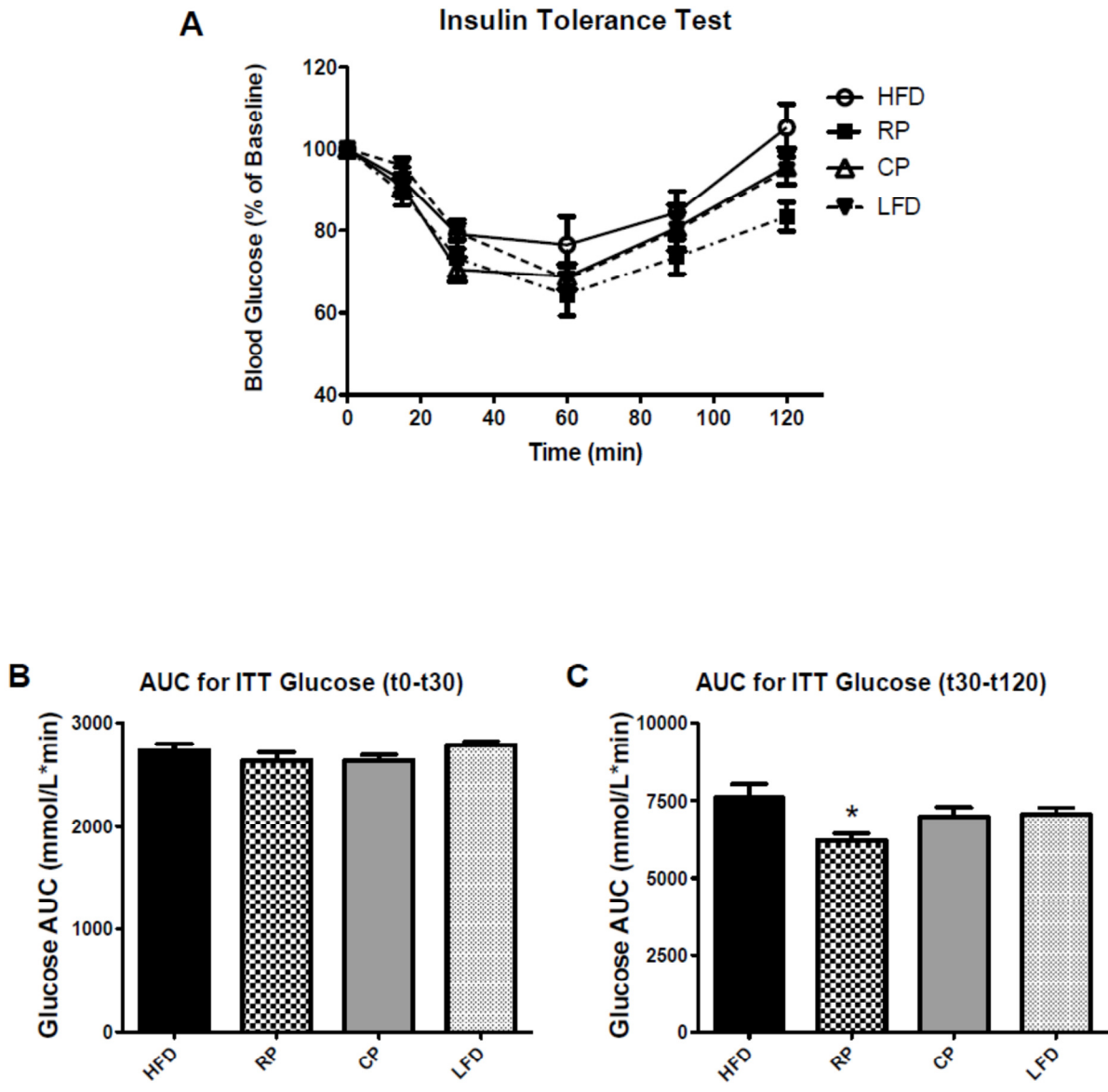


**FIGURE 10**

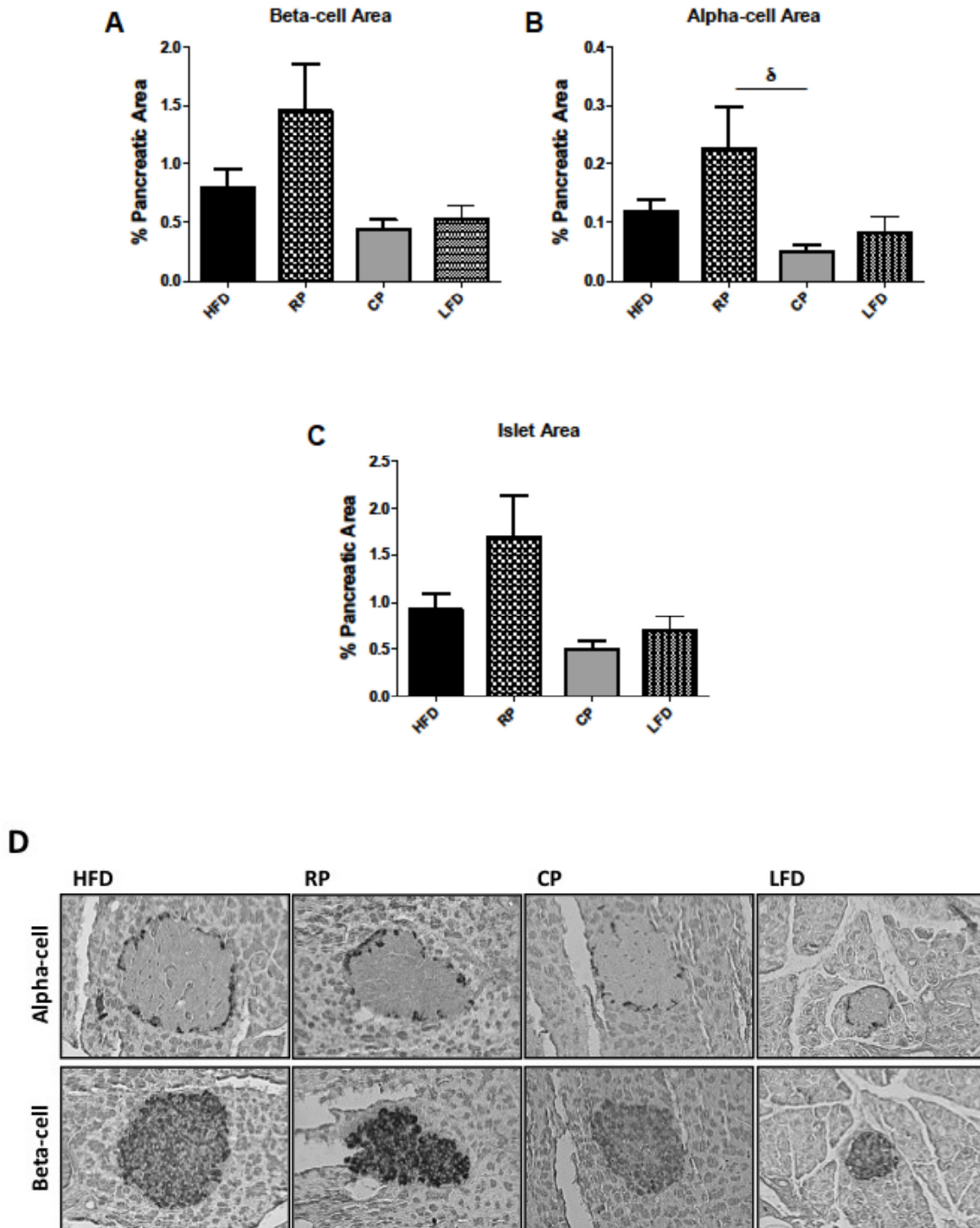




**FIGURE 11**

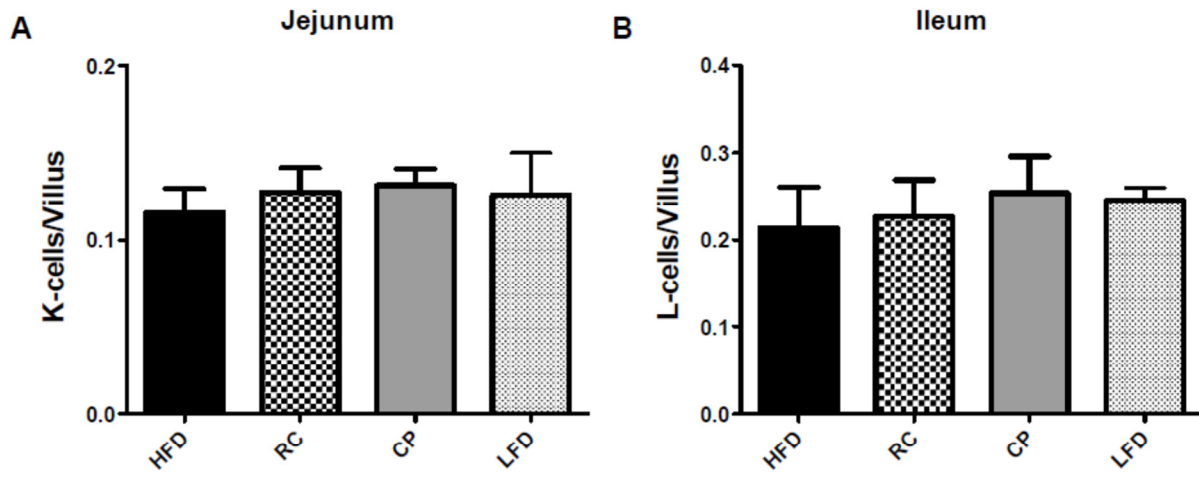
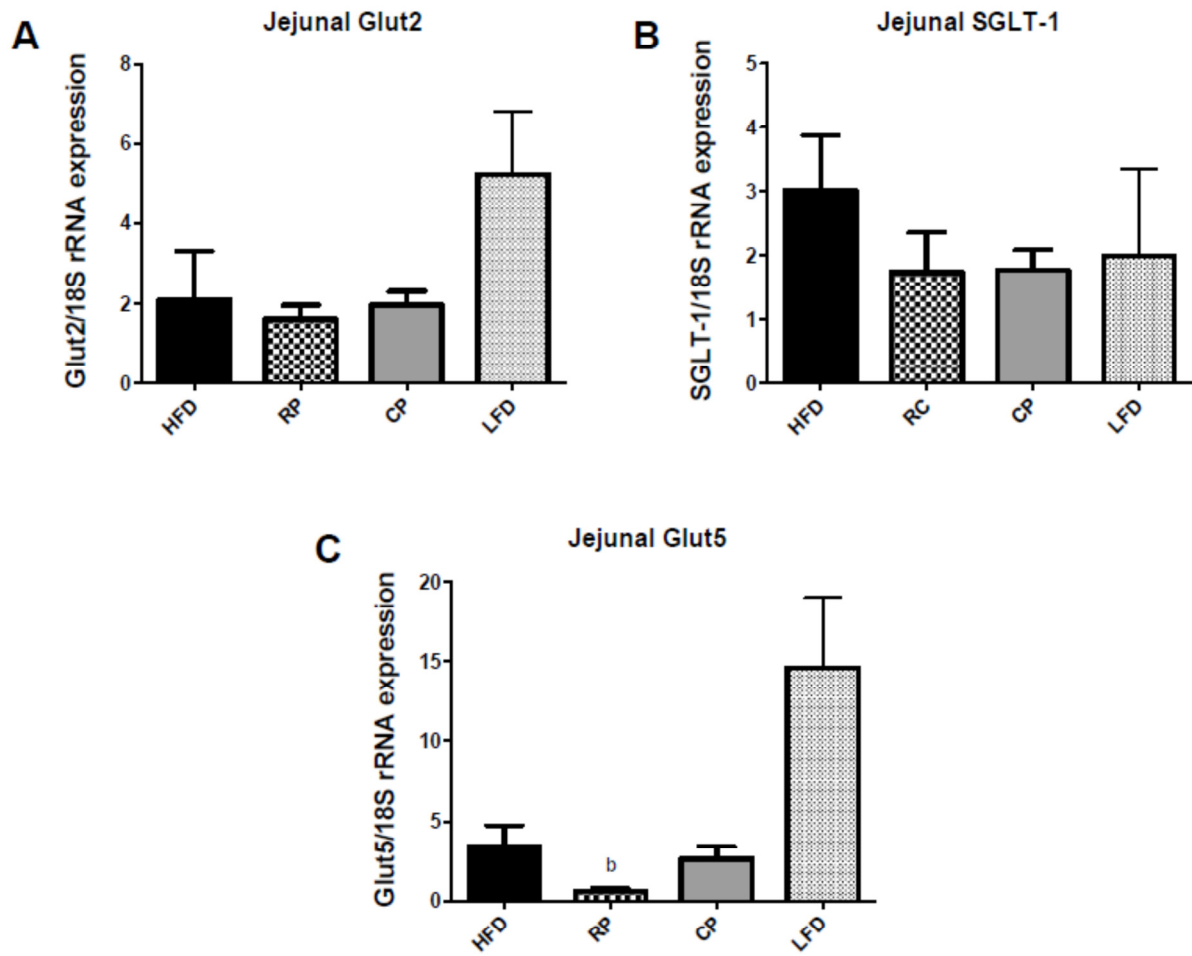


**FIGURE 12**



## References

- [1] Craig W, Beck L. Phytochemicals: Health Protective Effects. *Can J Diet Pract Res* 1999;60:78–84.
- [2] Ross J a, Kasum CM. Dietary flavonoids: bioavailability, metabolic effects, and safety. *Annu Rev Nutr* 2002;22:19–34.
- [3] Bravo L. Polyphenols: chemistry, dietary sources, metabolism, and nutritional significance. *Nutr Rev* 1998;56:317–33.
- [4] Scalbert A, Williamson G. Dietary Intake and Bioavailability of Polyphenols. *J Nutr* 2000;130:2073S–2085S.
- [5] Ovaskainen M-L, Törrönen R, Koponen JM, Sinkko H, Hellström J, Reinivuo H, et al. Dietary intake and major food sources of polyphenols in Finnish adults. *J Nutr* 2008;138:562–6.
- [6] Pérez-Jiménez J, Fezeu L, Touvier M, Arnault N, Manach C, Hercberg S, et al. Dietary intake of 337 polyphenols in French adults. *Am J Clin Nutr* 2011;93:1220–8.
- [7] Wang Y, Chung S, Song WO, Chun OK. Estimation of daily proanthocyanidin intake and major food sources in the U.S. diet. *J Nutr* 2011;141:447–52.
- [8] Wedick NM, Pan A, Cassidy A, Rimm EB, Sampson L, Rosner B, et al. Dietary flavonoid intakes and risk of type 2 diabetes in US men and women. *Am J Clin Nutr* 2012;95:925–33.
- [9] Zamora-Ros R, Andres-Lacueva C, Lamuela-Raventós RM, Berenguer T, Jakszyn P, Barricarte A, et al. Estimation of dietary sources and flavonoid intake in a Spanish adult population (EPIC-Spain). *J Am Diet Assoc* 2010;110:390–8.
- [10] Chen ZY, Chan PT, Ho KY, Fung KP, Wang J. Antioxidant activity of natural flavonoids is governed by number and location of their aromatic hydroxyl groups. *Chem Phys Lipids* 1996;79:157–63.
- [11] Rice-Evans CA, Miller NJ, Paganga G. Structure-antioxidant activity relationships of flavonoids and phenolic acids. *Free Radic Biol Med* 1996;20:933–56.
- [12] Evans JL. Oxidative Stress and Stress-Activated Signaling Pathways: A Unifying Hypothesis of Type 2 Diabetes. *Endocr Rev* 2002;23:599–622.
- [13] Bryans J a, Judd P a, Ellis PR. The effect of consuming instant black tea on postprandial plasma glucose and insulin concentrations in healthy humans. *J Am Coll Nutr* 2007;26:471–7.

- [14] Törrönen R, Sarkkinen E, Niskanen T, Tapola N, Kilpi K, Niskanen L. Postprandial glucose, insulin and glucagon-like peptide 1 responses to sucrose ingested with berries in healthy subjects. *Br J Nutr* 2011;1–7.
- [15] Kirkham S, Akilen R, Sharma S, Tsiami A. The potential of cinnamon to reduce blood glucose levels in patients with type 2 diabetes and insulin resistance. *Diabetes Obes Metab* 2009;11:1100–13.
- [16] El-Alfy AT, Ahmed A a E, Fatani AJ. Protective effect of red grape seeds proanthocyanidins against induction of diabetes by alloxan in rats. *Pharmacol Res* 2005;52:264–70.
- [17] Kim M-J, Ryu GR, Chung J-S, Sim SS, Min DS, Rhie D-J, et al. Protective effects of epicatechin against the toxic effects of streptozotocin on rat pancreatic islets: in vivo and in vitro. *Pancreas* 2003;26:292–9.
- [18] Cedó L, Castell-Auví A, Pallarès V, Ubaida Mohien C, Baiges I, Blay M, et al. Pancreatic islet proteome profile in Zucker fatty rats chronically treated with a grape seed procyanidin extract. *Food Chem* 2012;135:1948–56.
- [19] Ding Y, Zhang Z, Dai X, Jiang Y, Bao L, Li Y, et al. Grape seed proanthocyanidins ameliorate pancreatic beta-cell dysfunction and death in low-dose streptozotocin- and high-carbohydrate/high-fat diet-induced diabetic rats partially by regulating endoplasmic reticulum stress. *Nutr Metab (Lond)* 2013;10:51.
- [20] Zhu M, Hu J, Perez E, Phillips D, Kim W, Ghaedian R, et al. Effects of long-term cranberry supplementation on endocrine pancreas in aging rats. *Journals Gerontol* 2011;66A:1139–51.
- [21] Guyot S. Flavan-3-Ols and Proanthocyanidins. In: Nollet LML, Toldrá F, editors. *Handb. Anal. Act. Compd. ...*, Taylor & Francis Group; 2012, p. 317–48.
- [22] Stalmach A, Troufflard S, Serafini M, Crozier A. Absorption, metabolism and excretion of Choladi green tea flavan-3-ols by humans. *Mol Nutr Food Res* 2009;53:S44–53.
- [23] Stalmach A, Mullen W, Steiling H, Williamson G, Lean MEJ, Crozier A. Absorption, metabolism, and excretion of green tea flavan-3-ols in humans with an ileostomy. *Mol Nutr Food Res* 2010;54:323–34.
- [24] Kahle K, Kraus M, Scheppach W, Ackermann M, Ridder F, Richling E. Studies on apple and blueberry fruit constituents: do the polyphenols reach the colon after ingestion? *Mol Nutr Food Res* 2006;50:418–23.
- [25] Williamson G, Manach C. Bioavailability and bioefficacy of polyphenols in humans. II. Review of 93 intervention studies. *Am J Clin Nutr* 2005;81:243S–255S.

- [26] Halliwell B, Rafter J, Jenner A. Health promotion by flavonoids, tocopherols, tocotrienols, and other phenols: direct or indirect effects? Antioxidant or not? *Am J Clin Nutr* 2005;81:268S–276S.
- [27] Whitlock K a, Kozicky L, Jin A, Yee H, Ha C, Morris J, et al. Assessment of the mechanisms exerting glucose-lowering effects of dried peas in glucose-intolerant rats. *Br J Nutr* 2012;108 Suppl:S91–102.
- [28] Porter LJ, Hrstich LN, Chan BG. The conversion of procyanidins and prodelphinidins to cyanidin and delphinidin. *Phytochemistry* 1985;25:223–30.
- [29] Jin L. *Flavonoids in Saskatoon Fruits, Blueberry Fruits, and Legume Seeds*. University of Alberta, 2011.
- [30] Heikkinen S, Argmann CA, Champy M-F, Auwerx J. Evaluation of glucose homeostasis. *Curr Protoc Mol Biol* 2007;Chapter 29:Unit 29B.3.
- [31] Chan CB, MacPhail RM, Mitton K. Evidence for defective glucose sensing by islets of fa/fa obese Zucker rats. *Can J Physiol Pharmacol* 1993;71:34–9.
- [32] Chan CB, De Leo D, Joseph JW, McQuaid TS, Ha XF, Xu F, et al. Increased Uncoupling Protein-2 Levels in beta-cells Are Associated With Impaired Glucose-Stimulated Insulin Secretion: Mechanism of Action. *Diabetes* 2001;50:1302–10.
- [33] Zifkin M, Jin A, Ozga JA, Zaharia LI, Scherthner JP, Gesell A, et al. Gene expression and metabolite profiling of developing highbush blueberry fruit indicates transcriptional regulation of flavonoid metabolism and activation of abscisic acid metabolism. *Plant Physiol* 2012;158:200–24.
- [34] Chan CB, MacPhail RM, Mitton K. Evidence for defective glucose sensing by islets of fa/fa obese Zucker rats. *Can J Physiol Pharmacol* 1993;71:34–9.
- [35] Sutherland LN, Capozzi LC, Turchinsky NJ, Bell RC, Wright DC. Time course of high-fat diet-induced reductions in adipose tissue mitochondrial proteins: potential mechanisms and the relationship to glucose intolerance. *Am J Physiol Endocrinol Metab* 2008;295:E1076–83.
- [36] Thrush a B, Chabowski A, Heigenhauser GJ, McBride BW, Or-Rashid M, Dyck DJ. Conjugated linoleic acid increases skeletal muscle ceramide content and decreases insulin sensitivity in overweight, non-diabetic humans. *Appl Physiol Nutr Metab* 2007;32:372–82.
- [37] Borai A, Livingstone C, Ferns GAA. The biochemical assessment of insulin resistance. *Ann Clin Biochem* 2007;44:324–42.

- [38] Monagas M, Urpi-Sarda M, Sánchez-Patán F, Llorach R, Garrido I, Gómez-Cordovés C, et al. Insights into the metabolism and microbial biotransformation of dietary flavan-3-ols and the bioactivity of their metabolites. *Food Funct* 2010;1:233–53.
- [39] Saura-Calixto F, Pérez-Jiménez J, Touriño S, Serrano J, Fuguet E, Torres JL, et al. Proanthocyanidin metabolites associated with dietary fibre from in vitro colonic fermentation and proanthocyanidin metabolites in human plasma. *Mol Nutr Food Res* 2010;54:939–46.
- [40] Mateos-Martín ML, Pérez-Jiménez J, Fuguet E, Torres JL. Non-extractable proanthocyanidins from grapes are a source of bioavailable (epi)catechin and derived metabolites in rats. *Br J Nutr* 2012;108:290–7.
- [41] Hemingway RW, McGraw GW. Kinetics of Acid-Catalyzed Cleavage of Procyanidins. *J Wood Chem Technol* 1983;3:421–35.
- [42] Tsang C, Auger C, Mullen W, Bornet A, Rouanet J-M, Crozier A, et al. The absorption, metabolism and excretion of flavan-3-ols and procyanidins following the ingestion of a grape seed extract by rats. *Br J Nutr* 2005;94:170 – 181.
- [43] Shoji T, Masumoto S, Moriichi N, Akiyama H, Kanda T, Ohtake Y, et al. Apple procyanidin oligomers absorption in rats after oral administration: analysis of procyanidins in plasma using the porter method and high-performance liquid chromatography/tandem mass spectrometry. *J Agric Food Chem* 2006;54:884–92.
- [44] Stoupi S, Williamson G, Viton F, Barron D, King LJ, Brown JE, et al. In vivo bioavailability, absorption, excretion, and pharmacokinetics of [<sup>14</sup>C]procyanidin B2 in male rats. *Drug Metab Dispos* 2010;38:287–91.
- [45] Smith AH, Zoetendal E, Mackie RI. Bacterial Mechanisms to Overcome Inhibitory Effects of Dietary Tannins. *Microb Ecol* 2005;50:197–205.
- [46] Smith AH, Mackie RI. Effect of condensed tannins on bacterial diversity and metabolic activity in the rat gastrointestinal tract. *Appl Environ Microbiol* 2004;70:1104–15.
- [47] Yamakoshi J, Tokutake S, Kikuchi M, Kubota Y, Konishi H, Mitsuoka T. Effect of Proanthocyanidin-Rich Extract from Grape Seeds on Human Fecal Flora and Fecal Odor. *Microb Ecol Health Dis* 2001;13:25–31.
- [48] Cerf ME, Chapman CS, Louw J. High-fat programming of hyperglycemia, hyperinsulinemia, insulin resistance, hyperleptinemia, and altered islet architecture in 3-month-old wistar rats. *ISRN Endocrinol* 2012;2012:627270.
- [49] Ahrén B, Gudbjartsson T, Al-Amin a N, Mårtensson H, Myrsén-Axcrona U, Karlsson S, et al. Islet perturbations in rats fed a high-fat diet. *Pancreas* 1999;18:75–83.

- [50] Jayaprakasam B, Vareed SK, Olson LK, Nair MG. Insulin secretion by bioactive anthocyanins and anthocyanidins present in fruits. *J Agric Food Chem* 2005;53:28–31.
- [51] Deng S, Vatamaniuk M, Huang X, Doliba N, Lian M-M, Frank A, et al. Structural and functional abnormalities in the islets isolated from type 2 diabetic subjects. *Diabetes* 2004;53:624–32.
- [52] Clark A, Wells CA, Buley ID, Cruickshank JK, Vanhegan RI, Matthews DR, et al. Islet amyloid, increased A-cells, reduced B-cells and exocrine fibrosis: quantitative changes in the pancreas in type 2 diabetes. *Diabetes Res* 1988;9:151–9.
- [53] Ehses J a, Ellingsgaard H, Böni-Schnetzler M, Donath MY. Pancreatic islet inflammation in type 2 diabetes: from alpha and beta cell compensation to dysfunction. *Arch Physiol Biochem* 2009;115:240–7.
- [54] Quesada I, Tudurí E, Ripoll C, Nadal A. Physiology of the pancreatic alpha-cell and glucagon secretion: role in glucose homeostasis and diabetes. *J Endocrinol* 2008;199:5–19.
- [55] Dinneen S, Alzaid A, Turk D, Rizza R. Failure of glucagon suppression contributes to postprandial hyperglycaemia in IDDM. *Diabetologia* 1995;38:337–43.
- [56] Panickar KS. Effects of dietary polyphenols on neuroregulatory factors and pathways that mediate food intake and energy regulation in obesity. *Mol Nutr Food Res* 2013;57:34–47.
- [57] Rains TM, Agarwal S, Maki KC. Antiobesity effects of green tea catechins: a mechanistic review. *J Nutr Biochem* 2011;22:1–7.
- [58] Abd El Mohsen MM, Kuhnle G, Rechner AR, Schroeter H, Rose S, Jenner P, et al. Uptake and metabolism of epicatechin and its access to the brain after oral ingestion. *Free Radic Biol Med* 2002;33:1693–702.
- [59] Janle EM, Lila MA, Grannan M, Wood L, Higgins A, Yousef GG, et al. Pharmacokinetics and tissue distribution of <sup>14</sup>C-labeled grape polyphenols in the periphery and the central nervous system following oral administration. *J Med Food* 2010;13:926–33.
- [60] Wang J, Ferruzzi MG, Ho L, Blount J, Janle EM, Gong B, et al. Brain-targeted proanthocyanidin metabolites for Alzheimer's disease treatment. *J Neurosci* 2012;32:5144–50.
- [61] Venables MC, Hulston CJ, Cox HR, Jeukendrup AE. Green tea extract ingestion, fat oxidation, and glucose tolerance in healthy humans. *Am J Clin Nutr* 2008;87:778–84.
- [62] Hodgson AB, Randell RK, Jeukendrup AE. The effect of green tea extract on fat oxidation at rest and during exercise: evidence of efficacy and proposed mechanisms. *Adv Nutr* 2013;4:129–40.

- [63] Randell RK, Hodgson AB, Lotito SB, Jacobs DM, Boon N, Mela DJ, et al. No effect of 1 or 7 d of green tea extract ingestion on fat oxidation during exercise. *Med Sci Sports Exerc* 2013;45:883–91.

## REFERENCES

1. **Ahren J, Ahren B, Wierup N.** Increased beta-cell volume in mice fed a high-fat diet: a dynamic study over 12 months. *Islets* 2010;2(6):353-356.
2. **Almeida Costa GE et al.** Chemical composition, dietary fibre and resistant starch contents of raw and cooked pea, common bean, chickpea and lentil legumes. *Food Chem.* 2006; 94(3):327-330.
3. **Babio N, Balanza R, Basulto J, Bullo M, Salas-Salvadó J.** Dietary fibre: influence on body weight, glycemic control and plasma cholesterol profile. *Nutr Hosp.* 2010;25(3):327-340.
4. **Canadian Diabetes Association Clinical Practice Guidelines Expert Committee.** Canadian Diabetes Association 2008 clinical practice guidelines for the prevention and management of diabetes in Canada. *Can J Diabetes* 2008;32(Suppl 1):S1-S201.
5. **Chandalia M et al.** Beneficial effects of high dietary fiber intake in patients with type 2 diabetes mellitus. *The New England Journal of Medicine* 2000;5:1392-1398.
6. **Cani PD, Delzenne NM.** Interplay between obesity and associated metabolic disorders: new insights into the gut microbiota. *Current Opinion in Pharmacology* 2009;9(6):737-743.
7. **Delhanty PJ, van der Lely AJ.** Ghrelin and glucose homeostasis. *Peptides.* 2011; 32(11):2309-18.
8. **Duenas M, Estrella I, Hernandez T.** Occurrence of phenolic compounds in the seed coat and the cotyledon of peas (*Pisum sativum* L.). *Eur Food Res Technol.* 2004;219:116-123.
9. **Freeland KR, Wilson C, Wolever TMS.** Adaptation of colonic fermentation and glucagon-like peptide-1 secretion with increased wheat fibre intake for 1 year in hyperinsulinaemic human subjects. *British Journal of Nutrition* 2010;103:82–90.
10. **Galisteo M, Duarte J, Zarzuelo A.** Effects of dietary fibers on disturbances clustered in the metabolic syndrome. *J Nutr Biochem.* 2008;19(2):71-84.
11. **Goodlad JS & Mathers JC.** Digestion of complex carbohydrates and large bowel fermentation in rats fed on raw and cooked peas (*Pisum sativum*). *Br J Nutr* 1992;67(3):475-488.
12. **Grover GJ et al.** Effects of the soluble fiber complex PolyGlycopleX® (PGX®) on glycemic control, insulin secretion, and GLP-1 levels in Zucker diabetic rats. *Life Sciences* 2011;88:392–399.



13. **Hull RL et al.** Dietary-fat-induced obesity in mice results in beta cell hyperplasia but not increased insulin release: evidence for specificity of impaired beta cell adaptation. *Diabetologia* 2005;48(7):1350-1358.
14. **Jenkins DJ, Kendall CW, Axelsen M, Augustin LS, Vuksan V.** Viscous and nonviscous fibres, nonabsorbable and low glycaemic index carbohydrates, blood lipids and coronary heart disease. *Curr Opin Lipidol.* 2000;11:49–56.
15. **Kim W, Egan JM.** The Role of Incretins in Glucose Homeostasis and Diabetes Treatment. *Pharmacol Rev* 2008;60:470–512.
16. **Kutos̃ T, Golob T, Kac̃ M & Plestenjak A.** Dietary fibre content of dry and processed beans. *Food Chemistry* 2003;80(2):231–235.
17. **Liu Z et al.** Insulin and glucagon regulate pancreatic alpha-cell proliferation. *PLoS* 2011;One 6: e16096.
18. **Lu ZX et al.** Arabinoxylan fibre improves metabolic control in people with Type II diabetes. *Eur J Clin Nutr* 2004;58(4):621-628.
19. **Lunde MSH et al.** Variations in Postprandial Blood Glucose Responses and Satiety after Intake of Three Types of Bread *Journal of Nutrition and Metabolism* 2011.
20. **Ma Z et al.** Thermal processing effects on the functional properties and microstructure of lentil, chickpea, and pea flours. *Food Research International* 2011; 44: 2534–2544.
21. **Marconi E et al.** Physicochemical, nutritional, and microstructural characteristics of chickpeas (*Cicer arietinum* L.) and common beans (*Phaseolus vulgaris* L.) following microwave cooking. *Journal of Agricultural & Food Chemistry* 2000;48(12):5986-5994.
22. **Marinangeli CP, Jones PJ.** Whole and fractionated yellow pea flours reduce fasting insulin and insulin resistance in hypercholesterolaemic and overweight human subjects. *Br J Nutr.* 2011;105:110-117.
23. **Marinangeli CP, Krause D, Harding SV et al.** Whole and fractionated yellow pea flours modulate insulin, glucose, oxygen consumption, and the caecal microbiome in Golden Syrian hamsters. *Applied Physiology, Nutrition, & Metabolism = Physiologie Appliquee, Nutrition et Metabolisme* 2011; 36(6): 811-820.
24. **Massimino SP et al.** Fermentable Dietary Fiber Increases GLP-1 Secretion and Improves Glucose Homeostasis Despite Increased Intestinal Glucose Transport Capacity in Healthy Dogs. *J. Nutr.* 1998;128:1786–1793.
25. **Parnell JA & Reimer RA.** Prebiotic fibres dose-dependently increase satiety hormones and alter Bacteroidetes and Firmicutes in lean and obese JCR:LA-cp rats. *British Journal of Nutrition* 2012;107:601–613.

26. **Pick A et al.** Role of apoptosis in failure of beta-cell mass compensation for insulin resistance and beta-cell defects in the male Zucker diabetic fatty rat. *Diabetes* 1998;47(3):358-364.
27. **Prosky L & DeVries JW.** Controlling Dietary Fiber in Food Products. New York: Van Nostrand Reinhold 1992.
28. **Reimer RA et al.** Satiety Hormone and Metabolomic Response to an Intermittent High Energy Diet Differs in Rats Consuming Long-Term Diets High in Protein or Prebiotic Fiber. *J Proteome Res.* 2012; 11(8): 4065–4074.
29. **Schäfer G, Schenk U, Ritzel U, Ramadori G, Leonhardt U.** Comparison of the effects of dried peas with those of potatoes in mixed meals on postprandial glucose and insulin concentrations in patients with type 2 diabetes. *Am J Clin Nutr* 2003;78:99–103.
30. **Schenk S et al.** Different glycemic indexes of breakfast cereals are not due to glucose entry into blood but to glucose removal by tissue. *Am J Clin Nutr* 2003;78(4):742-748.
31. **Seino Y, Fukushima M, Yabe D.** GIP and GLP-1, the two incretin hormones: Similarities and differences. *Journal of Diabetes Investigation* 2010;1:8-23.
32. **Sievenpiper JL et al.** Effect of non-oil-seed pulses on glycaemic control: a systematic review and meta-analysis of randomised controlled experimental trials in people with and without diabetes. *Diabetologia* 2009;52:1479–1495.
33. **Tarini J, Wolever TMS.** The fermentable fibre inulin increases postprandial serum short-chain fatty acids and reduces free-fatty acids and ghrelin in healthy subjects. *Appl Physiol Nutr Metab.* 2010;35(1):9-16.
34. **Vyas U and Ranganathan N.** Probiotics, prebiotics, and synbiotics: gut and beyond. *Gastroenterol Res Pract.* 2012; 2012: 872716.
35. **Wang ZQ et al.** Effects of Dietary Fibers on Weight Gain, Carbohydrate Metabolism and Gastric Ghrelin Gene Expression in High Fat Diet Fed Mice. *Metabolism* 2007;56(12): 1635-1642.
36. **Weickert MO et al.** Cereal fiber improves whole-body insulin sensitivity in overweight and obese women. *Diabetes Care* 2006;29(4):775-780.
37. **Weickert MO, Pfeiffer AFH.** Metabolic Effects of Dietary Fiber Consumption and Prevention of Diabetes. *J. Nutr.* 2008;138: 439–442.
38. **Weiss R et al.** Basal alpha-cell up-regulation in obese insulin-resistant adolescents. *Journal of Clinical Endocrinology & Metabolism* 2011;96(1):91-97.
39. **Whitlock KA et al.** Assessment of the mechanisms exerting glucose-lowering effects of dried peas in glucose intolerant rats. *Br J Nutr* 2012; 108(S1):S91-S102.